ONREUR Report 91-2-W

WORKSHOP ON EXPLOSIVE AND PROPELLANT COMBUSTION MECHANISMS

R.W. Armstrong

July 25, 1991

Office of Naval Research, European Office

WORKSHOP ON EXPLOSIVE AND PROPELLANT COMBUSTION MECHANISMS

TABLE OF CONTENTS

WORKSHOP

ON

EXPLOSIVE AND PROPELLANT COMBUSTION MECHANISMS

This Workshop was sponsored by the Société Nationale des Poudres et Explosifs (SNPE), with the Office National d'Etudes et de Recherches Aérospatiale (ONERA), and the Office of Naval Research European Office (ONR Europe). The Workshop was held at the SNPE Centre de Recherches du Bouchet (CRB), Le Bouchet - B.P. no. 2, 91710 Vert-le-Petit, France, on June 3-4, 1991.

The early initiative for arranging this activity came from Dr. R.S. Miller, Chief Scientist, Mechanics Division, ONR, and Dr. Bernard Finck, Head, New Molecules Section, Defense Espace, SNPE. Dr. A.M. Diness, Director, Engineering Sciences, ONR, supported the effort. Assistance was provided by Dr. Jacques Boileau, SNPE (retired), and now an advisor to the Direction des Recherches, Etudes et Techniques, Division of Délégation Générale pour l'Armement.

Informal introductory meetings were arranged for Dr. R.W. Armstrong, Liaison Scientist, ONR Europe, with Dr. Bernard Wiedemann, Directeur, SNPE, and Dr. Alain Davenas, Directeur, Technologie et Recherche, SNPE, to gain approval for the proposed workshop. Dr. René Couturier is Manager of Research at SNPE/CRB. Dr. Gérard Doriath is Manager of the Propulsion Research Program. From this program and Bernard Finck's activity, respectively, Drs. Bernadette Gossant, Program Manager, Internal Ballistics, SNPE, and Marc Piteau, Energetic Material Synthesis, SNPE, provided coordination for developing the workshop with R.W. Armstrong, and with ONERA workshop participants, particularly, in the Energetics Department of ONERA headed by Dr. Guy Lengellé. Armstrong, in consultation with R.S. Miller, J. Boileau, and SNPE colleagues, arranged for the participation of U.S. scientists, especially including representatives from the Naval Research Laboratory.

In the subsequent pages of this report, corresponding largely to a description of research activities "in progress", a record is established of selected visual aids from the presentations that were given. A number of the U.S. participants were persuaded to add a written precis to their presentations. To all participants, a note of appreciation is given here.

R.W. Armstrong	B. Finck	R.S. Miller
ONR Europe	SNPE/CRB	ONR HQS

WORKSHOP ON EXPLOSIVE AND PROPELLANT COMBUSTION MECHANISMS

PARTICIPATION

Twenty participants took part in this workshop including a U.S. team of seven persons selected by Dr. R.S. Miller, Chief Scientist, Mechanics Division, Office of Naval Research. The French participants were from the host Société Nationale des Poudres et Explosifs (SNPE), Centre de Recherches du Bouchet (CRB), and from the Office National d'Etudes et de Recherches Aérospatiale (ONERA), Centre de Palaiseau. Dr. Jacques Boileau participated on behalf of Direction des Recherches, Etudes et Techniques, Delegation Générale pour l'Armement (DGA), and Dang Quang Vu was there on behalf of the DGA Direction des Missiles et de l'Espace, Service Technique des Poudres et Explosifs.

SUMMARY

First, selected visual aids are shown in this report as taken from the presentation by B. Gossant, giving a survey of internal ballistic programs at SNPE relating to solid propellant combustion mechanisms. This is followed by a visual aid package presented by G. Lengellé and ONERA colleagues, mostly on burning rate determinations. An overview is given by R.S. Miller (and A.W. Miziolek) of considerations relating to the combustion of high energy density materials, also with selected visual aids that were shown. The following presentations consist of extended abstracts and selected visual aids illustrating elements of U.S. programs now set to study combustion mechanisms in a new generation of energetic materials.

A main purpose of the workshop was to identify strengths of the French and U.S. programs as a forerunner of establishing specific collaborative U.S./France research activities on new energetic materials, known in the U.S. research community to involve new combustion considerations. The burning rate measurement capabilities at ONERA were an agreed strength as well as the availability of a new generation of energetic materials in the U.S., as described by R.S. Miller, with energies characteristic of metallic systems but without telltale signatures. The combustion properties approach theoretically limiting values and the comprehensive analytical description of these properties requires use of the fastest computers. New standardized combustion tests are being designed in the U.S. to evaluate the performances of these materials.

Agreement on a joint study of trinitroazetidine (TNAD), glycidyl azide polymer (GAP), and hexanitrohexaazaisowurtzitane (HNIW) materials resulted from the group discussions. A consensus was reached that it would be profitable for French investigators to increase their research efforts on the new ingredients that are available for propellant formulations. An important recommendation was to involve in this subject area researchers at French universities, particularly relating to SNPE activities.

WORKSHOP ON EXPLOSIVE AND PROPELLANT COMBUSTION MECHANISMS

Sponsored by the Société Nationale des Poudres et Explosifs,
with the Office National d'Etudes et de Recherches Aérospatiale,
and
the Office of Naval Research European Office

held at the

SNPE Centre de Recherches du Bouchet (CRB)
Le Bouchet - B.P. no. 2, 91710 Vert-le-Petit, France

June 3-4, 1991

SNPE-ONERA PRESENTATIONS

B. Finck, SNPE/CRB
Research done at SNPE,
particularly relating to new molecules

M. Piteau, SNPE/CRB
Formulation and characterization of new energetic materials

J.P. Bac, SNPE/CRB
Computational thermochemistry of energetic materials

B. Gossant, SNPE/CRB
Comprehensive combustion mechanisms related to motor firing

G. Lengellé, ONERA/Centre de Palaiseau
Decomposition and combustion
of existing and new energetic materials

J.R. Duterque, ONERA/CP
Methods and measurements for characterizing the combustion
of energetic ingredients

J.F. Trubert, ONERA/CP
Gas sampling and mass spectrometry analysis
at the decomposition surface and in the flame

WORKSHOP ON EXPLOSIVE AND PROPELLANT COMBUSTION (CONT'D)

Sponsored by SNPE with ONERA and the ONR at the
SNPE Centre de Recherches du Bouchet
Le Bouchet - B.P. no.2, 91710 Vert-le-Petit, France

June 3-4, 1991

U.S. PRESENTATIONS

R.S. Miller, Office of Naval Research, Arlington, VA, (and A.W. Miziolek, Ballistic Research Lab., Aberdeen Proving Ground, MD)
High Energy Density Materials Combustion

T.B. Brill, University of Delaware, Newark, DE
1. Chemical phenomena at burning surfaces
2. Decomposition of energetic materials at high temperature

T. (and D. Hanson-) Parr, Naval Weapons Center, China Lake, CA
Solid propellant flame structure,
monitored with advanced laser diagnostics

E.W. Price, Georgia Institute of Technology, Atlanta, GA
(presented by T. Parr)
Kinetically limited leading edge of diffusion flames (KLLEFs)

C.F. Melius*, Sandia National Laboratories, Livermore, CA.
*Visiting Professor at Universite Pierre et Marie Curie.
Theoretical determination of thermochemistry
and reaction mechanisms

R. Gilardi, Naval Research Laboratory, Washington, D.C.
Structure analyses of energetic and strained organic compounds

R.W. Armstrong*, Office of Naval Research European Office, London, U.K.
*On leave from the University of Maryland, College Park, MD, following a sabbatical research stay at the Cavendish Laboratory, University of Cambridge, U.K.
Thermomechanical influences on the combustion
of RDX crystals

B. Gossant

Propellant and Combustion Mechanisms

SNPE
DEFENSE ESPACE
RECHERCHE PROPULSION

WORKSHOP ON COMBUSTION MECHANISMS

June 3–4 , 1991

Comprehensive combustion mechanisms related to motor firing

B. GOSSANT

07/25/91

SNPE
DEFENSE ESPACE
RECHERCHE PROPULSION

BURNING RATE CHARACTERIZATION

1– ON SMALL PROPELLANT SAMPLES:

1.1– STRAND BURNER method:

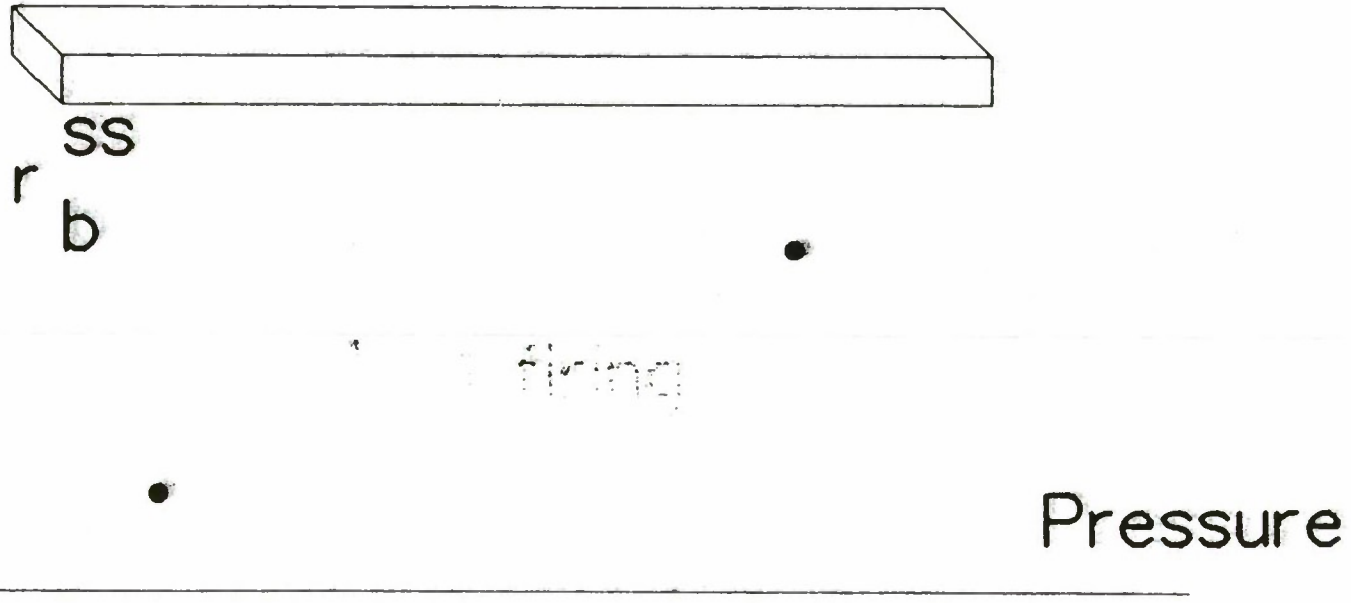

SNPE
DEFENSE ESPACE
RECHERCHE PROPULSION

1.2– DIRECT ULTRASONIC METHOD:

– Closed vessel

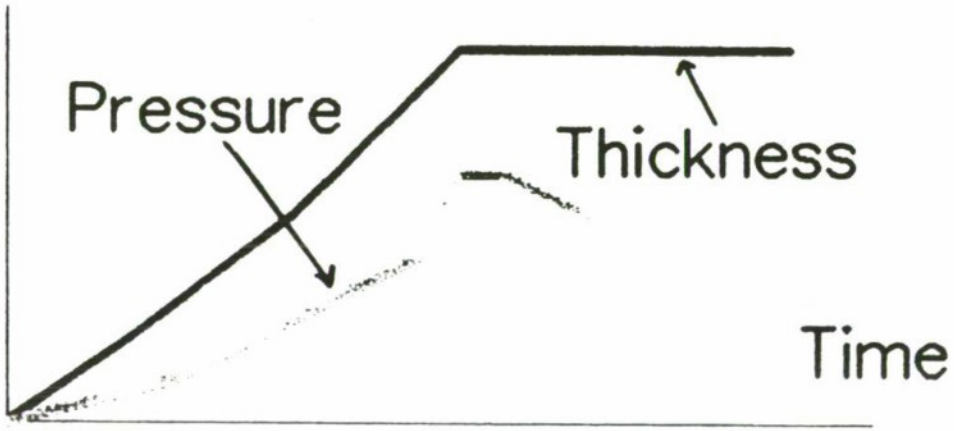

SNPE
DEFENSE ESPACE
RECHERCHE PROPULSION

2– ON SUBSCALED TEST MOTORS:

2.1– Neutral:

- Star–shaped (Campanule)
- Cylindrical (Bates)

2.2– With surface evolution:

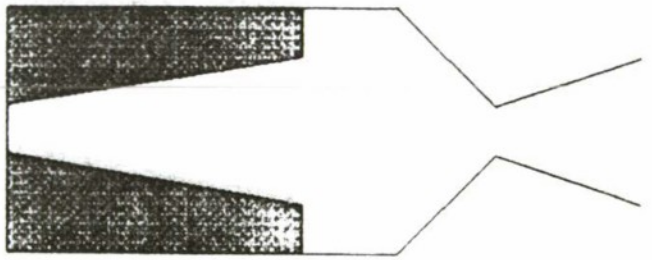

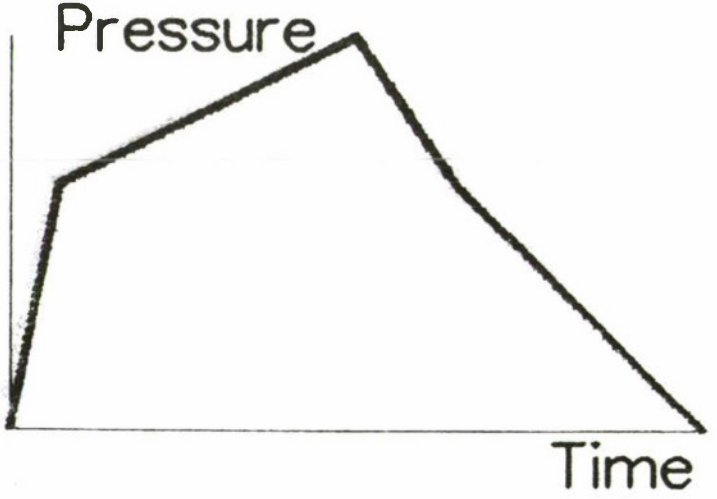

SNPE
DEFENSE ESPACE
RECHERCHE PROPULSION

CHARACTERIZATION UNDER TRANSIENT FLUX

1– PRESSURE COUPLING RESPONSE:

Determine propellant mass flow rate in presence of an acoustic field

SNPE: T–burner

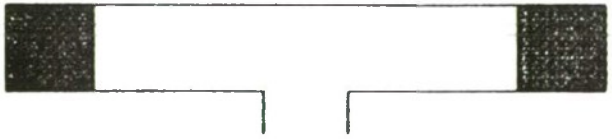

ONERA: PEM

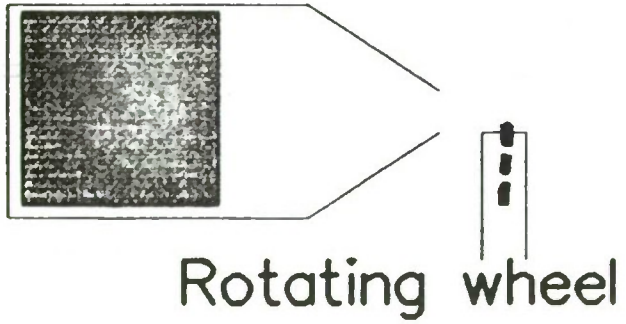

SNPE
DEFENSE ESPACE
RECHERCHE PROPULSION

2– IGNITION TESTS:

Characterize ignition delays for various propellant compositions

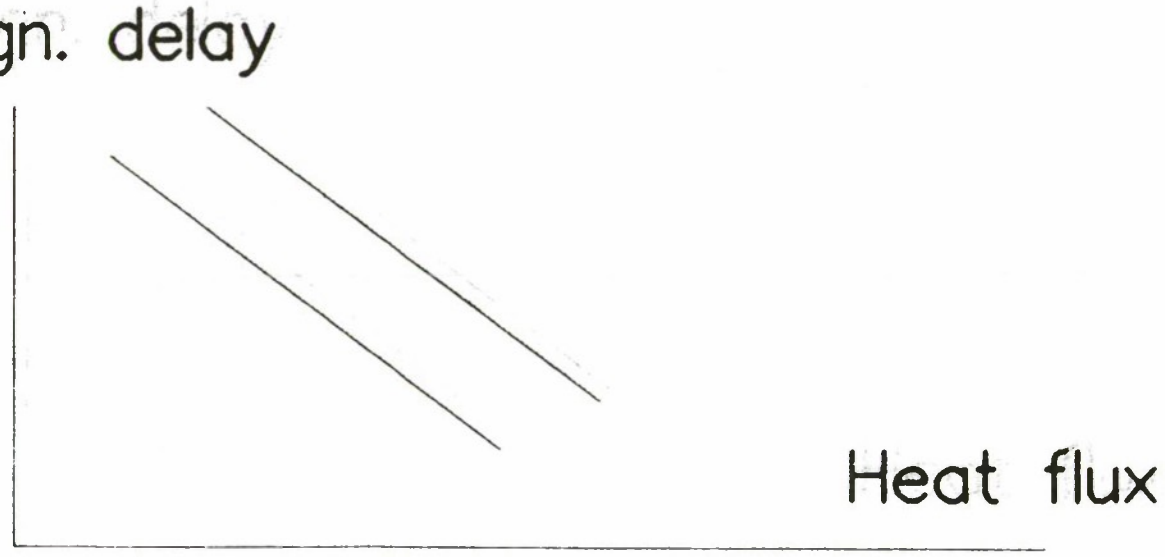

07/25/91

SNPE
DEFENSE ESPACE
RECHERCHE PROPULSION

COMBUSTION MECHANISMS

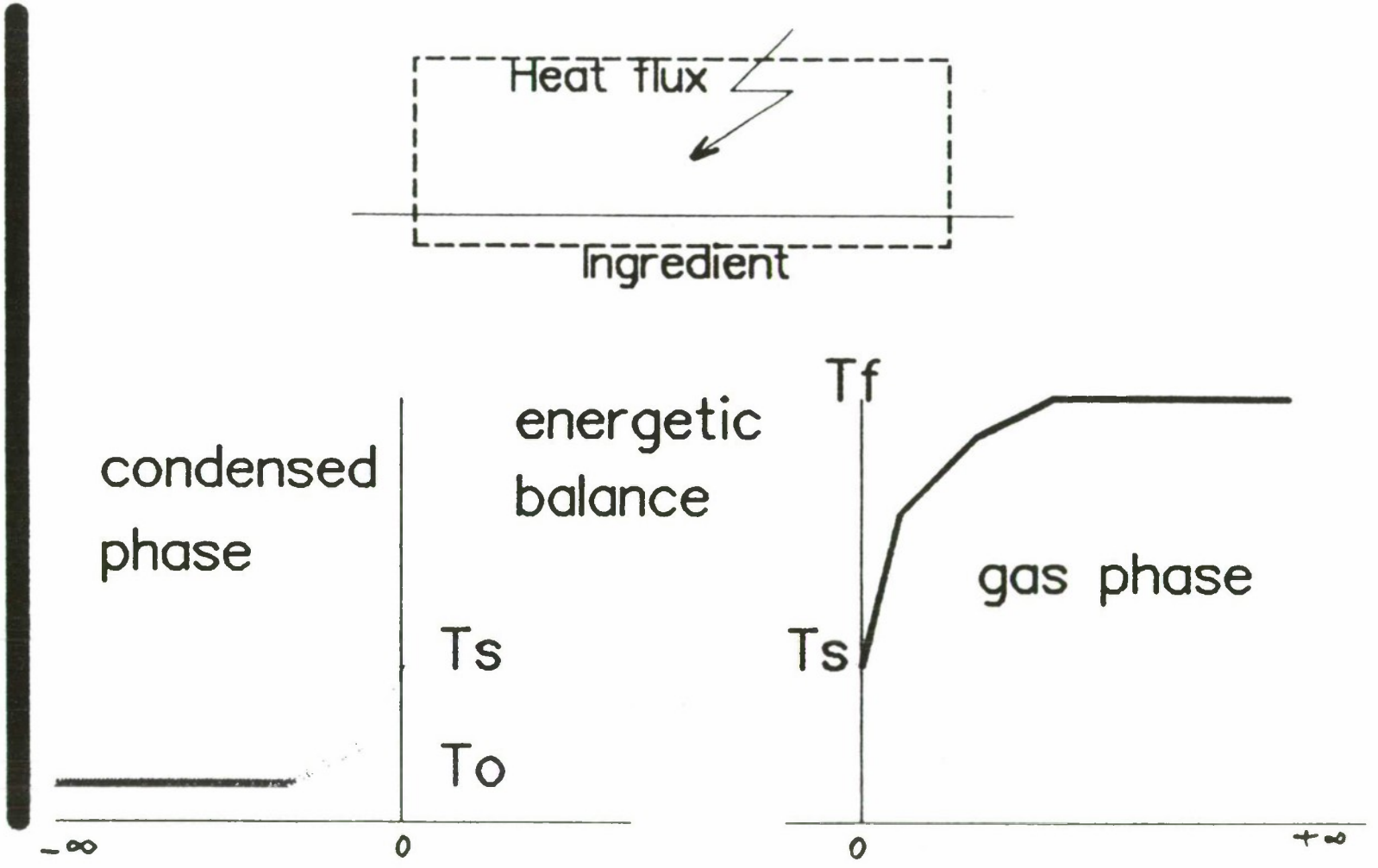

SNPE
DEFENSE ESPACE
RECHERCHE PROPULSION

CONDENSED PHASE BEHAVIOR

Energetic balance at ingredient surface:

$$\rho_{s,i}\, r_{b,i}^{ss} \left[c_{s,i} \left(T_{s,i}^{ss} - T_0 \right) - Q_{s,i} \right] = \lambda_{g,i} \left. \frac{dT}{dx} \right|_{0^+}$$

In this eq., two main characteristics depend on $T_{s,i}^{ss}$: $Q_{s,i}$ and $r_{b,i}^{ss}$

1– DETERMINATION OF Qs,i: experimentally

a) Record temperature profiles in condensed and gas phases (embedded thermocouples)

b) Evaluate Ts,i, $\lambda_{g,i} \left. \frac{dT}{dx} \right|_{0^+}$ (knowing $\lambda_{g,i}$).

SNPE
DEFENSE ESPACE
RECHERCHE PROPULSION

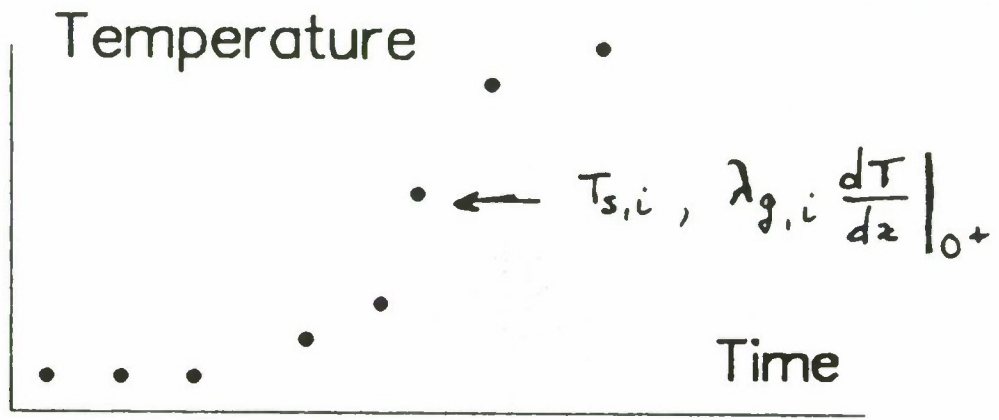

c) Evaluate Qs,i (knowing Cs,i , $\rho_{s,i}$, $r_{b,i}^{ss}$)

2– DETERMINATION OF PYROLYSIS LAWS:

experimentally

a) Record $r_{b,i}^{ss}$ and associated $T_{s,i}^{ss}$

b) Record DSC results giving Ai, $E_{g,i}$
(but pb. of temperature range)

SNPE
DEFENSE ESPACE
RECHERCHE PROPULSION

GASEOUS PHASE BEHAVIOR

Combustion model for a self–burning ingredient

1– FLAME CHARACTERISTICS:

$T_{F,i}$ = adiabatic flame temperature

$Q_{F,i}$ = heat release in the flame

$$f^- = \lambda_{g,i} \left.\frac{dT}{dx}\right|_{x_F^-}$$

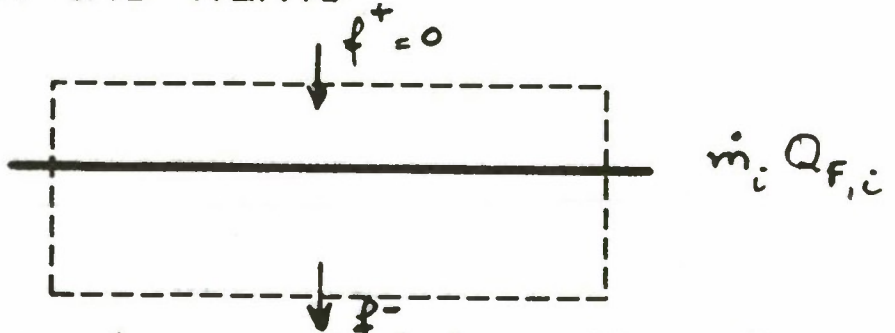

In an elementary domain containing the flame:

$$\lambda_{g,i} \left.\frac{dT}{dx}\right|_{x_F^-} = \dot{m}_i Q_{F,i} \quad ; \quad \dot{m}_i = \rho_{s,i} r_{b,i}$$

SNPE
DEFENSE ESPACE
RECHERCHE PROPULSION

2– DESCRIPTION OF THE GASEOUS PHASE:

Heat conduction from the flame to the surface

$$\begin{cases} \lambda_{g,i} \dfrac{d^2T}{dx^2} = \dot{m}_i\, C_{g,i} \dfrac{dT}{dx} + \dot{\omega}_i \qquad \dot{\omega}_i = 0 \text{ Assumption of thin sheet flame} \\ \quad + \text{B.C.} \end{cases}$$

Integration of eq. gives the temperature profile and heat flux in any point x

$$\begin{cases} T_i^{(ss)}(x) = T_{s,i} + \left(T_{F,i} - T_{s,i}\right)\left(\exp \dfrac{\dot{m}_i C_{g,i}\, x}{\lambda_{g,i}} - 1\right) \Big/ \left[\exp \dfrac{\dot{m}_i C_{g,i}\, x_{F,i}}{\lambda_{g,i}} - 1\right] \\ \dfrac{d\,T_i^{(ss)}}{dx}(x) = \left(T_{F,i} - T_{s,i}\right) \dfrac{\dot{m}_i C_{g,i}}{\lambda_{g,i}} \exp \dfrac{\dot{m}_i C_{g,i}\, x}{\lambda_{g,i}} \Big/ \left[\exp \dfrac{\dot{m}_i C_{g,i}\, x_{F,i}}{\lambda_{g,i}} - 1\right] \end{cases}$$

SNPE
DEFENSE ESPACE
RECHERCHE PROPULSION

3- FLAME HEIGHT DETERMINATION:

Need a model for $x_{F,i}$ (or $\xi_{F,i} = \frac{\dot{m}_i \, C_{g,i}}{\lambda_{g,i}} x_{F,i}$)
Depends on the flame structure
For a self-burning ingredient, assumption of a premixed flame gives:

$x_{F,i} = v_{g,i} \, \tau_i$; $v_{g,i}$ = gas velocity = $\dot{m}_i / \rho_{g,i}$
τ_i = reaction time = $\left[k_i \, P_{g,i}^{\delta_i} \right]^{-1}$; $k_i = B_i \exp\left(- \frac{E_{F,i}}{R T_{F,i}} \right.$

$$\Longrightarrow \quad x_{F,i} = \frac{\dot{m}_i}{K_i \, P^{\delta_i}} \qquad \left(\text{or } \xi_{F,i} = \frac{C_{g,i}}{\lambda_{g,i}} \frac{\dot{m}_i}{K_i P^{\delta_i}} \right)$$

SNPE
DEFENSE ESPACE
RECHERCHE PROPULSION

4– SURFACE TEMPERATURE DETERMINATION:

Flux expression in $x = x_F$ – $\Longrightarrow$ $T_{s,i}(x) = T_{F,i} - \frac{Q_{F,i}}{C_{g,i}}\left[1 - \exp\left(-\frac{\dot{m}_i C_{g,i}}{\lambda_{g,i}} q_{F,i}\right.\right.$

5– A BASIC COMBUSTION MODEL:

a) Guess one $T_{s,i}^{ss}$

b) Solve for $\xi_{F,i} = -\ln\left[1 - \left(T_{F,i} - T_{s,i}^{(ss)}\right)\frac{C_{g,i}}{Q_{F,i}}\right.$

c) Solve for $\dot{m}_i = \left(\frac{\lambda_{g,i}}{C_{g,i}} K_i P^{\delta_i}\right)^{1/2}$

d) Solve for $T_{s,i}^{ss} = -\frac{E_{s,i}}{R} \ln \frac{\dot{m}_i}{A_{s,i}}$

SNPE
DEFENSE ESPACE
RECHERCHE PROPULSION

6– MAIN DATA:

a) $T_{F,i}$: Obtained by enthalpy conservation

$$I \xrightarrow{\Delta H_i} n_2 N_2 + n_{20} N_2O + h_{20} H_2O + \cdots$$

$$\Delta H_{f,i}^{298} + \int_{298}^{T_0} C_{s,i}(T)\, dT = \sum_j Y_j \left\{ \Delta H_{f,j}^{298} + \int_{298}^{T_{F,i}} C_{g,i}(T)\, dT \right\}$$

b) FLAME HEAT RELEASE:

$Q_{F,i} \propto \Delta H_i$ depends on the scheme

1st $\quad I \xrightarrow{\Delta H_i} n_2 N_2 + n_{20} N_2O + h_{20} H_2O + \cdots$

2nd $\quad I \longrightarrow I_1 + I_2 + \cdots \xrightarrow{\Delta H_i} n_2 N_2 + n_{20} N_2O + h_{20} H_2O + \cdots$

SNPE
DEFENSE ESPACE
RECHERCHE PROPULSION

c) THERMAL PROPERTIES OF GAS:

Assuming realistic values for $T_{s,i}^{ss}$ and $T_{F,i}$

$$\overline{C_{g,i}} = \int_{T_{s,i}}^{T_{F,i}} C_{g,i}(T)\, dT \Big/ \left(T_{F,i} - T_{s,i}\right)$$

$$\overline{\lambda_{g,i}} = \text{---}$$

SNPE
DEFENSE ESPACE
RECHERCHE PROPULSION

COMBUSTION MODEL FOR A PROPELLANT

It is an extension of the model presented for one ingredient. With multi–ingredients, new specific features arrise.

1– DESCRIPTION OF CONDENSED PHASE:

$$a_{fill} = \frac{M_{fill}}{M_P}$$

SNPE
DEFENSE ESPACE
RECHERCHE PROPULSION

a) Determine $r_{b,p}^{ss}$ (or $\dot{m}_p^{ss}$)

+ If binder + filler (1 particle size)

Different models:

@ BDP considers an average configuration at the surface

Binder and filler are simoultaneously recessed:

$$\Longrightarrow \dot{m}_p^{ss} = \frac{\dot{m}_{fill}^{ss}}{\alpha_{fill}} \frac{S_{fill}}{S_p}$$

@ ONERA considers combustion in direction normal to the surface and alternate burning of filler and binder (Beckstead)

$$\Longrightarrow \dot{m}_p^{ss} = \frac{\dot{m}_{fill\ pp}^{ss}\ \dot{m}_{binder}^{ss}}{\alpha_{fill}\dot{m}_{binder}^{ss} + (1-\alpha_{fill})\dot{m}_{fill}^{ss}}$$

This previous eq. may be modified to take into account an ignition delay for the solid particle of filler.

SNPE
DEFENSE ESPACE
RECHERCHE PROPULSION

+ Binder + filler (various particle sizes)

$$\alpha_{fill} = \sum_j \alpha_{fill}(j)$$

PEM model considers j pseudo-propellants, one for each particle size. $\Longrightarrow \dot{m}_p^{ss} = \alpha_{fill} \Big/ \sum_j \left[\alpha_{fill}(j) / \dot{m}_p^{ss}(j) \right]$

b) Determine $\dot{m}_{fill}$ and $\dot{m}_{bind}$

By pyrolysis laws:

$$\dot{m}_{fill}^{ss} = A_{fill} \exp\left(-\frac{E_{s,fill}}{R T_{s,fill}}\right)$$

$$\dot{m}_{bind}^{ss} = A_{bind} \exp\left(-\frac{E_{s,bind}}{R T_{s,bind}}\right)$$

SNPE
DEFENSE ESPACE
RECHERCHE PROPULSION

2– FLAME STRUCTURE:

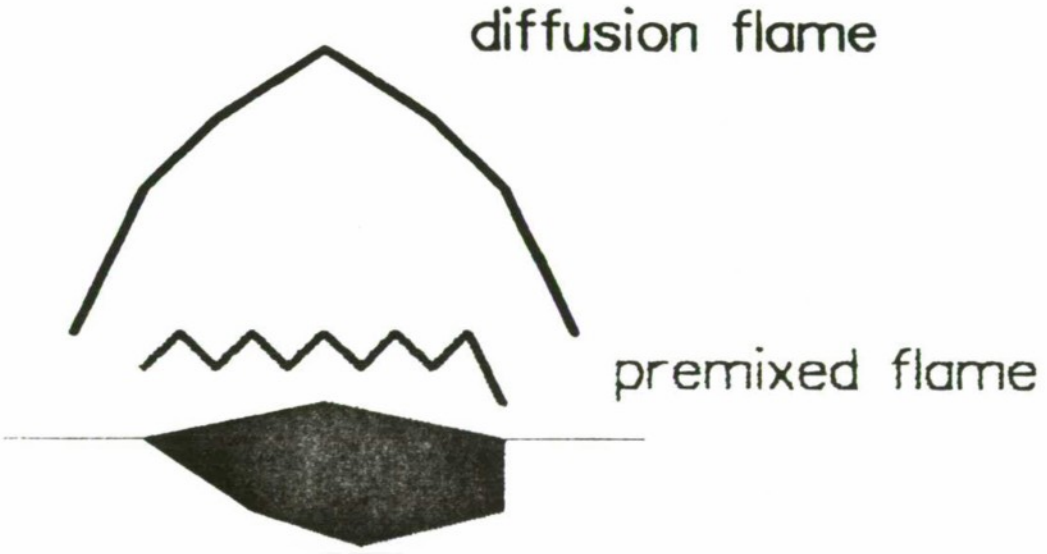

07/25/91

SNPE
DEFENSE ESPACE
RECHERCHE PROPULSION

a) Model for a diffusion flame height:

$$x_F = x_D + x_R$$

x_D = evaluated by Burke – Schumann analysis
= f (mixing ratio, geometry, D_g , ρ_g)

D_g ← Diffusion coefficient

1–D approach $x_D = A_{fh}\, x_D$

A_{fh} = height factor for equivalent thin sheet flame

SNPE
DEFENSE ESPACE
RECHERCHE PROPULSION

b) Energetic balance above ingredients:

Depends on flame structure. It is necessary to know which part of reactions fluxes must be accounted for assessing surface temperatures.

EX: HTPB/AP assuming (ONERA model)

- premixed AP flame
- Diffusion flame between fuel rich gas (binder) and oxidizing species (from AP flame)

+ Above HTPB (heated by diff. flame only):

$$\left.\begin{array}{ll} x = x_F & T = T_F \\ & \lambda_g \left.\frac{dT}{dx}\right|_{x_F^-} = \dot{m}_p Q_F \\ x = 0 & T = T_{s,HTPB} \\ & \lambda_g \left.\frac{dT}{dx}\right|_{0^+} \end{array}\right\} \Longrightarrow T_{s,HTPB} = T_F - \frac{Q_F}{\lambda_g}\left[1 - \exp\left(-\frac{\dot{m}_p \lambda_g x_F}{\lambda_g}\right)\right]$$

SNPE
DEFENSE ESPACE
RECHERCHE PROPULSION

+ Above AP (interaction of the two flames)

Influence of final diffusion flame on AP flame

$$x = x_F \quad T = T_F \quad \bar{\lambda}_g \left.\frac{dT}{dx}\right|_{x_F^-} = \dot{m}_p Q_F$$

$$x = x_{AP} \quad T = T_{AP} \quad \bar{\lambda}_g \left.\frac{dT}{dx}\right|_{x_{AP}^+} = \dot{m}_p \left[Q_F - \bar{C}_g (T_F - T_{AP}) \right]$$

$$\Longrightarrow T_{AP} = T_F - \frac{Q_F}{\bar{C}_g} \left\{ 1 - \exp\left[-\frac{\dot{m}_p \bar{C}_g}{\bar{\lambda}_g} (x_F - x_{AP}) \right] \right.$$

+ Energetic balance at AP surface:

$$x = x_{AP} \quad T = T_{AP} \quad \bar{\lambda}_g \left.\frac{dT}{dx}\right|_{x_{AP}^-} = \bar{\lambda}_g \left.\frac{dT}{dx}\right|_{x_{AP}^+} + \dot{m}_{AP} Q_{AP}$$

$$x = 0 \quad T = T_{s,AP} \quad \bar{\lambda}_g \left.\frac{dT}{dx}\right|_{0^+}$$

$$\Longrightarrow T_{s,AP} = T_{AP} - \frac{\bar{\lambda}_g}{\dot{m}_p \bar{C}_g} \left.\frac{dT}{dx}\right|_{x_{AP}^-} \left[1 - \exp\left(-\frac{\dot{m}_p \bar{C}_g}{\bar{\lambda}_g} x_{AP} \right) \right.$$

SNPE
DEFENSE ESPACE
RECHERCHE PROPULSION

CONCLUSIONS

1– Models have the capability to evaluate the burning rate of a propellant as a function of pressure, initial temperature.

Problems: knowledge of physical parameters flame structure, behavior of each ingredient validity, role of catalysts

2– Problems for modelling unsteady combustion behavior Also what kind of experiments could be conducted on the ingredients

J. Duterque, G. Lengellé, and J.F. Trubert

Decomposition and Combustion Measurements

O N E R A

Energetics Department

Centre de Palaiseau

DEA 5660 USA-FRANCE

Working Group n° 4 - 3/4 june 1991

Decomposition and combustion of existing and new energetic materials.

- Existing ingredients and corresponding propellants
- Methods for characterizing the combustion of energetic ingredients
- Gas sampling and mass spectrometry analysis at the decomposition surface and in the flame

J. DUTERQUE, G. LENGELLÉ, J.F. TRUBERT

Existing ingredients and corresponding propellants

- Double-base propellants and active binders
  Numerous results, Kubota/Japan,
  Zenin-Korobeinichev/URSS,
  N.S. Cohen - M. Beckstead/USA, ONERA/France.

Should serve as reference for methods of investigation and for modelization efforts.

- HMX - RDX
  Approach similar to that of DB propellants.

- Composite propellants
  AP - PB binder/HMX - active binder

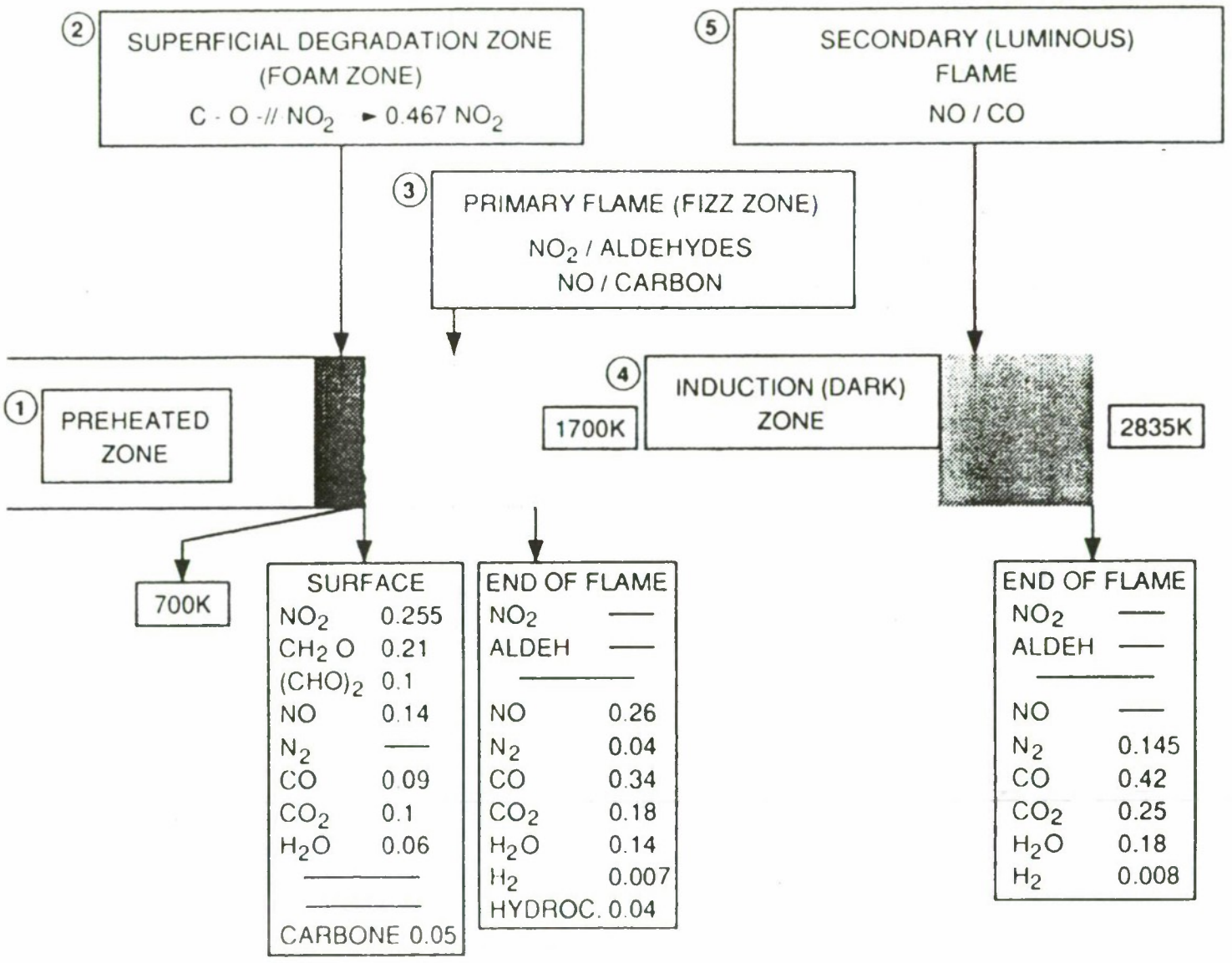

Figures for an 1100 cal/g propellant. Surface and primary flame (at 11 atm) mass fractions from gas analysis

VARIOUS ZONES IN THE COMBUSTION OF A DOUBLE BASE - PROPELLANT

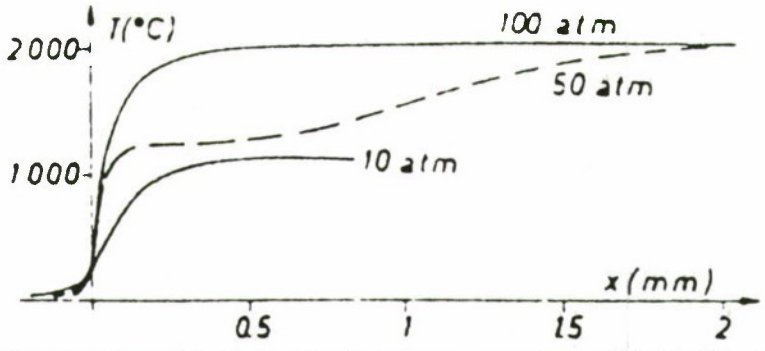

Pressure atm.	10	50	100
v_b mm/s	1.9	6.7	10.6
T_s, K	610	662	685
Preheated zone, µm (measured/ computed)	140/ 194	50/55	45/35
Residence time in preheated zone, ms	100	8	3
Superficial degradation zone µm	11	3	2
Residence time in superficial zone, ms	6	0,.5	0,2
Flame thickness, µm (measured)	200	75	110 (secon- dary flame)

Measured results from Zenin

Characteristics of the combustion zones.

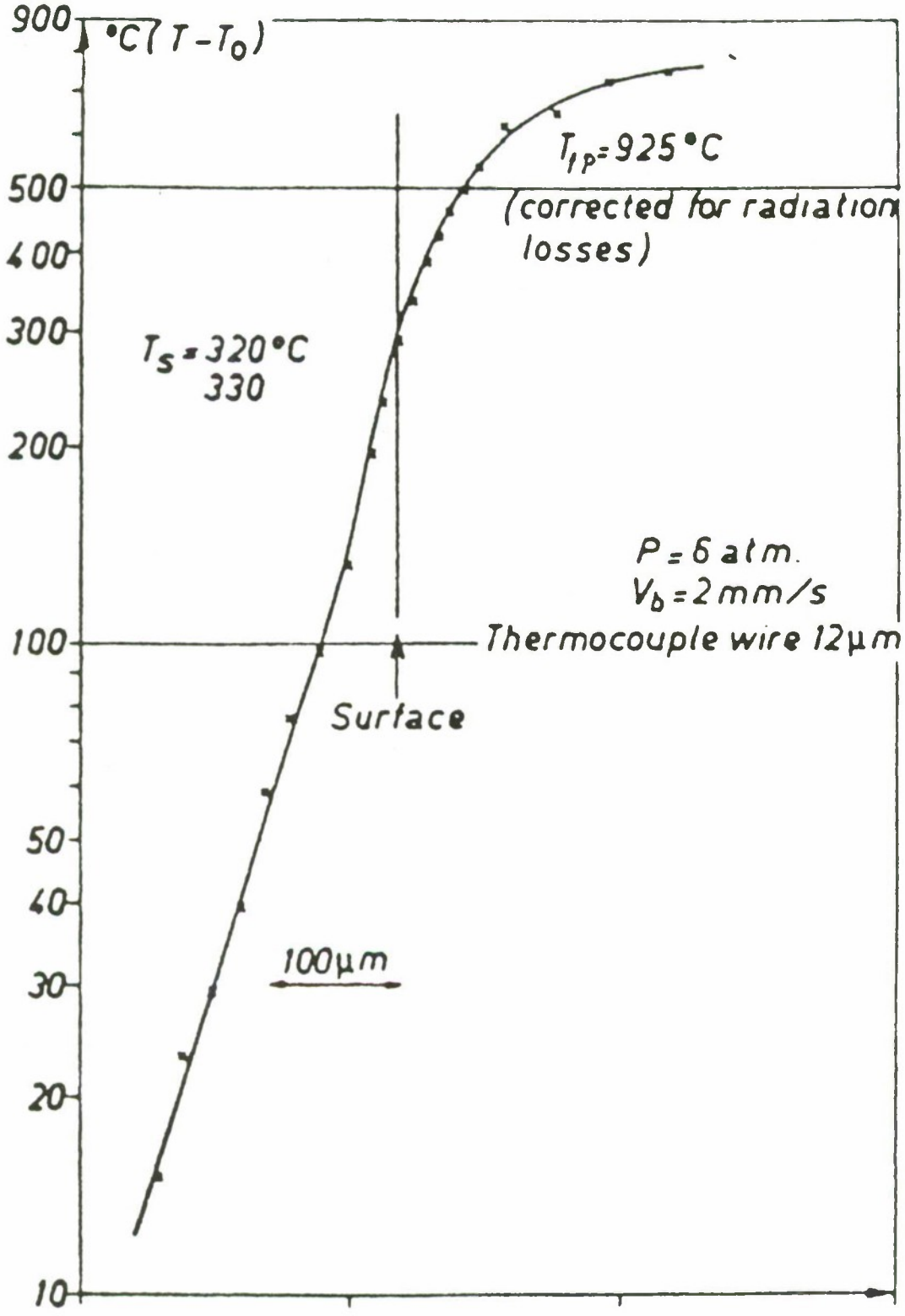

TEMPERATURE PROFILE IN THE CONDENSED PHASE

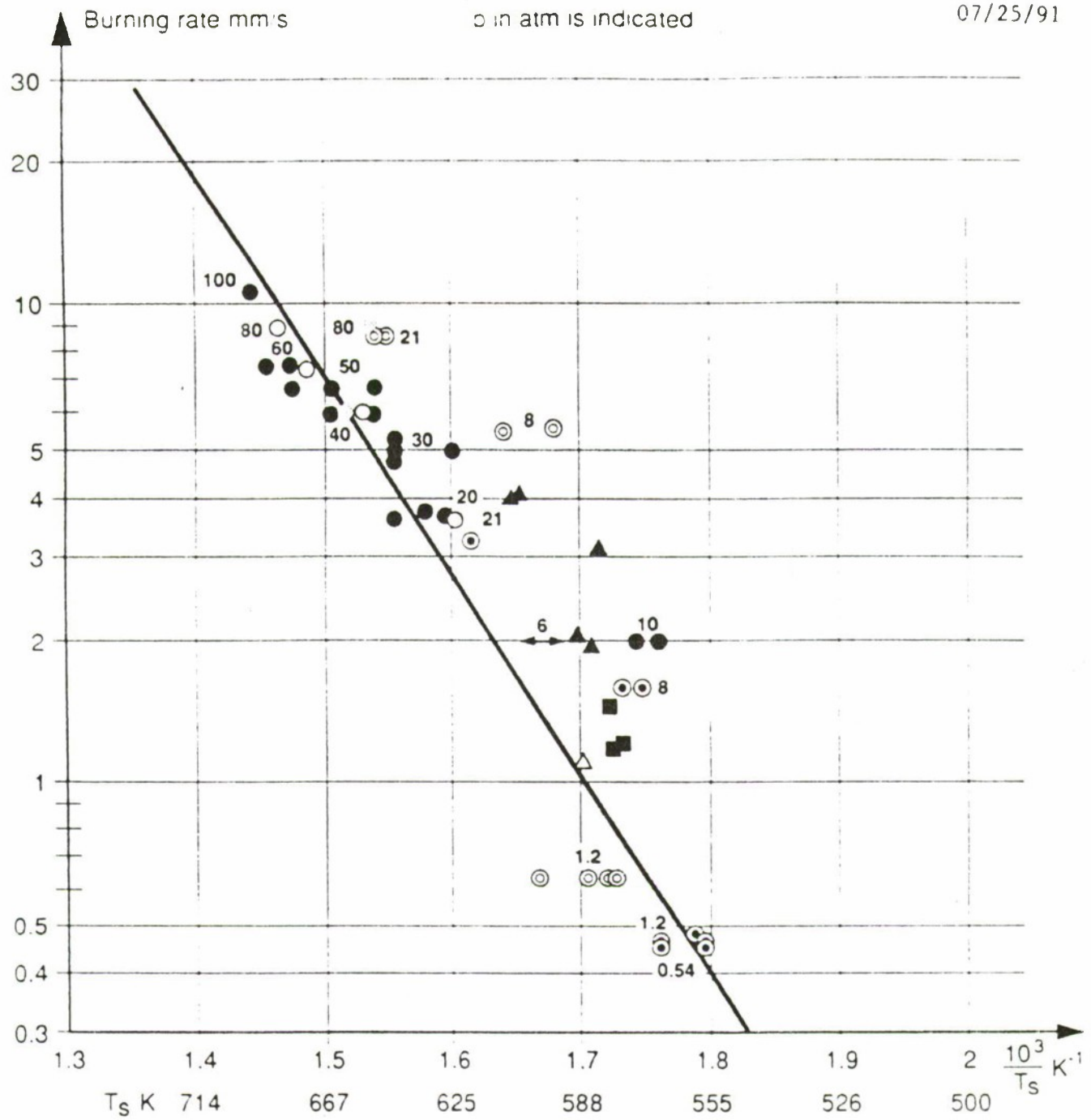

Corresponds to $A_c = 110^{17}$ s^{-1}, $E_c = 40\ 10^3$ cal/mole

$Q_s = 100$ cal/g , $T_o = 20$°C , $d_p = 0.8\ 10^{-3}$ cm^2 s

◄►▲	Microthermocouple	ONERA (1100 cal/g)	
△	Microthermocouple	SUH	
⊙	Reference, microthermocouple	KUBOTA	
◎	+ additives, microthermocouple	KUBOTA	
●	Microthermocouple	ZENIN	Propellant "N" (reference)
○	"Light pipe method"	SELEZNEV	
	"Thermal noise method"		
■	Microthermocouple	DENISYUK	$T_o = 120$°C

PYROLYSIS LAW FOR DOUBLE - BASE PROPELLANTS

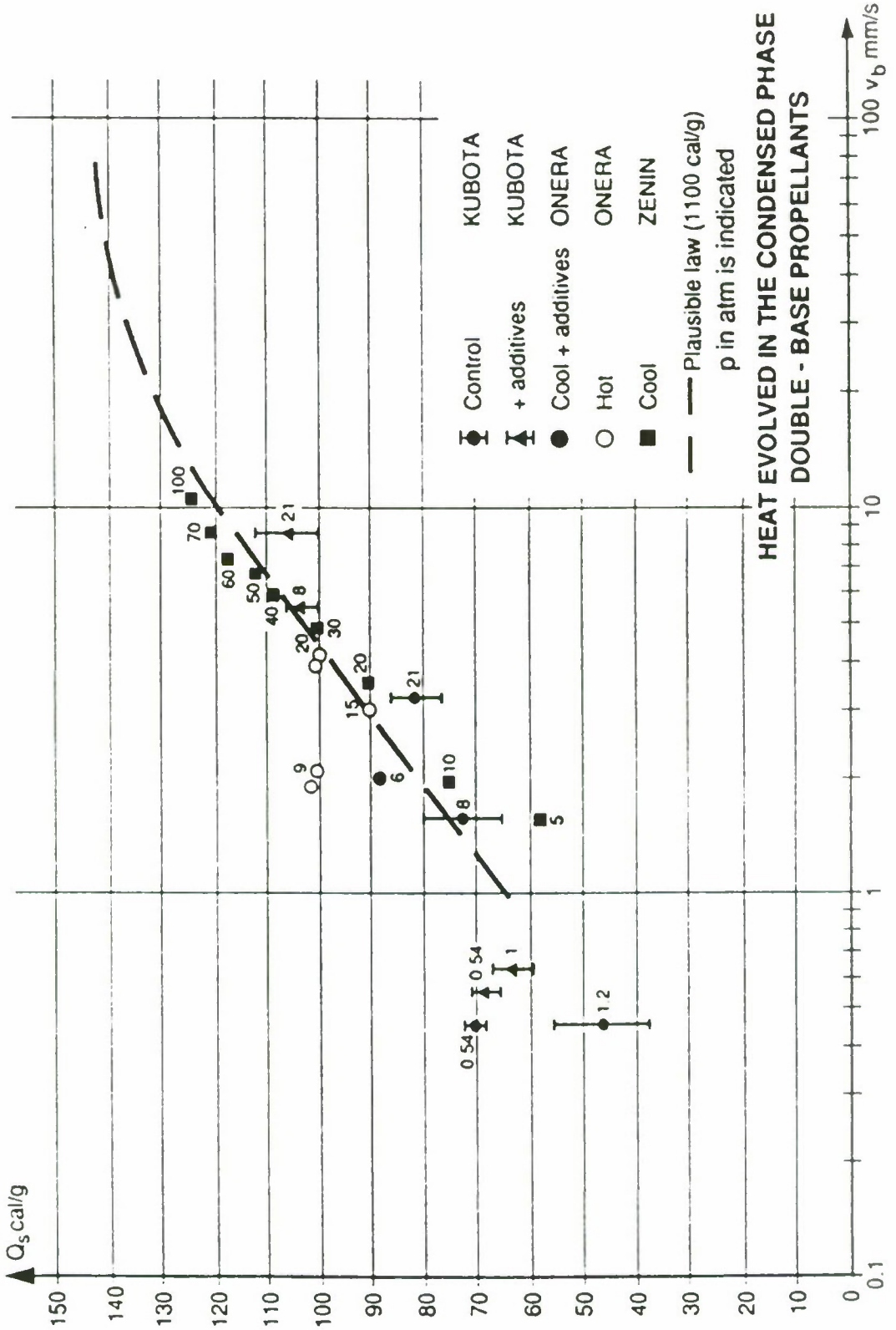
HEAT EVOLVED IN THE CONDENSED PHASE
DOUBLE - BASE PROPELLANTS
Q_s cal/g
100 v_b mm/s
Control KUBOTA
+ additives KUBOTA
Cool + additives ONERA
Hot ONERA
Cool ZENIN
Plausible law (1100 cal/g)
p in atm is indicated

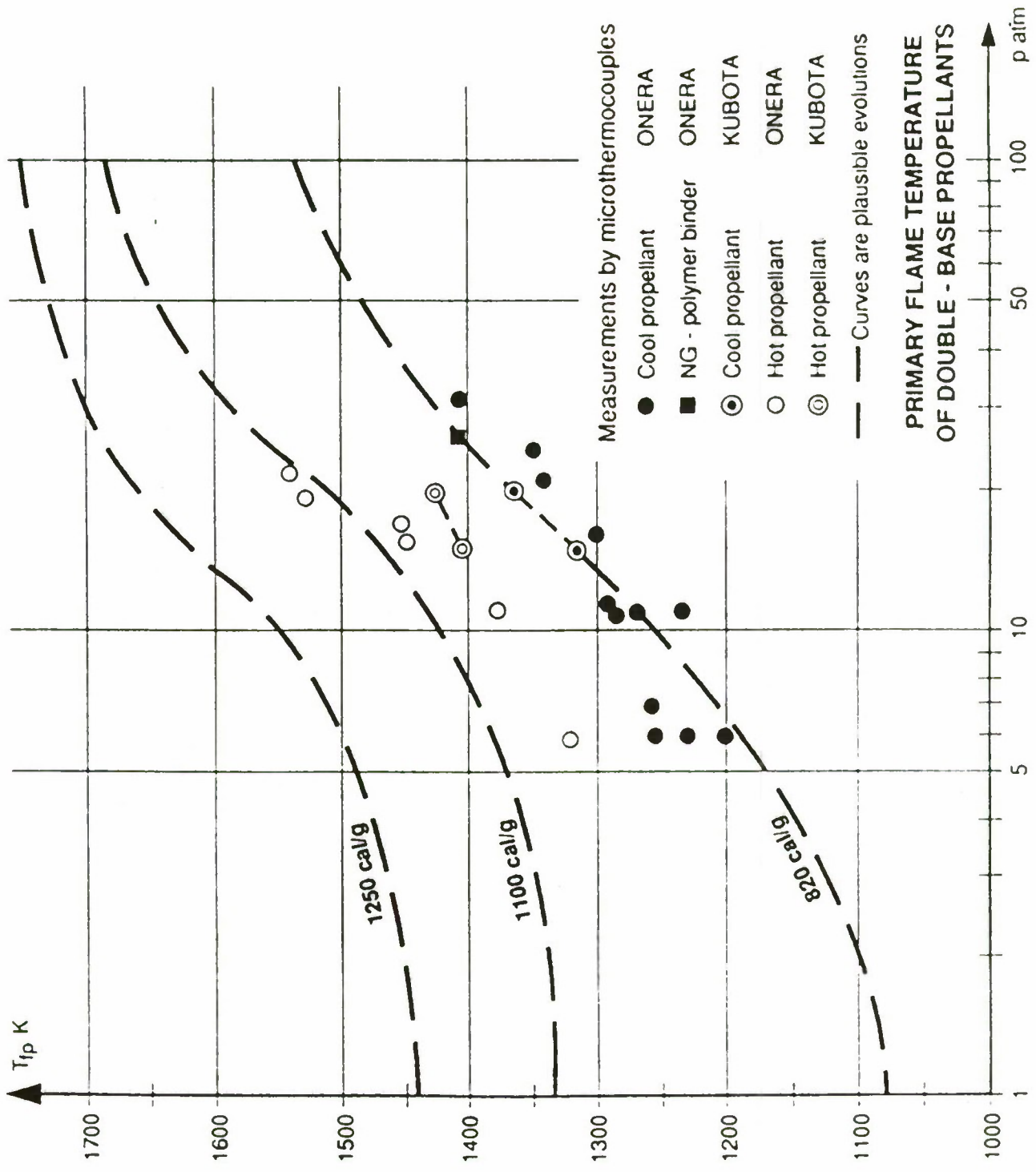
PRIMARY FLAME TEMPERATURE
OF DOUBLE - BASE PROPELLANTS
T_{fp} K
p atm
1700
1600
1500
1400
1300
1200
1100
1000
1
5
10
50
100
1250 cal/g
1100 cal/g
820 cal/g
Measurements by microthermocouples
Cool propellant ONERA
NG - polymer binder ONERA
Cool propellant KUBOTA
Hot propellant ONERA
Hot propellant KUBOTA
Curves are plausible evolutions

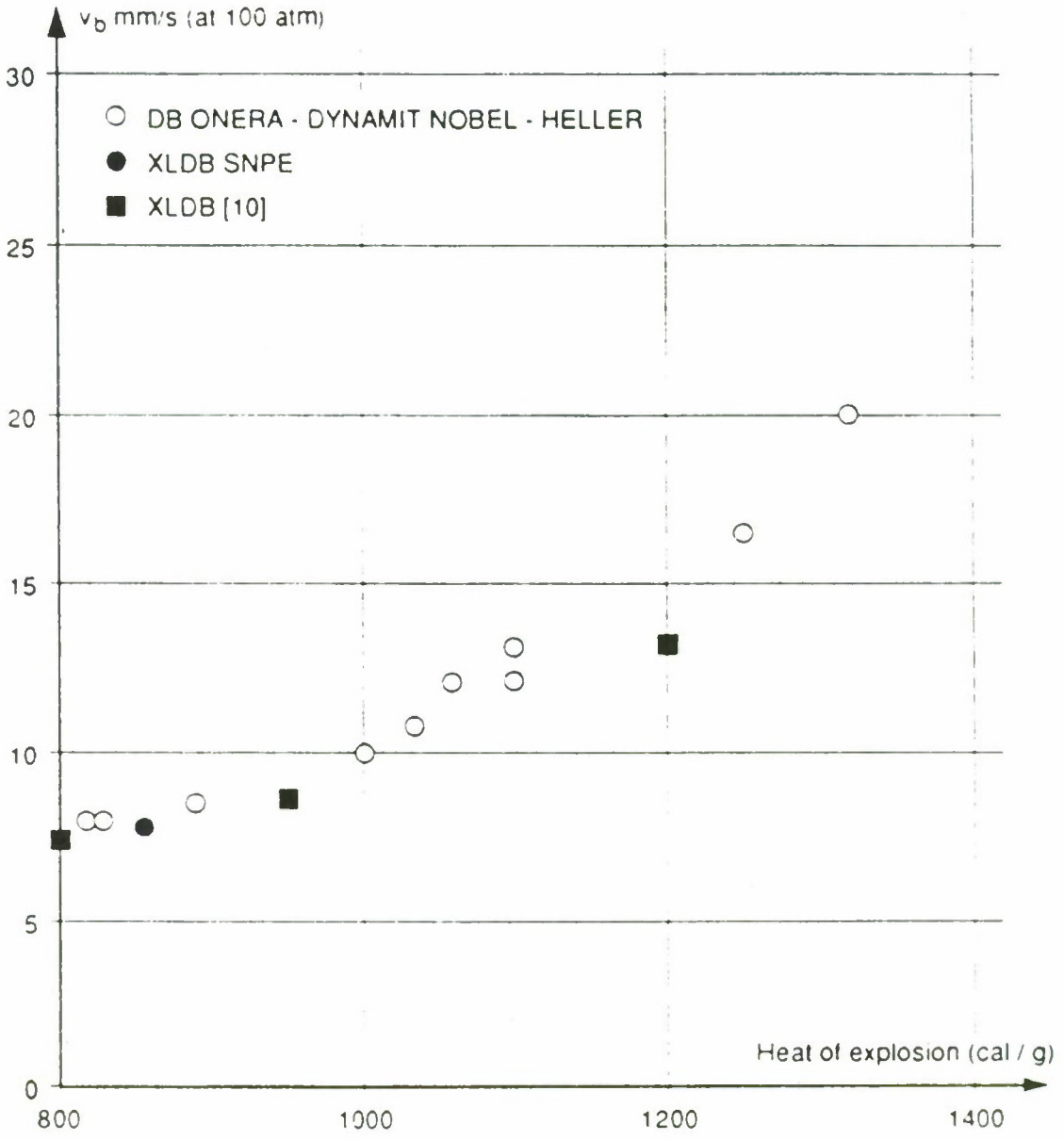

BURNING RATE VS HEAT OF EXPLOSION.DOUBLE-BASE PROPELLANTS AND XLDB BINDERS

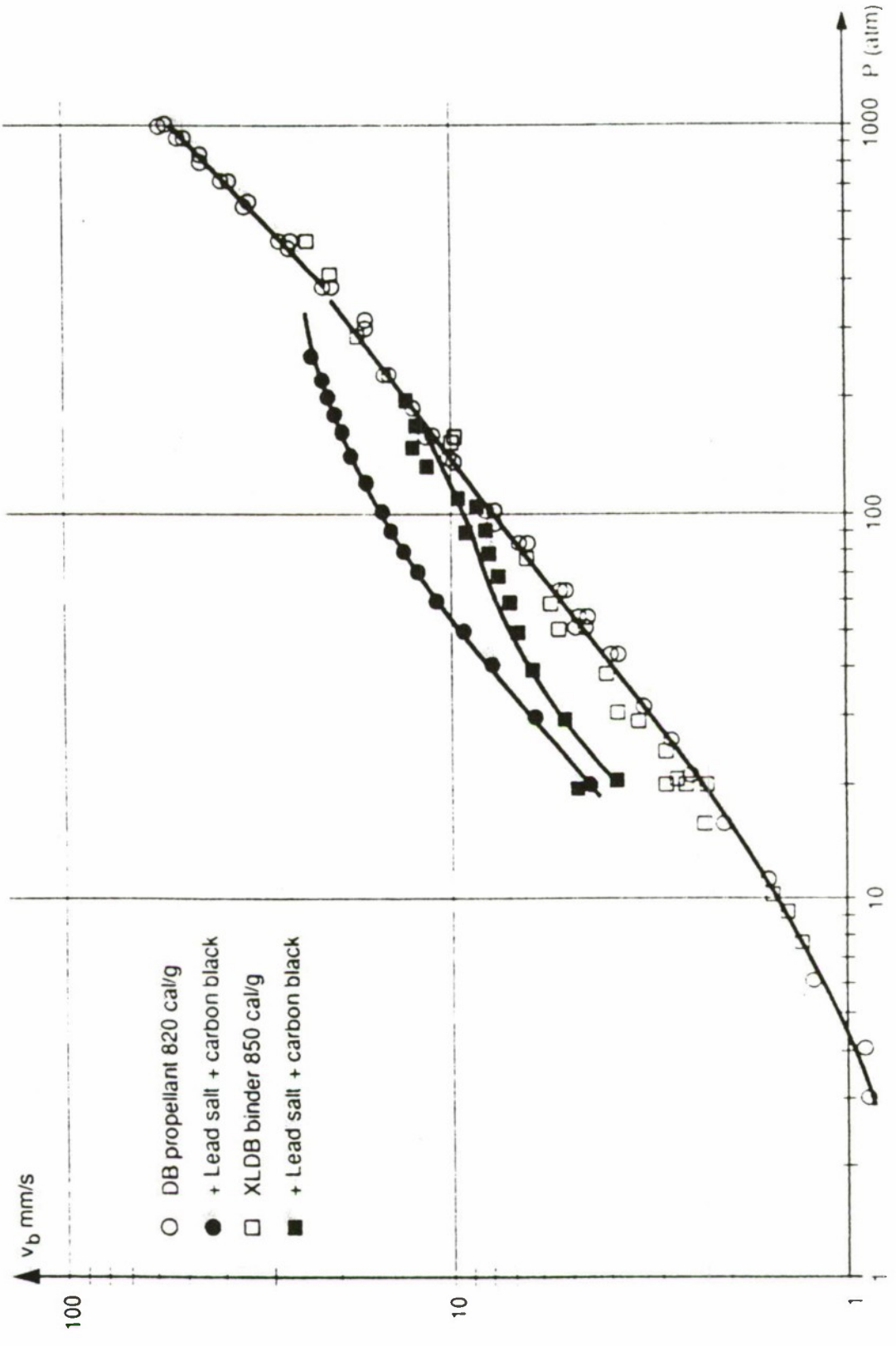

DOUBLE - BASE PROPELLANT AND ACTIVE BINDER BURNING RATES

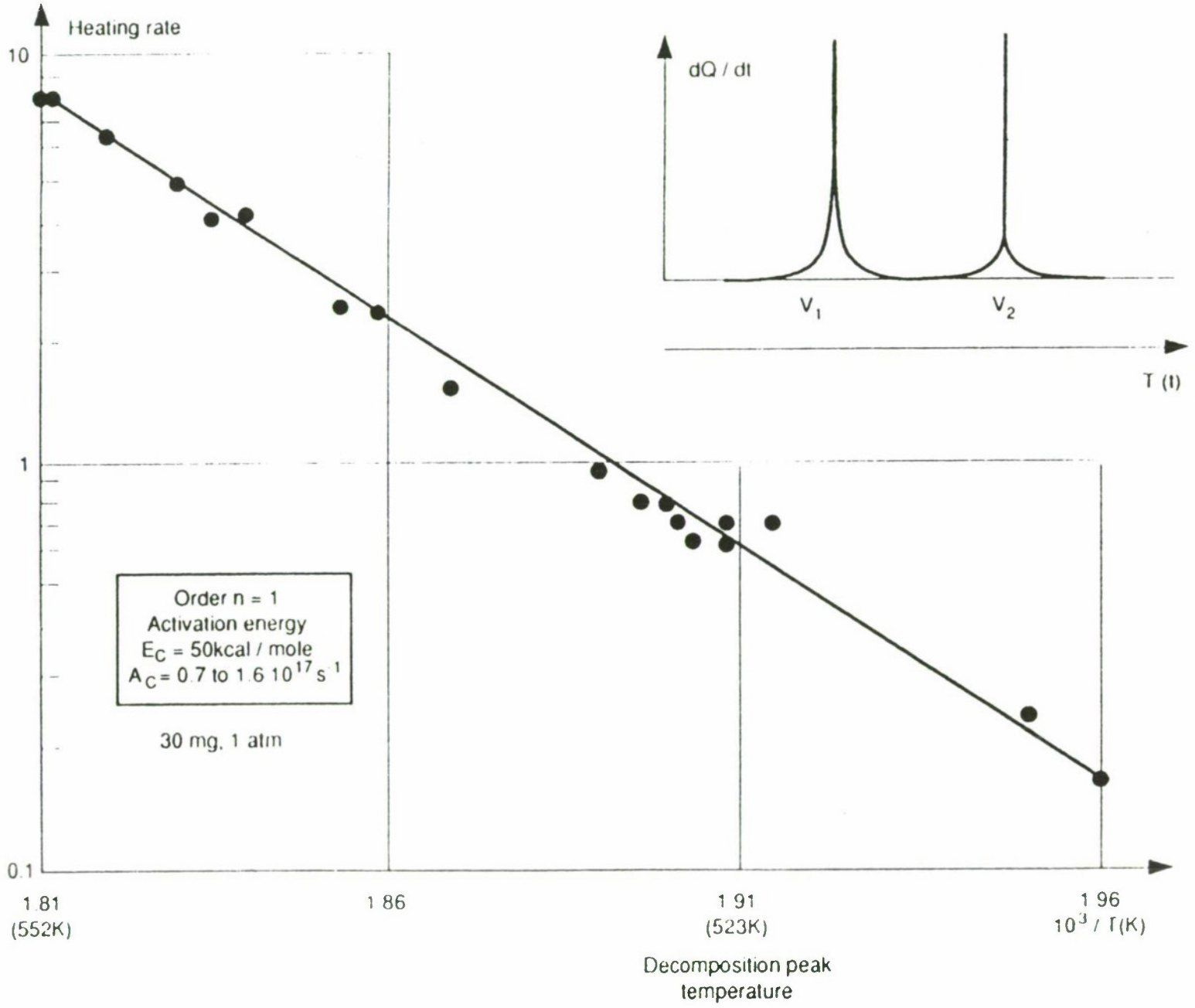

DIFFERENTIAL THERMAL ANALYSIS OF HMX DECOMPOSITION

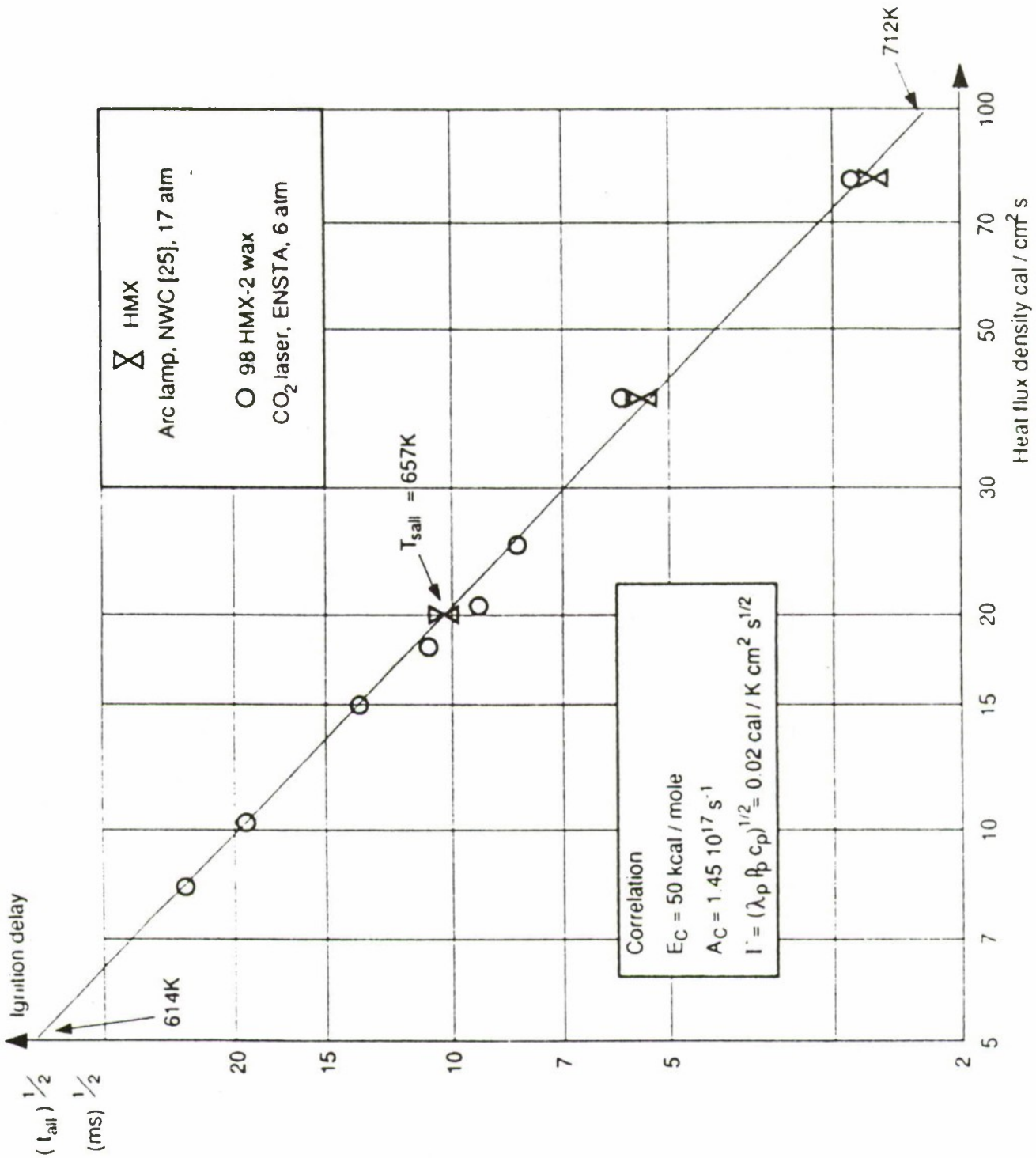

IGNITION OF HMX

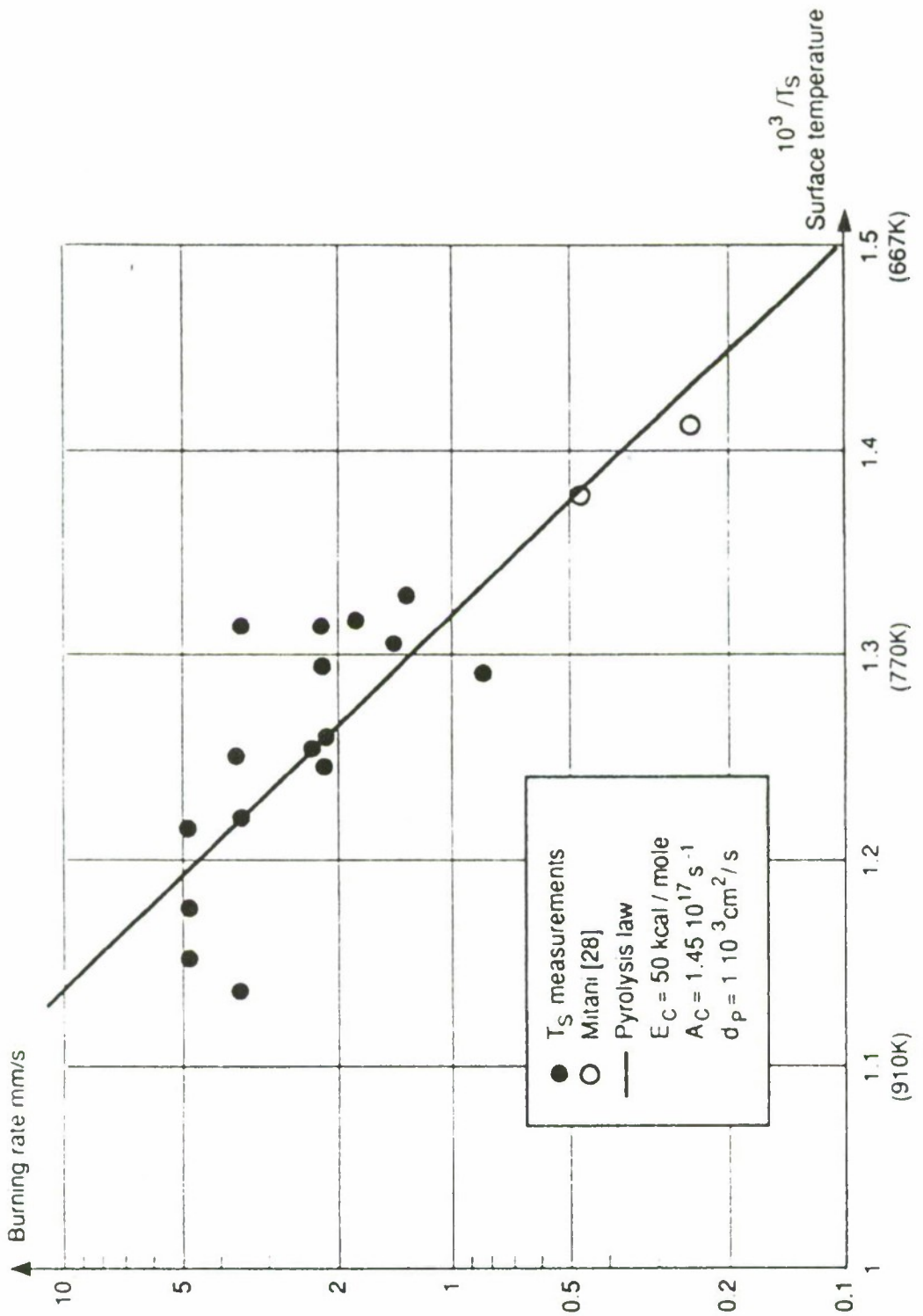

PYROLYSIS LAW FOR HMX

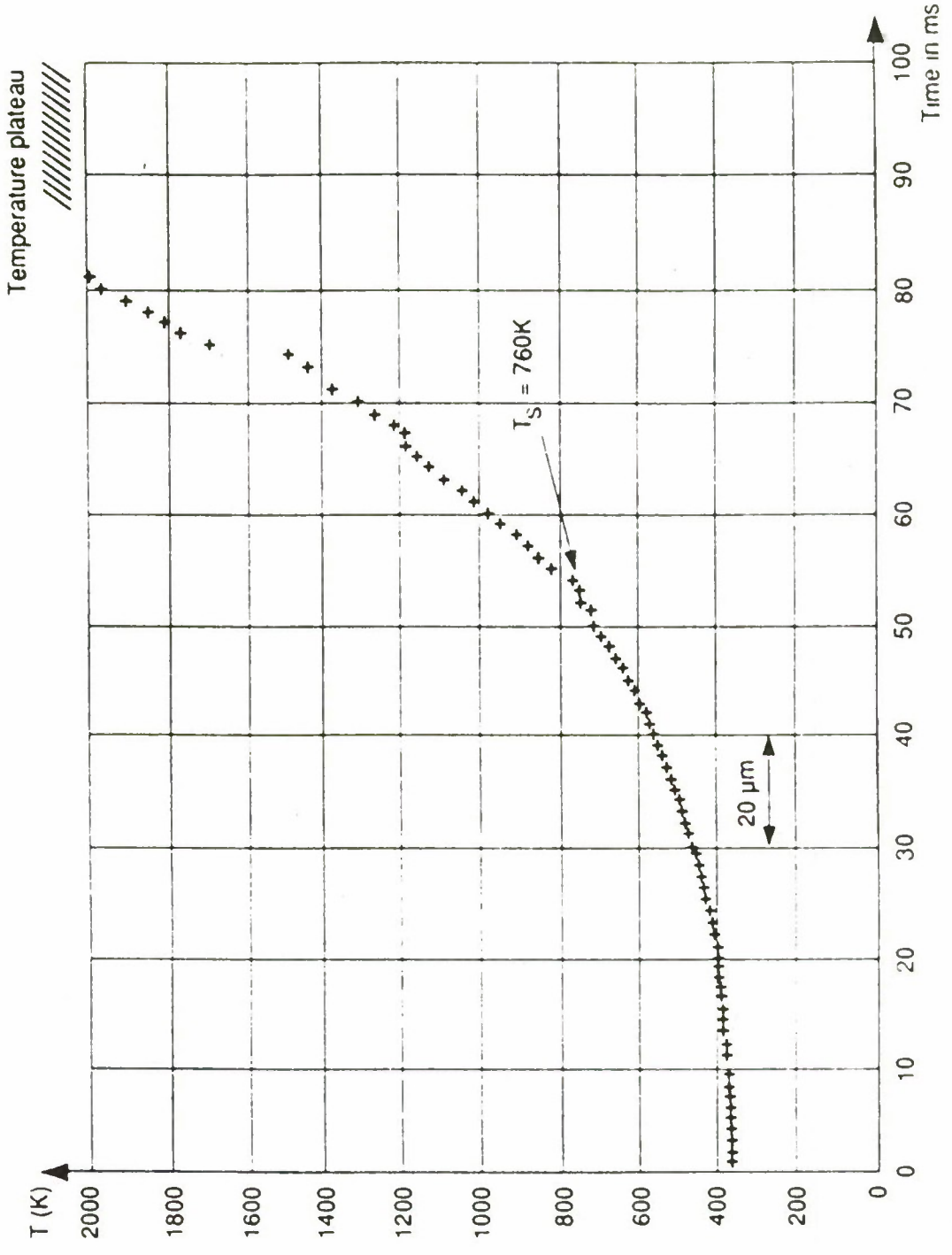

p = 11atm $V_b \simeq 2.1$ mm/s — $d_p = 1.110^{3}$ cm^2/s

HMX + wax (2%)

TEMPERATURE PROFILE, UNDER COMBUSTION, WITH MICROTHERMOCOUPLE

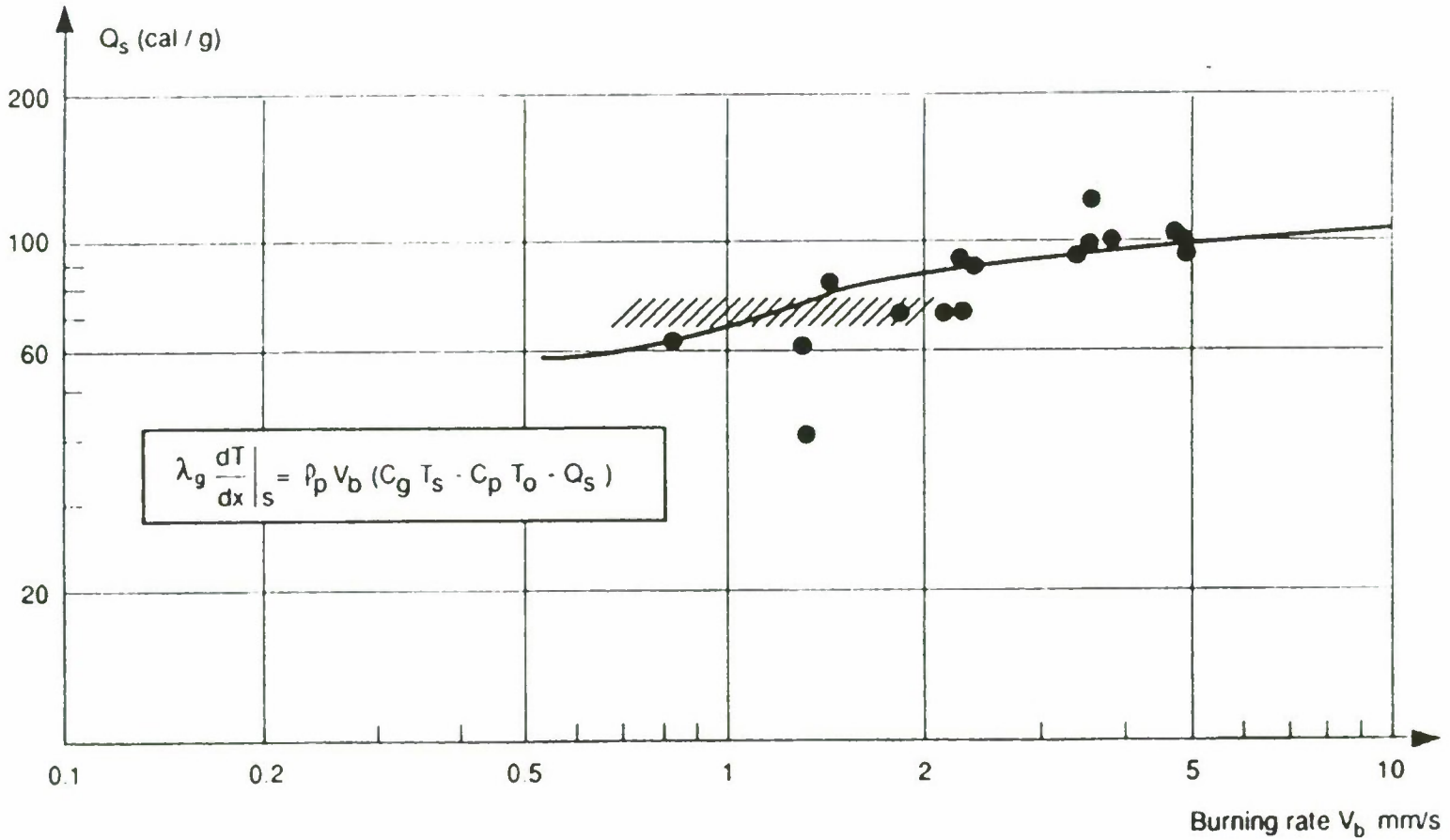

● Thermocouple measurements

//// Kubota [27]

HEAT EVOLVED IN THE CONDENSED PHASE OF HMX

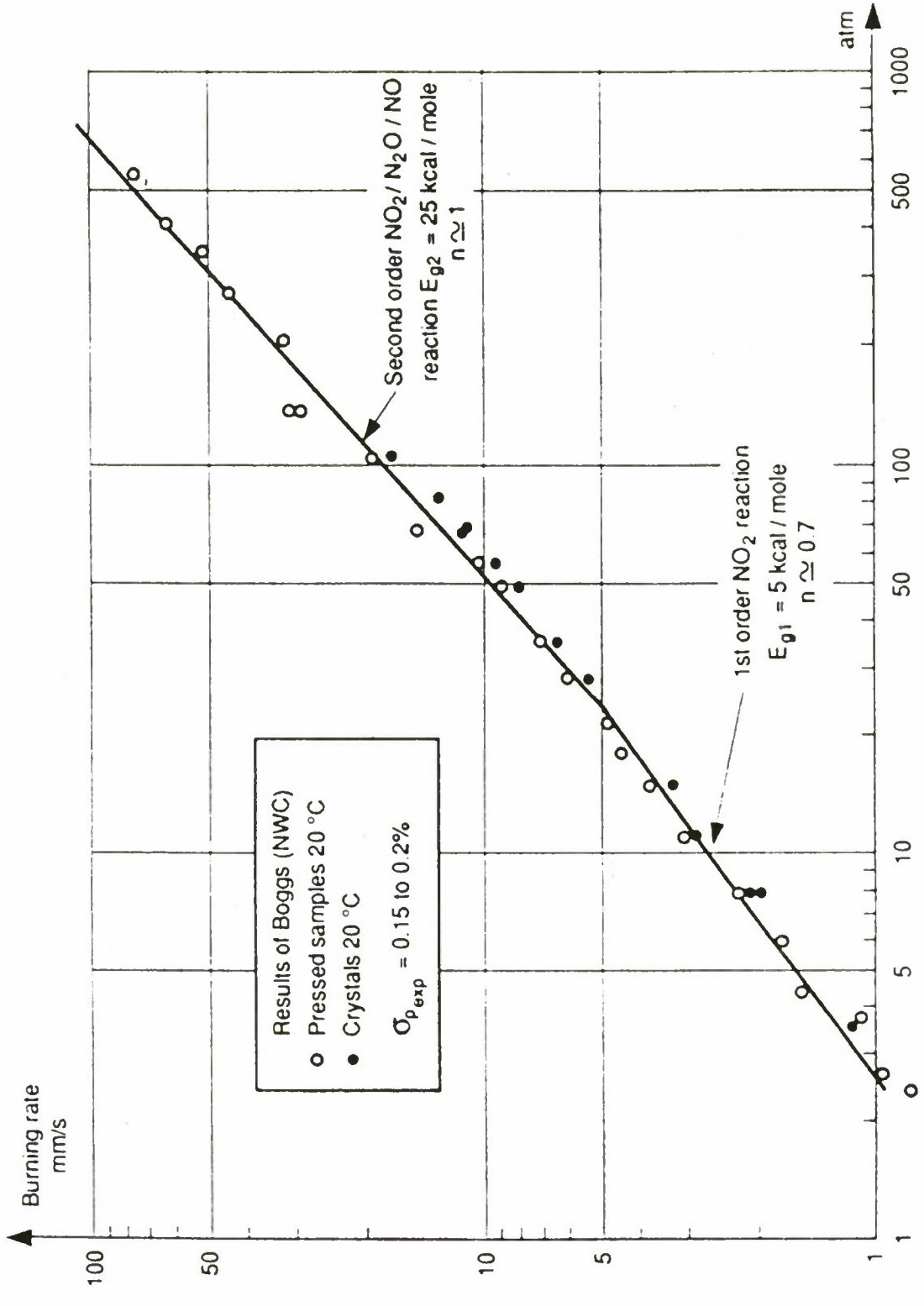

VITESSE DE COMBUSTION DE L'OCTOGENE

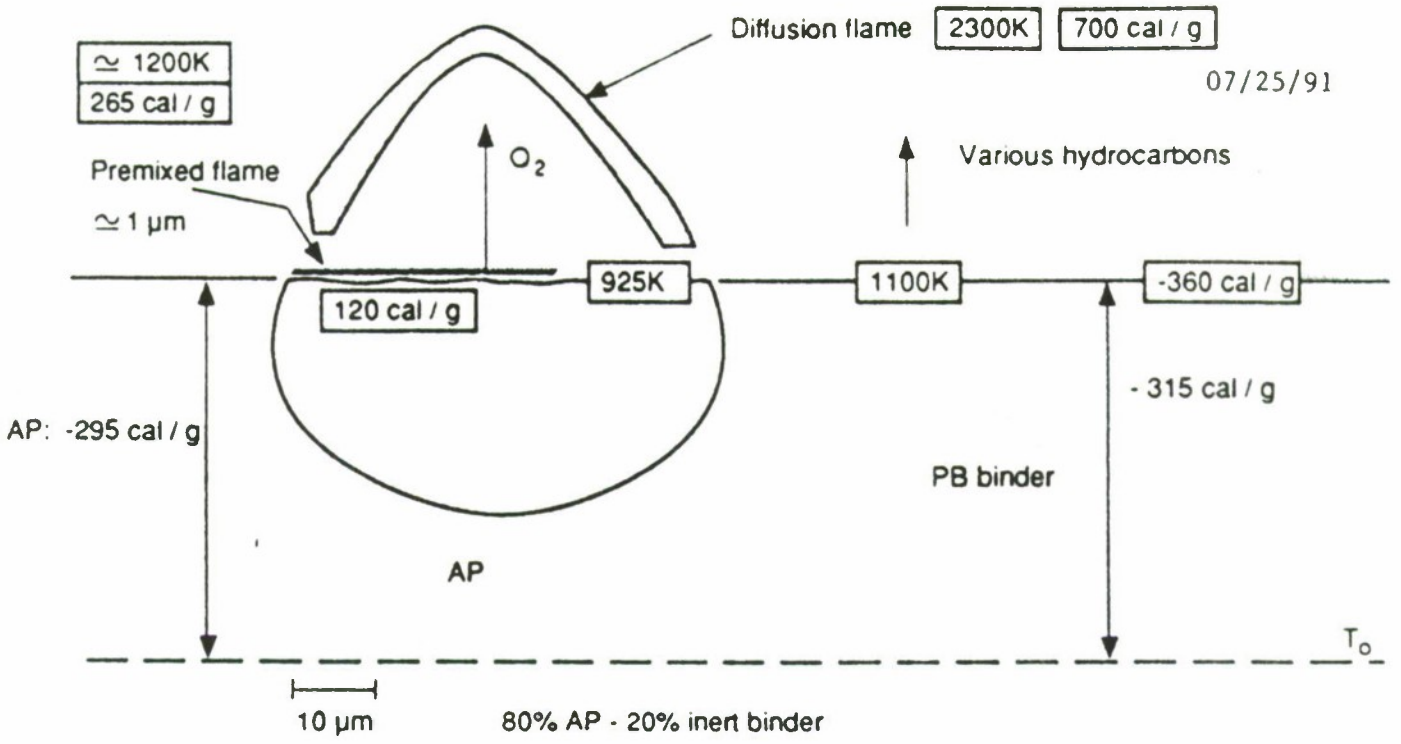

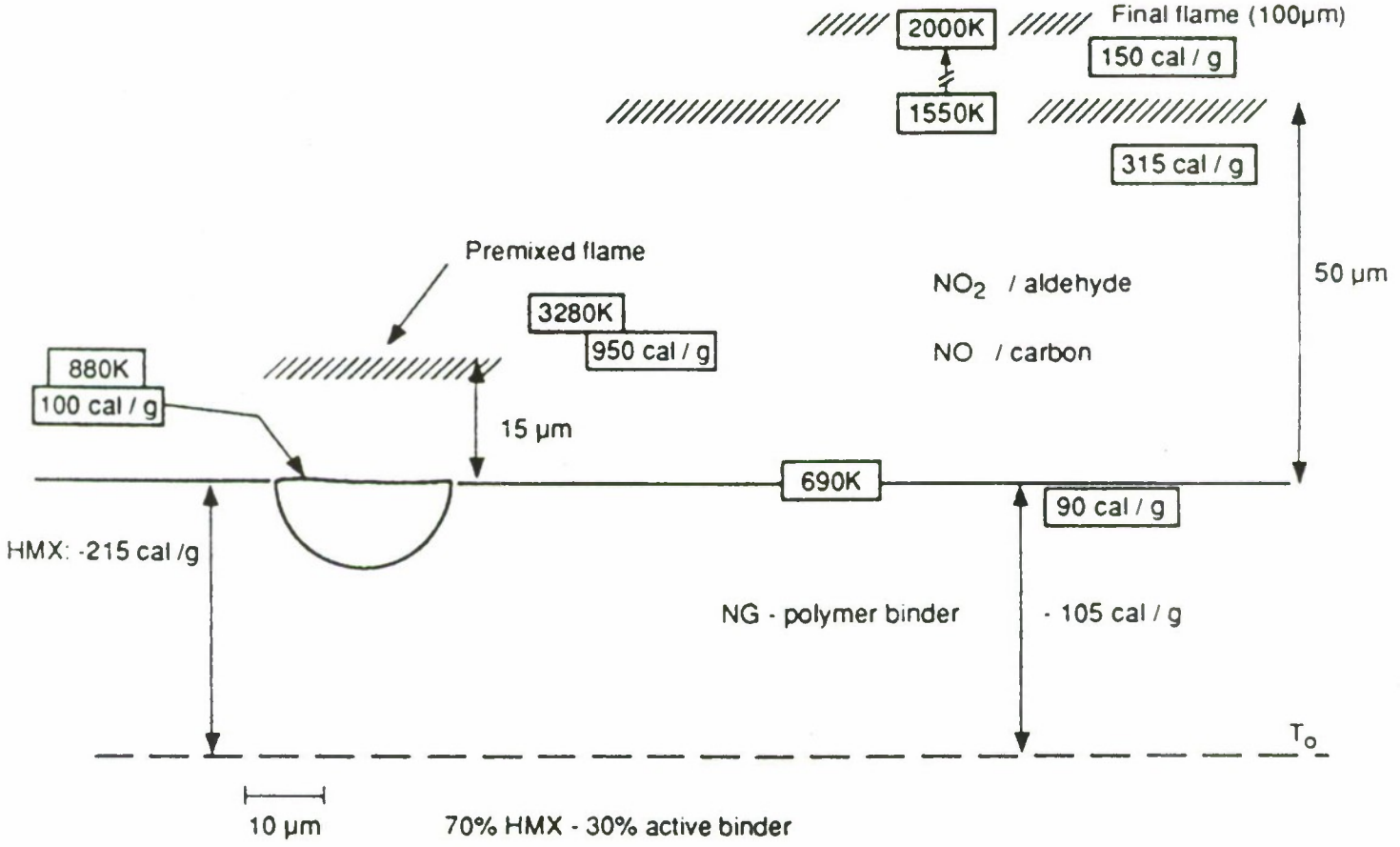

Figures for a burning rate of 10 mm / s. Positive heats are exothermic.
COMPARATIVE PICTURE OF AP-INERT BINDER AND HMX-ACTIVE BINDER COMBUSTION

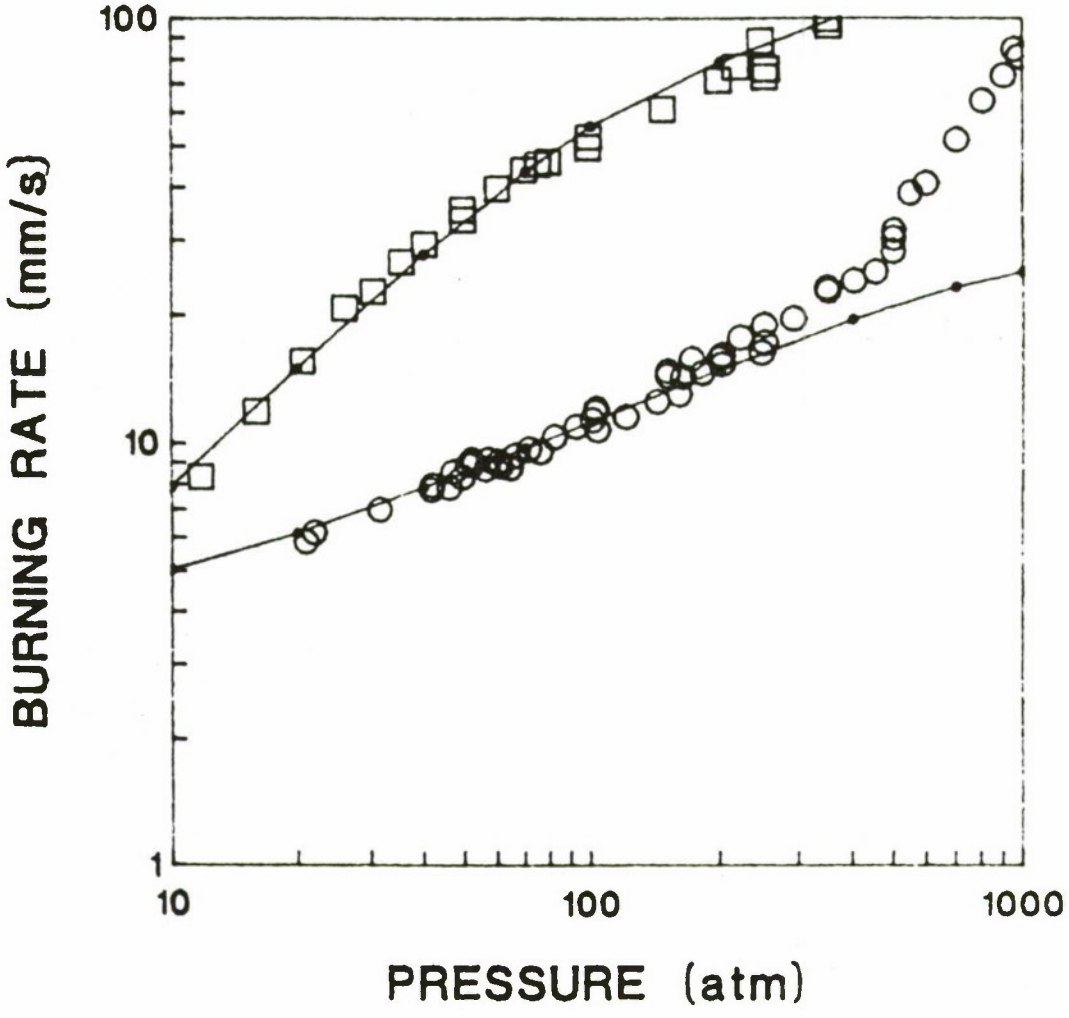

□ 80% 5μm AP-CTPB
○ 80% 90μm AP-CTPB

—•— Computed burning rate

AP-INERT BINDER PROPELLANTS.

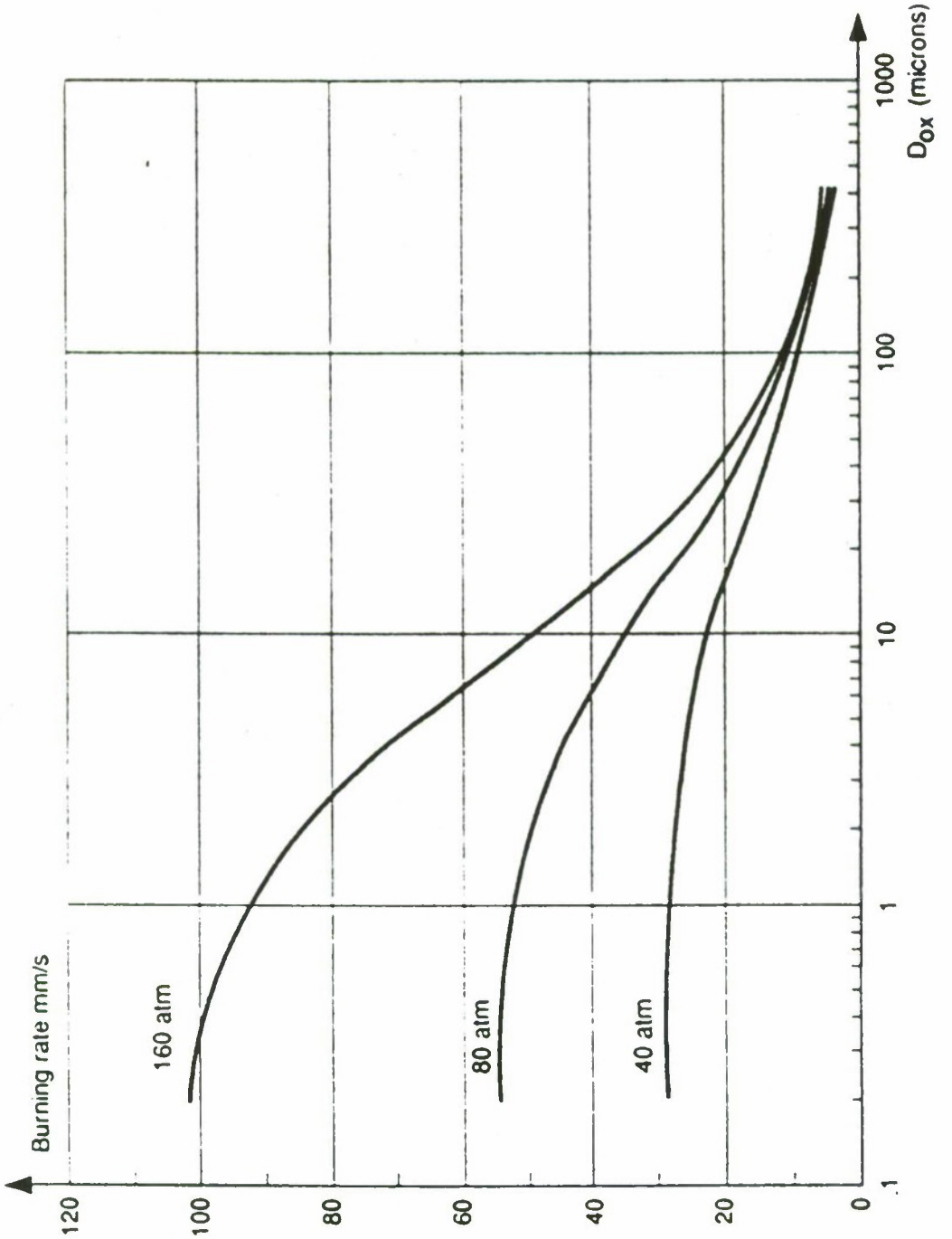

80% AP - 20% CTPB
BURNING RATE (COMPUTED RESULTS) VS AP PARTICLE SIZE

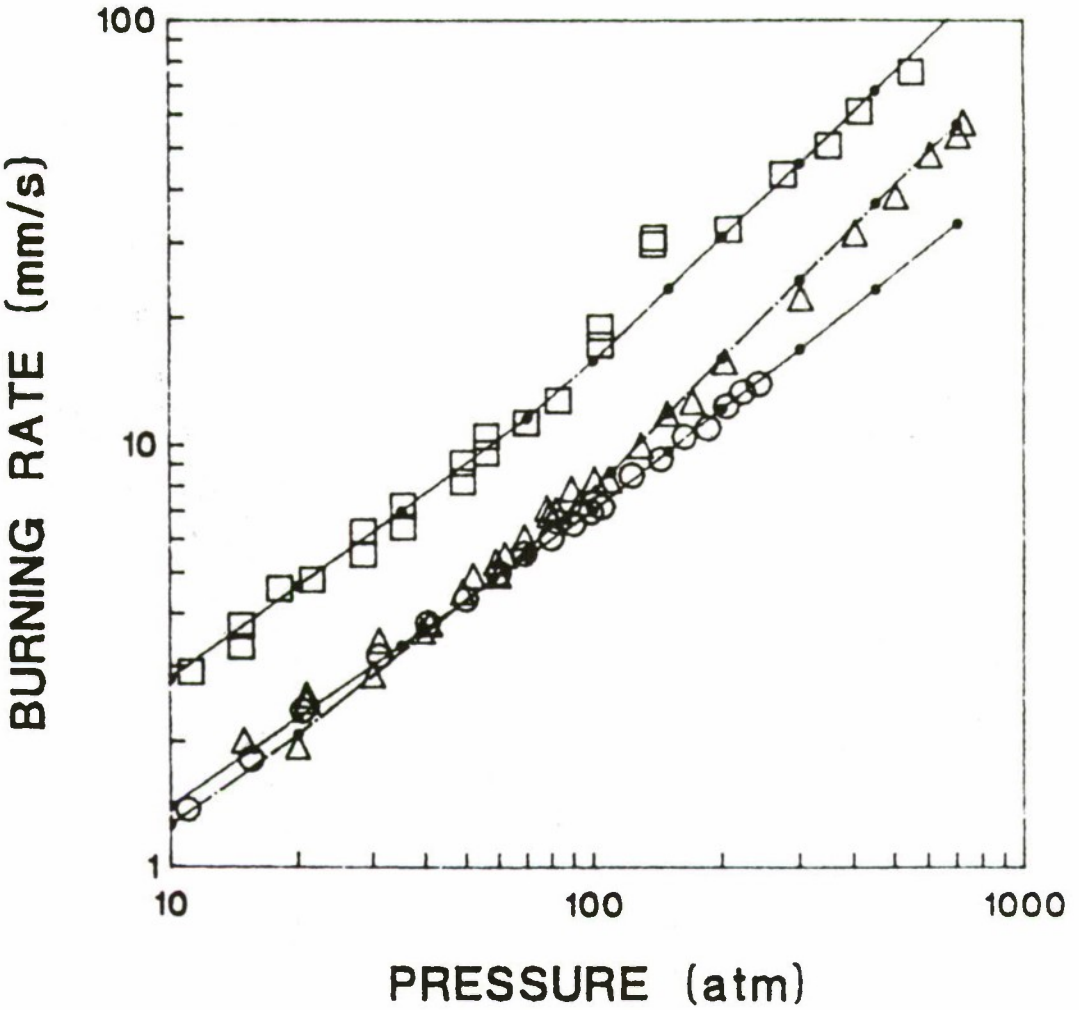

□ HMX
○ ENERGETIC BINDER (Heat of explosion=850 cal/g)
△ 70% HMX [20μm] + 30% BINDER

—•— Computed burning rate

EXPERIMENTAL AND COMPUTED BURNING RATE OF A NITRAMINE BASED PROPELLANT.

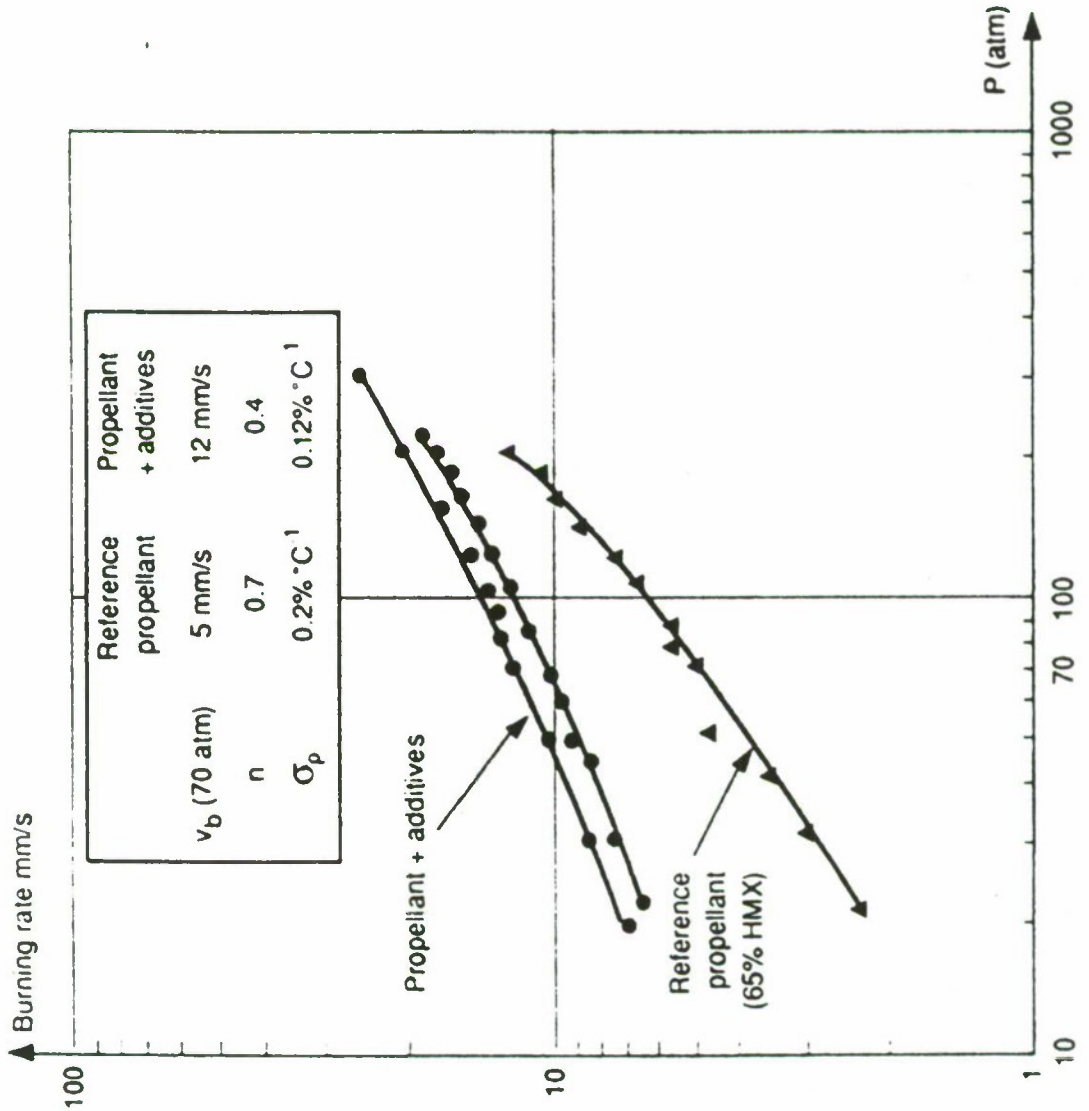

HMX - ACTIVE BINDER PROPELLANT WITH ADDITIVES

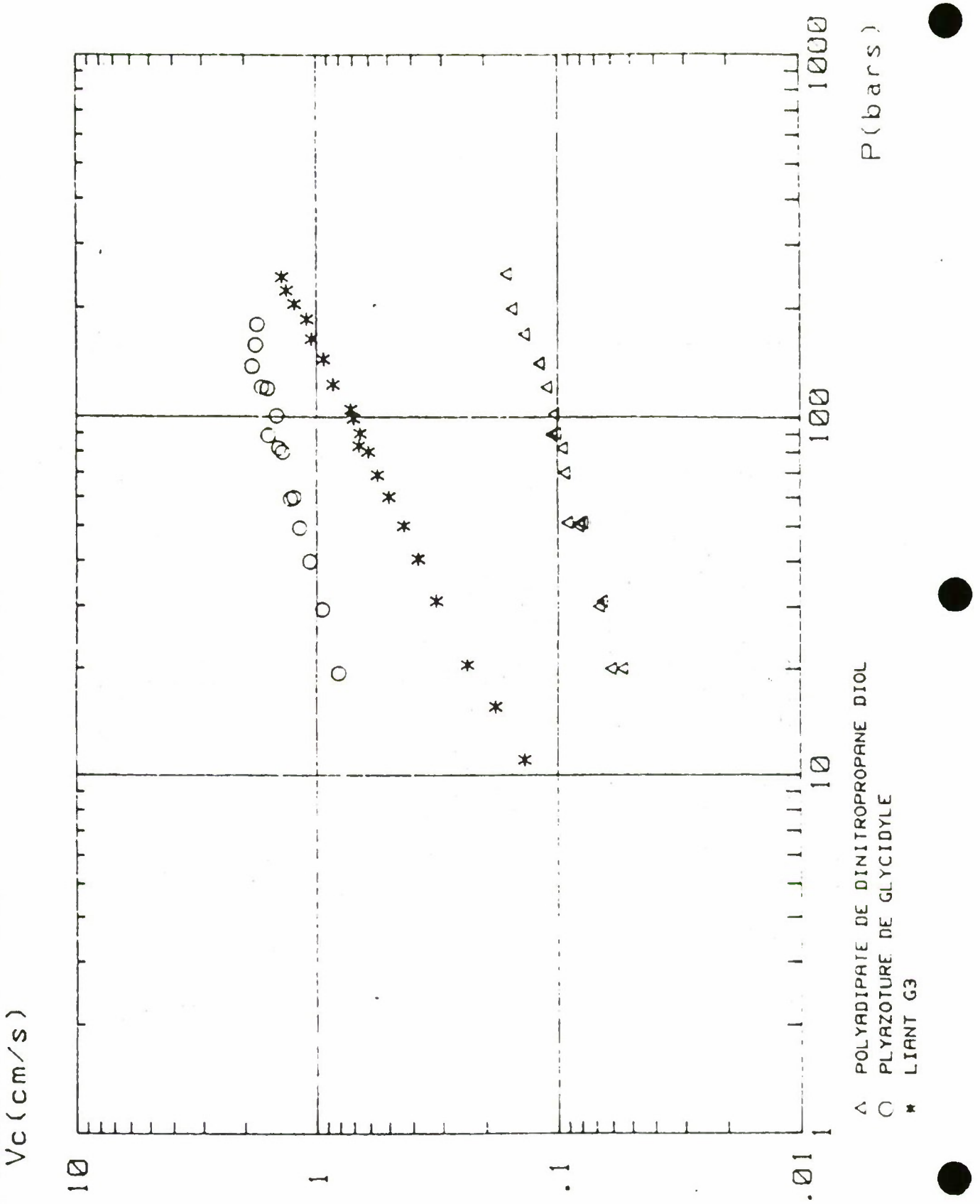

VITESSE DE COMBUSTION DES LIANTS

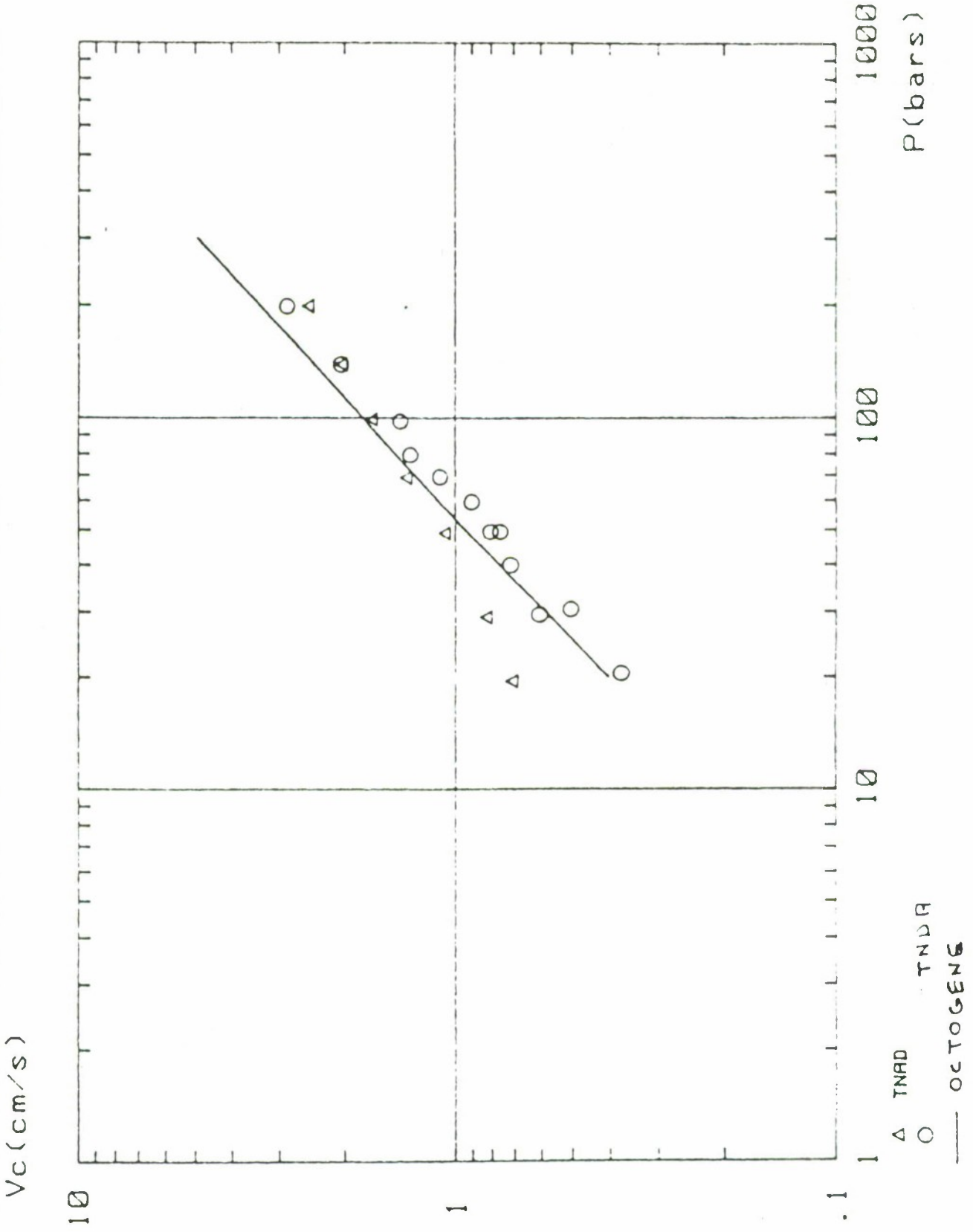

VITESSE DE COMBUSTION DES NOUVELLES CHARGES

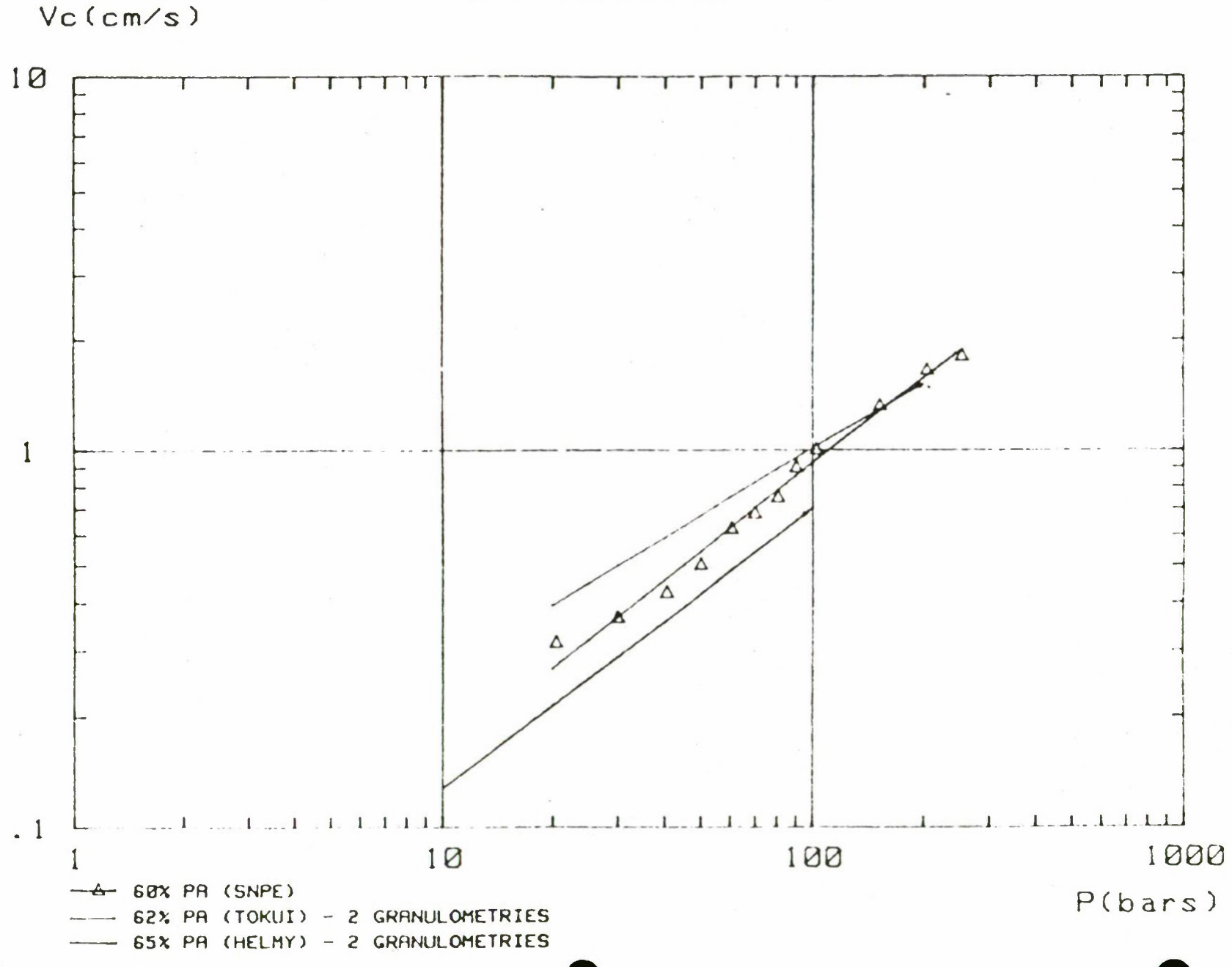

Vitesses de combustion de propergols PA6 - NBI

07/25/91

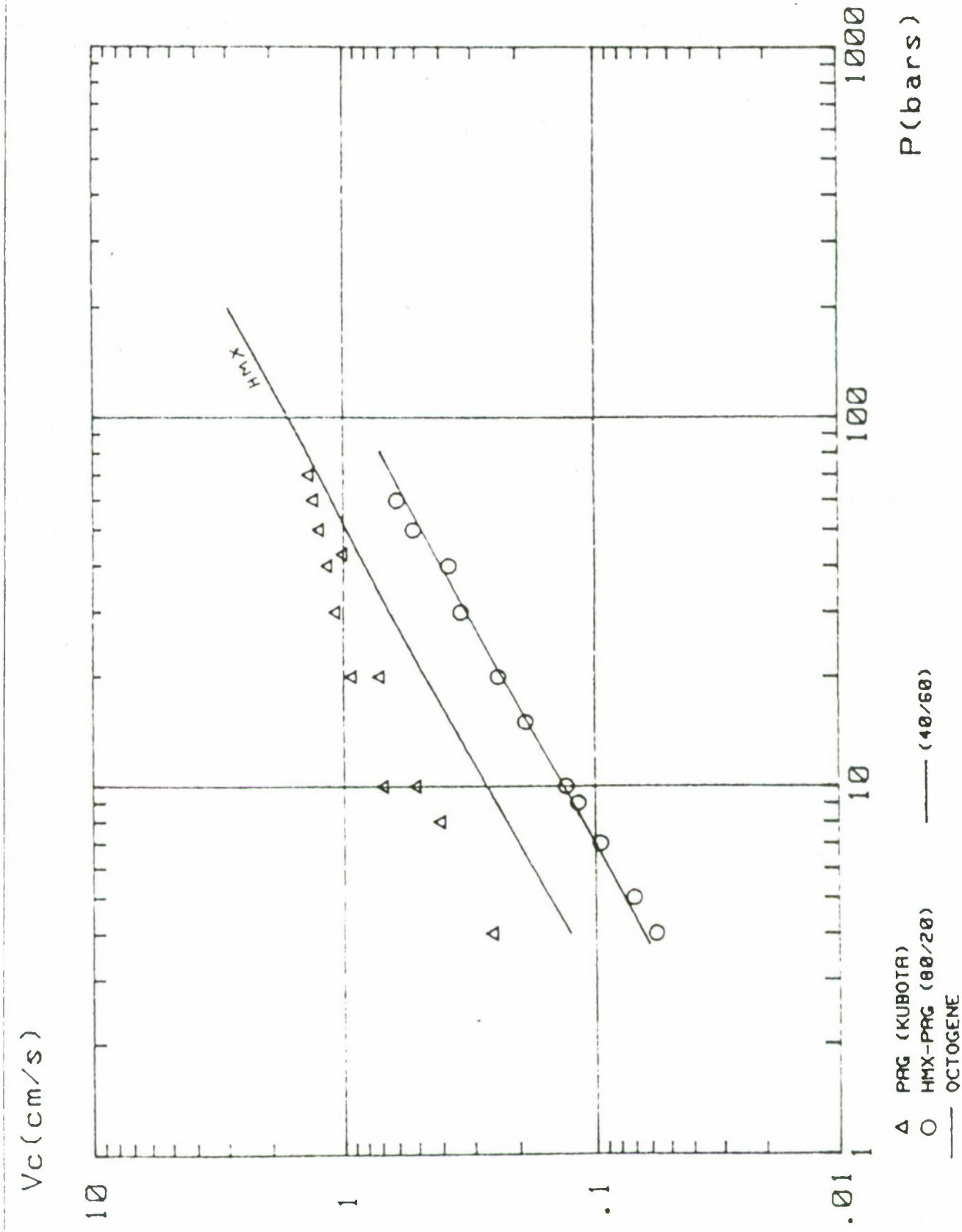

VITESSE DE COMBUSTION DES CONSTITUANTS ET DU PROPERGOL

R.S. Miller and A.W. Miziolek

High Energy Density Materials Combustion

HIGH ENERGY DENSITY MATERIALS COMBUSTION

Richard. S. Miller
Office of Naval Research
Arlington, VA 22217

Andrzej W. Miziolek
Ballistic Research Laboratory
Aberdeen Proving Ground, MD 21005

I. - Introduction:

Dramatic advances in nitramine oxidizer chemistry, energetic polymer chemistry, combustion diagnostics, computational combustion simulation, processing simulation, and detonation hazards simulation science and technology will provide the framework for major advances in the energy density and the control of energy release rates of rockets and explosives. High energy density materials makes possible the development of new generations of (a) high energy, low signature, minimum sensitivity missile propellants, with tailorable high burning rates, and (b) new generations of high energy, minimum sensitivity explosives, for both enhanced armor penetration and underwater structural damage.

The current solid rocket propulsion and armaments technology is based on materials that have been employed world-wide during most of the 20th century. Monocyclic nitramines (RDX and HMX), nitrate esters of cellulose and glycols, non-energetic crosslinkable polymers, aluminum powder, and inorganic oxidizers (e.g. ammonium perchlorate) are materials employed widely in current high performance compositions. RDX and HMX, for example, were synthesized in the time period from 1890 to 1940, and came into first military use in World War II. Nitrate esters, such as nitroglycerin and nitrocellulose, are even older materials. Limitations of RDX and HMX based propellants and explosives are densities of 1.9 gram per cubic centimeter or less, heats of formation substantially less than those of advanced nitramines, and a "burning-rate box" - a burning rate resistant to tailoring. Significant increases in energy density and in the control of the energy release rates in solid rocket propellants with reduced signatures, in explosives with high metal-accelerating detonation energy, and in underwater explosives with high shock and bubble energy, are potential consequences of ongoing major advances in nitramine oxidizer and energetic polymer chemical sciences. A specific example is a family of high energy density, low signature rocket propellants which will employ advanced nitramine oxidizers in combination with energetic poly(oxirane) and poly(oxetane) crosslinkable polymers plasticized with conventional high energy nitrate esters, or other advanced materials. The first advanced nitramine oxidizer was synthesized in February of 1987 at the Naval Weapons Center; US Air Force, Navy, and industrial energetic poly(oxirane) and poly(oxetane) polymer research and development has also been successful.

The computational combustion, processing, and hazards simulations of composites composed of advanced nitramine oxidizers and energetic polymers will reduce the cost and risk of successful US missile and gun propellant development because combustion and processing instabilities as well as detonation hazards will be predictable and hence avoided. Increases in underwater explosive performance will accrue as nitramine oxidizer science is extended to

discover crystalline oxidizers with mixed halogenated functional groups and nitramine combustion simulation capability is extended to include halogen metal/boron combustion and their corresponding high pressure kinetics and transport processes.

II. - High Energy Density Materials/Explosive Combustion Science

The goal is to establish the computational combustion science base for understanding and controlling the energy release processes at the microstructural level of high energy density non-metallized propellants and new metallized all-gas-product underwater explosive concepts.

A. - General Description of Non-Metallized Propellant Combustion Science

An understanding of the coupled condensed and gas phase chemical processes occurring during mono-propellant steady state combustion, using high energy nitramine oxidizers and energetic polymers as separate substances, will first be established. Complementary experimental quantitative methods, at low pressure, that spatially resolve gas phase species and gas and condensed phase temperature profiles will be used. Using this understanding of the mono-propellant condensed phase and gas phase combustion processes, coupled condensed phase and gas phase models, containing detailed kinetic theory transport and finite rate chemistry, will be developed. Using these developed mono-propellant combustion models, two dimensional computational combustion and transport simulations of the coupled condensed and gas phase processes during crystalline oxidizer and energetic polymer model propellant (2-D) diffusion flame combustion will be made. At low pressure, using complementary experimental techniques to those used in the monopropellant combustion investigations, a quantitative understanding of microscopic two dimensional diffusion flames at the propellant microstructural level will be established. The two dimensional simulations with coupled gas and condensed phase chemistry models will be validated using these experimental, spatially resolved investigations of gas phase species and gas and condensed phase temperature profiles of two dimensional model propellants.

This two dimensional simulation will provide the first microstructurally based solid propellant combustion modeling tool to the US solid propulsion industry. This will be a point of departure towards future three dimensional solid propellant combustion modeling requiring massively parallel computer computational capabilities, and presently conceptual, multidimensional kinetics and transport sensitivity and lumping mathematics.

A1. Gas Phase Combustion Process Measurement & Simulation

Quantitative measurement of gas phase species and temperature distributions above the deflagrating solids using complementary advanced optical spectroscopic diagnostics, mass spectrometric techniques along with temperature distributions in the condensed phase will be established. Experimental measurements of gas phase combustion processes in the immediate vicinity of the regressing propellant surface are very difficult and present a substantial challenge to the combustion diagnostics community. However, powerful techniques have been developed over the last two decades that allow for the measurement of important flame parameters such as temperature and species concentration profiles. None of these techniques, or any of the emerging new ones, have yet been brought to bear on any of the nitramine flames with the goal of thoroughly testing the existing 1-D flame models to verify their validity. Such

tests, which are typically done in hydrocarbon combustion research, require accurate temperature measurements as well as relative and absolute concentration profiles to be made for major and minor chemical species throughout the flame zone. This kind of quantitative data requires extensive careful laboratory work and frequent cross-checking between different laboratories using different techniques to measure the same flame parameter.

The techniques currently used for this type of work can be divided into two groups; spectroscopic and mass spectrometric. The spectroscopic diagnostic tools can yield either point measurements (such as laser-induced fluorescence (LIF)) or line-of-sight measurements (such as absorption). Many of the spectroscopic techniques are laser-based and are considered to be non-intrusive. Among the important ones that need to be applied to advanced nitramine oxidizer and energetic polymer flames are; (a) Coherent Anti-Stokes Raman Scattering (CARS), which is used primarily for flame temperature measurements and major species detection, (1) (b) LIF, which is used for reactive (radical) species measurements like OH, O, H, CN, NCO, etc., (2-3) and (c) Resonance Enhanced Multi-Photon Ionization (REMPI), which is used for detecting non-fluorescing species like H2CN, and methyl radicals (4-5). For a more complete summary of propellant diagnostics and modelling see reference (6,8). A new technique called Degenerate Four-Wave Mixing (DFWM) appears to hold great promise to complement LIF experiments in that it appears to work well with minor species (unlike CARS), but seems to avoid the quenching and quantification problems that accompany LIF measurements.(7) The applicability of this technique will be explored for advanced nitramine, energetic polymer and model propellant diffusion flames.

Another spectroscopic technique that needs to be applied to these flames is infrared absorption spectroscopy. Fourier Transform Infrared Spectroscopy (FTIR) has been applied very successfully to hydrocarbon flame research and appears to be very promising for nitramine flames since a number of important species like HONO, HNO, HNCO and HCNO have known infrared absorption bands. Tunable infrared lasers should also be useful due to their increased time and spatial resolution. (8)

Mass spectrometry is yet another powerful tool for chemical detection that has been applied extensively to hydrocarbon flame research but not yet applied to nitramine flames. Although probing of a sample volume of the flame zone is not strictly non-intrusive, in many cases the nature of the intrusion (flow field and thermal perturbation) can be minimized as well as accounted for in the data analysis. There are primarily two types of mass spectrometric sampling: molecular beam as well as quartz microprobe. The molecular beam technique allows for the detection of reactive species which are "frozen out" in the beam formation/expansion process, but due to the size and shape of the sampling cone, is more susceptible to perturbing the flame. (9) The quartz microprobe sampler, on the other hand, minimizes the flame perturbation, but is not sensitive to highly reactive, minor species. An appropriate model validation program will require a comprehensive experimental approach utilizing all of the above techniques, and by the nature of the requirement, will require a very high degree of coordination between the laboratories engaged in this research.

These species and temperature profiles will test and establish the validity of gas phase nitrogen combustion chemistry and transport networks simulations based on elementary reaction kinetics being established under coordinated DoD and DoE Sandia Combustion Research

Facility Laboratory programs. The Sandia Combustion Research Facility combustion simulation is presently capable of handling 1-dimensional mono-cyclic nitramine gas phase flame chemistry and transport on a detailed chemical level using the CHEMKIN nitrogen, carbon, hydrogen, oxygen chemical kinetics package. (10)

The Sandia combustion simulation has predicted these profiles as well as the pressure and temperature dependencies of RDX combustion. RDX flames are presumably simulated in this analysis because RDX reaction chemistry is largely initiated in the gas phase for which the 1-D premixed flame code is most applicable. The gas phase 1-D flame simulation does not include the currently unknown physics and chemistry of condensed phase energy release processes which are now known to be dominant in advanced nitramine combustion. However, before these models can undergo further development, they have to be verified experimentally to establish their accuracy. Currently, even the verification of the existing RDX flame model has been inadequate with the only experimental data available for comparison coming from limited Russian literature.

In addition, the heterogeneous nature of the solid/gas interface has been ignored in all of the propellant combustion models that have been developed to date. (11) The challenge, therefore, is not only to study this interfacial region experimentally and to develop appropriate models for it, but also to determine the importance of heterogeneous processes in the overall combustion of nitramine oxidizers, some of which are already known to undergo substantial condensed phase chemistry. Oxidizers with substantial condensed phase energy release have never before been known. The coupling of combined condensed phase and gas phase energy release processes in a nitrogen based oxidizer is heretofore an unknown phenomena. The heterogeneous chemistry portion of this program represents a pioneering effort. It will require the development of better diagnostic tools that can probe the gas composition and the temperature gradient in the immediate vicinity of the surface. Also, appropriate interface computational models will need to be developed to simulate this process accurately. Work that has been initiated in coal combustion, in which heterogeneous processes are very important, will be extended to include condensed phase energy release and nitrogen chemistry networks.

A2 - Condensed Phase Chemical Processes

Experimental investigation of micron thick nitramine oxidizer and polymer films heated by fast microsecond laser substrate heating coupled with: (a) time of flight mass spectrometry, for identifying gas phase species, (b) transient time resolved infrared spectroscopy, for condensed phase species identification, (c) time resolved ellipsometry, for film thickness observations, and (d) time resolved infrared thermometry, for substrate temperature measurement, will permit the condensed phase chemical processes to be investigated and understood.(12) These coupled experimental measurements, made at heating rates from 100,000 to 1,000,000 degrees per second and at attained temperatures that are reflective of solid propellant combustion conditions, will provide the first observations of subsurface condensed and gas phase chemical processes. The interpretation of these observations when coupled with the results of molecular level behavior research that includes: (a) high temperature solution decomposition study results, (b) very low pressure pyrolysis results, (c) detailed subsurface product combustion studies, (d) low temperature reactive defect formation studies, and (e) unimolecular molecular beam decomposition results, will establish

the condensed phase combustion chemistry model.

B. Advanced Underwater Explosive All-Gas-Product Concepts Combustion Modeling

Advanced underwater explosive all-gas-product concepts, which may employ mixed nitramine difluoroamino explosives, dinitramino salts, novel plasticizers, energetic polymers and aluminum or boron particles, have evolved that will maximize both shock and bubble underwater structural damage. The control of the post-detonation bubble energy release rates of these new underwater explosive concepts, to maximize bubble structural damage effectiveness, will require an understanding and the ability to control metal, aluminum and boron combustion. The ability to understand and control distributed boron or aluminum particle combustion in high pressure fluorine and chlorine rich detonation product gases will require validated simulations. As the very first step in establishing this multi-dimensional boron/aluminum combustion simulation, a kinetic model for the boron and aluminum in combination with carbon, hydrogen, fluorine, chlorine, and oxygen species must be established. The future development of a kinetic model of homogeneous combustion of boron and aluminum combustion in halogen F or Cl containing O/H/C detonation product gases will establish a point of departure for the simulation of the heterogeneous combustion of boron and aluminum in underwater detonation product gases.

III. CONCLUSIONS

A. Impact on Future Weapons Systems

High energy density materials coupled with combustion, processing and detonation hazards simulation science and technology will enable the US to utilize non-metalized, low observable, high performance missile propellants with tailorable burning rates, high performance shaped charges for armor penetration, advanced low vulnerability gun propellants, and new generations of underwater explosives to maximize underwater structural damage. Additional advantages of the advanced propellant and explosive technology include: (a) improved mechanical properties and reduced vulnerability because of improved polymers and higher polymer content, (b) improved processability because of lower solids loading, (c) possible elimination of plasticizer migration because plasticization may not be necessary, (d) higher thermal stability and lower vulnerability, (e) higher combustion efficiency and no two-phase flow losses with the use of advanced nitramine oxidizers and energetic binders in non-metallized propellant formulations, (f) less impact on the environment with no or less hydrogen chloride production because of elimination or decreased use of ammonium perchlorate, and (g) minimum waste disposal with thermoplastic elastomer based propellant reprocessing.

B. Impact on the Industrial Base:

The major impact on the US industrial base will be to produce propellants that simultaneously satisfy the requirements for reduced infrared signatures, controlled detonation hazards and tailorable, stable, controllable burning rates for tactical as well as for potential new generations of strategic missile propulsion systems. A predictive propellant and explosive simulation capability for ballistics, processing and hazards design will be utilized as it is developed. Current empirical design techniques based on decades of propellant development

using conventional ingredients (RDX, HMX, non energetic polymers, aluminum powder and ammonium perchlorate) in batch processing equipment will be used initially but with little hope of direct applicability due to very different combustion behavior of the high energy density materials.

ACKNOWLEDGEMENTS: The authors acknowledge the contributions of the many scientists and engineers who participated in a series of workshops that established the structure of the nonmetallized combustion simulation science hierarchy described in this paper. RSM would like to thank Andrzej Miziolek for the many months he spent working on this endeavor as a Scientific Advisor to the Mechanics Division of the Office of Naval Research.

REFERENCES:

1. J. H. Stufflebeam and A. C Eckbreth, "CARS Diagnostics of Solid Propellant Combustion at Elevated Pressure", Combustion Science and Technology, Vol. 66, p. 163, 1989; also "Multiple Species CARS Measurements of High Pressure Solid Propellant Combustion", AIAA Aerospace Sciences Meeting, Paper Number ATAA-89-0060, 1989; J. H. Stufflebeam, "Temperature and Multiple Species CARS Measurements of Solid Propellant Flames", 26th JANNAF Combustion Meeting, CPIA Publication 529, vol. II, p. 107, Oct 1989.

2. D. R. Crosley, ed., "Laser Probes for Combustion Chemistry", ACS Sym. Series 134, 1980.

3. B. E. Forch, J. B. Morris, and A. W. Miziolek, "Laser Induced Fluorescence and Ionization Techniques for Combustion Diagnostics", Laser-Based Approaches in Luminescence Spectroscopy", T. Vo-Dinh and D. Eastwood, eds., ASTM STP 1066, p. 50, 1990.

4. M. C. Lin, and W. A. Sanders,"Detection and Spectroscopy of Methyl and Substituted Methyl Radicals by Resonance Enhanced Multiphoton Ionization", Adv. Multiphoton Processes and Spectroscopy, S. H. Lin ed., World Scientific Pub., p 333, 1986; also T. G. DiGiuseppe, J. W. Hudgens, and M. C. Lin, "Detection of Gas Phase Methyl Radicals using Multiphoton Ionization"; Chem. Phys. Lett., 82, p. 267, 1981; "Multiphoton Ionization of CH3 in the Gas Phase J. Phys. Chem., 86, p. 780, 1982; "New Electronic States in CH3 Observed Using Multiphoton Ionizations", J. Chem. Phys., 76, p. 3338, 1982; and J. W. Hudgens, T. G. DiGiuseppe, and M. C. Lin, "Two-Photon Resonance Enhanced Multiphoton Ionization Spectroscopy and State Assignments of the Methyl Radical", J. Chem. Phys., 79, 571, 1983.

5. T. A. Cool, J. S. Bernstein, X-M. Song, and P. M. Goodwin, "Profiles of HCO and CH3 in CH4/O2 and C2H4/O2 Flames By Resonance Ionization", 22nd Symposium (International) on Combustion, p. 142, 1988.

6. A. W. Miziolek, ed., "Kinetic and Related Aspects of Propellant Combustion Chemistry", CPIA Publication 503, May 1988.

7. D.J. Rakestraw, L. R. Thorne, and T. Dreier, "Detection of NH Radicals in Flames Using Degenerate Four Wave Mixing", 23rd Symposium (International) on Combustion, 1990 (in press).

8. M. H. Alexander, P. J. Dagdigian, M. E. Jacox, C. D. Kolb, C. F. Melius, H. Rabitz, M. D. Smooke, and W. Tsang, "Nitramine Propellant Ignition and Combustion Research: New Tools and New Directions, "U.S. Army Research Office Technical Report, February 1989.

9. N. E. Ermolin, O. P. Korobelnichev, L. V. Kulbida, and V. M. Fomin, Fiz. Goreniya i Vzryva, 22, No. 5, p. 54 (1986). Orlginal data is O. P. Korobeinichev et. al. in Mass-Spectrom. Khim. Kinet., 1985, p. 73. (Mass Spectrometry and Chemical Kinetics, Moscow (1985)). Article was translated for Dr. Carl Melius at Sandia Combustion Research Facility.

10. C. F. Melius and J. S. Binkley, "Reactions of NH and NH2 with O and O2: Theoretical Studies", American Chemical Society Symposium Series, No. 249, Chemistry of Combustion Processes, ed. T. M. Sloane (Am. Chem. Soc., Washington, DC, 1984), pp. 103-115; also C. F. Melius and J. S. Binkley, "Energetics of the Reaction Pathways for NH2 + NO- > Products, Twentieth Symposium (International) on Combustion, (The Combustion Institute, Pittsburgh, PA, 1985), p. 575; C. F. Mellus and J. S. Binkley, "Thermochemistry of the Decomposition of Nitramines in the Gas Phase, Twenty-First Symposium (International) on Combustion, (The Combustion Institute, Pittsburgh, PA, 1986) p. 1953; C. F. Melius and J. S. Binkley, "Quantum Chemical Calculations of the Decomposition of Nitramines": Thermochemistry and Reaction Pathways, Proceedings of Twenty-Third JANNAF Combustion Meeting, Vol. I, p. 241, October 1986; C. F. Mellus, "Molecular Decomposition Mechanisms of Energetic Materials, J. de Physique 48, C4-341 (1987); A. W. Mlziolek, C. F. Melius, L. R. Thorne, P. J. Dagdigian, and M. H. Alexander, "Gas Phase Combustion Chemistry of Nitramine Propellants," BRL-TR-2906 (1988); C. F. Mellus, "The Gas-Phase Chemistry of Nitramine Combustion, Twenty-Fifth JANNAF Combustion Meeting, Vol. II, p. 155, October, 1988; L. R. Thorne and C. F. Melius: "The Structure of Hydrogen Cyanide - Nitrogen Dioxide Premixed Flames; 26th JANNAF Combustion Meeting, CPIA Publication 529, vol. I, p. 63, Oct. 1989; L. R. Thorne and C. F. Melius, "The Structure of Hydrogen Cyanide - Nitrogen Dioxide Premixed Flames, The Combustion Institute, Pittsburgh, PA, 1990) In press; C. F Melius; "Thermochemical Modeling: I. Application to Decomposition of Energetic Materials"; in Chemistry and Physics of Energetic Materials; NATO ASI 309, p. 21, S. Bulusu, ed., 1990; C. F. Melius; "Thermochemical Modeling: II. Application to Ignition and Combustion of Energetic Materials"; Chemistry and Physics of Energetic Materials; NATO ASI 309, p. 51, S. Bulusu, ed., 1990; C. Y. Lin, H. T. Wang, M. C. Lin, and C. F. Mellus, "A Shock Tube Study of the CH2O + NO2 Reaction at High Temperatures," Int'l. J. Chem. Kinetics, 22, p. 455, 1990.

11. R. C. Brown, C. E. Kolb, H. Rabitz, S. Y. Cho, R.A. Yetter, F. L. Dryer, "A Model for B2O3 Gasification in Hydrocarbon Combustion Environments: Heterogeneous Surface Reaction Mechanisms", Combustion and Flame, to be submitted. and S. Y. Cho, R.A. Yetter, F. L. Dryer, "Computer Model for Chemically Reactive Flow with Complex Chemistry/Multi-component Molecular Diffusion/Heterogeneous Processes", J. of Compuational Physics, in press.

12. K. L. Erickson, R. D. Skocypec, W. M. Trott, and A. M. Renlund, "Development of Thin-Film Samples for Examining Condensed-Phase Chemical Mechanisms Affecting Combustion of Energetic Materials," Proc.15th International Pyrotechnics Seminar (IIT Research Institute, Chicago, IL) 239-260 (1990); R. D. Skocypec and K. L. Erickson, "Time-Resolved Mass Spectrometry Technique for Studying Fast Transient CHNO Explosive Decomposition Kinetics," Proc. 9th Symposium (International on Detonation (1989); R. D. Skocypec, K. L. Erickson, A. M. Renlund and W. M. Trott, "Fast Transient Gas- and Condensed-Phase Chemistry of Energetic Materials," 26th JANNAF Combustion Meeting, CPIA Pub. 529, v. II, p. 117, Oct (1989).

MICRO-STRUCTURALLY BASED HIGH ENERGY DENSITY MATERIAL SCIENCE

UNDERSTAND, CONTROL AND PREDICT ENERGY RELEASE RATES AT MICROSTRUCTURAL LEVEL

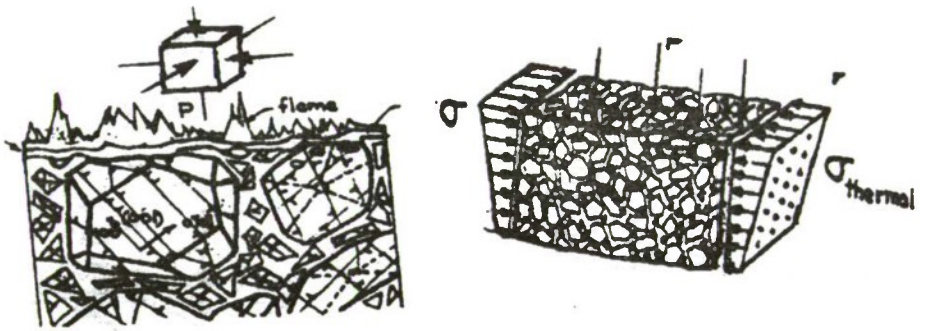

PROCESSING SCIENCE

HAZARDS SCIENCE

COMBUSTION & DETONATION SCIENCE

MICRO-STRUCTURALLY BASED HIERARCHICAL COMBUSTION & DETONATION SIMULATION SCIENCE

GOAL: LINK ATOMIC & MOLECULAR DECOMPOSITION PROCESSES OF ENERGETIC OXIDIZER CRYSTALS & POLYMERS TO MICRO-STRUCTURALLY BASED ENGINEERING PREDICTIONS OF ENERGY RELEASE MECHANISMS & RATES

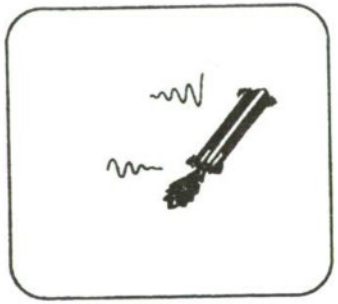

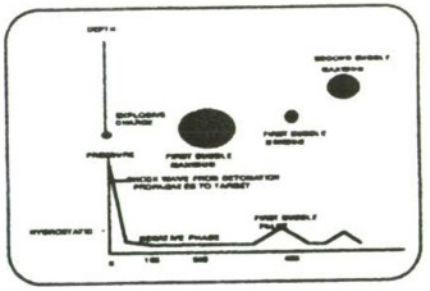

ENGINEERING PREDICTIONS

PROPELLANT COMBUSTION

DETONATIONS & (EXPLOSIONS)

MOLECULAR LEVEL BEHAVIOR

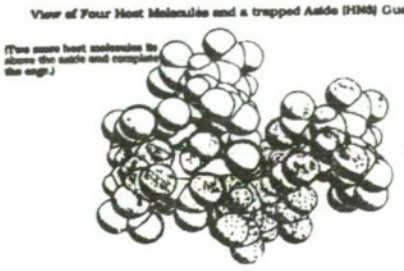

SYNTHESIS

PHYSICAL

SYNTHETIC

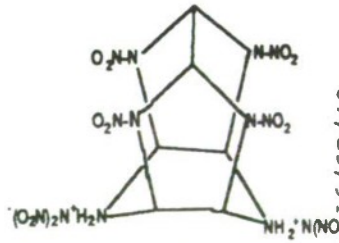

$NH_4^+ N(NO_2)_2^-$

07/25/91

IONIC DINITRAMIDES: DISCOVERY, PROCESS IMPROVEMENTS & ELECTRONIC & CRYSTAL STRUCTURES

NH4+ AMMONIUM CATION

N,N-DINITRAMIDE- ANION

AMMONIUM DINITRAMIDE

OBJECTIVES:

- *O UNDERSTAND THE CHEMISTRY OF THE DINITRAMINE FUNCTIONAL GROUP*
- *O DETERMINE STRUCTURES OF IONIC DINITRAMIDES*
- *O DETERMINE ELECTRONIC STRUCTURE AND PROPERTIES OF N(NO2)2-; ESTIMATE RELATIVE ACIDITY OF HN(NO2)2*

ACCOMPLISHMENTS:

- *O DINITRAMIDE SALTS SYNTHESIS MADE PRACTICAL*
- *O X-RAY AND CALCULATED STRUCTURES OF THE DINITRAMIDE ANION AGREE*
- *O CONJUGATION OF NO2 GROUPS WITH NITROGEN LONE PAIRS EXPLAINS TWISTED N(NO2)- CONFORMATION*
- *O ELECTROSTATIC POTENTIAL OF N(NO2)2- SURFACE GOVERNS INTERACTIONS WITH CHARGED SPECIES*

APPROACH:

- *O SYNTHESIZE COVALENT DINITRAMINES TO DETERMINE REACTION PATHWAYS AND RELATIVE STABILITIES*
- *O X-RAY CRYSTALLOGRAPHY*
- *O QUANTUM MECHANICS*

DR. ROBERT SCHMITT & JEFFREY BOTTARO @ SRI INTERNATIONAL
PROF. PETER POLITZER @ UNIV. OF NEW ORLEANS
DR. RICHARD GILARDI @ /NRL

COVALENT CUBYL DINITRAMINE CHEMISTRY

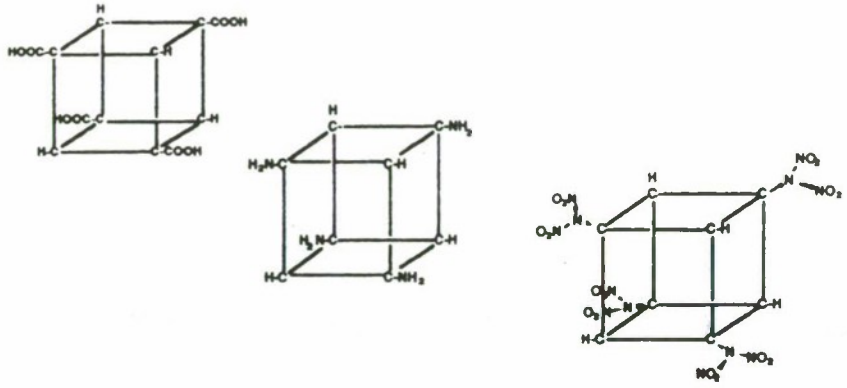

OBJECTIVES:

O INTRODUCE AND STABILIZE COVALENT DINITRAMINE CHEMICAL BONDS ON THE CUBANE MOLECULAR FRAMEWORK

ACCOMPLISHMENTS:

O ESTABLISHED METHODS TO SYNTHESIZE 1,3,5,7 CUBANE TETRA ACID

O DISCOVERED THAT ELECTRON WITHDRAWING GROUPS STABILIZE THE COVALENT CUBYL DINITRAMINE BONDS

O DISCOVERED NEW METHODS TO INTRODUCE COVALENT DINITRAMINO GROUPS

APPROACH:

O UNDERSTAND THE FUNCTIONALIZATION CHEMISTRY OF CUBANE

O ESTABLISH NEW METHODS TO SYNTHESIZE COVALENT DINITRAMINO BONDS

O INTRODUCE AND STABILIZE COVALENT CARBON -DINITRAMINE GROUPS ON THE CUBANE MOLECULAR FRAMEWORK

PROFS. EATON & OLAH , DRS. WILLER & SCHMITT
@ UNIV. OF CHICAGO, USC, THIOKOL ELKTON, & SRI

07/25/91

7/1/91

MIXED DIFLUOROAMINO-NITRAMINO CRYSTALLINE OXIDIZERS SYNTHESIS & CRYSTAL STRUCTURE

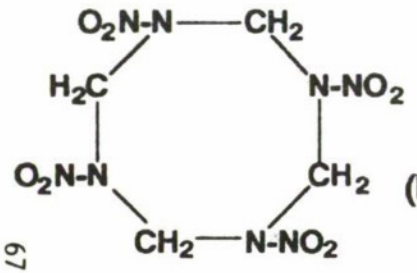

HMX -1920

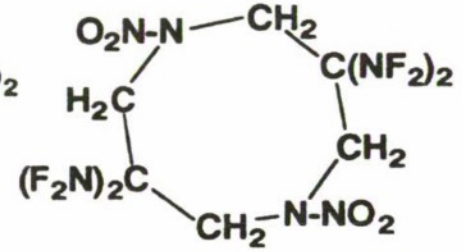

DFADA - 1990

67

OBJECTIVES:

- O DEVELOP CHEMICAL METHODS TO SYNTHESIZE MONOCYLIC OXIDIZERS WITH MIXED NITRAMINO AND DIFLUOROAMINON FUNCTIONALITY
- O ESTABLISH DENSITY PREDICTION METHODS FOR DIFLUOROAMINE AND NITRAMINE OXIDIZERS
- O ESTABLISH NEW METHODS OF DIFLUOROAMINATION

ACCOMPLISHMENTS:

- O FIRST MONOCYCLIC MIXED DIFLUOROAMINO NITRAMINE OXIDIZER SYNTHESIZED
- O NEW STORABLE SALT OF DIFLUOROAMINIC ACID SYNTHESIZED
- O DENSITY PREDICTION METHOD ESTABLISHED FOR MIXED NITRAMINE - DIFLUOROAMINE OXIDIZERS
- O SECOND NITRAMINE -DIFLUOROAMINE UNDERWAY

APPROACH:

- O DEVELOP CHEMICAL METHODS TO SYNTHESIZE MONOCYLIC SUBSTRATES AMENABLE TO NITRAMINE & DIFLUOROAMINE FUNCTIONALIZATION
- O INTRODUCE NITRAMINE & DIFLUOROAMINE FUNCTIONALITY IN THE SE SUBSTRATES

DR. KURT BAUM @ FLUOROCHEM
PROF. HERMAN AMMON/ @ UNIV. OF MARYLAND
DR. RICHARD GILARDI @ NRL

07/25/91

7/1/91

POLYMORPHIC PHASE SPACE OF HNIW

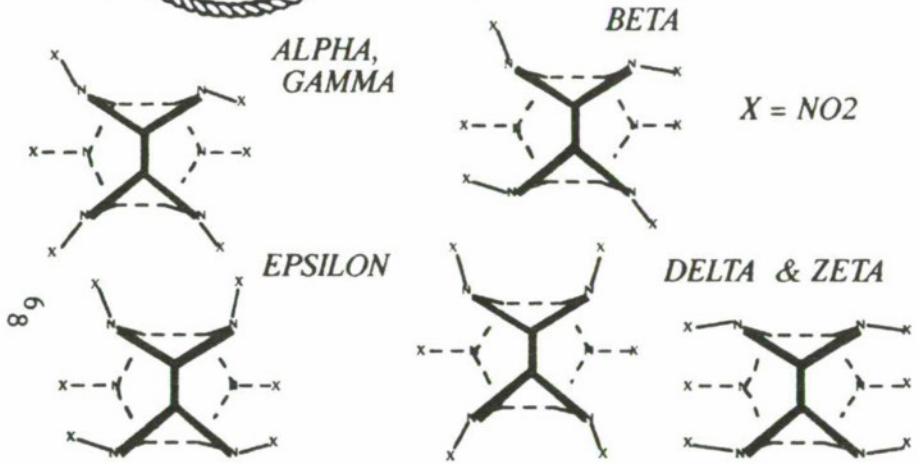

OBJECTIVES:

- O DISCOVER THE STABILITY FIELDS OF THE POLYMORPHIC PHASE SPACE OF HNIW
- O ESTABLISH ANALYTICAL TOOLS TO DISTINGUISH POLYMORPHS
- O UNDERSTAND THE AFFINITIES OF HNIW CONFORMERS FOR HYDROGEN CONTAINING SOLUTE MOLECULES

ACCOMPLISHMENTS:

- O SOLVENT RECRYSTALLIZATION OF ALPHA, GAMMA, BETA EPSILON POLYMORPHS
- O HIGH PRESSURE TRANSITION OF GAMMA TO DELTA OR ZETA POLYMORPH
- O POLYMORPHS AND IMPURITIES IDENTIFIED BY FTIR
- O ELECTROSTATIC POTENTIALS ON SURFACES OF HNIW MOLECULES IN POLYMORPHIC CONFORMATION

APPROACH:

- O HIGH PRESSURE INTER-CONVERSION
- O FTIR & X-RAY DIFFRACTION COUPLED ANALYSES
- O CO-SOLVENT RECRYSTALLIZATION OF DENSE POLYMORPHS
- O COMPUTATION OF ELECTROSTATIC POTENTIALS FOR POLYMORPHIC CONFORMERS

DRS.. D. VANDERAH, M. NADLER/ R. NISSAN, R. YEE,A..NIELSEN @ NWC DR.T.RUSSELL @ NSWC-WO, DR. R. GILARDI @ NRL
DR. P. POLITZER @ UNIV OF NEW ORLEANS
MR. G. MANSER @ AEROJET

KINETICS OF NITRAMINE OXIDIZER FRAGMENTATION PRODUCTS

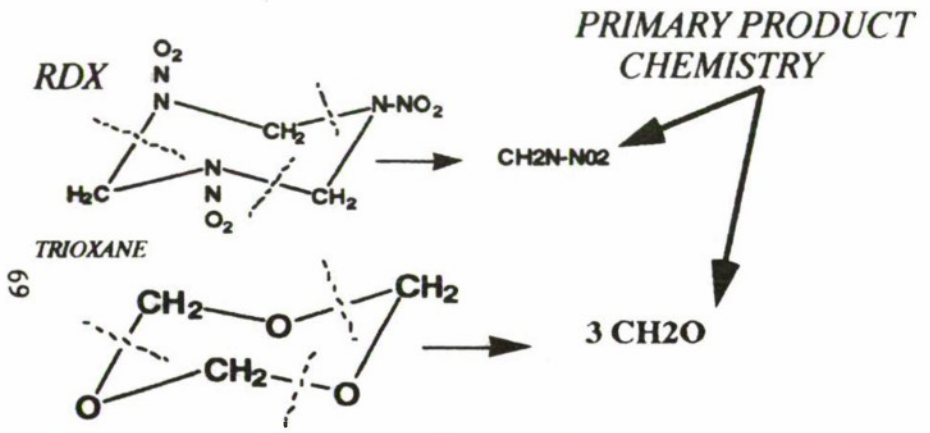

OBJECTIVES:

- O IDENTIFY AND DETERMINE RATE CONSTANTS AND MECHANISMS FOR KEY ENERGY RELEASE PROCESS IN NITRAMINE COMBUSTION
- O ESTABLISH MODELS FOR THE COMBUSTION OF ADVANCED ENERGETIC MATERIALS

ACCOMPLISHMENTS:

- O RATE CONSTANT S COMPUTED & THEN MEASURED FOR PRIMARY AND SECONDARY REACTIONS
- O CONCERTED MOLECULAR ELIMINATION PREDICTED FOR METHYLENE NITRAMINE
- O ELUCIDATION OF THE KINETICS/MECHANISMS OF CN +N2O,OH + HNO, HNCO + NO, H +NH3 REACTIONS
- O ESTABLISHMENT OF SHOCK TUBE /LASER DIAGNOSTICS FOR CN REACTIONS

APPROACH:

- O LARGE SCALE AB INITIO CALCULATIONS OF POTENTIAL ENERGY SURFACES
- O COMPUTATION OF THERMOCHEMISTRY & COMPLEX REACTION RATES
- O REACTION RATE MEASUREMENTS BY ADVANCED OPTICAL TECHNIQUES

PROFS. M. C. LIN ,R. HANSON & DRS. C. MELIUS & M. PAGE @ EMORY UNIV., STANFORD UNIV. & SNL @ LIVERMORE & NRL

7/1/91

07/25/91

RATE CONSTANT S COMPUTED & THEN MEASURED FOR PRIMARY AND SECONDARY REACTIONS

UNIMOLECULAR REACTIONS - EXPERIMENTALLY ACCESSIBLE

TRIOXANE TO FORMALDEHYDE

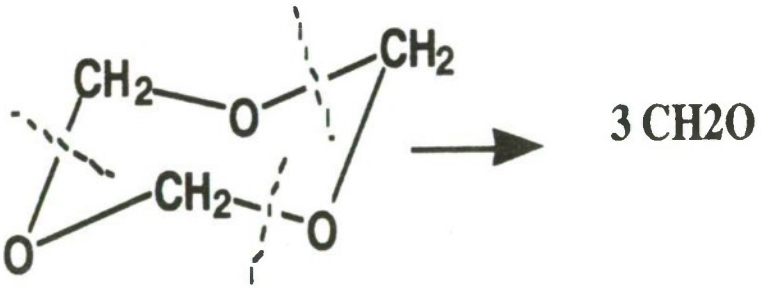

CONCERTED MOLECULAR ELIMINATION MECHANISM

QUANTUM MECHANICS COMPUTATION BY MELIUS @ SNL AT LIVERMORE

$$k = 10^{15.67\pm0.01}\, e^{-(51{,}200\pm40)/RT}\ s^{-1}$$

EXPERIMENTAL BY LIN @ EMORY

$$k = 10^{15.78\pm0.19}\, e^{-(50{,}900\pm505)/RT}\ s^{-1}$$

LIN & MELIUS @ EMORY UNIV. & SNL

07/25/91

7/1/91

RATE CONSTANT S COMPUTED & THEN MEASURED FOR PRIMARY AND SECONDARY REACTIONS

BIMOLECULAR REACTIONS - EXPERIMENTALLY ACCESSIBLE

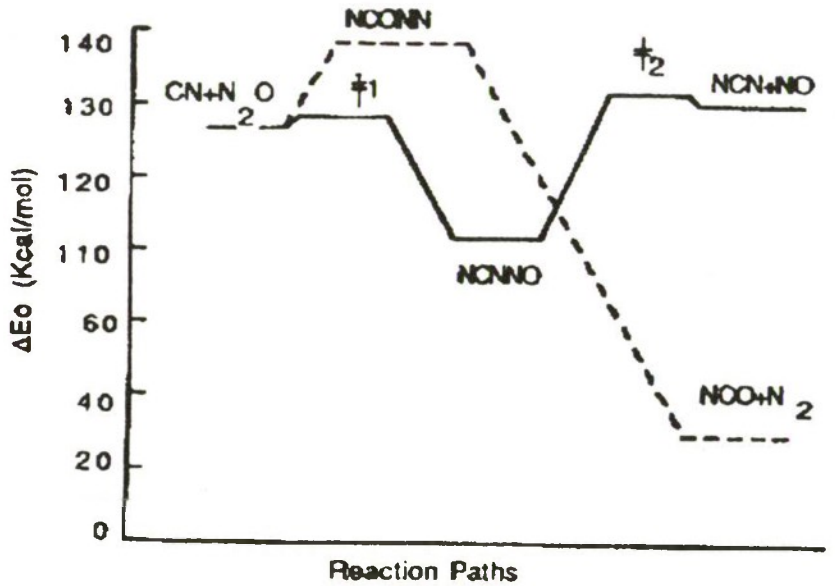

ESTABLISHMENT OF A NEW MECHANISM IN THE NITROGEN NETWORK

ACCURATE THERMOCHEMICAL DATA IS PREDICTED FOR COMPLEX SPECIES

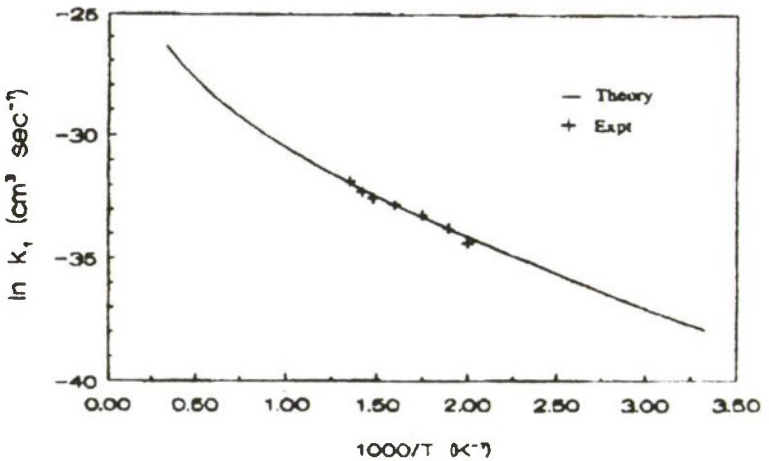

CONFIDENCE IS BUILDING TO TRUST QUANTUM MECHANICAL ESTIMATES OF MECHANISMS AND RATE CONSTANTS FOR REACTIONS OF 6 TO 6 HEAVY ATOMS

LIN & MELIUS @ EMORY UNIV. & SNL

CONCERTED MOLECULAR ELIMINATION PREDICTED FOR METHYLENE NITRAMINE

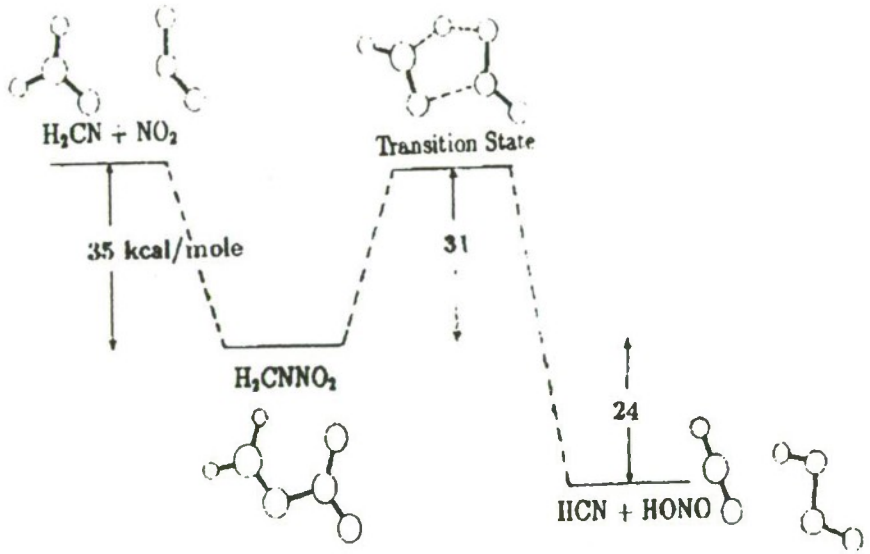

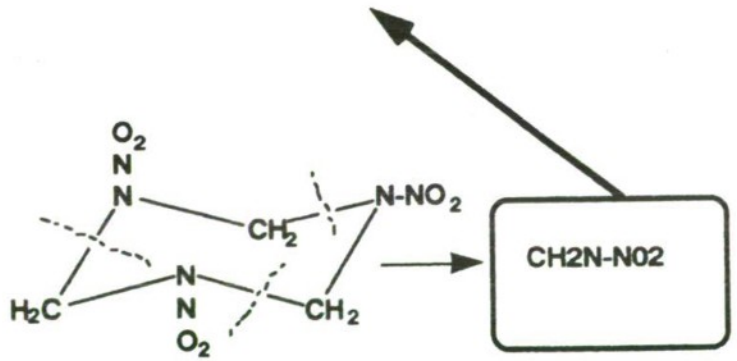

- *LOW ENERGY BARRIER INDICATES DIRECT CONCERTED REACTION TO HCN + HONO*
- *MECHANISM IS CONSISTENT WITH LEE'S MOLECULAR BEAM EXPERIMENTS*
- *LARGE SCALE AB INITIO MULTIREFERENCE CONFIGURATION INTERACTION USED TO DETERMINE DETAILS OF THE POTENTIAL ENERGY SURFACE*

DR. MICHAEL PAGE @ NRL

MONOPROPELLANT GAS PHASE COMBUSTION CHEMISTRY

MASS SPECTROMETRIC

LASER DRIVEN COMBUSTION OF ENERGETIC POLYMERS

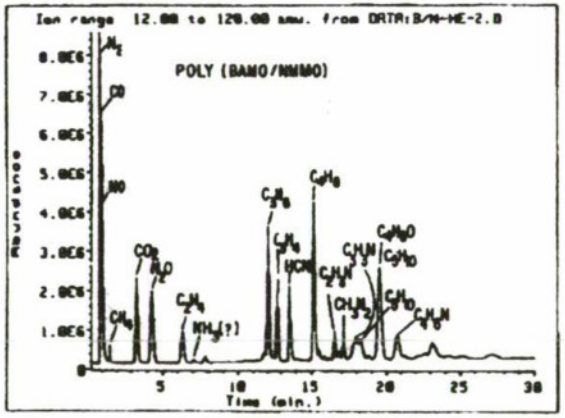

LITZINGER @ PENN STATE
QUARTZ MICROPROBE MASS SPEC OPERATIONAL
1 JUNE 1990

OPTICAL DIAGNOSTICS

LASER DRIVEN IGNITION & COMBUSTION

PLANAR LASER INDUCED FLUORESCENCE FOR:
RADICALS
o DISCOVERED HNIW CONDENSED PHASE SELF SUSTAINED HEAT RELEASE

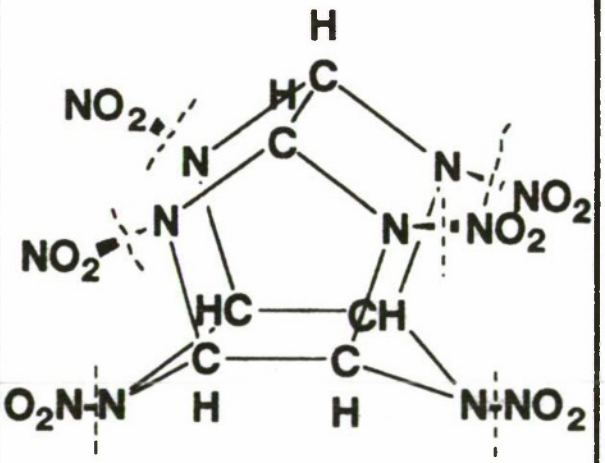

PROPOSED POLYMERIZATION OF HCN RESIDUE
PARR @NWC -
HNIW UNDERWAY AT 1 ATM.
GOING TO 10 ATM.

STEADY STATE COMBUSTION

CARS FOR:
- TEMP & MAJOR SPECIES
DEGENERATE FOUR WAVE MIXING FOR:
-MINOR SPECIES

Table 1. Optical Diagnostics for Nitramine Combustion

Molecule	Method	Sensitivity	Relative Error
N_2, O_2, H_2, CO, NO, HCN, H_2O, CO_2, N_2O, CH_2O	CARS	1%	±5%
H, O, OH, NO, NH, CH, CN, HNO, NCO NO_2, NH_2, CH_2O	LIF, DFWM	ppm	±20-30%*

LASER-SERVO SYSTEM FOR PROPELLANT COMBUSTION

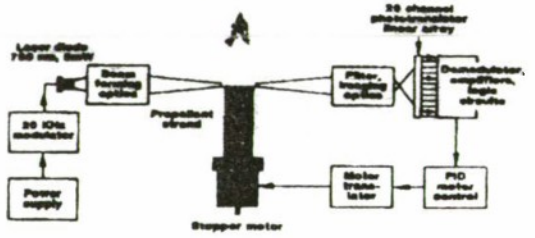

STUFFLEBEAM @ UTRC
START 1 JULY 1990
RDX & HNIW

OPTICAL & THERMAL WAVE DIAGNOSTICS OF NITRAMINE MICROSTRUCTURAL COMBUSTION PROCESSES

HNIW MICROCOMPOSITE PROPELLANT FLAME MICROSTRUCTURE

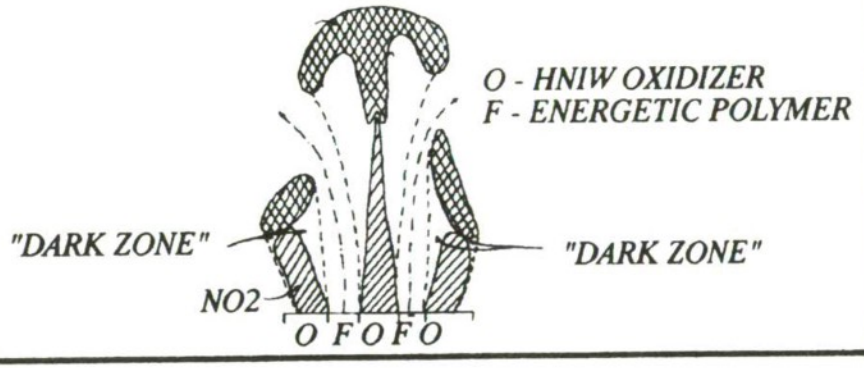

OBJECTIVES:

- O UNDERSTAND THE FLAME STRUCTURE , KINETICS AND CHEMISTRY OF NITRAMINE MONOCYCLIC AND POLYCYCLIC OXIDIZERS
- O ESTABLISH THE STEADY STATE AND TRANSIENT COMBUSTION RESPONSES

ACCOMPLISHMENTS:

- O OH ROTATIONAL GAS PHASE TEMPERATURE MEASUREMENTS EXTENDED TO SUBSURFACE
- O FIRST PLIF STUDIES OF PROPELLANT MICROCOMPOSITE FLAME STRUCTURES
- O DISCOVERED RADICAL COUNTER DIFFUSION SHOULD BE INCLUDED IN MICROCOMPOSITE COMBUSTION SIMULATIONS

APPROACH:

- O PLANAR LASER INDUCED FLUORESCENCE FOR 2-D MEASUREMENTS OF SPECIES, CONCENTRATION AND ROTATIONAL TEMPERATURE
- O SPATIALLY RESOLVED UV/VIS ABSORPTION MEASUREMENTS ARE USED TO ESTABLISH ABSOLUTE PROFILES
- O MICROTHERMOCOUPLES USED FOR CONDENSED PHASE TEMPERATURE PROFILES

DRS. TIM & DONNA PARR @ NWC

KINETICALLY LIMITED LEADING EDGE DIFFUSION FLAMES (KLLEF'S)

(NUMERICAL SIMULATION & EXPERIMENT)

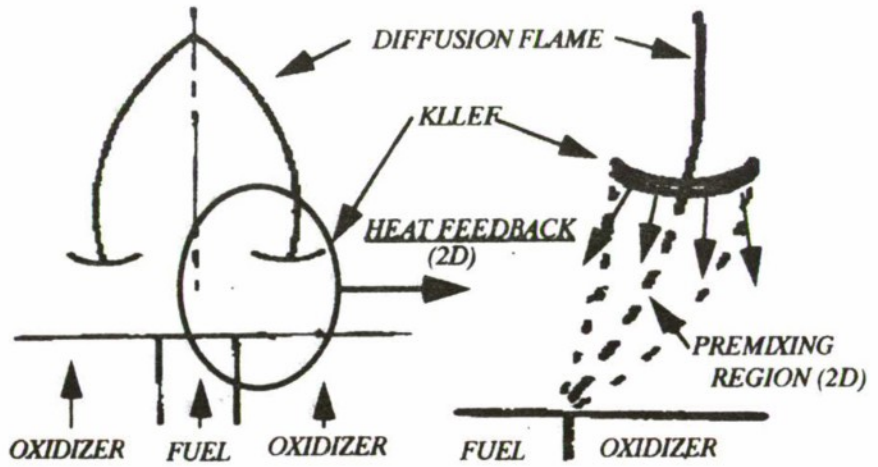

OBJECTIVES:

- O UNDERSTAND THE MICROSCOPIC COMBUSTION PROCESSES OF LAMINAR FUEL/OXIDIZER FLAMELETS
- O VERIFY THE CRITICAL ROLE OF THE KLLEF AND ESTABLISH VERIFIED ANALYTICAL-COMPUTATIONAL MODEL
- O DISCOVER MECHANISMS TO CONTROL & STABILIZE KLEEF BEHAVIOR, SUPPRESS OSCILLATIONS

ACCOMPLISHMENTS:

- O KLEEF SHOWN TO DOMINATE BEHAVIOR AND STABILITY OF LAMINAR DIFFUSION FLAMES
- O CONTROLLING PROCESSES DEMONSTRATED IN GAS BURNER EXPERIMENTS
- O NUMERICAL MODEL OF RIGOROUS KLLEF MODEL ACHIEVED THAT SUPPORTS EXPT'S
- O OSCILLATORY PROPELLANT BURNER TESTS SHOW CRITICAL ROLE OF KLLEF STABILITY

APPROACH:

- O GAS BURNER STUDIES OF LEADING EDGE FLAMES
- O NUMERICAL SOLUTIONS OF LEADING EDGE FLAMES
- O COMBUSTION OF AP/BINDER/AP MICRO-COMPOSITE SANDWICHES
- O DYNAMIC PROPELLANT COMBUSTION RESPONSE

PROF. EDWARD PRICE @ GEORGIA TECH

7/1/91

07/25/91

RIGOROUS 2-D SOLUTION OF METHANE -AIR REACTIVE FLOW IN WOLFARD BURNER

HEAT RELEASE PLOT

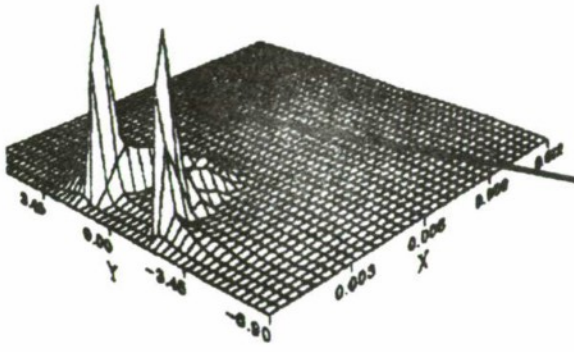

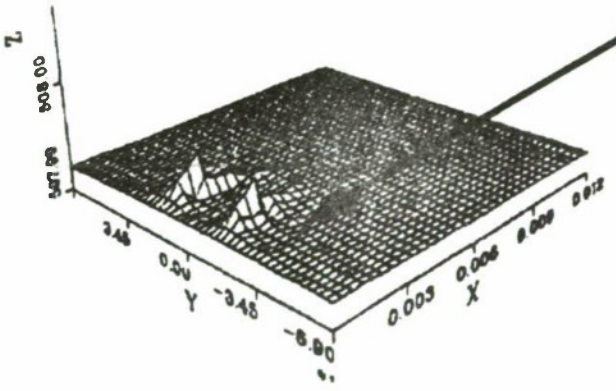

- O 2-D NON-STEADY, COMPRESSIBLE NAVIER STOKES CODE WITH TEMPERATURE DEPENDENT TRANSPORT AND THERMODYNAMIC SPECIES PROPERTIES USING A FULL SET OF PRIMARY CHEMICAL SPECIES (18) AND 48 REACTIONS
- O 2-D STEADY STATE SOLUTION VERIFIES:
  - OO PRESENCE OF CONCENTRATED (KLLEF) REACTION REGION
  - OO PRESSURE PEAK IN KLLEF
  - OO FLOW DIVERGENCE IN KLLEF APPROACH FLOW

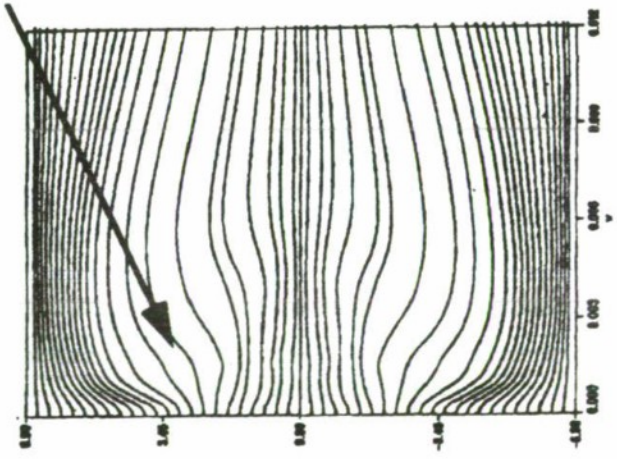

T.B. Brill

Simulation of Burning and Explosion

EXPERIMENTAL SIMULATION OF THE BURNING SURFACE DURING COMBUSTION/EXPLOSION

07/25/91

Thomas B. Brill

Department of Chemistry
University of Delaware
Newark, DE 19716
USA

SUMMARY/OVERVIEW:

A chemical and physical description of the surface reaction zone during propellant burning is essential to any advanced model of combustion. Because chemical details have not been obtainable during actual combustion, two simulation experiments have been developed to determine the kinetics and mechanisms. The burn rate is predicted by the measured kinetics. The observed gas products, therefore, very probably initiate the first stage of the flame zone.

TECHNICAL DISCUSSION

New high energy rocket propellants formulated without metal fuels present an enormous challenge to the rocket propulsion community. Instability, safe ignitability, and tailorability are all potential problems that have to be surmounted. Modeling will play a major role in guiding development because of the expense of large scale testing.

The ultimate goal of modeling combustion and combustion stability of rocket propellants requires, among other inputs, a chemical and physical description of the reacting surface at the microscale level. Such detail has not been forthcoming from direct measurements during combustion. This is because the surface is transient, heterogeneous, non-equilibrium and is obscured by the flame. Therefore, it is necessary to design experiments that simulate the condensed phase and surface during combustion, but release the gases into a cool unreactive atmosphere where they are quenched and detected immediately.

The burning surface can be imagined to be a film of material 20-100μM thick in which a phase change occurs driven by chemical reactions and heat transfer. In effect, it is a "thin-film" reaction zone that regresses through the condensed phase on one side leaving gas products behind on the other side. Therefore, an instantaneous simulation of this reaction zone would be a thin film of sample experiencing a heating rate in the 100-2000°C/sec range at a pressure of atmospheric or higher. The choice of the heating rate of 100-2000°C/sec is based on recent work of Sakamoto and Kubota with thermocouples imbedded in HMX propellants. Their measurements indicate that dT/dt in the condensed phase (foam) reaction zone is 1000±500°C/sec.

Two approaches to the reaction zone simulation have been developed: Fast-Heat-and-Hold/FTIR Spectroscopy (also called T-jump/FTIR) and Simultaneous Mass and Temperature Change/FTIR Spectroscopy (SMATCH/FTIR). Measurement of both high rate kinetics and the gas products released is important because it needs to be demonstrated that the kinetics predict the burn rate in order to have confidence that the gas products observed are the ones that feed the dark zone of the combustion region.

The Fast-Heat-and-Hold/FTIR method is designed to permit heating of a sample at 2000°C/sec to a preselected final temperature. In this way, most of the interfering chemical processes that are operative in decomposition studies at slow heating rates and that result from "cooking" are minimized. Figure 1 shows a diagram of the method. The thermal response trace of the sample is obtained from the control voltage of the circuit that maintains constant resistance of the Pt ribbon filament. The gas products are evolved into a cool argon atmosphere where they quench and are identified and quantified by absorbance of the IR beam of a rapid-scan FTIR spectrometer. Figure 2 shows the composite of these data for HMX heated at 2000°C/sec to 300°C. The ignition exotherm is the sharp negative spike in the control voltage.

The fact that gas products are detected in advance of the exotherm is strong evidence that autocatalysis is operative in HMX. The fact that NO_2 and N_2O appear in advance of the fuels (CH_2O and HCN) indicates that these fuel and oxidizer-producing reactions are not coupled. That is, NO_2 and HCN are not produced in the same elementary reaction and N_2O and CH_2O are not produced in the same elementary reaction. Instead, N_2O and NO_2 are released and CH_2O and HCN are then produced in later stage degradation of the residue. The fact that the gas product concentrations are not changing through the exotherm implies that the mechanism of decomposition before the exotherm and during the exotherm is essentially the same throughout. More of the HMX is simply decomposing.

The most useful new data from this experiment so far are gas product ratios as a function of temperature. The N_2O/NO_2 ratio shown in Figure 3 reflects the ratio of rate constants for the two global decomposition paths of HMX: the $N_2O + CH_2O$ branch and the NO_2 + HCN branch. At lower temperature the $N_2O + CH_2O$ branch dominates, while at higher temperature the NO_2 + HCN branch dominates. Temperatures in the range of 350°C are believed to exist on the surface of burning HMX propellants. Thus, Figure 3 gives the ratio of the rate constants for the two "feeder" reactions that should be used as inputs in models of the gas phase during the ignition of HMX.

The SMATCH/FTIR technique enables the dynamic weight change of the sample to be recorded as a function of time and temperature as the sample is rapidly heated. From this, a kinetics simulation of the burning surface is obtained. Simultaneously, the near surface gas products are recorded by rapid-scan FTIR spectroscopy.

Recently, it has been found that the Arrhenius constants from SMATCH/FTIR studies of thin films accurately predict the burn rate ($\dot{r}$) measured in the same pressure and temperature range. Figure 4 shows the simultaneously acquired weight-loss, temperature increase and near surface gas product data for 13%N nitrocellulose. A non-isothermal kinetics model was applied. The Arrhenius constants obtained and the known sample thickness predict $\dot{r}$ = 0.3 mm/sec. The value is in excellent agreement with the experiment $\dot{r}$ of 0.4 mm/sec for a double base propellant (80% nitrocellulose) determined under the same pressure conditions. The SMATCH/FTIR data for glycidylazide polymer (GAP) predict $\dot{r}$ = 1.35 mm/sec compared to the experimental value of 1.7 mm/sec under the same pressure conditions. The similarity of the predicted and measured $\dot{r}$ gives confidence that the gas products and concentrations measured by SMATCH/FTIR are the reactants for the flame were a flame to be present. The gas products from SMATCH/FTIR are essentially the same as those measured by the Fast-Heat-and-Hold/FTIR method and all of our previous fast thermolysis/FTIR studies. As a result, the connection between the chemical composition of a material and its ultimate flame characteristics is beginning to be made.

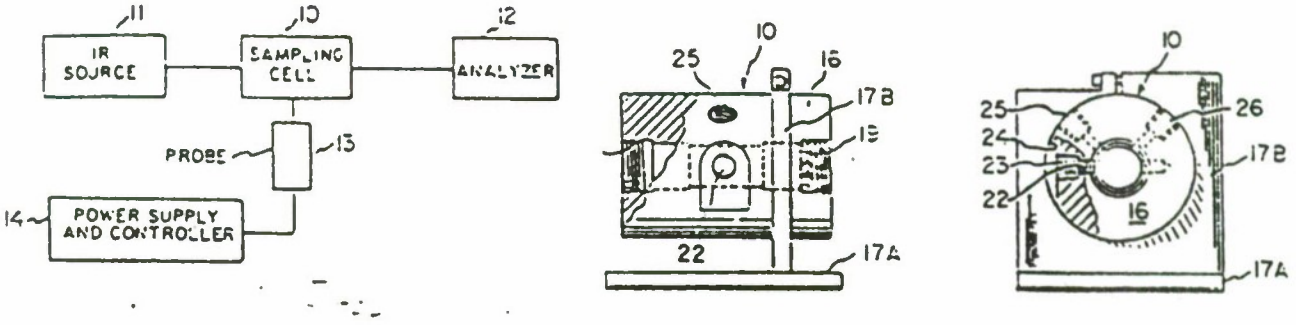

Figure 1. The physical layout (left) and cell design for the Fast Heat and Hold/FTIR experiment. A thin film of 200μg of sample is placed on a Pt ribbon filament and inserted through the cell wall at site 22.

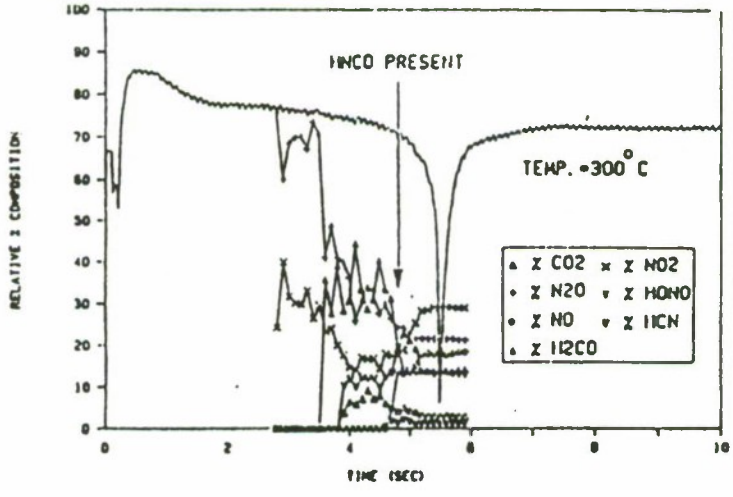

Figure 2. The control voltage response of the Pt filament superposed on the quantified gas products from 200μg of HMX. The heating rate was 2000°C/sec to a constant temperature of 300°C. The negative spike is the exotherm of HMX. See text for more details.

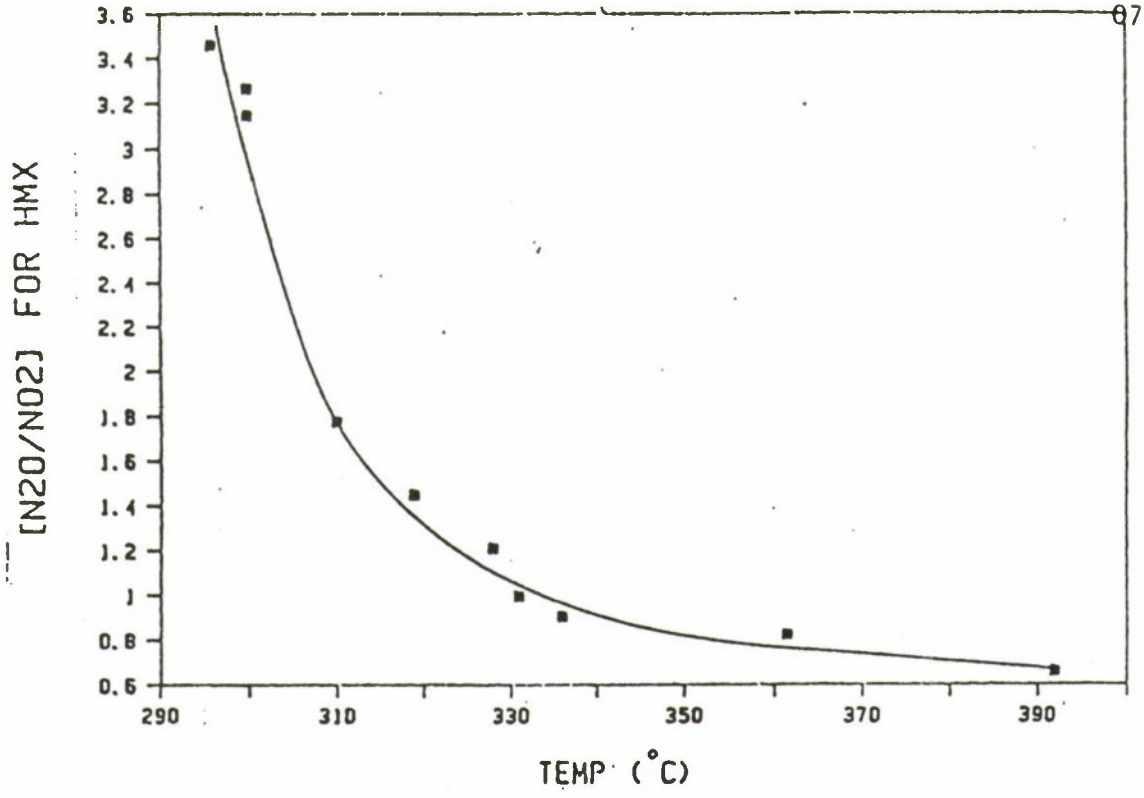

Figure 3. The N_2O-CH_2O/NO_2-HCN branching ratio of HMX as a function of temperature. The rates of these two reactions are approximately equal at the burning surface temperature of HMX (340-360°C).

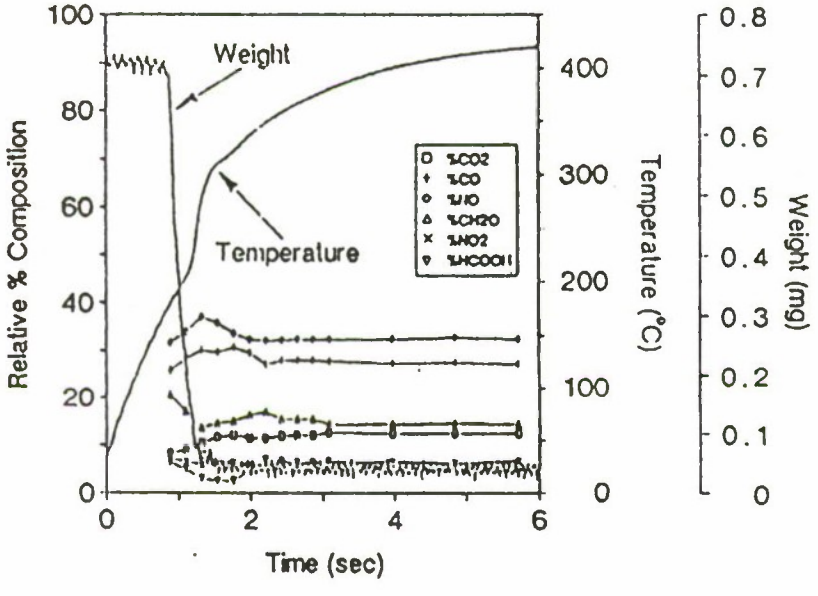

Figure 4. SMATCH/FTIR data for a 30μM thick film of 13%N nitrocellulose showing the dynamic weight change, temperature change and near surface gas products. The mass change and temperature profile enables a non-isothermal kinetics model to be applied. The gas products are the species that leave the surface under this simulated combustion situation.

TECHNIQUES DEVELOPED TO APPROXIMATE IGNITION AND COMBUSTION OF SOLIDS MORE CLOSELY

SMATCH/FTIR Spectroscopy

Simultaneous measurement of the mass change, temperature change and near-surface gas species of thin films heated at $dT/dt \leq 320 K/sec$

Fast-Heat-and-Hold FTIR Spectroscopy

$dT/dt = 2000 k/sec$ to an isothermal temperature.

SMATCH/FTIR SPECTROSCOPY

a

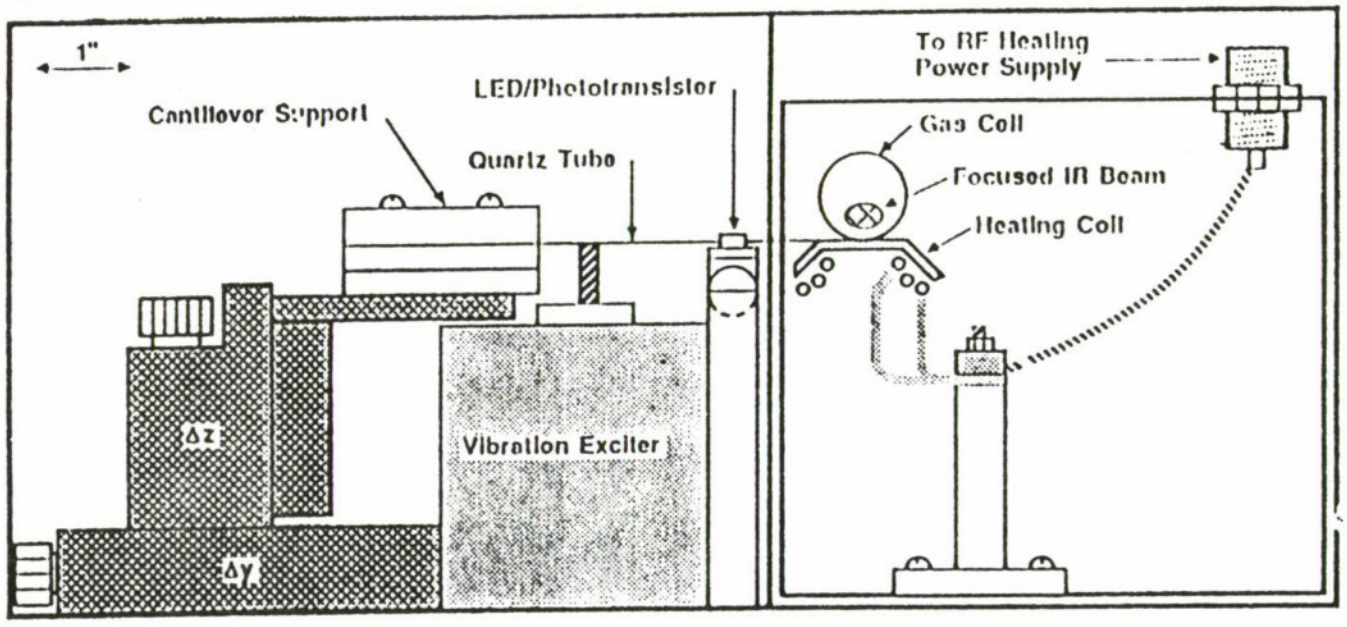

b

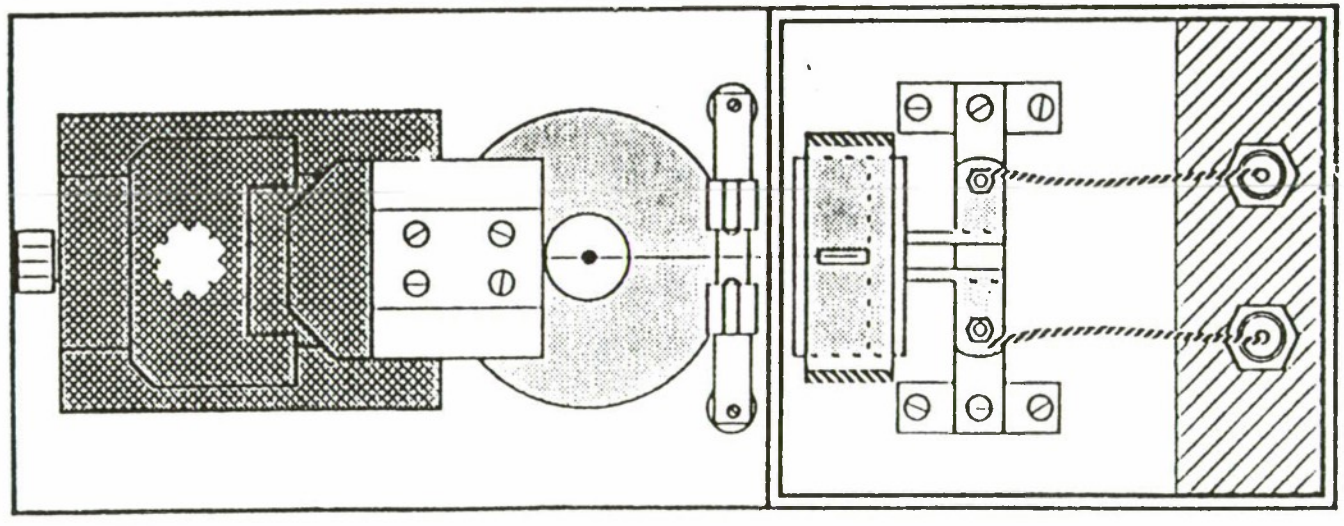

evolved gas + temperature change + mass change

Block Diagram of the SMATCH/FTIR Experiment

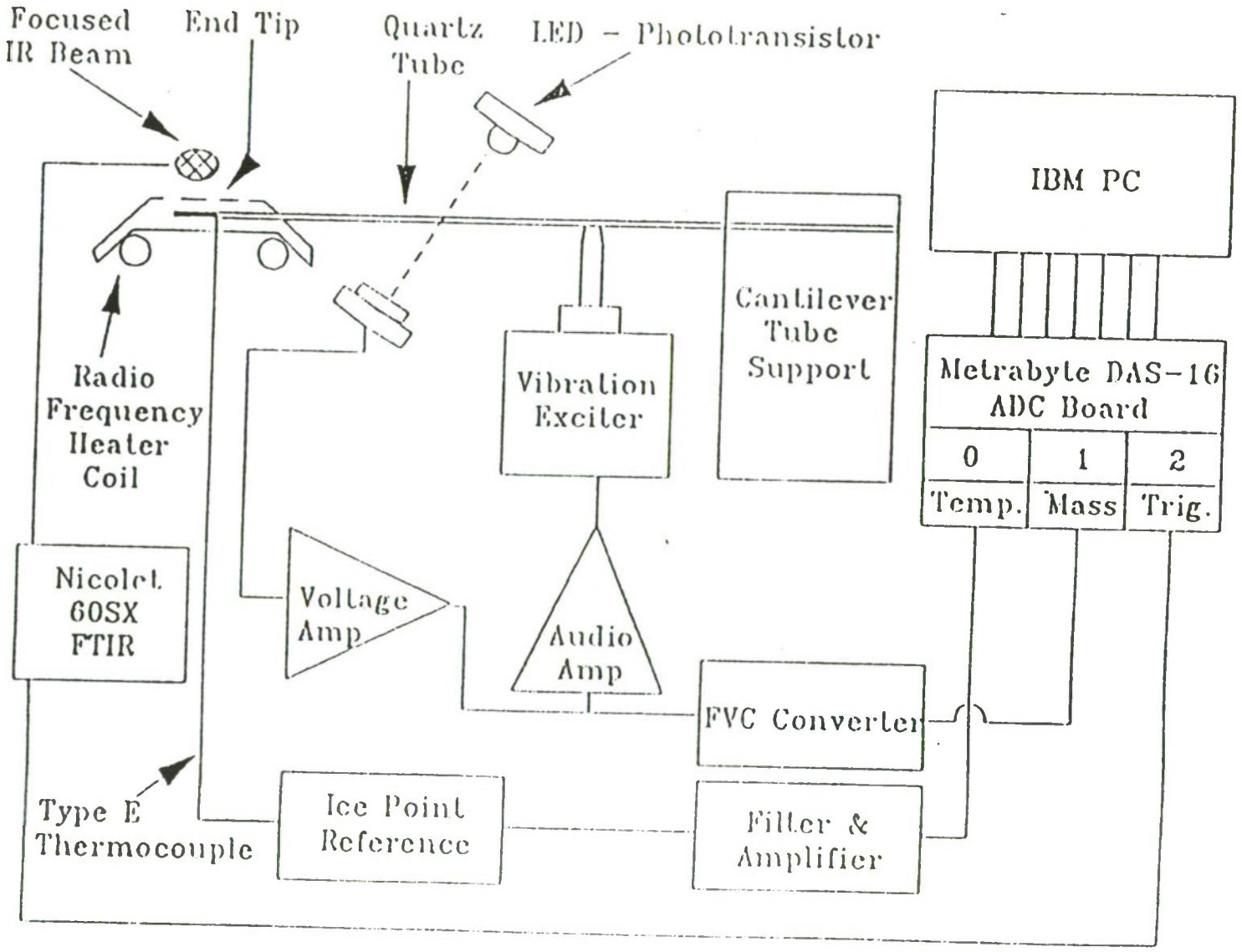

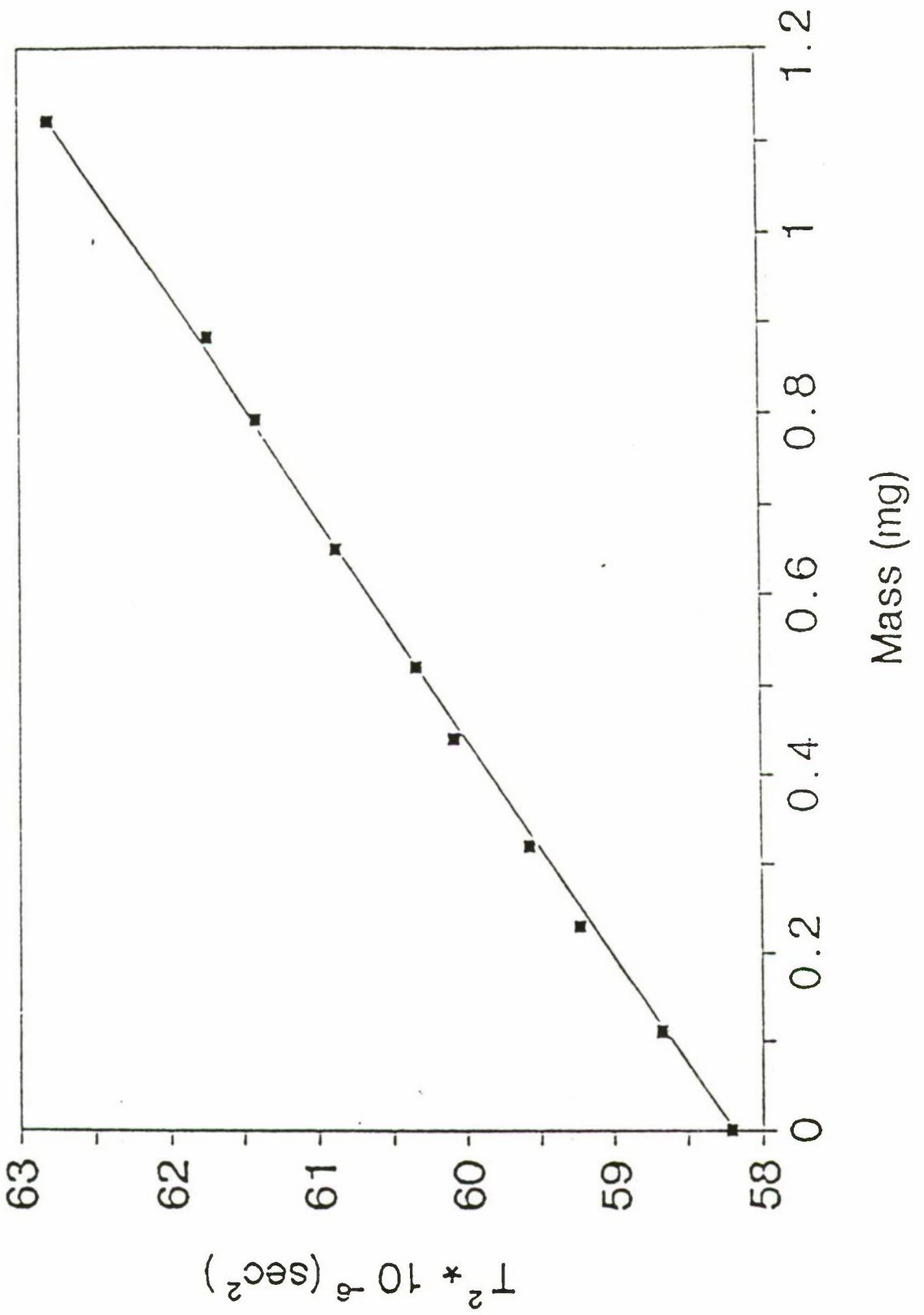
63
62
61
60
59
58
0
0.2
0.4
0.6
0.8
1
1.2
Mass (mg)
T² * 10⁻⁶ (sec²)

Simultaneous Mass, Temperature, and Gas Product Measurements of AMMO

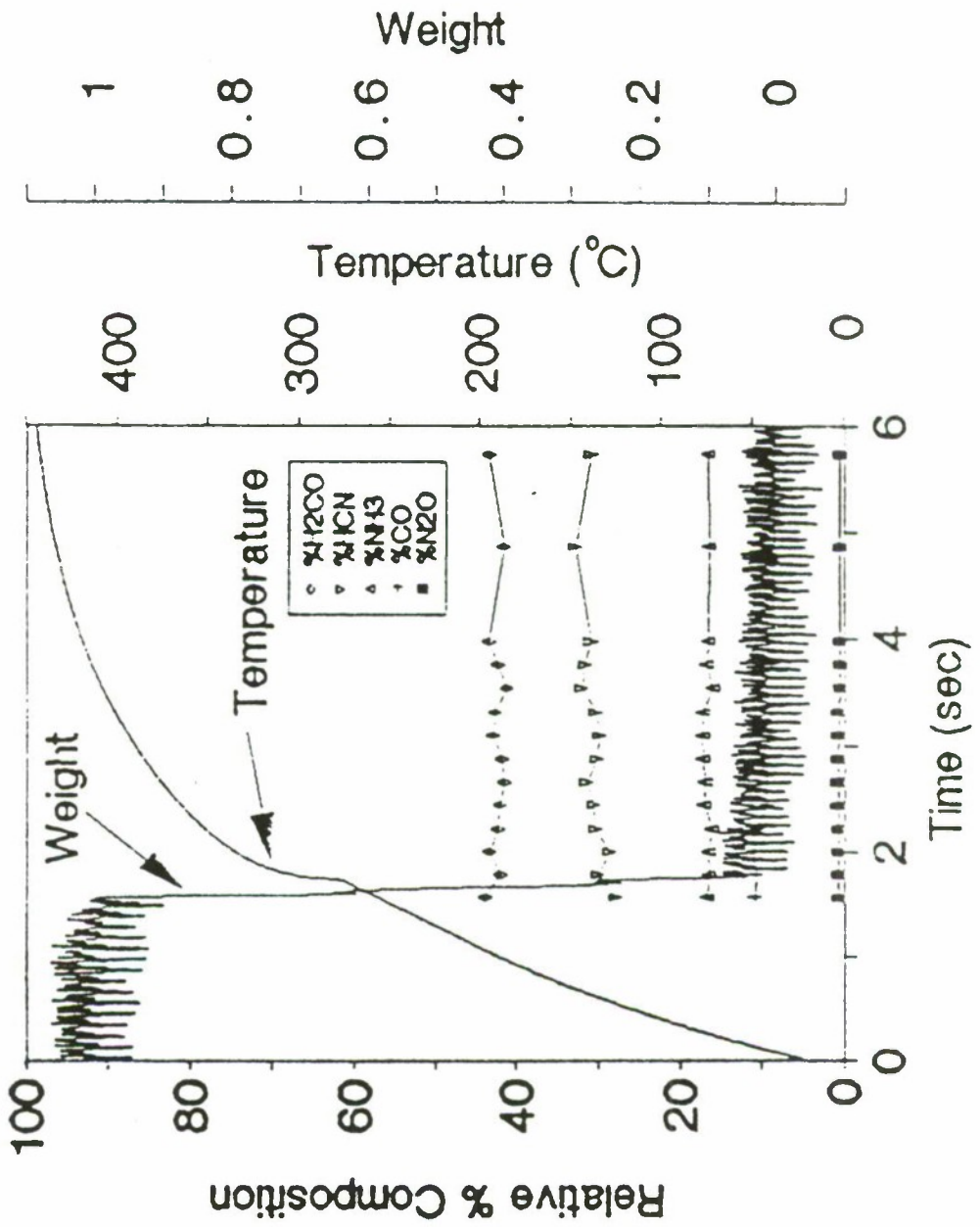

Arrhenius Plots for Azide Polymers Measured by SMATCH/FTIR Spectroscopy

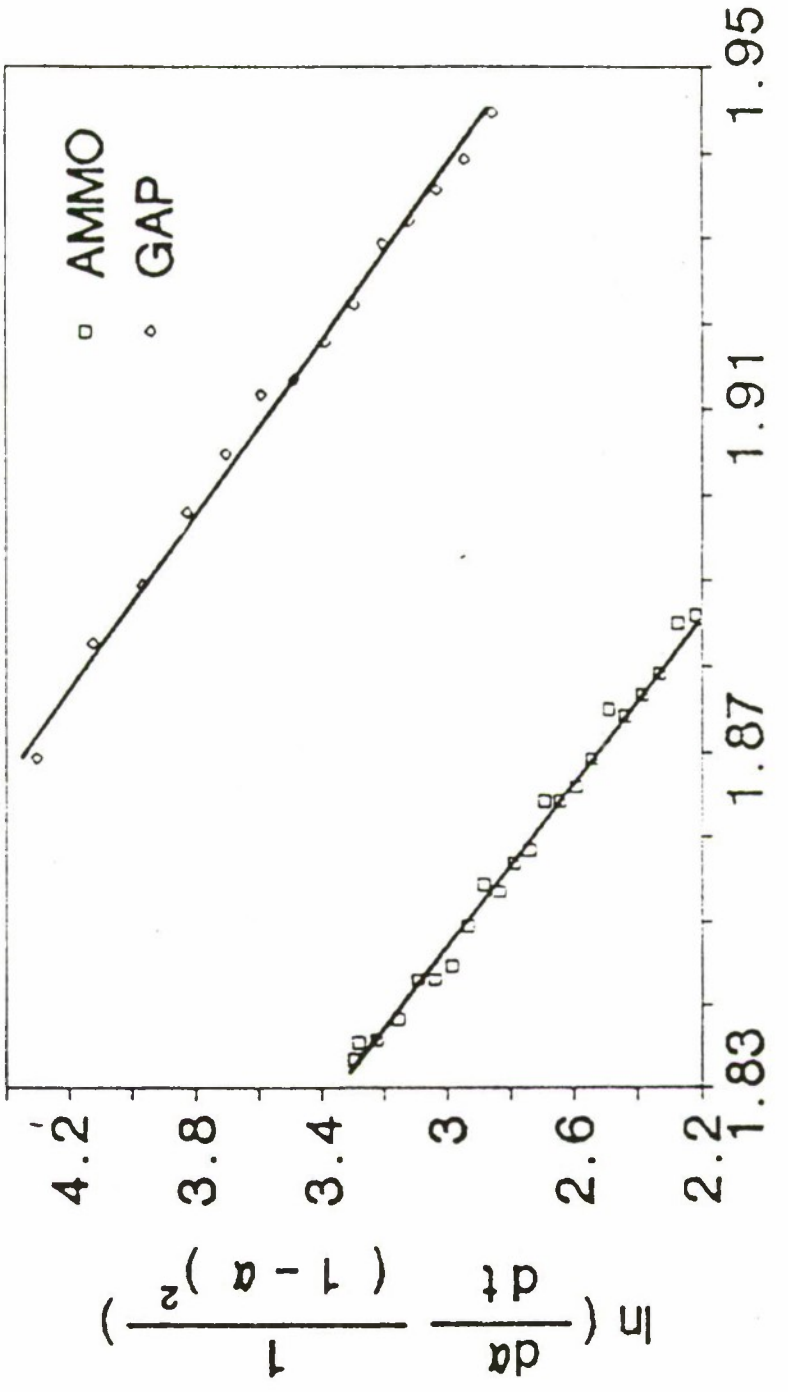

Table 4. Kinetic Parameters of Azide Polymers for Thermal Decomposition at dT/dt=150°C/sec by SMATCH/FTIR Spectroscopy

polymer	E_a (kcal/mol)[a,b]	log A (sec^{-1})
GAP	42.3 ± 2.4	19.0 ± 0.9
AMMO	43.2 ± 2.8	18.9 ± 1.3

[a] apparent reaction order n=2
[b] the average of two experiments

Problem: Combustion and explosions incorporate high temperature reactions of the condensed phase.

What is the chemistry of an energetic material at a temperature well above its normal "slow" decomposition temperature?

A Solution: T-Jump/FTIR Spectroscopy

Heat 200ug of sample at 2000 C/sec to a set temperature and hold at that temperature while recording the temperature and measuring the gas product concentrations next to the surface.

Cell Design

- Heat a thin film of material at a controlled high rate and stop at a desired temperature (CDS Pyroprobe)
- Record the thermal response of the sample
- Evolve the gases into a cool inert atmosphere to quench them in near-surface zone.
- Identify and quantify products in near-real time (Nicolet 20SX or 60SX)

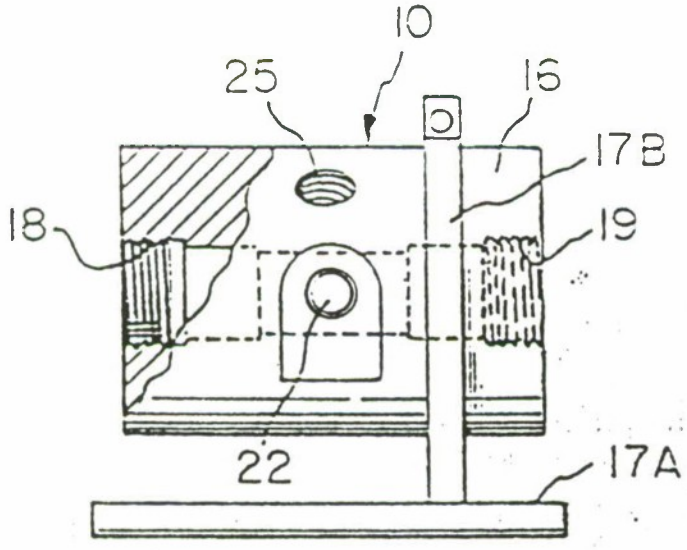

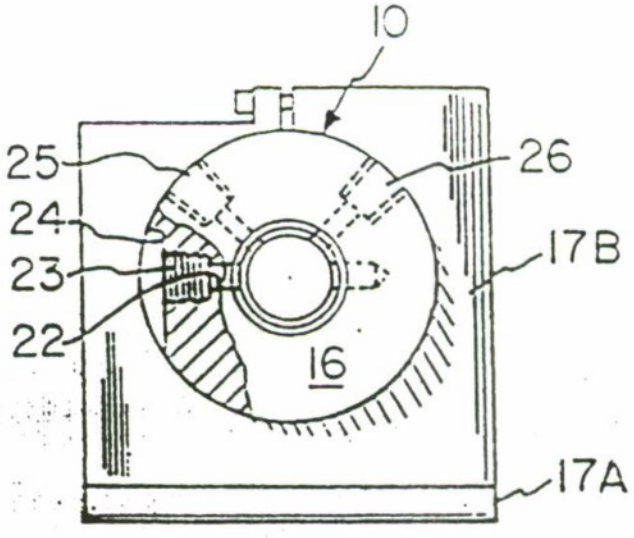

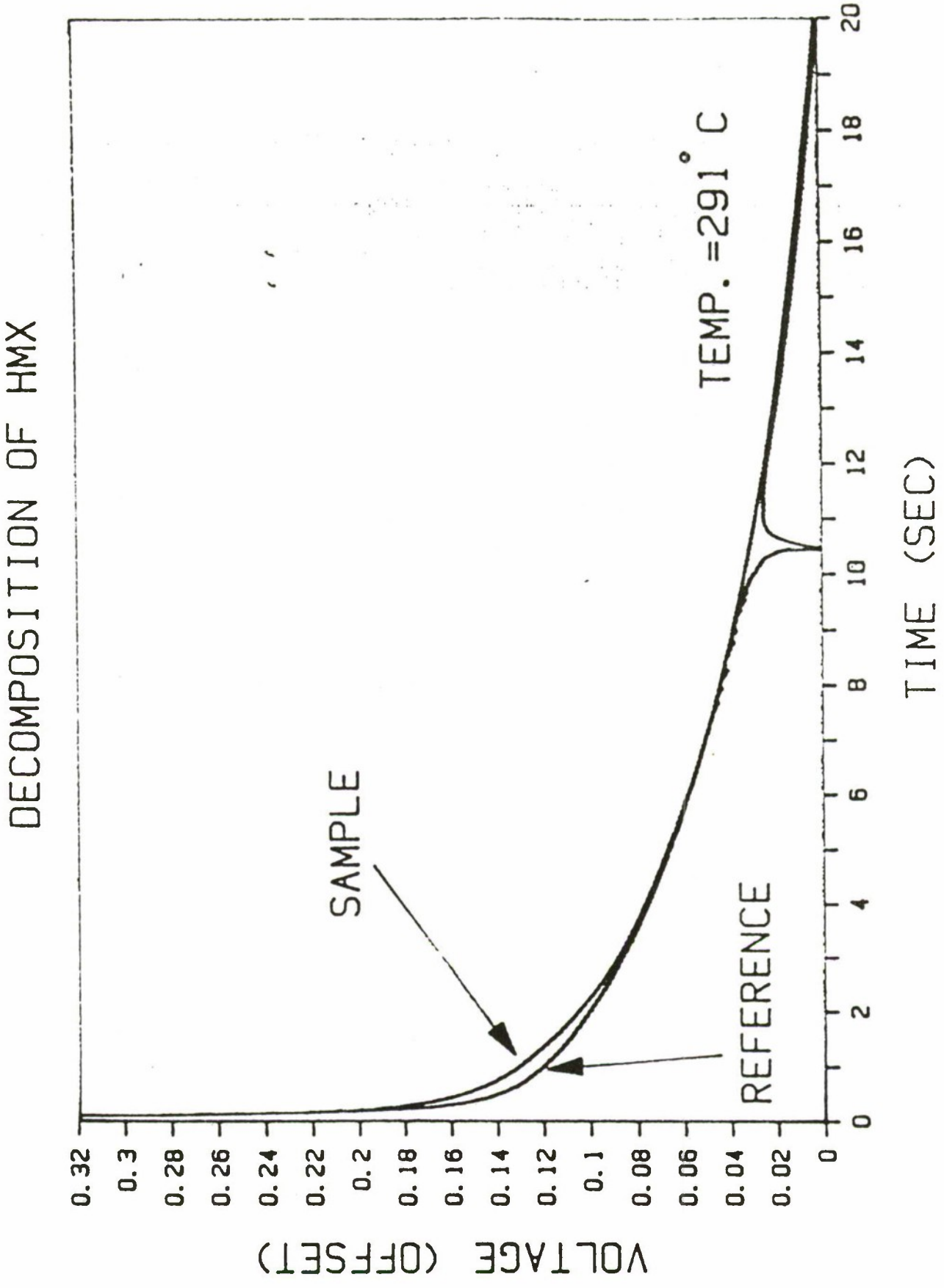
DECOMPOSITION OF HMX
TEMP. =291° C
SAMPLE
REFERENCE
VOLTAGE (OFFSET)
TIME (SEC)
0.32
0.3
0.28
0.26
0.24
0.22
0.2
0.18
0.16
0.14
0.12
0.1
0.08
0.06
0.04
0.02
0
2
4
6
8
10
12
14
16
18
20

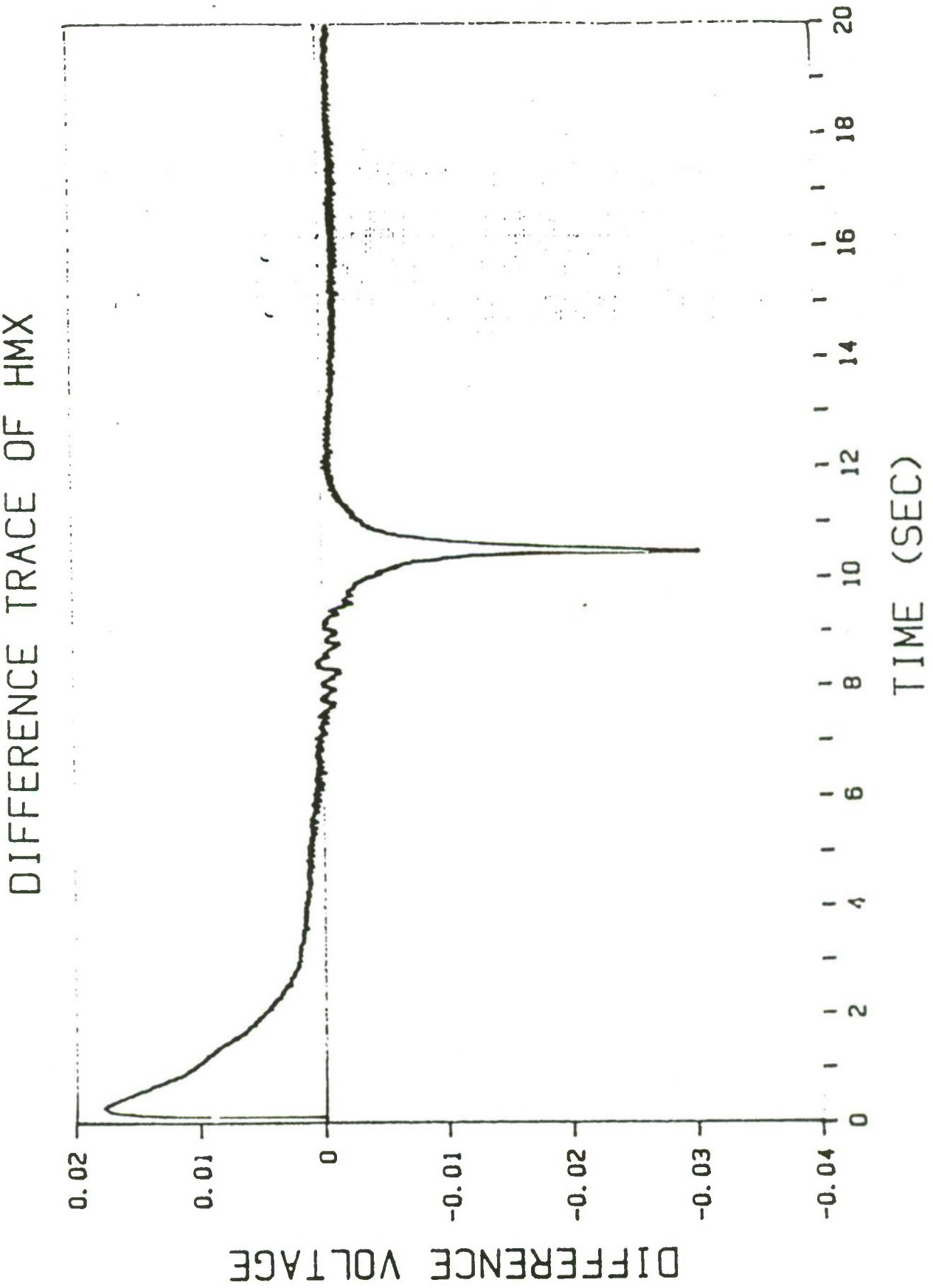
DIFFERENCE TRACE OF HMX
DIFFERENCE VOLTAGE
0.02
0.01
0
-0.01
-0.02
-0.03
-0.04
0
2
4
6
8
10
12
14
16
18
20
TIME (SEC)

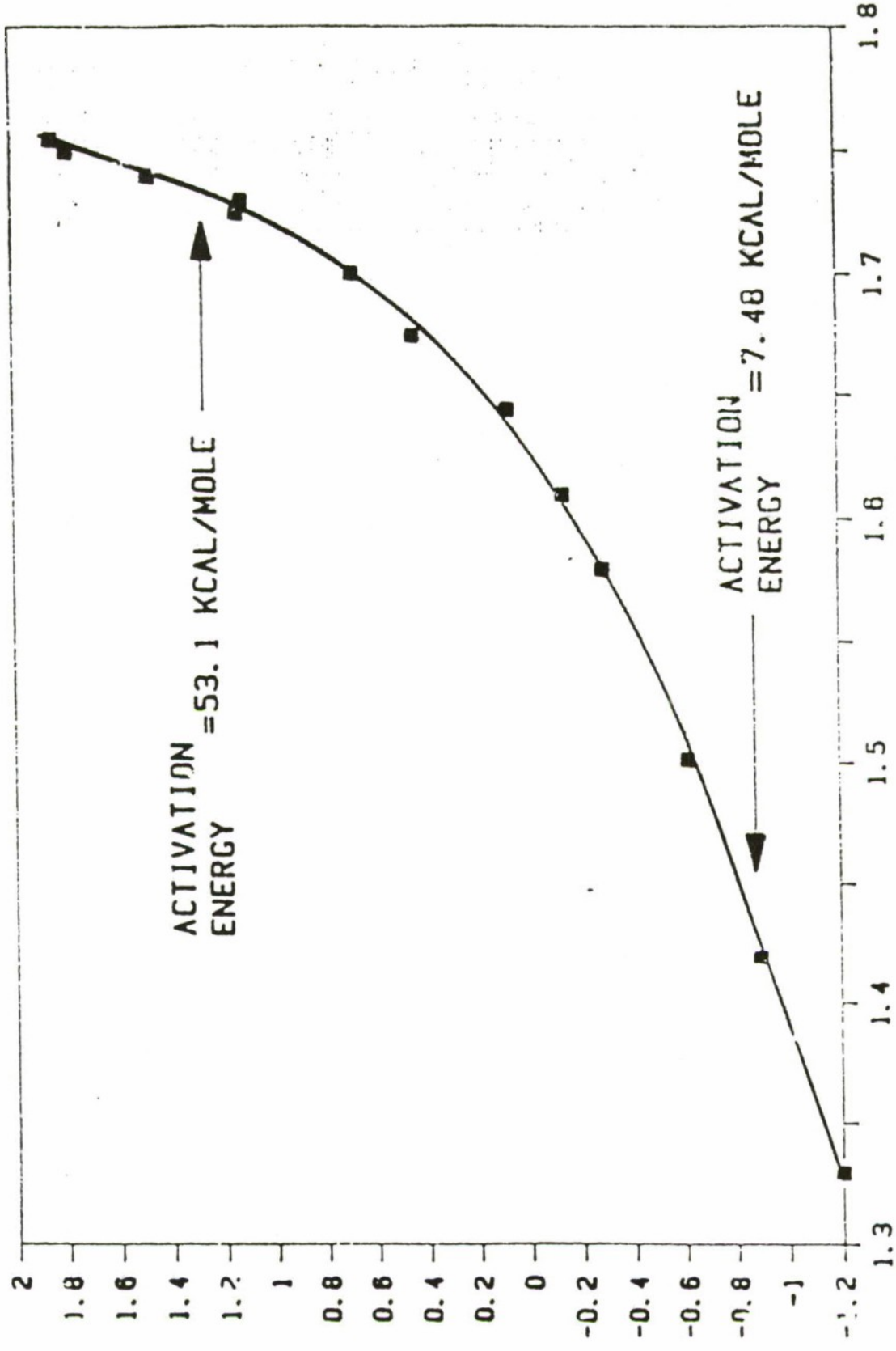
HMX under 40 psi Ar
ln [Time to Exotherm]
TEMP^{-1}(K) *10^{3}
ACTIVATION ENERGY =53.1 KCAL/MOLE
ACTIVATION ENERGY =7.48 KCAL/MOLE
2
1.8
1.6
1.4
1.2
1
0.8
0.6
0.4
0.2
0
-0.2
-0.4
-0.6
-0.8
-1
-1.2
1.3
1.4
1.5
1.6
1.7
1.8

Decomposition of HMX

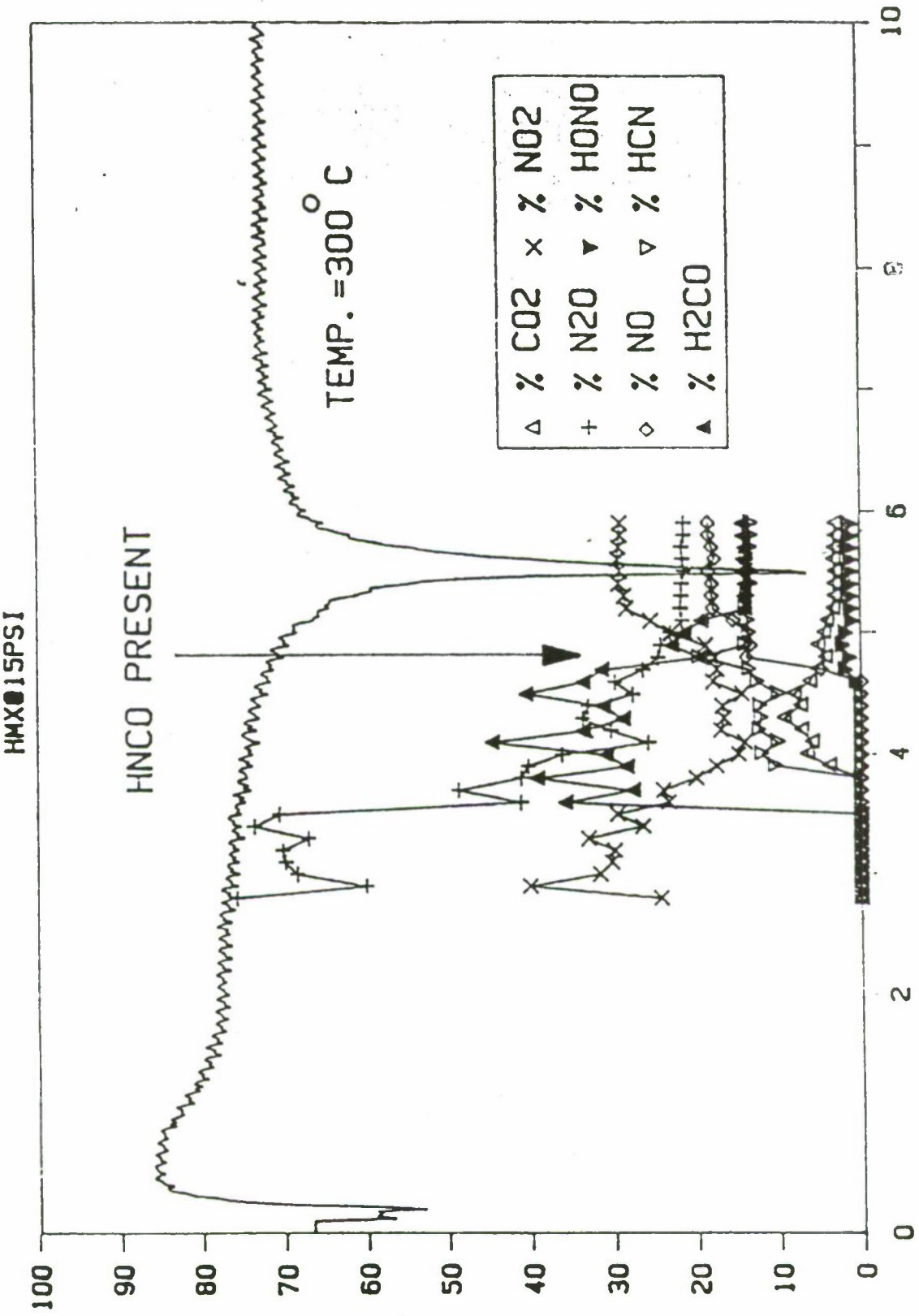

T. Parr and D. Hanson-Parr

Laser Diagnostics for Flame Structures

SOLID PROPELLANT FLAME STRUCTURE MONITORED WITH ADVANCED LASER DIAGNOSTICS

Tim Parr and Donna Hanson-Parr
Research Department
Naval Weapons Center
China Lake, CA 93555-6001

OBJECTIVE This presentation summarizes work done at NWC utilizing advanced laser diagnostics, as well as other techniques, to measure solid propellant flame structure and chemistry. The ultimate goal of such studies is a better understanding of the fundamentals of solid propellant combustion on a detailed chemical kinetic level. Such an understanding would allow for the development of a computer code for the a-priori prediction of propellant ballistic properties such as burn rate, pressure exponent, temperature sensitivity, ballistic catalysts, combustion instability, ignitability, and hazard properties such as DDT. Such a code would afford general improvements in formulation capabilities as well as shortened development times and a move away from expensive trial and error formulation testing. The development of such a code requires direction and validation by experimental work aimed, in part, at directly measuring propellant flame chemistry and structure.

The direct objective of our work is to measure temperature and species profiles in deflagrating samples of neat energetic materials, composite propellants, and controlled geometry composite sandwich propellants. We will discuss the experimental techniques used, including transient UV/Vis absorption and Planar Laser Induced Fluorescence (PLIF). PLIF results for ignition and deflagration at 1 atm of neat and composite samples will be presented and the effect of elevated pressure on propellant flame structure shown. Deflagration temperature profiles, measured using PLIF and thermocouples will be presented. Calibration of PLIF measured relative species profiles using transient absorption will be discussed. Finally composite sandwich propellant diffusion flame structure will be presented.

TECHNIQUE The samples we work with are pressed pellets of neat nitramines or sliced pieces of composite propellants. A CO_2 laser is used to supply up to 150 cal/cm^{2}s igniting flux, affording temperature gradients to above 100K deg/s. We study flames at ambient pressure and up to 4 atms.

The PLIF diagnostic technique allows measurement of 2D profiles of flame species and temperature in a single laser shot. The Nd-YAG/dye/non linear crystal laser beam is formed into a sheet, passed over the samples surface and through the center of the flame, and tuned in resonance with an absorption transition of a species of interest (we have studied CN, NH, OH, CH, C_2, NO, NO_2, NCO, H_2CO). Fluorescence from that species is measured at right angles to the laser sheet using a gated image intensified CCD camera. The technique allows spatial resolution of better than 50 microns (10 microns possible) and temporal resolution below 10 ns.

For transient absorption measurements on steady state deflagration the sample pellets deflagrating surface is held at a constant height using spring loading from below and a taught tungsten wire stretched over the surface. The path of a Xe arc lamp is placed at the desired height above this surface and absorption monitored using a spectrometer and an intensified OMA (Optical Multichannel Analyzer). The spatial resolution is better than 250 microns using this configuration. Absorption measurements have been made on OH, NO_2, NO and CN using this apparatus.

PLIF RESULTS ON IGNITION PLIF measurements of the time evolution of ignition of neat HMX (at 1 atm) show the following. At times less than 2 msec no gaseous species are evolved; calculations show that at the heating flux used, 2 msec are required to heat the HMX surface up to the 'melting' temperature. After the surface melts, a plume of NO_2 begins to grow, reaching about 2.5 mm off the surface at 4 msec. At 5 msec a spherical gaseous ignition kernel forms, as evidenced by the CN PLIF images, and this kernel consumes a hole in the NO_2 plume leaving an outward accelerating thin shell. The ignition kernel rapidly

forms into a thin flame sheet the edges of which then attach to the sample surface. The NO_2 plume is reduced in intensity and limited in extent to the region below the thin flame sheet. PLIF measurements on other species show that NH generally follows the CN time/space behavior with the exception of peaking slightly closer to the surface. The OH radical forms only after the ignition kernel forms and peaks beyond the flame sheet, staying at a high concentration higher into the flame because it is an equilibrium product. The NO profile largely follows the NO_2 behavior but the concentration is so high that the laser beam is totally absorbed and PLIF profiles not accurate.

Addition of a binder to HMX, as in a composite propellant, causes longer ignition kernel delays and higher flame standoff distances. The PLIF technique has shown efficacy even for relatively dirty highly aluminized propellant flames.

ELEVATED PRESSURES When the backing pressure is raised the ignition kernel delays decrease and the flame standoff distance drop. As pressure is increased the flame sheet standoff distances drop approximately inversely with pressure while the flame thickness decreases much more slowly. This implies that at realistic rocket motor pressures the flame sheet will be very close to the surface, ca 25 microns, and will extend onto the surface, pointing out the importance of radical attack on the condensed phase.

TEMPERATURE Kinetics are exponentially dependent on temperature so it is imperative to accurately measure temperature profiles to facilitate kinetic modeling of propellant flames. The rotational temperature of a species can be obtained by ratioing rotationally specific population density measurements, which can be obtained using PLIF by pumping different resonant lines. Such measurements done on OH radicals show that the flame kernel mentioned above correlates with the secondary flame of HMX deflagration, ie total thermodynamic heat release. A Boltzmann plot for OH rotational level distribution in HMX deflagration lead to a slope indicating a rotational temperature of 2772 K ± 35K, which is very close to the adiabatic flame temperature for HMX at 1 atm (2922K) showing that the PLIF technique has reasonable accuracy even in a hostile environment. Combining these PLIF results for gaseous flame temperature profiles with our micro-thermocouple measurements of condensed phase and near surface temperatures clearly shows the two stage nature of the HMX and RDX flames. Table I shows the important results:

TABLE I.

Ingredient	Melt Thick.	T_s	Primary Flame Thickness	Secondary Flame Height
RDX	80 μm	610K	100 μm	1.5 mm
HMX	40 μm	660K	140 μm	2.2 mm

TRANSIENT ABSORPTION Measurements have been made on OH, NO_2, NO and CN. The line of sight nature of the absorption measurements are deconvolved using measured PLIF profile shapes. The peak concentrations found using this method in HMX self deflagration were: 0.083 mole fraction for NO_2, 0.13 mole fraction for NO, and 340 ppm for CN.

DIFFUSION FLAME STRUCTURE Controlled geometry sandwiches of solid oxidizers and fuel were used to study composite propellant diffusion flame structure using 2D PLIF imaging. The sandwiches were manually fabricated and the minimum oxidizer and binder thickness studied so far were 250 μm and 200 μm respectively. PLIF measurements on a propellant that had no diffusion flame showed NO_2 plumes coming from the oxidizer but no diffusion flame between the oxidizer and the fuel plumes. A different combination clearly showed a diffusion flame between the oxidizer and binder plumes. These flames, as evidenced by CN radicals, had kinetically limited delay standoff distances associated with them and appeared downstream within the diffusional mixing fans.

SUMMARY We have used advanced laser diagnostics to study the chemistry and structure of neat energetic material, composite solid propellant, and controlled geometry sandwich flames. Spatially and temporally resolved concentration profiles have been obtained for NO_2, NO, CN, CH, OH, H_2CO, CH, and C_2; all in two dimensions. Spatial resolution to 50 microns was demonstrated. Pressures to 4 atm were studied. Concentration profiles were calibrated using transient absorption. State resolved population distributions were measured for OH and CN to provide 2D flame temperature profiles. Condensed phase and near surface temperature profiles were measured using micro thermocouples. Direct images of composite propellant diffusion flame structures were obtained.

Our results, along with those of Stufflebeam (UTRC), Edwards (AFAL), Vanderhoff (BRL), Lengelle (ONERA, France), and other groups in the US, Netherlands, and Soviet Union, are beginning to lead to an understanding of solid propellant combustion on a fundamental level and providing data for direction and validation of modeling efforts.

APPROACH

- **SAMPLES**

  PRESSED PELLETS OF NEAT NITRAMINES

  COMPOSITE PROPELLANTS

  CONTROLLED GEOMETRY COMPOSITE SANDWICHES

- **FLAME**

  CO2 LASER IGNITION

  CO2 LASER SUPPORTED DEFLAGRATION

  SELF DEFLAGRATION

  1-4 ATM

- **DIAGNOSTICS**

  PLANAR LASER INDUCED FLUORESCENCE (PLIF)

  2D SPECIES PROFILES

  2D TEMPERATURE PROFILES

  TRANSIENT UV/VIS ABSORPTION

  ABSOLUTE CALIBRATION OF CONCENTRATION

FIRST PLIF STUDIES OF PROPELLANT MICROCOMPOSITE FLAME STRUCTURES

DIRECT IMAGING OF DIFFUSION FLAME STRUCTURE

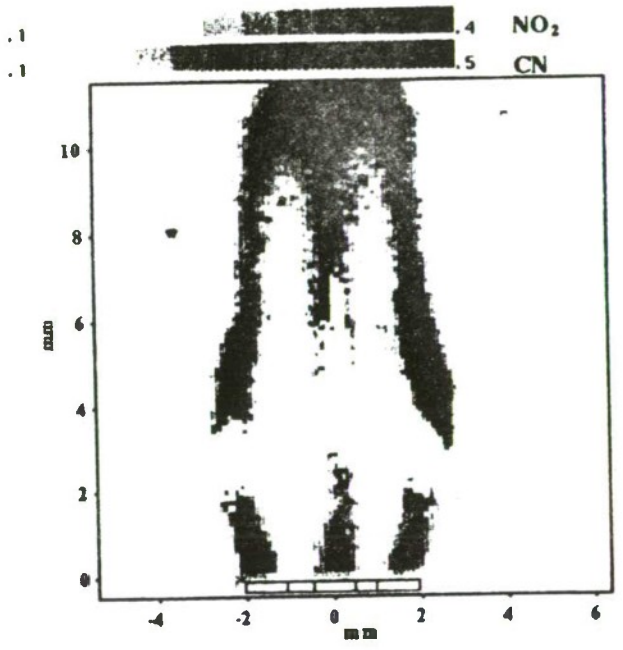

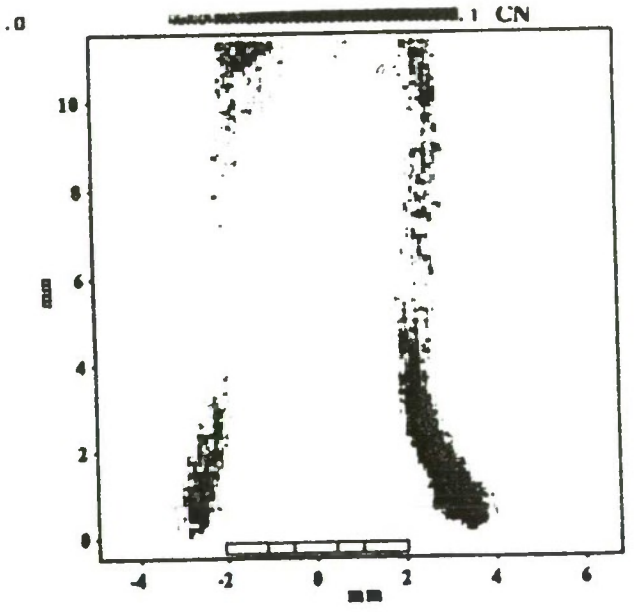

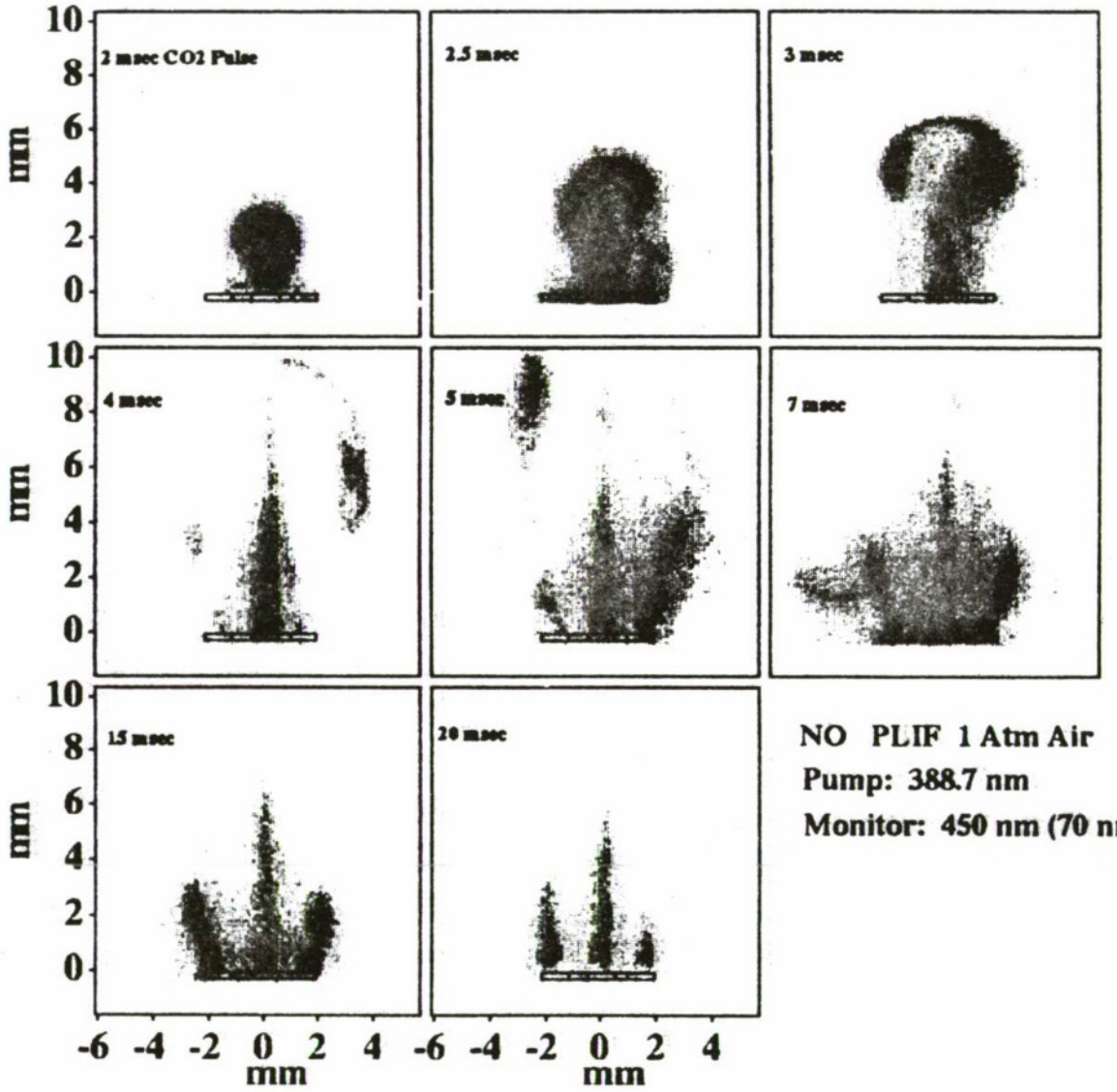

NO PLIF 1 Atm Air
Pump: 388.7 nm
Monitor: 450 nm (70 nm FWHM)

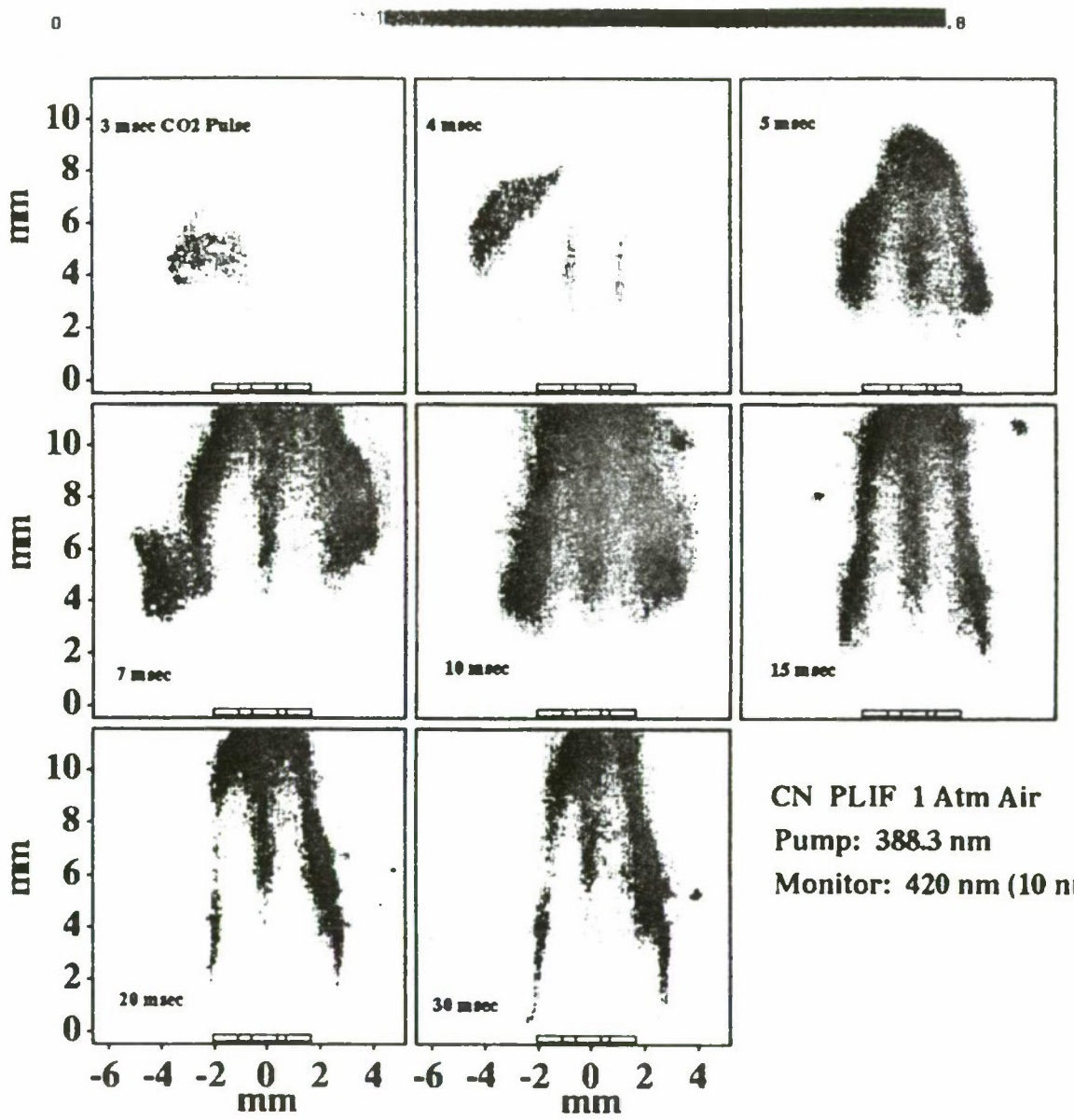

CN PLIF 1 Atm Air
Pump: 388.3 nm
Monitor: 420 nm (10 nm FWHM)

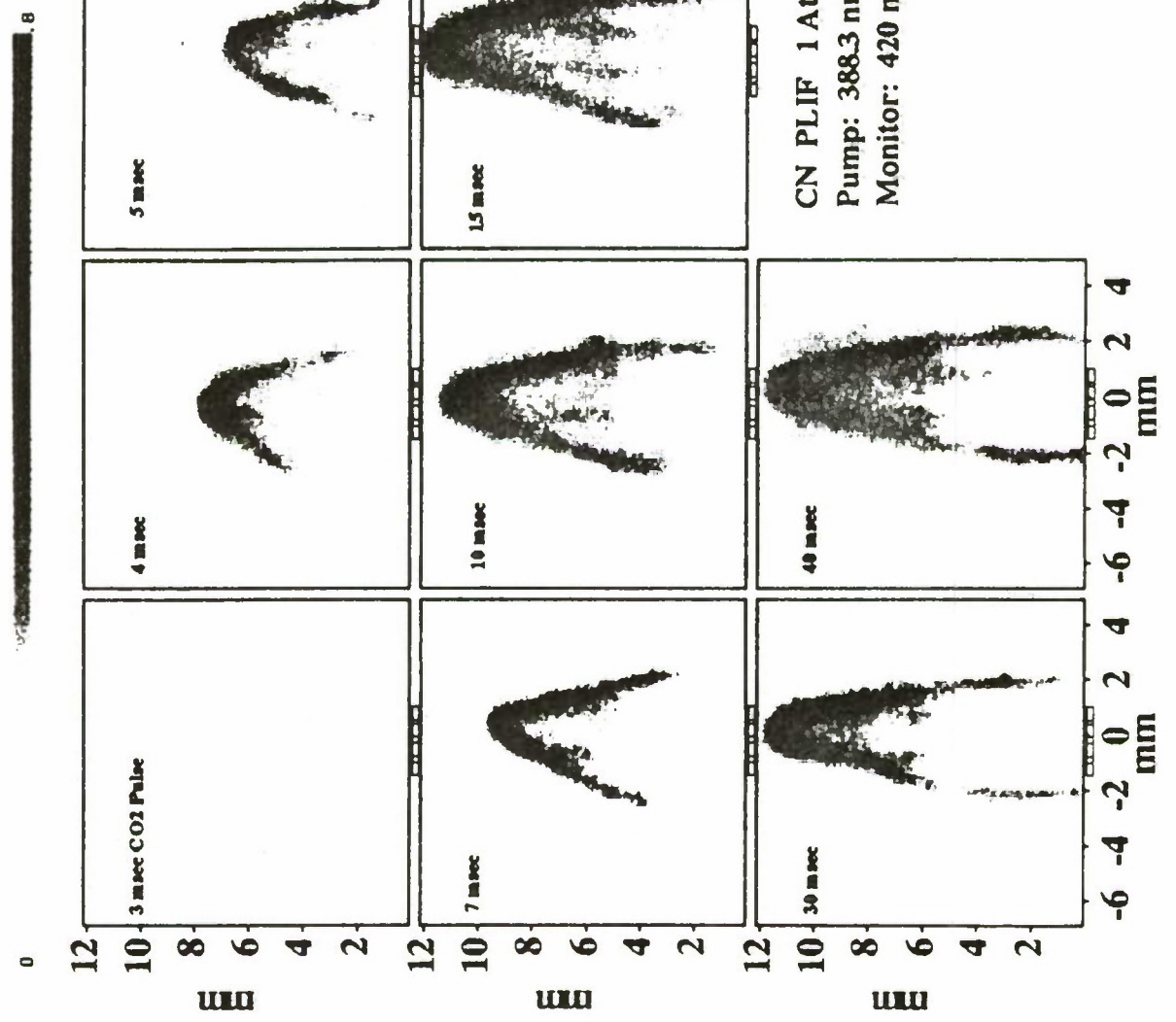
3 msec CO2 Pulse
4 msec
5 msec
7 msec
10 msec
15 msec
30 msec
40 msec
mm
mm
CN PLIF 1 Atm Air
Pump: 388.3 nm
Monitor: 420 nm (10 nm FWHM)

MICROCOMPOSITE PROPELLANT FLAME MICROSTRUCTURE

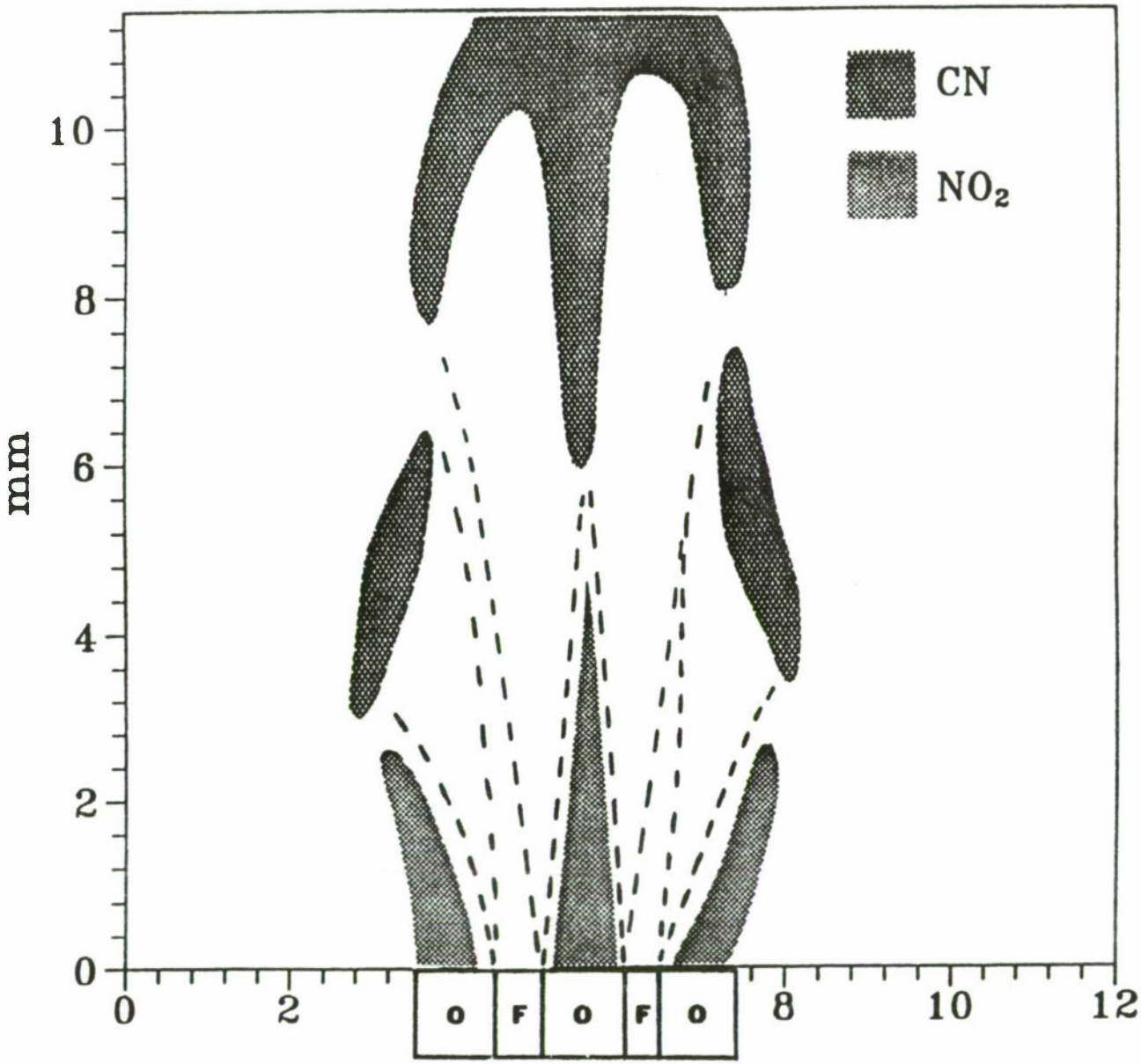

DISCOVERED RADICAL BACKDIFFUSION SHOULD BE INCLUDED IN SOLID COMBUSTION SIMULATIONS

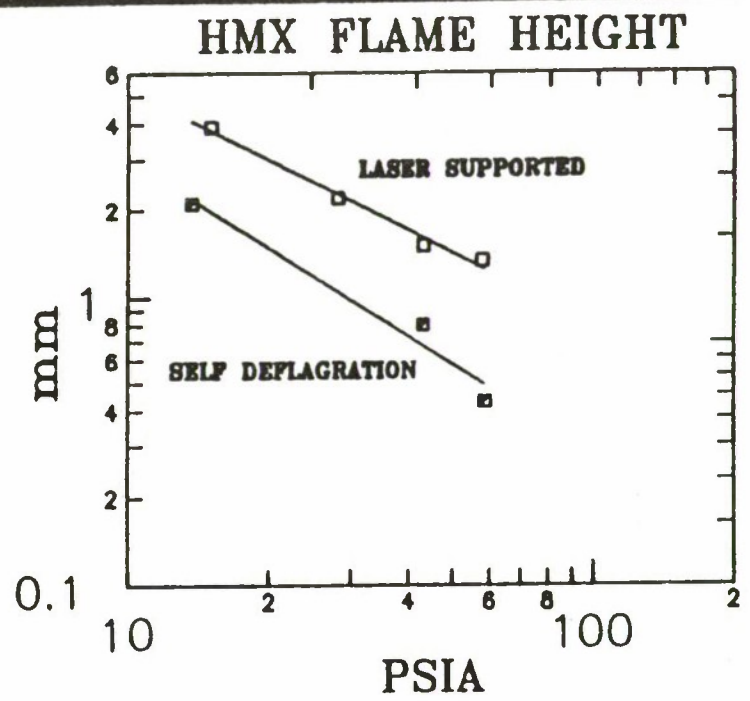

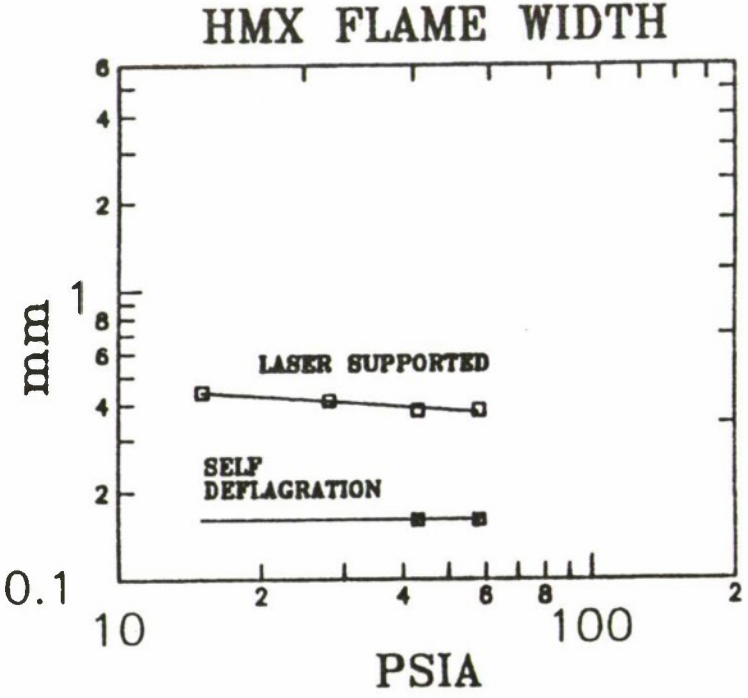

- *AS PRESSURE RISES FLAME SHEET HEIGHT DROPS SHARPLY BUT FLAME SHEET THICKNESS DOES NOT*
- *AT ROCKET MOTOR PRESSURES THICKNESS WILL INCLUDE SURFACE AND RADICAL ATTACK ON SURFACE MUST BE INCLUDED IN SIMULATIONS*

DRS. TIM & DONNA PARR @ NWC

SUMMARY

- **STUDIED NEAT NITRAMINES, COMPOSITE, SANDWICHES**
- **SPATIALLY AND TEMPORALLY RESOLVED CONCENTRATION PROFILES**
  NO_2 NO CN NH OH H_2CO CH C_2 ALL 2D
- **STATE RESOLVED POPULATION DISTRIBUTIONS**
  OH NO CN T_r PROFILES inc 2D
- **50 μm RESOLUTION (COULD BE < 20 μm)**
- **DEMONSTRATED TO 4 atm (PLAN > 10 atm)**
- **CALIBRATED CONC. via UV/Vis ABSORPTION**
  NO_2 NO CN OH
- **CONDENSED PHASE AND NEAR SURFACE TEMPERATURE PROFILES**
- **CONTROLLED HEATING FLUX FOR TRANSIENT COMBUSTION, IGNITION, OSCILLATORY COMBUSTION with TEMPORALLY RESOLVED DIAGNOSTICS**
- **PROPELLANT DIFFUSION FLAME STRUCTURE DIRECTLY IMAGED**

Our results along with Stufflebeam (UTRC), Edwards (AFAL), Vanderhoff (BRL), and other research groups in the US, France, Netherlands, and the Soviet Union are beginning to lead to an understanding of solid propellant combustion on a fundamental level and providing data for direction and validation of modeling efforts.

E. Price

Kinetically Limited Leading Edge of Diffusion Flames (KLLEFs)

KINETICALLY LIMITED LEADING EDGE of DIFFUSION FLAMES (KLLEFs)

Prof. ED PRICE
Georgia Institute of Technology

(Presented by Tim Parr, NWC)

- INTRODUCTION
- METHANE/AIR DIFFUSION FLAME EXPERIMENTS
- METHANE/AIR DIFFUSION FLAME MODELING
- COMPOSITE PROPELLANT RESPONSE PREDICTIONS AND EXPERIMENTAL VALIDATION

OSCILLATORY PROPELLANT BURNER TESTS SHOW CRITICAL ROLE OF KLLEF STABILITY

O RESPONSE FUNCTION SHOWS A LARGE PEAK AROUND 250 PSI

O A PREDICTED SINGULAR "BLOW OFF" RESPONSE OF KLLEFS WAS CONFIRMED THAT HAD BEEN PREDICTED

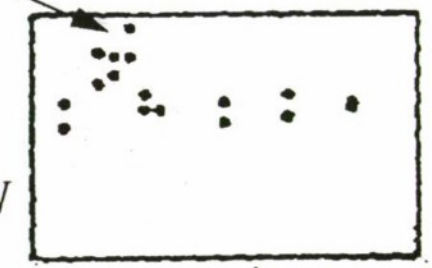

109

KLLEF AT 3 PRESSURES

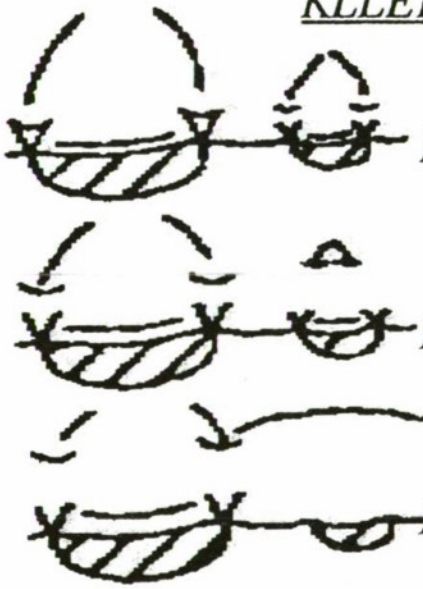

O BIMODAL AP/PBAN PROPELLANTS DESIGNED TO SHOW ROLE OF KLLEF

O NWC PREPARED PROPELLANTS

0 T- BURNER AT NWC USED TO ESTABLISH RESPONSE FUNCTION

O DYNAMIC COMBUSTION RESPONSE WAS DETERMINED AT TWO FREQUENCIES OVER A WIDE RANGE OF PRESSURES

PROF. EDWARD PRICE @ GEORGIA TECH

1/21/91

07/25/91

KINETICALLY LIMITED LEADING EDGE DIFFUSION FLAMES (KLLEF'S)

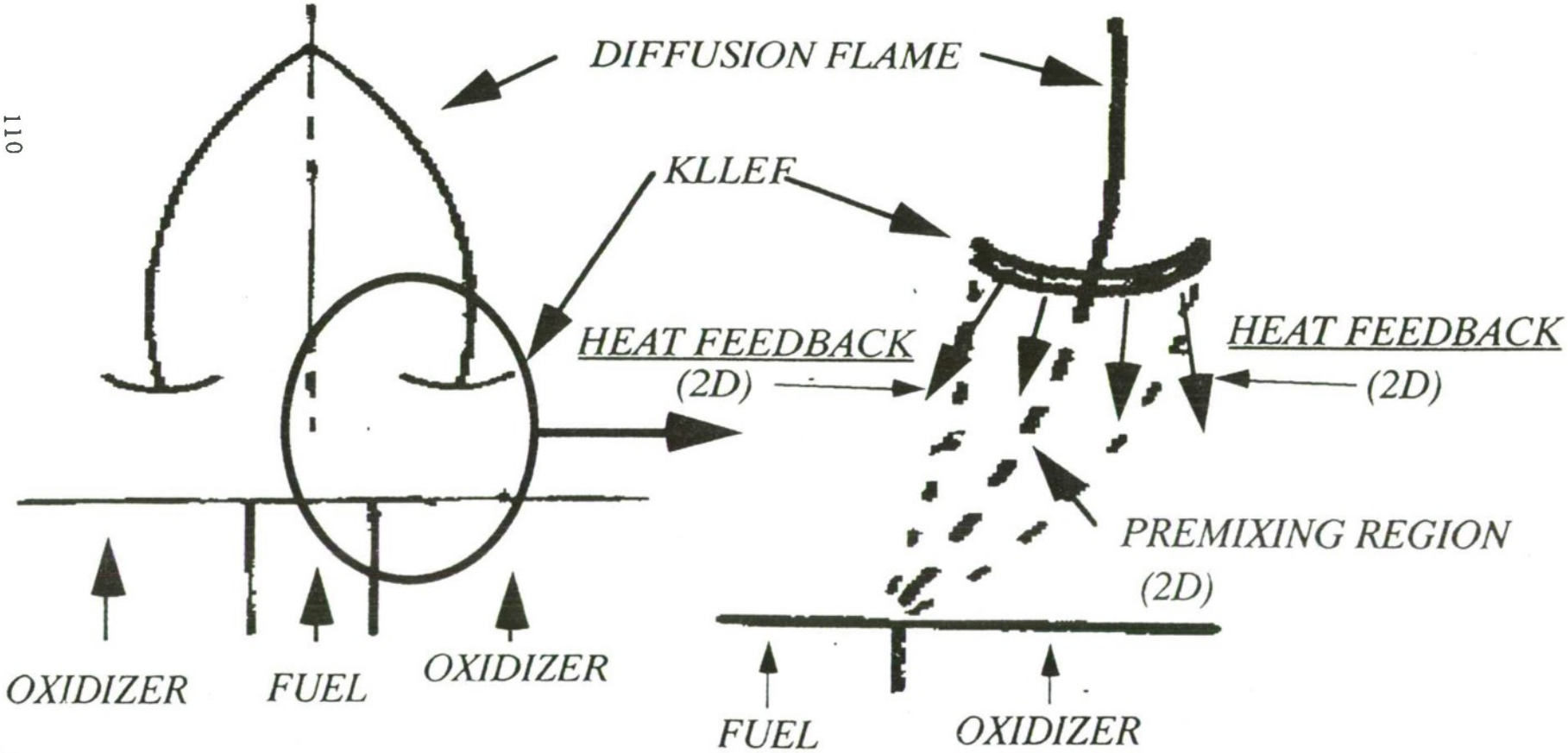

CONCLUSIONS OF PRICE KLLEF PHENOMEOLOGICAL MODEL:

O HEAT FLOW FROM OUTER CLASSICAL DIFFUSION FLAME SHOWN TO BE A MINOR CONTRIBUTION THEAT TRANSFER

O FLAME SPEED IS MUCH LESS THAN INFLOW GAS SPEED INTO THE LEADING EDGE FLAME

O DIVERGENCE OF FLOW AROUND KLLEF GENERATED PRESSURE PEAK AFFECTS LEF POSITION

O LATERAL HEAT LOSSES IN 2-D FLAME DOMINATE THE FLAME STANDOFF DISTANCE AND THE CORRESPONDING MIXING TIMES

O QUALITATIVE AND QUANTITATIVE MODELLING OF KLEEF IS ESSENTIAL T O THE PREDICTION AND CONTROL OF BURNING IN HETEROGENEOUS SYSTEMS

C.F. Melius

Thermochemistry and Reaction Mechanisms

The Thermochemistry and Reaction Mechanisms of Decomposition of Energetic Materials*

Carl F. Melius
Combustion Research Facility
Sandia National Laboratories
Livermore, CA 94550

Abstract

The decomposition mechanism of energetic materials have been studied theoretically using detailed chemical kinetics models. The thermochemistry of the intermediate molecular species as well as the reaction pathways are determined using the BAC-MP4 quantum chemistry method. Examples are given for the ignition of nitromethane and the cyclic nitramine, RDX. Differences between the cyclic nitramines and caged nitramines due to hydrogen content of the energetic material are discussed. Formalisms have been developed for treating non-idealities of high pressure and condensed phase solvation. Results for water-catalyzed reactions are presented.

Introduction

The decomposition of energetic materials represents a hostile environment of high temperatures and pressures and short time scales. While it is difficult to experimentally study the molecular processes of decomposition under these conditions, these processes are computationally accessible to theoretical chemistry and detailed chemical kinetics modeling. The ability to model energetic materials requires a knowledge of the thermochemical properties of the initial energetic compound as well as those of the intermediates formed during the decomposition process. From the thermochemical properties, one can determine the bond dissociation energies of a molecular species and its subsequent intermediates. One can also determine reaction pathways and the activation energies involved in going from reactants to products. In this paper, we use the BAC-MP4 (Bond-Additivity-Corrected Møller-Plesset 4th order perturbation theory) quantum chemical procedure[1] to investigate dissociation energies of various energetic molecules and decomposition pathways for various energetic materials, including nitromethane and nitramines[2]. Finally, we present a formalism for treating non-ideal gas effects in the detailed kinetics modeling.[3]

Bond Energies of Nitro Groups

In Table I, we present the bond dissociation energies for selected nitro compounds involving C-NO_2 and N-NO_2 compounds. We find that the R_2N-NO_2 compounds (nitramines) have weaker bond strengths than the R_3C-NO_2 compounds. Also, nitramine (NH_2NO_2), methyl nitramine (CH_3NHNO_2), and dimethylnitramine ($(CH_3)_2NNO_2$) have similar N-NO_2 bond dissociation energies (~ 47-51 kcal-mol-1),

*This work supported by the Office of Naval Research under contract N00014-90-F-0078.

even when strain energy is introduced, such as in N-nitro azetidine. This indicates that group-additivity concepts can be applied to estimating heats of formation of larger nitramine compounds.

On the other hand, neighboring groups can affect the bond dissociation energy for the C-nitro class. Replacing a hydrogen atom of nitromethane by a methyl or amino group has little effect on the BDE. Replacing the hydrogens by an imino (C=N) double bond also has little effect on the BDE. Thus, it is surprising to find that oxynitrotriazole, which has a neighboring amino and imino bond has increased its nitro bond energy by ~13 kcal-mol^{-1}. This is comparable to the increase in the C-NO_2 bond energy due to a neighboring C=C double bond.

Table I. Calculated bond dissociation energies for various nitro compounds. BDE's are determined from BAC-MP4 heats of formation at 298 K. (Energies in kcal-mol-1.)

C-Nitro Compounds		N-Nitro Compounds	
CH_3--NO_2	58.9	NH_2--NO_2	51.4
C_2H_5--NO_2	60.8	CH_3NH--NO_2	50.6
NH_2CH_2--NO_2	59.2	$(CH_3)_2N$--NO_2	47.2
HN=CH--NO_2	59.8		50.6
CH_2=CH--NO_2	70.2		
Oxynitrotriazole	71.8		

Nitromethane Ignition

The detailed chemical kinetics modeling approach is used to study the chemistry of nitromethane ignition and detonation[2]. The chemical reaction mechanism included 35 species and 150 elementary reactions. In Fig. 1, we present the temperature, pressure, and species profiles as a function of time for the ignition of CH_3NO_2 at 6.85 atmospheres and 1202 K, representative of the experimental conditions in Ref. 4. We see from the figure that the overall reaction chemistry of the first stage ignition is primarily

$$2\ CH_3NO_2 \rightarrow CH_3OH + CH_2O + 2\ NO, \qquad \Delta H_{Rxn} = +1.9 \qquad (R1)$$

with the later conversion of formaldehyde to carbon monoxide

$$CH_2O \rightarrow CO + H_2. \qquad \Delta H_{Rxn} = -0.5 \qquad (R2)$$

The reactions are essentially thermoneutral, yielding very little temperature rise. The increase in pressure arises from the conversion of one mole of nitromethane into

two moles of intermediates. The overall reaction, which reduces the free energy, is driven by the increase in entropy of phase space resulting from the increase in the number of molecules formed. The majority of heat release in nitromethane occurs in the second stage ignition which converts NO to N_2. A reaction flow diagram for the first stage ignition is given in Fig. 2. In nitromethane, the conversion of CH_3O to CH_3OH and CH_2O provides the source of heat for the short (microsecond) first ignition stage, after which CH_3OH is converted back to CH_2O and then to CO during the first stage ignition. We find the same role of CH_3OH occurring in methyl nitrate ignition. In Fig. 3 we present the temperature, pressure, and species concentration profiles as a function of time for nitromethane following shock detonation. The time is plotted on a logarithmic scale in order to see both the first and second stages of ignition. The main difference in the chemistry from that in the low pressure, constant volume ignition is that more of the CH_2O is converted to CO and H_2 under detonation conditions. It is important to note that in the detonation process, the time scale for the chemical reactions to occur for the decomposition and first stage of ignition is hundreds of picoseconds.

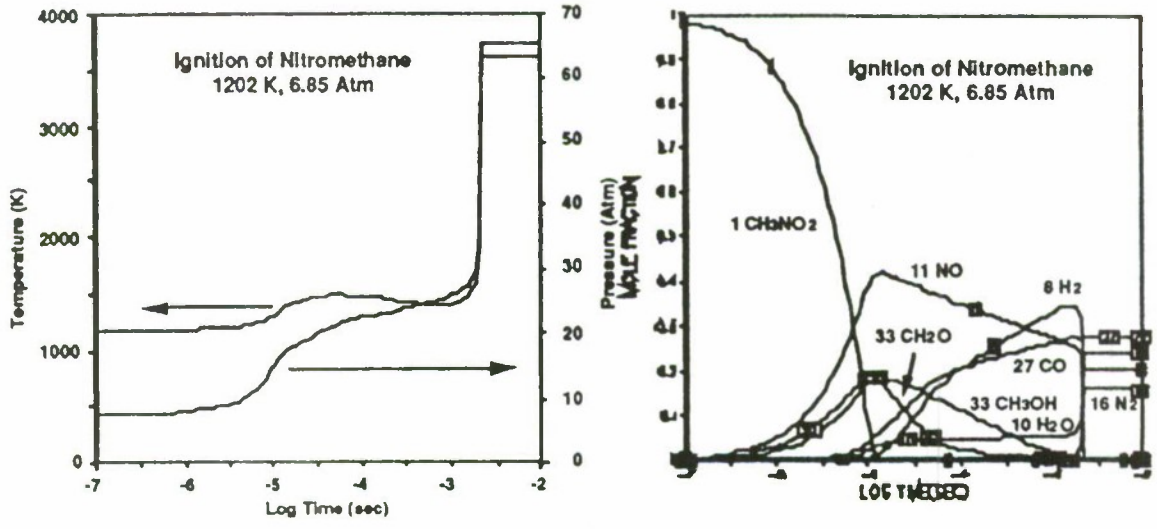

Fig. 1. Temperature and major species concentration (mole fraction) profiles as a function of time for the ignition of nitromethane in a shock tube. Starting conditions were 1202 K and 6.85 atm.

Decomposition Reaction Mechanism for the First Stage Ignition of CH_3NO_2

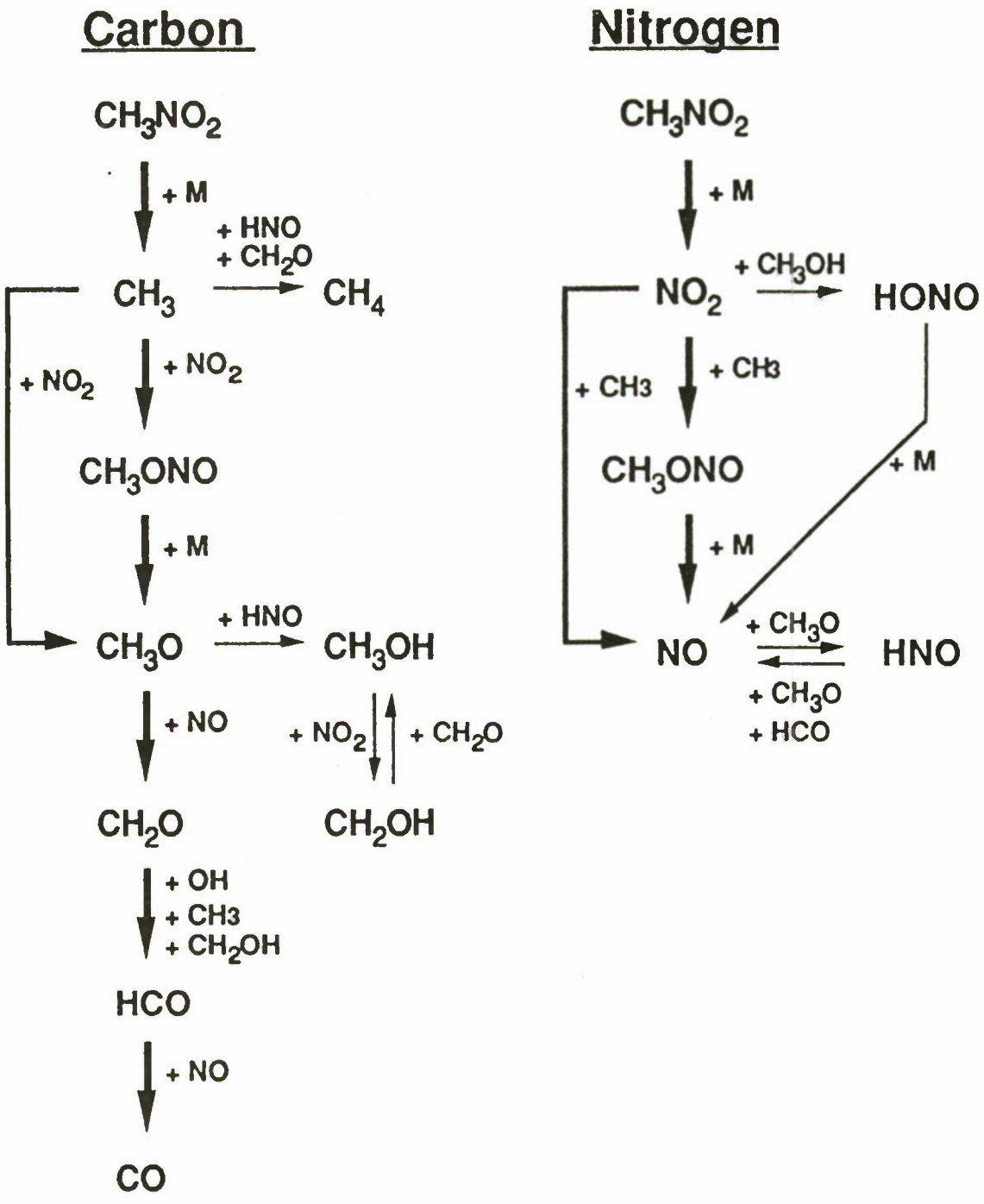

Fig. 2. Reaction mechanism diagrams for the carbon-containing and nitrogen-containing species during the ignition of nitromethane. Starting conditions are 1202 K and 6.85 atm. Unimolecular decomposition is indicated by the third-body notation +M. Thick arrows indicate major reaction pathways.

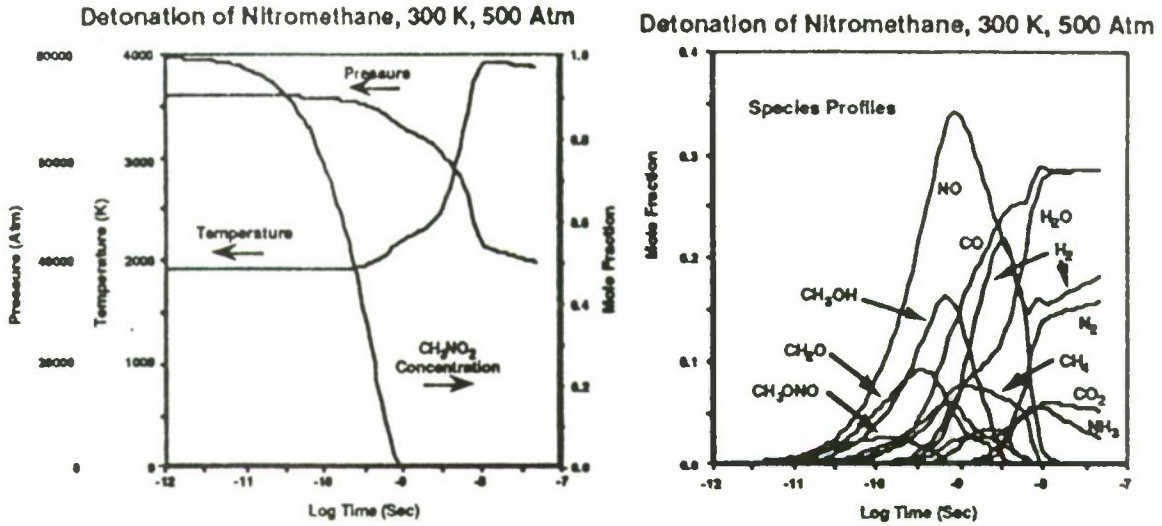

Fig. 3. Temperature and major species concentration (mole fraction) profiles as a function of time for the detonation of nitromethane. Starting conditions were 300 K and 500 atm.

RDX Flame

We have solved the one-dimensional flame problem, including mass and species diffusion as well as detailed kinetics modeling, to study the reaction chemistry of an RDX flame.[2,5] The resulting temperature and species profiles as a function of distance above the gas/solid surface of the steady-state RDX flame at 1 atm are given in Fig. 4. In Fig. 5, we present the chemical reaction flow diagrams for the RDX flame. The results indicate two-stage flame chemistry. The OH radical dominates the primary zone chemistry. The thermal decomposition of HONO provides the source of OH radicals in the primary flame. HONO plays an analogous role to CH_3OH in nitromethane by providing a temporary source of heat for the first stage ignition. The HONO is formed from NO_2 by reactions with weakly bound hydrogenated species, such as H_2CN, CH_2O, and HCO. Since the C-H bond in HCN is very strong, the majority of HCN remains until the second oxidation stage zone. The N_2O formed during the initial decomposition stage also remains relatively inert until the high temperature second oxidation stage.

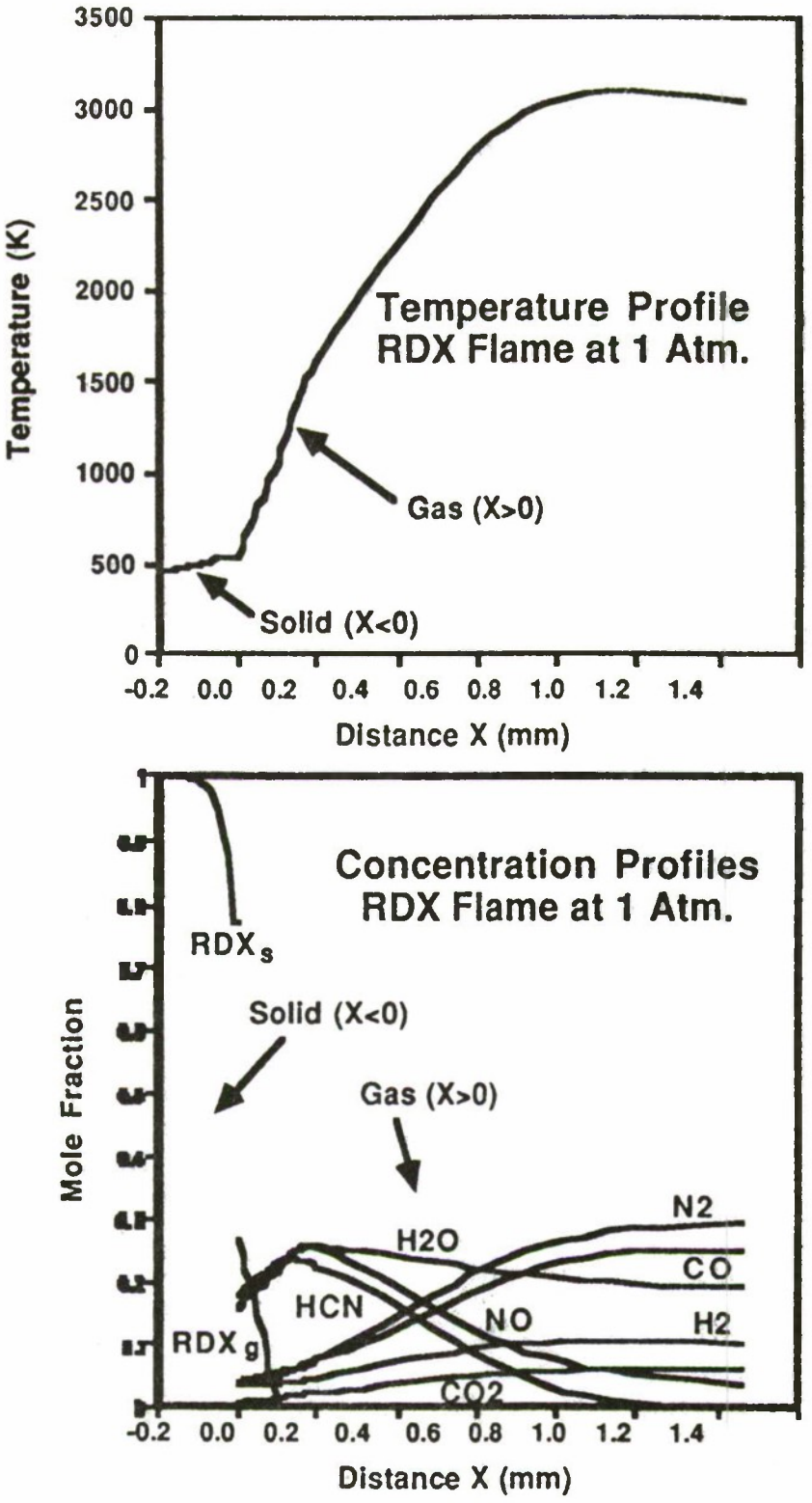

Fig. 4. Temperature and species concentration (mole fraction) profiles as a function of distance (mm) for the RDX flame at 1 atm. Origin corresponds to the gas-solid interface.

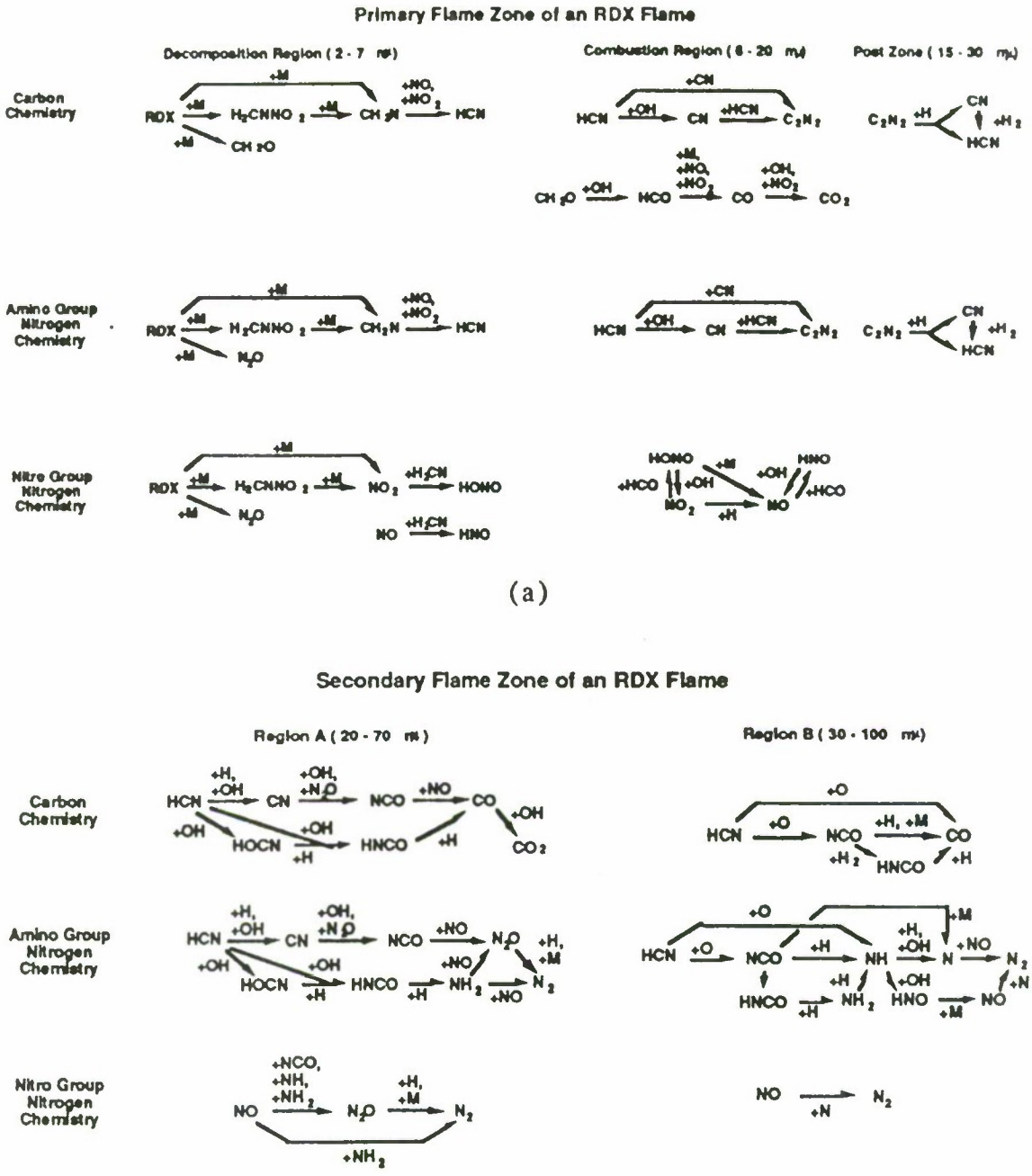

Fig. 5. Chemical reaction flow diagrams for the (a) primary and (b) secondary stages (or zones) in the RDX flame at 17 atm. The spatial extent of the zones is indicated by the distances given in μm. We have separately indicated the reaction chemistry of the carbon species, the nitrogen species of the amino group of the RDX ring, and the nitrogen chemistry of nitro group of RDX. A similar reaction flow diagram exists for other flame pressures except that the distances must be scaled. Thick arrows indicate major pathways, while thin arrows indicate minor pathways.

HCN / NO_2 Flame

To understand the difference in chemistry between cyclic nitramines and caged nitramines, we have developed a detailed chemical kinetics model of the HCN/NO_2 flame.[6] In collaboration with M. C. Lin, we have been combining experiments with BAC-MP4 calculations and detailed chemical kinetics modeling to develop improved chemical reaction mechanisms.[7] Unlike RDX, the hydrogen content for this system is half as much, i.e., $C_1H_1N_2O_2$ vs. $C_1H_2N_2O_2$. Several changes were made in the chemical reaction mechanism, including the new species NCN. Based on BAC-MP4 calculations, we have included possible reaction steps involving the NCN radical within the overall reaction mechanism. The resulting chemical reaction flow diagram is shown in Fig. 6.

Comparing the HCN / NO_2 flame with the RDX flame, we find that the reaction mechanisms in the HCN / NO_2 flame resemble primarily the secondary flame chemistry of RDX. This is not surprising, since the primary flame chemistry of RDX involves the formation and decomposition of HONO. For the HCN / NO_2 flame, there is only one hydrogen atom per NO_2 group (as typical for the caged nitramines), while RDX and HMX have two hydrogen atoms per NO_2 group. The extra hydrogen in the case of RDX and HMX is readily extracted by the NO_2 to form HONO. The decomposition of the HONO to form OH radicals generates the radical pool responsible for the first stage flame chemistry. On the other hand, the hydrogen in HCN is strongly bound, so HONO cannot be readily formed. The hydrogen is not available until after oxygen atoms are produced. Thus, we expect the combustion chemistry of caged nitramines to be similar to that of HCN / NO_2 flames but significantly different from that of the cyclic nitramines, RDX and HMX.

Real-Gas Effects on Chemical Thermodynamics and Reaction Mechanisms

The stability of decomposition intermediates as well as the reaction mechanisms will be affected by the real-gas behavior of high pressures and condensed phases. We have recently developed a procedure using equations of state whose critical properties could be obtained theoretically from the BAC-MP4 method.[3] The procedure uses transition state theory to treat transition state structures as additional species whose thermodynamic properties can be determined using the same equations of state. The relationship between the real gas partial molar Gibbs energy μ_i, the pure species ideal gas Gibbs energy μ_i^o (equal to the standard Gibbs energy of formation $\Delta G^o_{f\,298}$ computed by the BAC-MP4 method), and the partial molar departure functions μ_i^D (computed from the equation of state) is given by:

$$\mu_i = \mu_i^o + RT\, ln\, (P / P^o) + \mu_i^D + RT\, ln\, x_i = G_i^* + RT\, ln\, x_i, \qquad (7)$$

where x_i is the mole fraction of species i and G_i^* is an effective Gibbs energy for a species in the high-density environment.

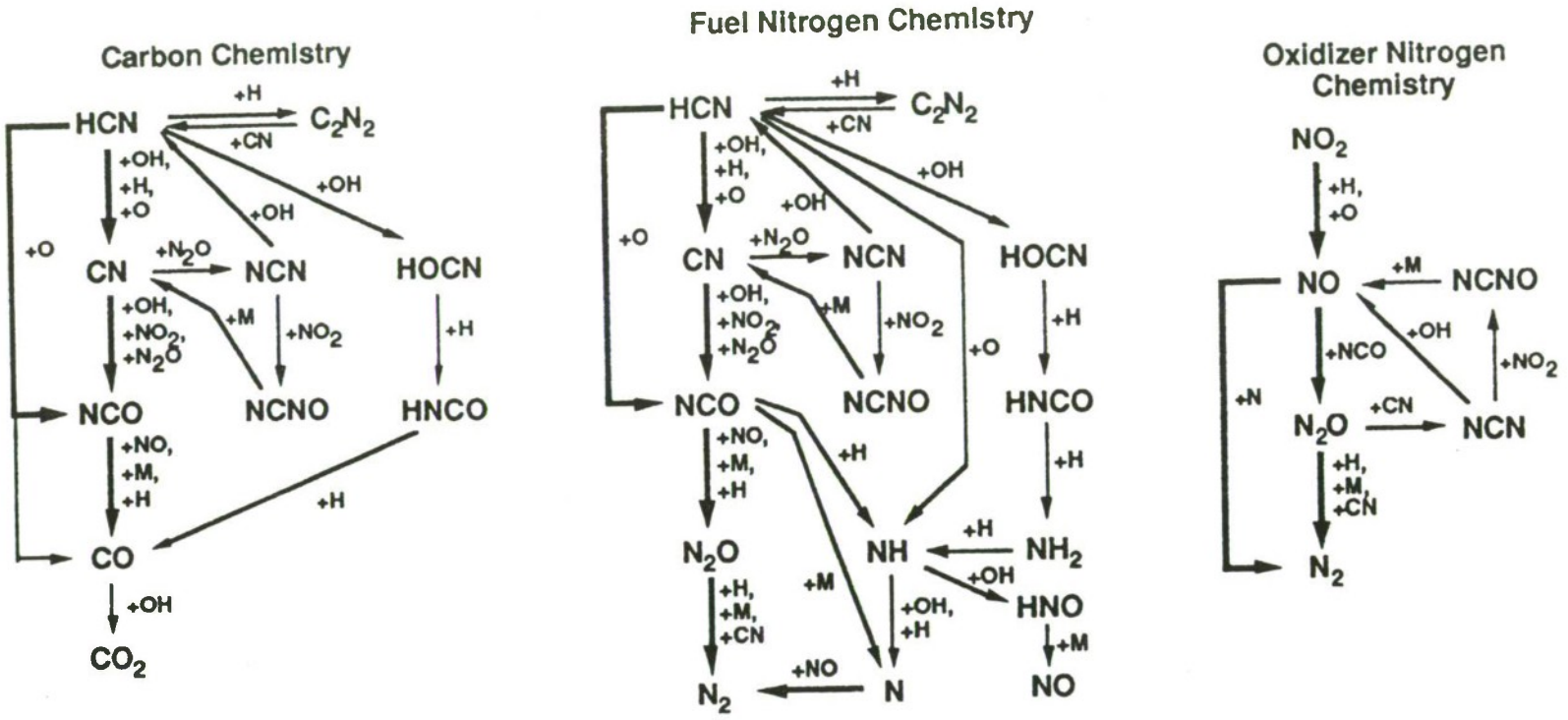

Fig. 6. Reaction flow diagrams for various chemical species occurring in a 1 : 1 HCN / NO_2 flame (ϕ = 1.24) at 25 torr. Shown separately are the pathways for (a) the carbon, (b) the fuel-bound nitrogen, arising from HCN, and (c) the nitrogen arising from the oxidizer, NO_2. The thick arrows indicate major pathways while the thinner arrows indicate other pathways.

Parameters for the critical volumes and critical temperatures of transition state structures and other molecules are obtained from scaling relations based on the atomic charges within the molecule. The resulting heats of formation, $\Delta H^{o}_{f\,298}$, and free energies, $\Delta G^{o}_{f\,298}$, for the OH + H_2 → H_2O + H reaction are given in Table II and Fig. 7. The results indicate that the transition state is intermediate in polarity between reactants and products. We have developed a solvation model based on the boundary-element method[8] to obtain solvation energies and volume parameters. Preliminary results for the H + HN_3 → H_2 + N_3 are given in Table III. The results indicate a trade-off between the solvation effect, which assists the reaction, and the volume effect, which hinders the reaction at high pressure..

Table II. Changes in chemical potential for the reaction H + H_2O ⇄ H_2 + OH, relative to reactants (energies in kcal-mol^{-1}) for two different temperature and pressure regimes.

	298 K, 1 Atm.				700 K, 300 Atm.				
	$\Delta\mu^o$	$\Delta\mu^D$	ΔG^*	ΔV	$\Delta\mu^o$	$\Delta\mu^{IG}$	$\Delta\mu^D$	ΔG^*	ΔV
TS	23.0	-4.2	18.9	-6	31.6	23.7	-0.7	23.0	-366
Products	14.9	3.3	18.1	+12	14.3	14.3	0.5	14.7	+108

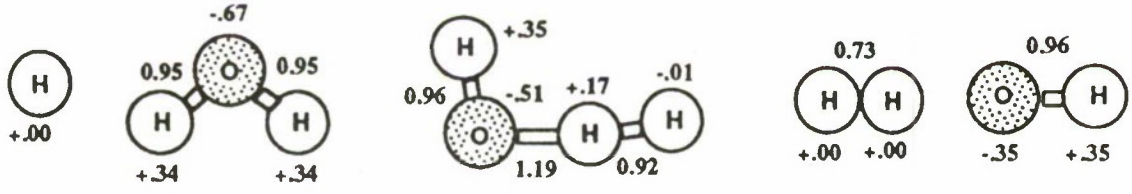

Fig.7. Geometries and atomic charges for the reaction H + H_2O ⇄ H_2 + OH,

---

Table III. Condensed Phase Effects on H + HN_3 → H_2 + N_3. Volumes, surface areas, and free energies of cavitation and electrostatic solvation are given for the reactants, transition state, and products.

Species:	H		HN_3	TS		H_2		N_3
Volume (Å^3):	7.0		47.8	67.9		10.7		44.1
		0.0			+13.1		-0.0	
Area (Å^2):	17.7		59.6	68.2		23.1		56.8
		0.0			-9.1		+2.6	

Free Energy (Kcal-mol^{-1}):

Cavitation	1.9	6.4	7.4	2.5	6.1
	0.0		-1.0	+0.3	
Electrostatic	0.0	-4.5	-3.6	0.0	-2.1
	0.0		+0.9	+2.5	

Water-assisted Reactions

During the initial stages of decomposition in the condensed phase, the formation of water can autocatalyze the decomposition process through hydration and hydrolysis. For example, the transition state structures for the breaking of the C-N bond is indicated in Fig. 8. The concerted proton transfer among several water molecules along with the increased ionic character of the transition states significantly lowers the activation energies of the reaction.[9]

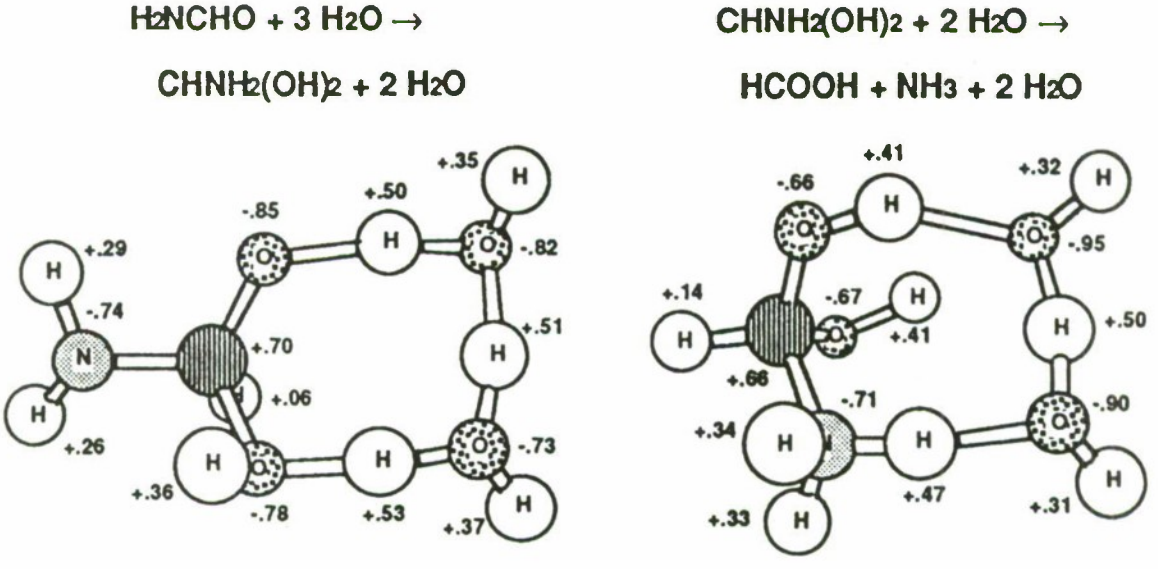

Fig. 8. Transition state structures and atomic charges for the hydrolysis of formamide to formic acid, corresponding to the breaking of the C-N bond. The additional water molecules autocatalyze the reaction. The increased ionic charges on the hydrogen atoms undergoing proton transfer enhance the solvation energy, thereby lowering the activation energy of reaction.

Conclusions

The BAC-MP4 quantum chemistry method and detailed kinetics modeling has been used to investigate the decomposition mechanism of energetic materials at the

molecular level. Thermochemical properties of intermediate species and transition state structures are used to determine initial bond breaking in energetic molecules. Chemical kinetics modeling using these results provide reaction pathways by which decomposition and oxidation during ignition and deflagration occur. These results can be used to understand the processes that will occur in new energetic materials under development.

References

[1]C. F. Melius; "Thermochemical Modeling: I. Application to Decomposition of Energetic Materials;" in Chemistry and Physics of Energetic Materials;" NATO ASI **309**, p. 21, S. Bulusu, ed., 1990.

[2]C. F. Melius; "Thermochemical Modeling: II. Application to Ignition and Combustion of Energetic Materials;" in Chemistry and Physics of Energetic Materials;" NATO ASI **309**, p. 51, S. Bulusu, ed., 1990.

[3]C. F. Melius, N. Bergan, and J. E. Shepherd, "Effects of Water on Combustion Kinetics at High Pressure," *Twenty-Third Symposium (International) on Combustion* (The Combustion Institute, Pittsburgh, PA, 1990), in press.

[4]R. Guirguis, D. Hsu, D. Bogan, and E. Oran, Comb. and Flames 61, 51 (1985).

[5]C. F. Melius, Proceedings of the 25th JANNAF Combustion Meeting, Vol. II, p. 155, October 1988.

[6]L. R. Thorne and C. F. Melius, "The Structure of Hydrogen Cyanide-Nitrogen Dioxide Premixed Flames," *Twenty-Third Symposium (International) on Combustion* (The Combustion Institute, Pittsburgh, PA, 1990), in press.

[7]C.-Y. Lin, H.-T. Wang, M. C. Lin, and C. F. Melius, "A Shock Tube Study of the $CH_2O + NO_2$ Reaction at High Temperatures," Int'l. J. Chem. Kinetics, **22**, p. 455, 1990; H. K. Aldridge, X. Liu, M. C. Lin, and C. F. Melius, "Thermal Unimolecular Decomposition of 1,3,5-Trioxane: Comparison of Theory and Experiment", Intern. J. Chem. Kinetics, 1990, in press; Y. He, X. Liu, M. C. Lin, and C. F. Melius, "The Thermal Reaction of HNCO at Moderate Temperatures,", Int'l. J. Chem. Kinetics, submitted.

[8]R. J. Zauhar and R. S. Morgan, "The Rigorous Computation of the Molecular Electric Potential," J. Comp. Chem. **9**, 171 (1990).

[9]B. C. Garrett and C. F. Melius, Variational Transition State Theory Calculations of Concerted Hydrogen Atom Tunneling in Water Clusters and Formaldehyde/Water Clusters," in Theoretical and Computational Models for Organic Chemistry, NATO ASI, in press.

BAC-MP4 Quantum Chemical Calculations of Thermochemical Data and Reaction Mechanisms

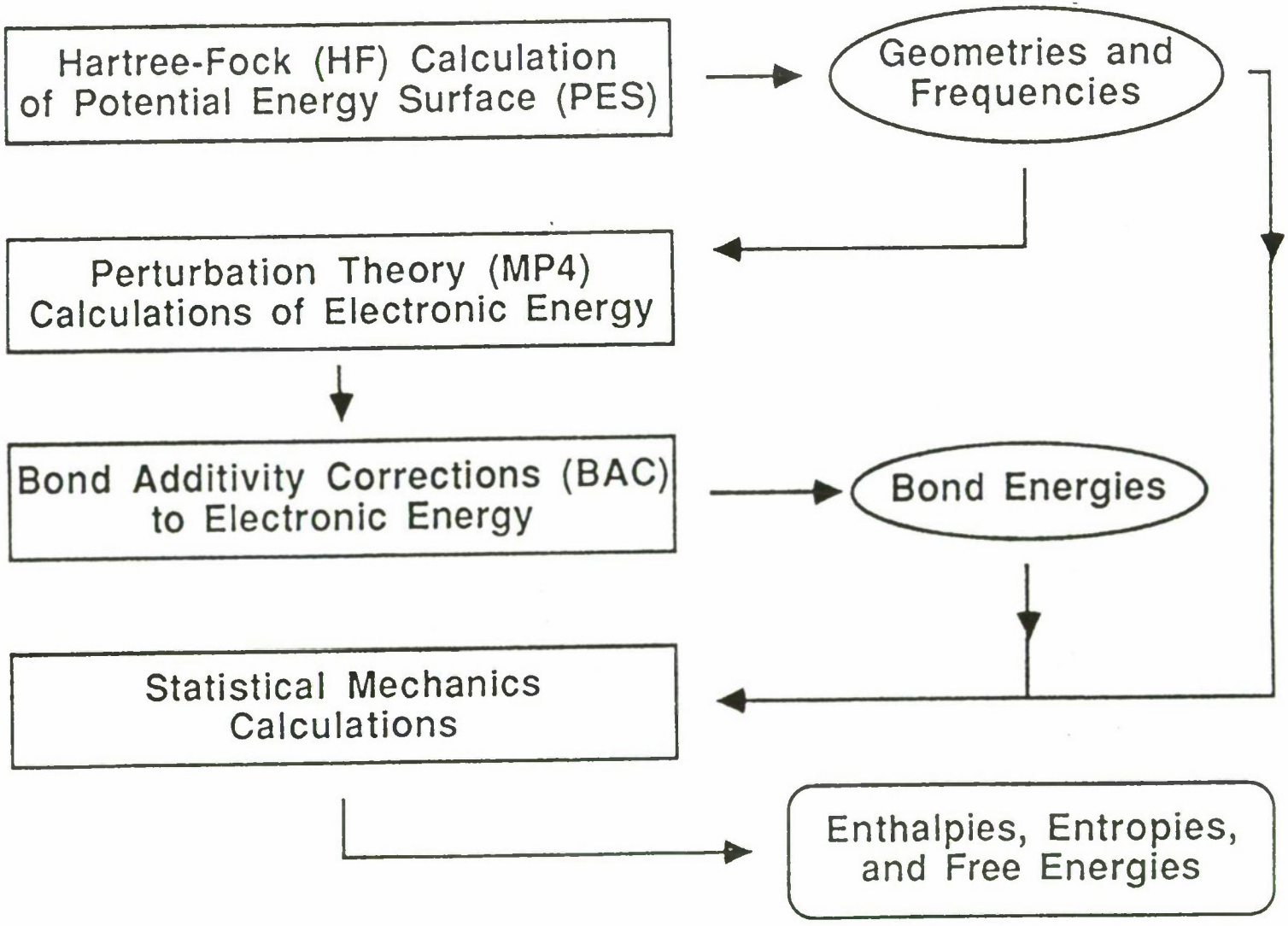

BAC-MP4 Heats of Formation (ΔH^{o}_{f298}'s) Comparisons with Experiments

Molecule	ΔH^{o}_{f298}	Error Est.	Th. - Exp.	Molecule	ΔH^{o}_{f298}	Error Est.	Th. - Exp.
CH_3NO_2	-16.8	2.1	1.0	NO	21.6	1.2	0.0
CH_3ONO	-15.3	1.3	0.3	NO_2	7.1	4.2	-0.8
CH_3ONO_2	-26.1	3.6	2.5	NO_3	22.7	9.5	5.7
$C_2H_5NO_2$	-24.8	1.8	-0.4	OH	9.5	1.1	0.1
$C_6H_5NO_2$	14.2	2.6	-1.5	HO_2	3.6	1.8	1.1
$(CH_3)_2N_2H_2$	21.1	2.1	1.0	CH_3	34.9	1.2	0.1
HONO	-19.1	1.1	-0.8	C_2H_5	28.8	1.3	0.5
$HONO_2$	-30.2	3.9	2.1	NH_2	46.1	1.1	0.6
N_2O	18.6	1.2	-1.0	NH	87.0	1.1	5.1
HN_3	69.5	1.0	-0.9	CN	108.2	6.4	4.2

Energies in kcal-mole^{-1}

Bond Energies for Various C-nitro, N-nitro, and O-nitro Compounds

C-Nitro Compounds

CH_3--NO_2	58.9
C_2H_5--NO_2	60.8
NH_2CH_2--NO_2	59.2
$HN{=}CH$--NO_2	59.8
$HOCH_2CH_2$--NO_2	61.8
O_2N-CH_2CH_2--NO_2	61.1
$CH_2{=}CH$--NO_2	70.2
$CH_3CH{=}CH$--NO_2	69.5
$HOCH{=}CH$--NO_2 (no h.b.)	70.0
$HOCH{=}CH$--NO_2 (h.b.)	77.0
cis-$NH_2CH{=}CH$--NO_2	78.2
trans-$NH_2CH{=}CH$--NO_2	76.5
C_6H_5--NO_2	72.4
O_2N-CH_2--NO_2	55.5
$HC(O)$--NO_2	49.8

H-Nitro Compounds

H--NO_2	73.4

N-Nitro Compounds

NH_2--NO_2	51.4
CH_3NH--NO_2	50.6
$(CH_3)_2N$--NO_2	47.2
 --NO_2	50.6
O_2NNH--NO_2	47.8
$CH_2{=}N$--NO_2	37.1

O-Nitro Compounds

HO--NO_2	46.8
CH_3O--NO_2	39.9

Using BAC-MP4 ΔH_{f298}'s (Energies in kcal-mol-1)

07/25/91

Nitroethane Decomposition

Five-centered Elimination

$$CH_3CH_2NO_2 \rightarrow CH_2CH_2 + HONO \quad \Delta E = 41 \text{ kcal-mol}^{-1}$$

$$k = 10^{11.9} e^{-42.3/RT} \quad \text{near } T = 600K$$

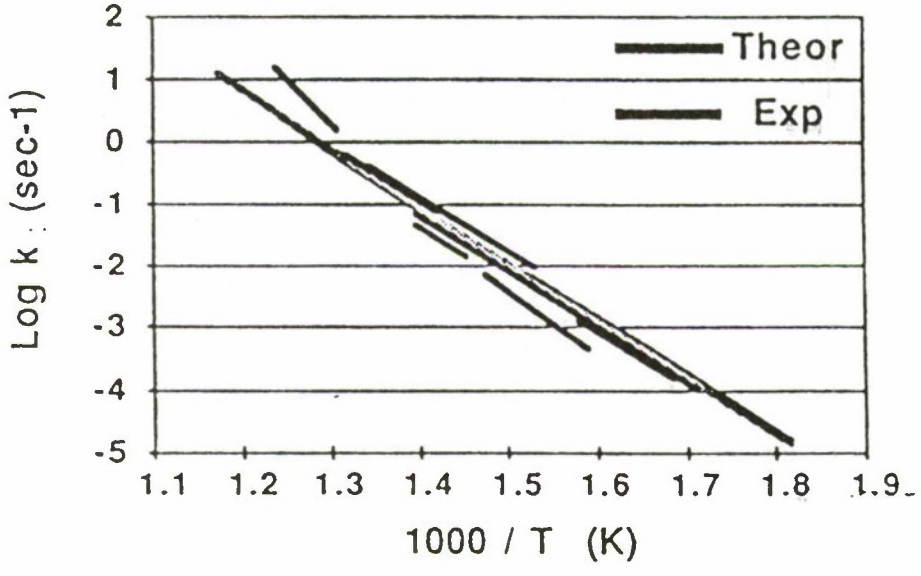

At higher T, C-N bond scission occurs

$$CH_3CH_2NO_2 \rightarrow CH_3CH_2 + NO_2 \quad \Delta E = 58 \text{ kcal-mol}^{-1}$$

(Theoretical rate constant k and activation energies ΔE are based on BAC-MP4 method)

Decomposition of RDX

At Fast Heating Rates

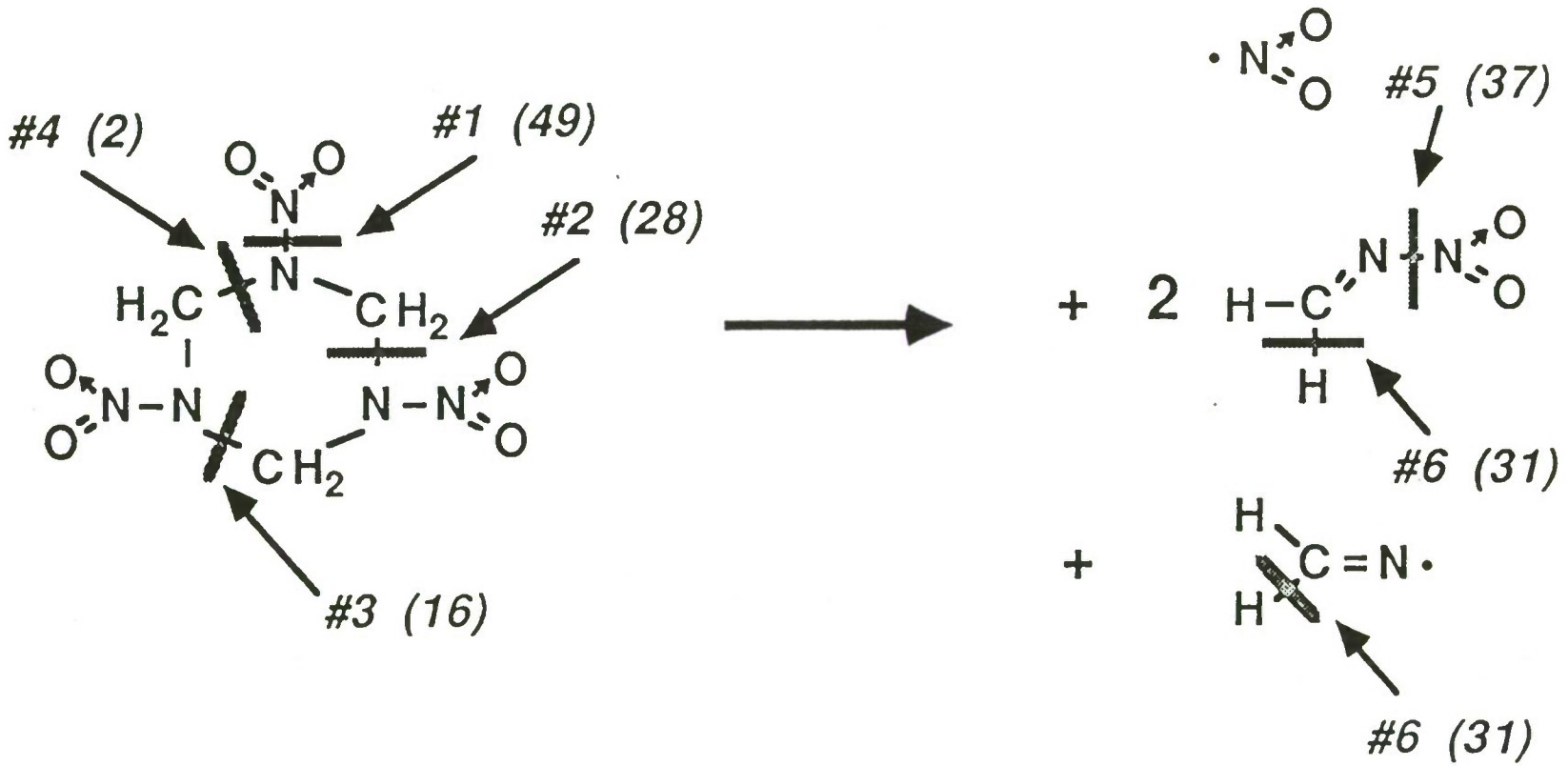

#n (Δ E) : Position, Order, and Energy of Chain Bond Breaking (Energy in kcal/mole)

Modelling of RDX Flame

Gas Phase:

$$\rho_g V_g A = \dot{M} = \text{constant}; \qquad \rho_g = \frac{p \bar{W}}{RT}$$

$$\dot{M} \frac{dT}{dx} = \frac{1}{c_p} \frac{d}{dx} (\lambda_g A \frac{dT}{dx}) - \frac{A}{c_p} \sum_{k=1}^{K} \rho_g Y_k V_k c_{pk} \frac{dT}{dx} - \frac{A}{c_p} \sum_{k=1}^{K} \dot{\omega}_k h_k W_k$$

$$\dot{M} \frac{dY_k}{dx} = - \frac{d}{dx} (\rho_g A Y_k V_k) + A \dot{\omega}_k W_k \quad (k = 1, ..., K)$$

Gas/Solid Interface:

$$\lambda_g \frac{dT^+}{dx} = \lambda_s \frac{dT^-}{dx} + \sum_{k=1}^{K} \rho_g Y_k V_k h_k + \rho_g V_g \Delta H_{vap}$$

$$\rho_s V_s \varepsilon_k - \rho_g V_g Y_k = \rho_g Y_k V_k$$

$$\rho_s V_s = \dot{\omega}_{evap} - \dot{\omega}_{cond}$$

Chemistry: 62 Gas Phase Chemical Species; 353 Chemical Reactions

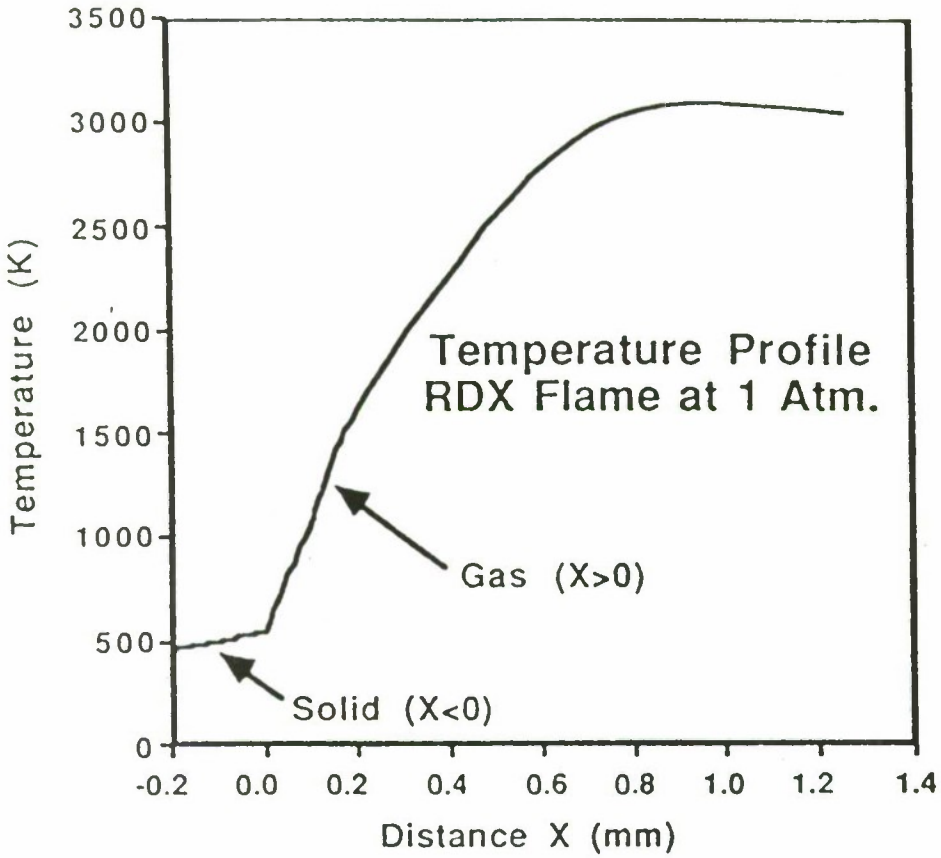
Temperature Profile
RDX Flame at 1 Atm.
Gas (X>0)
Solid (X<0)
Temperature (K)
3500
3000
2500
2000
1500
1000
500
0
-0.2
0.0
0.2
0.4
0.6
0.8
1.0
1.2
1.4
Distance X (mm)

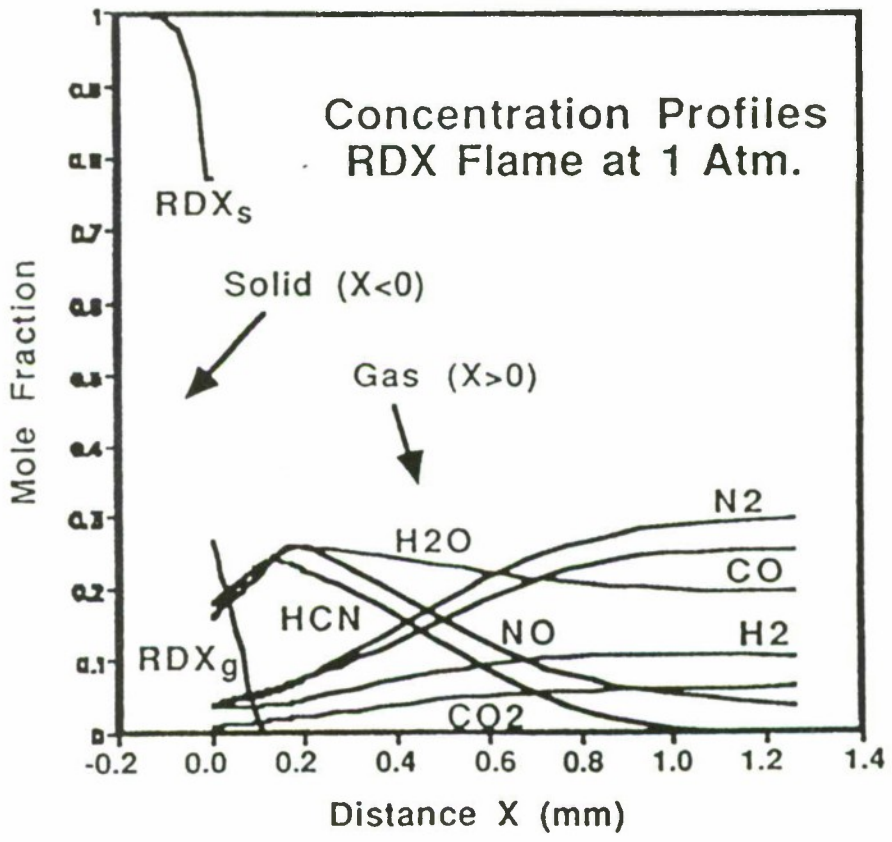
Concentration Profiles
RDX Flame at 1 Atm.
RDXs
Solid (X<0)
Gas (X>0)
N2
H2O
CO
HCN
NO
H2
RDXg
CO2
Mole Fraction
-0.2
0.0
0.2
0.4
0.6
0.8
1.0
1.2
1.4
Distance X (mm)

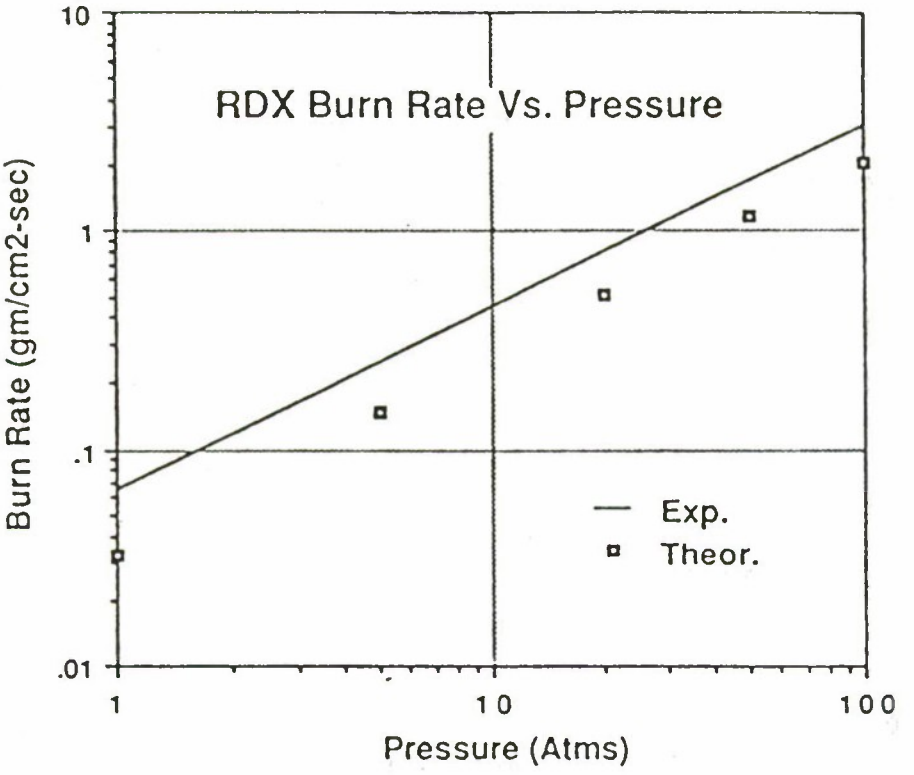
RDX Burn Rate Vs. Pressure
Burn Rate (gm/cm2-sec)
10
1
.1
.01
1
10
100
Pressure (Atms)
Exp.
Theor.

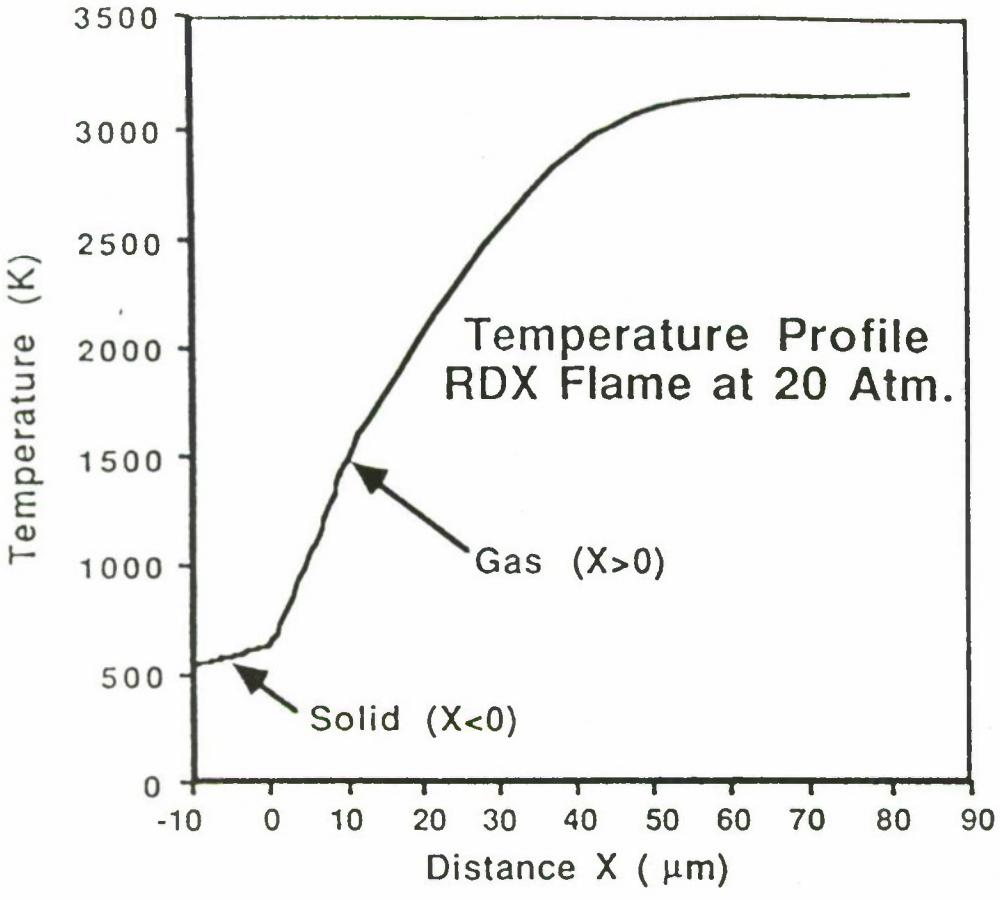
Temperature Profile
RDX Flame at 20 Atm.
Temperature (K)
3500
3000
2500
2000
1500
1000
500
0
Gas (X>0)
Solid (X<0)
-10
0
10
20
30
40
50
60
70
80
90
Distance X (μm)

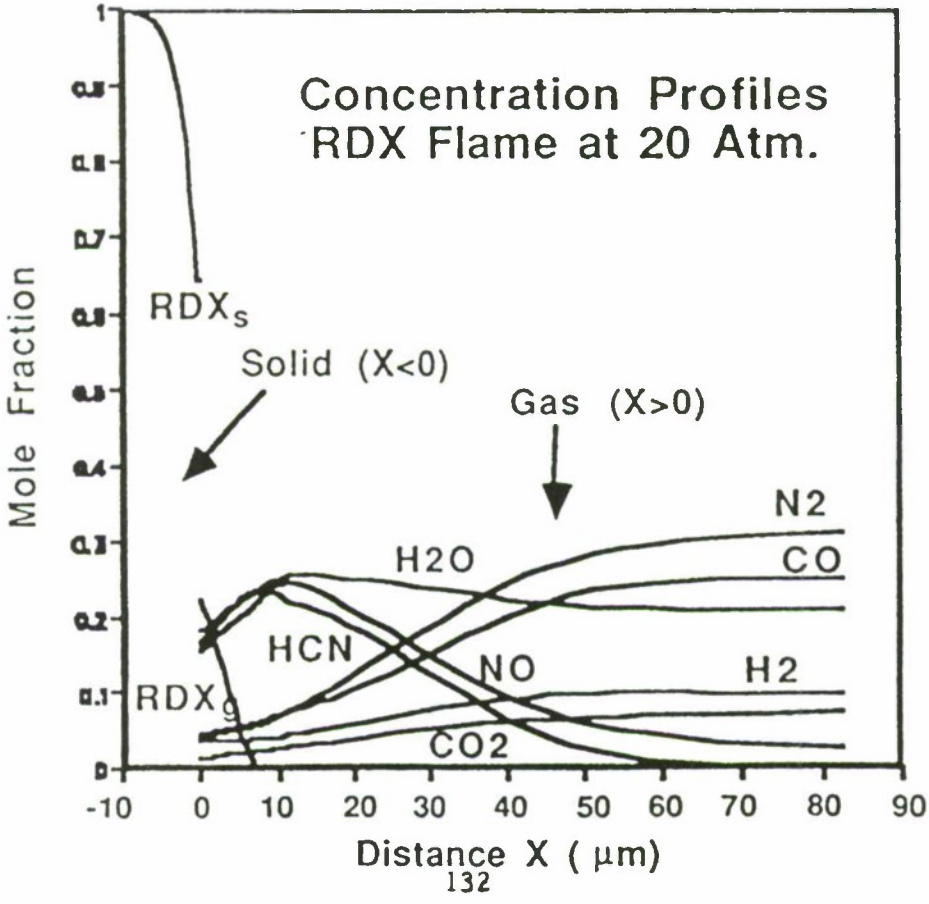
Concentration Profiles
RDX Flame at 20 Atm.
Mole Fraction
RDXs
Solid (X<0)
Gas (X>0)
N2
H2O
CO
HCN
NO
H2
RDXg
CO2
-10
0
10
20
30
40
50
60
70
80
90
Distance X (μm)

RDX Solid/Gas Interface

Flame Pressure:	1 Atm	20 Atm
Surface Temperature:	549K	634K
Mass Transport ($gm/cm^2/sec$):		
Rate of Evaporation:	7.582	120.06
Rate of Condensation:	7.550	119.55
Burn Rate:	0.032	0.51
Fraction of Solid Reacted:	0.047	0.073
Heat Transport (10^8 $erg/cm^2/sec$):		
$\lambda_g (dT/dx)^+$:	2.58	45.2
$\lambda_s (dT/dx)^-$:	1.42	30.0
$\rho v \Delta H_{vap}$:	0.19	-2.4
$\Sigma \rho_i v_i h_i$:	0.96	17.6

where

$\lambda_{RDX} = 2.918\ 10^4$ erg/cm/K/sec

$\Delta H_{vap} = 133.9\ 10^{10}$ erg/mol

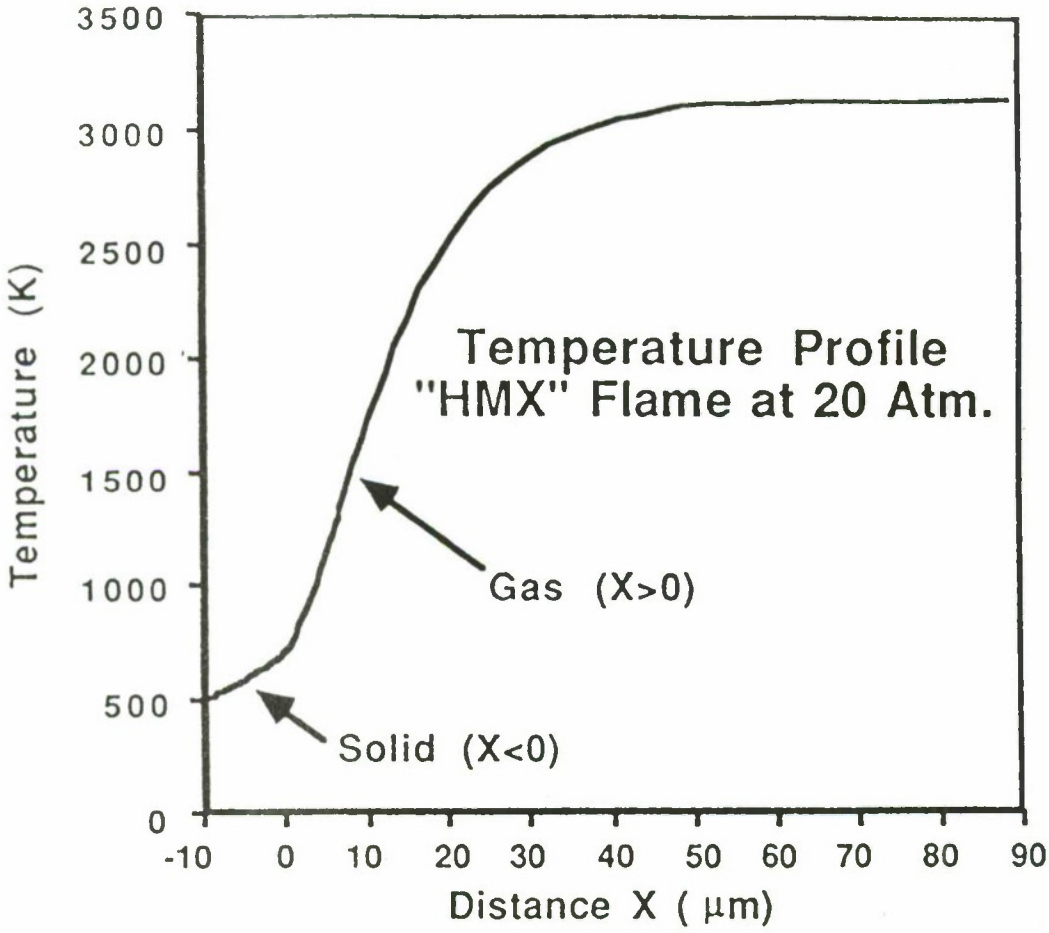
Temperature Profile
"HMX" Flame at 20 Atm.
Gas (X>0)
Solid (X<0)
Temperature (K)
Distance X (μm)
3500
3000
2500
2000
1500
1000
500
0
-10
0
10
20
30
40
50
60
70
80
90

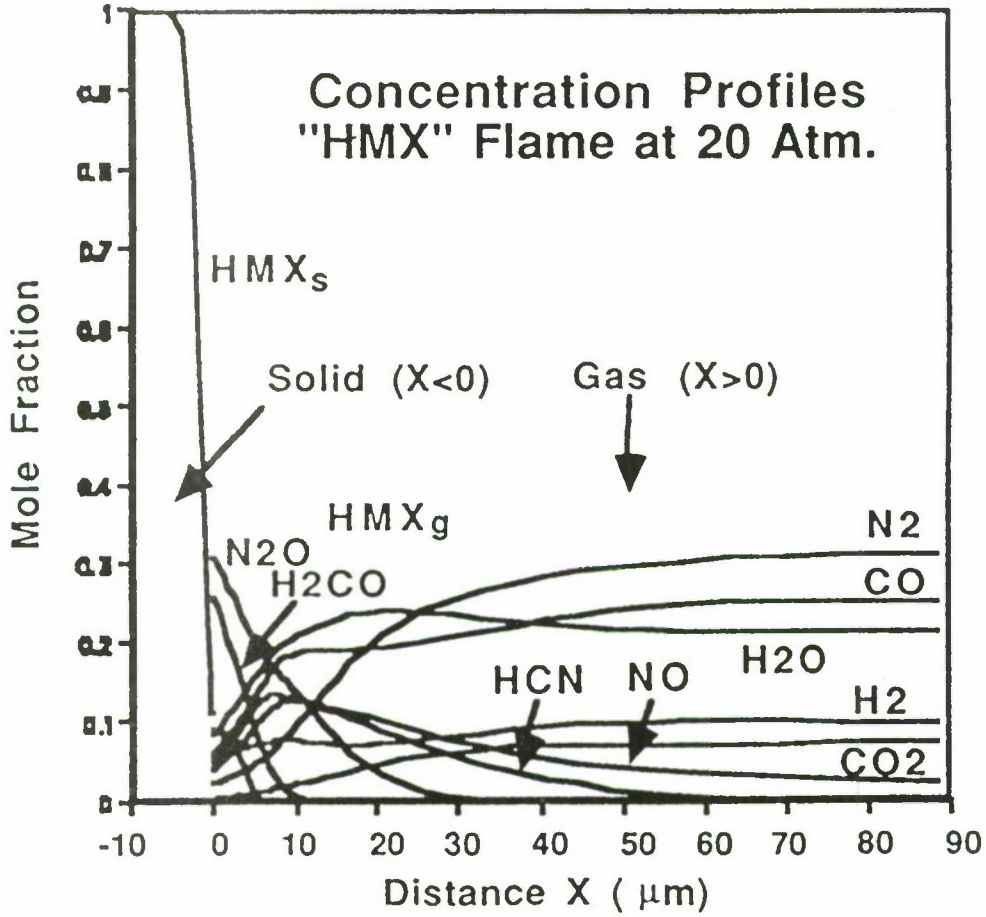
Concentration Profiles
"HMX" Flame at 20 Atm.
HMXs
Solid (X<0)
Gas (X>0)
HMXg
N2O
H2CO
N2
CO
H2O
HCN
NO
H2
CO2
Mole Fraction
Distance X (μm)
-10
0
10
20
30
40
50
60
70
80
90

RDX/HMX Solid/Gas Interface

Flame:	RDX	"HMX"
Flame Pressure:	20 Atm	20 Atm
Surface Temperature:	634K	703K
Mass Transport ($gm/cm^2/sec$):		
Rate of Evaporation:	118.06	47.01
Rate of Condensation:	117.56	45.86
Burn Rate:	0.50	1.15
Fraction of Solid Reacted:	0.085	0.568
Heat Transport (10^8 $erg/cm^2/sec$):		
$\lambda_g (dT/dx)^+$:	43.3	39.4
$\lambda_s (dT/dx)^-$:	29.0	56.6
$\rho v \Delta H_{vap}$:	-2.4	-38.6
$\Sigma \rho_i v_i h_i$:	16.7	21.4

where

$\lambda_{RDX} = 2.918\ 10^4$ erg/cm/K/sec

$\Delta H_{vap} = 133.9\ 10^{10}$ erg/mol

Fuel Nitrogen Chemistry

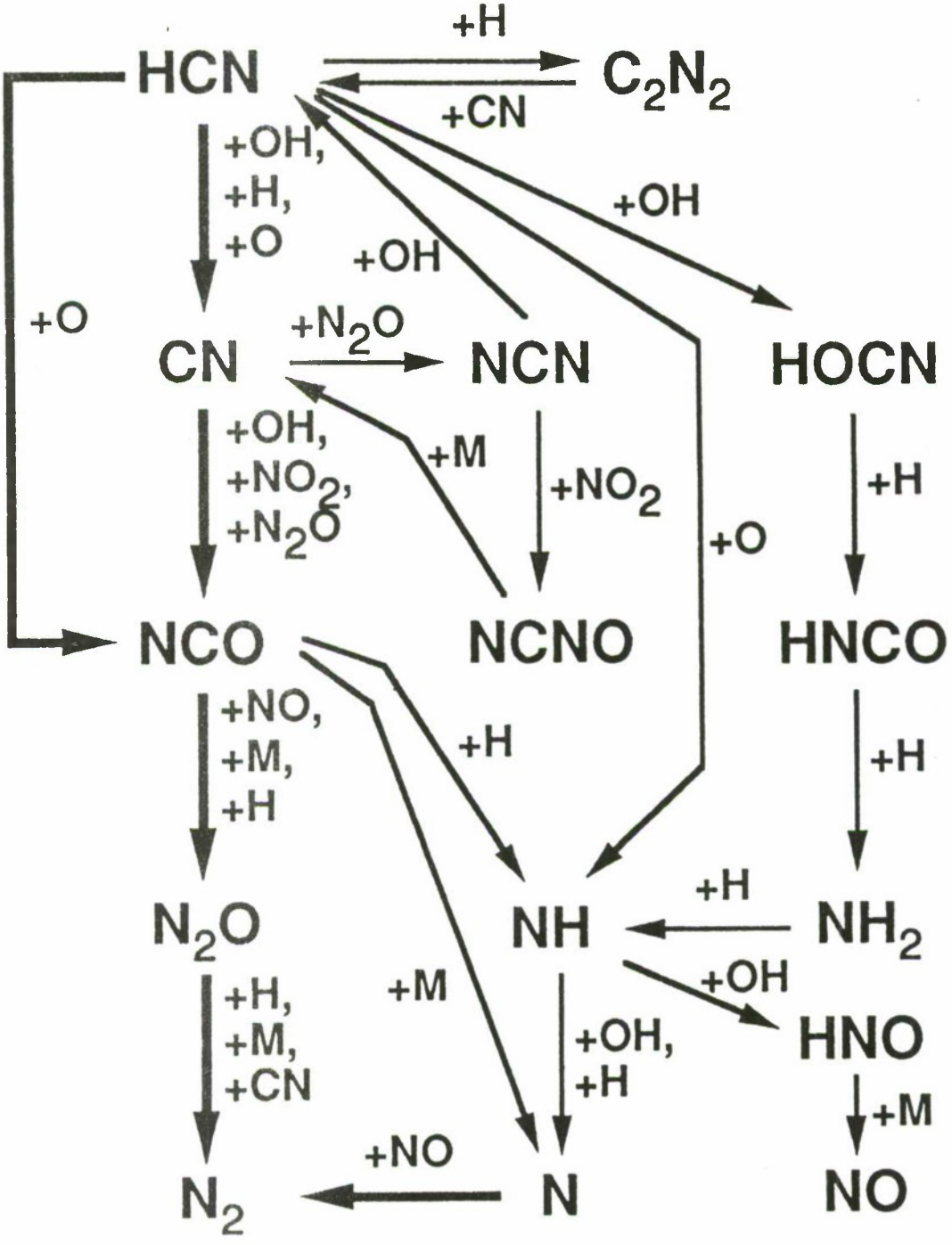

Energetics of $H_3CCCH \rightarrow H_2CCCH_2$

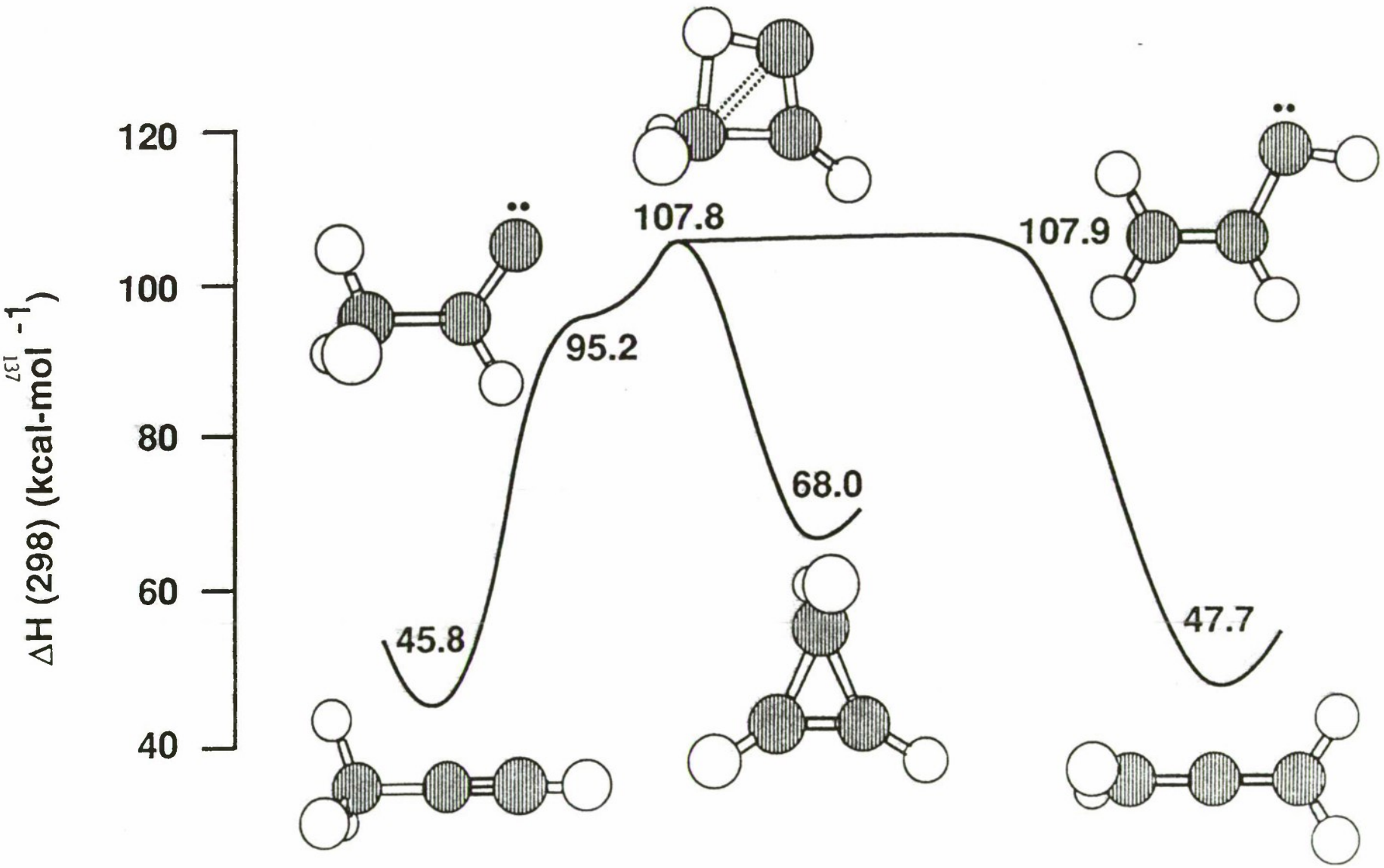

07/25/91

Energetics of Cyclobutene → Butadiene

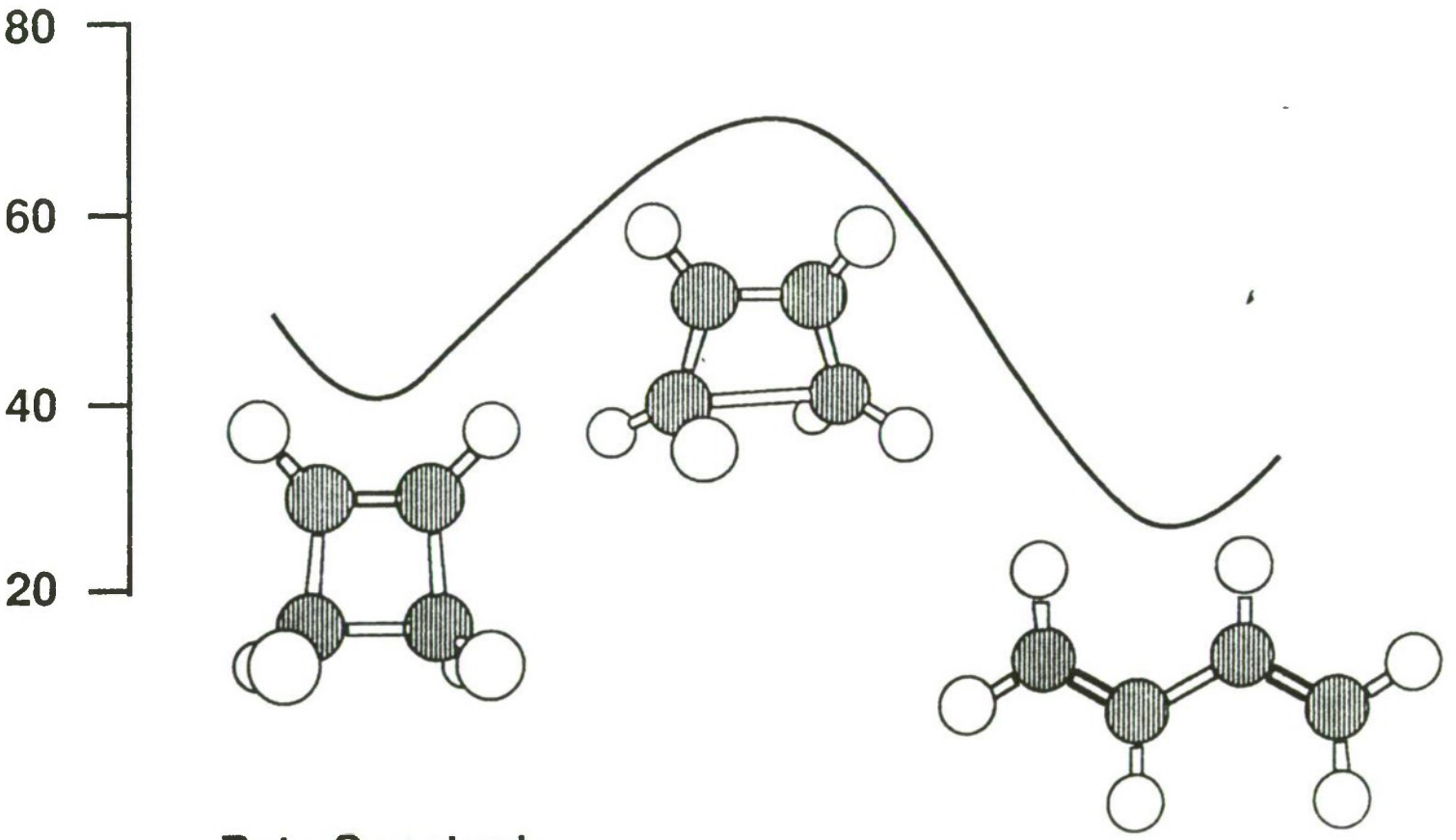

Rate Constant:

Exp. $k = 10^{13.4} \exp(-32.9 / RT)$

Theor. $k = 10^{13.3} \exp(-29.2 / RT)$

07/25/91

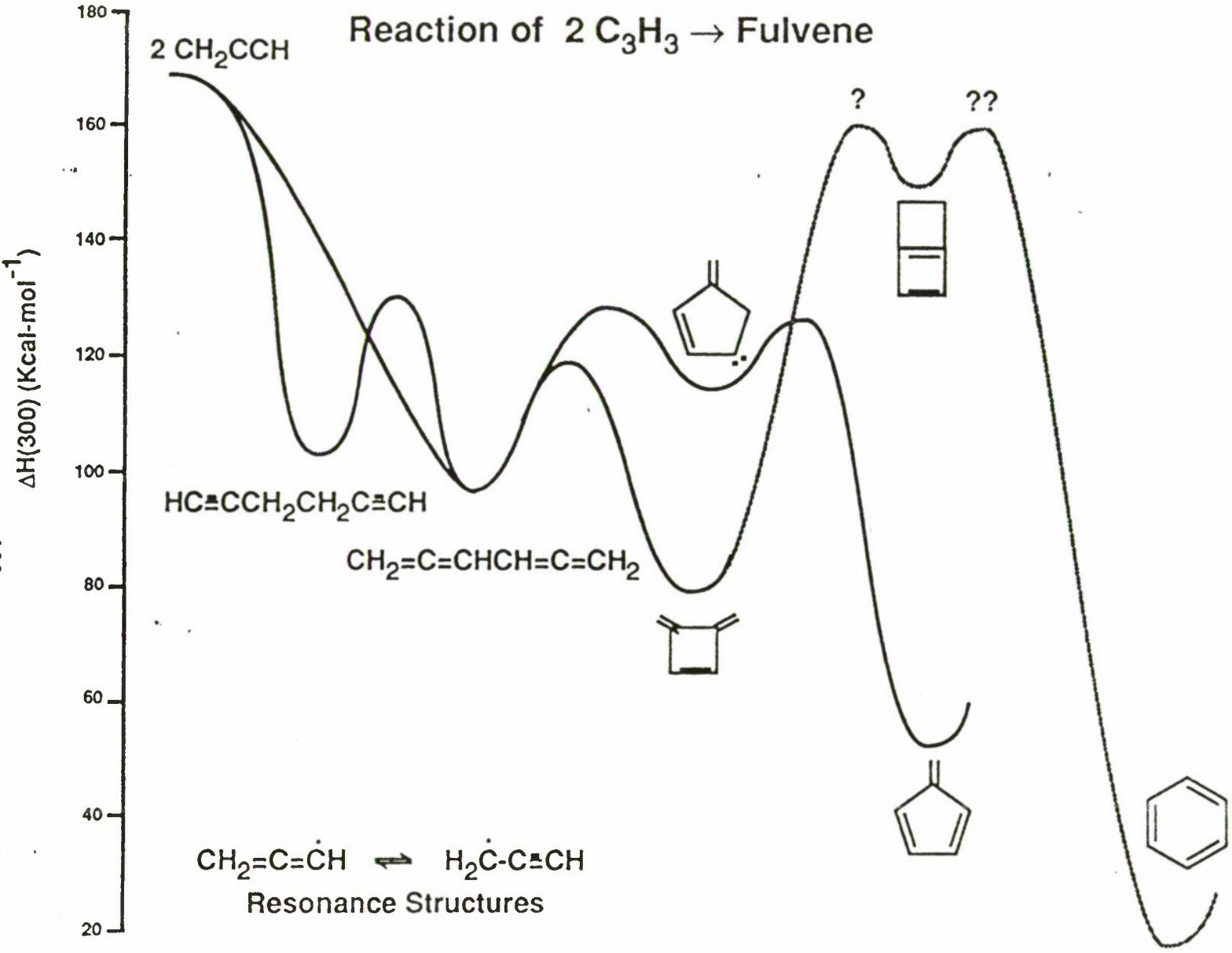
Reaction of 2 C_3H_3 → Fulvene
2 CH_2CCH
?
??
$HC{\equiv}CCH_2CH_2C{\equiv}CH$
$CH_2{=}C{=}CHCH{=}C{=}CH_2$
$CH_2{=}C{=}\dot{C}H \rightleftharpoons H_2\dot{C}{-}C{\equiv}CH$
Resonance Structures
$\Delta H(300)$ (Kcal-mol^{-1})
180
160
140
120
100
80
60
40
20

Reaction of $2\ C_3H_3 \rightarrow C_6H_5 + H$

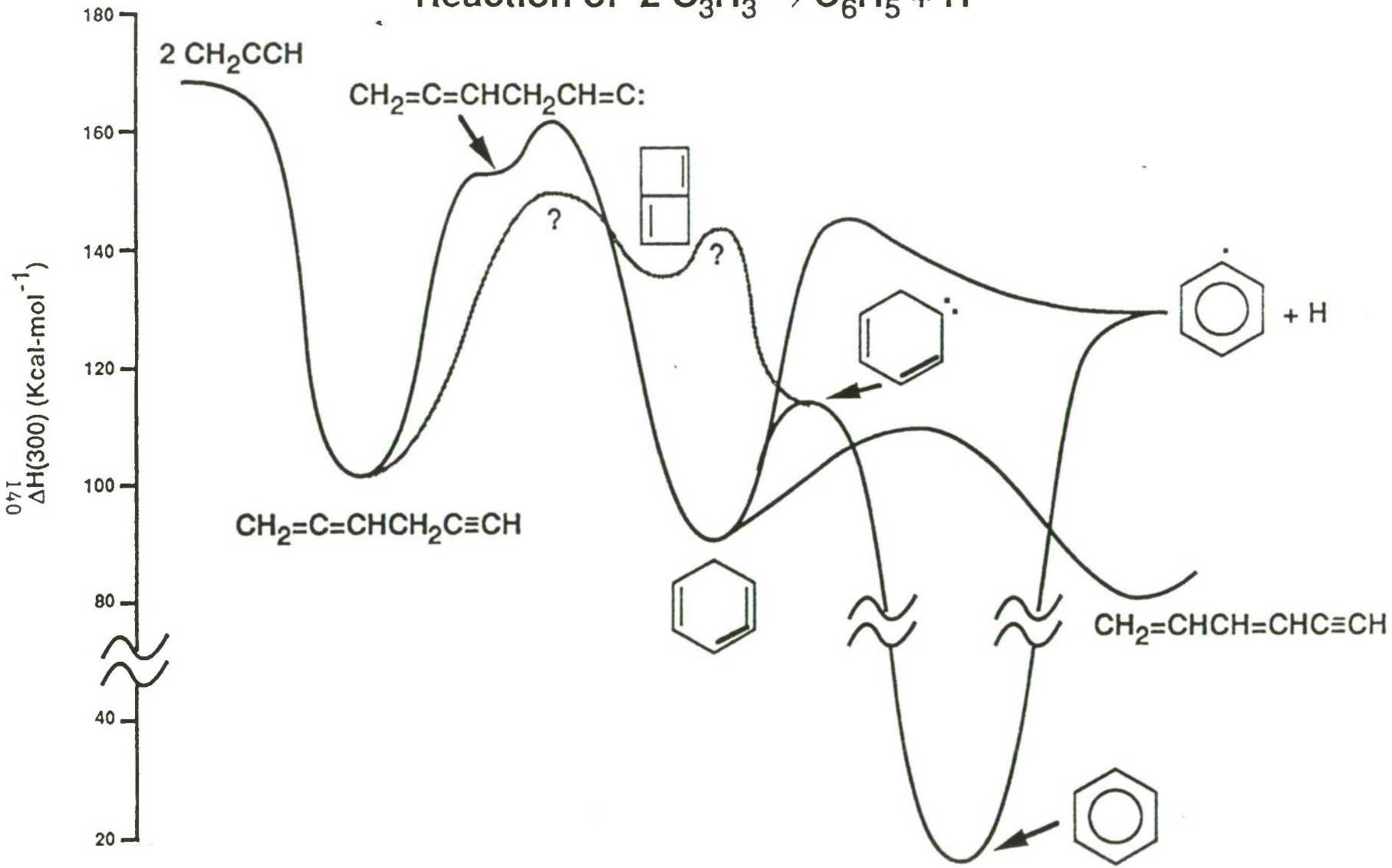

07/25/91

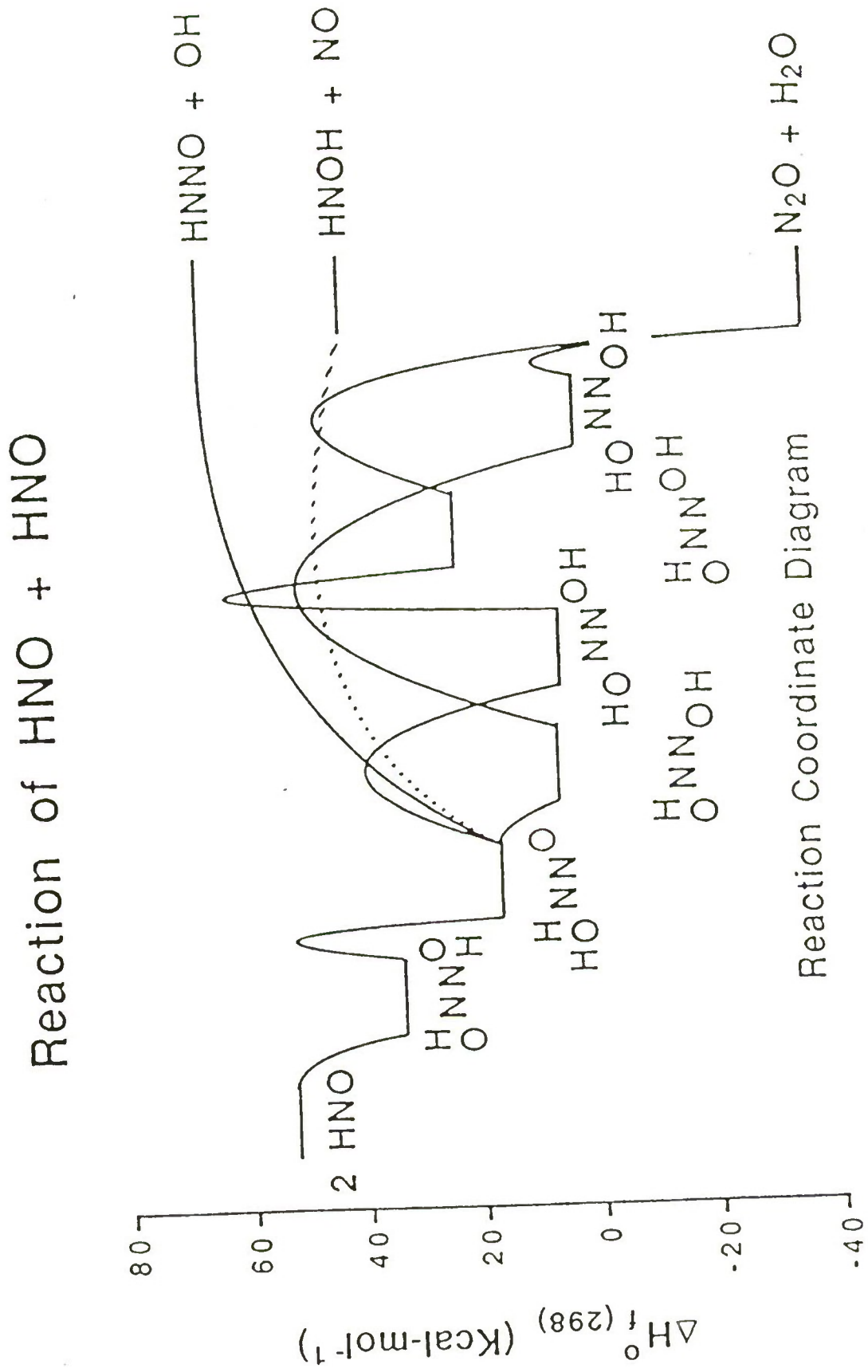
Reaction of HNO + HNO
HNNO + OH
HNOH + NO
$N_2O + H_2O$
2 HNO
Reaction Coordinate Diagram
ΔH^o_f (298) (Kcal-mol^{-1})
80
60
40
20
0
-20
-40

Conversion of Nitramine to N_2O

$$NH_2NO_2 + n\ H_2O \rightarrow N_2O + H_2O + n\ H_2O$$

With and Without Additional Water Molecules n

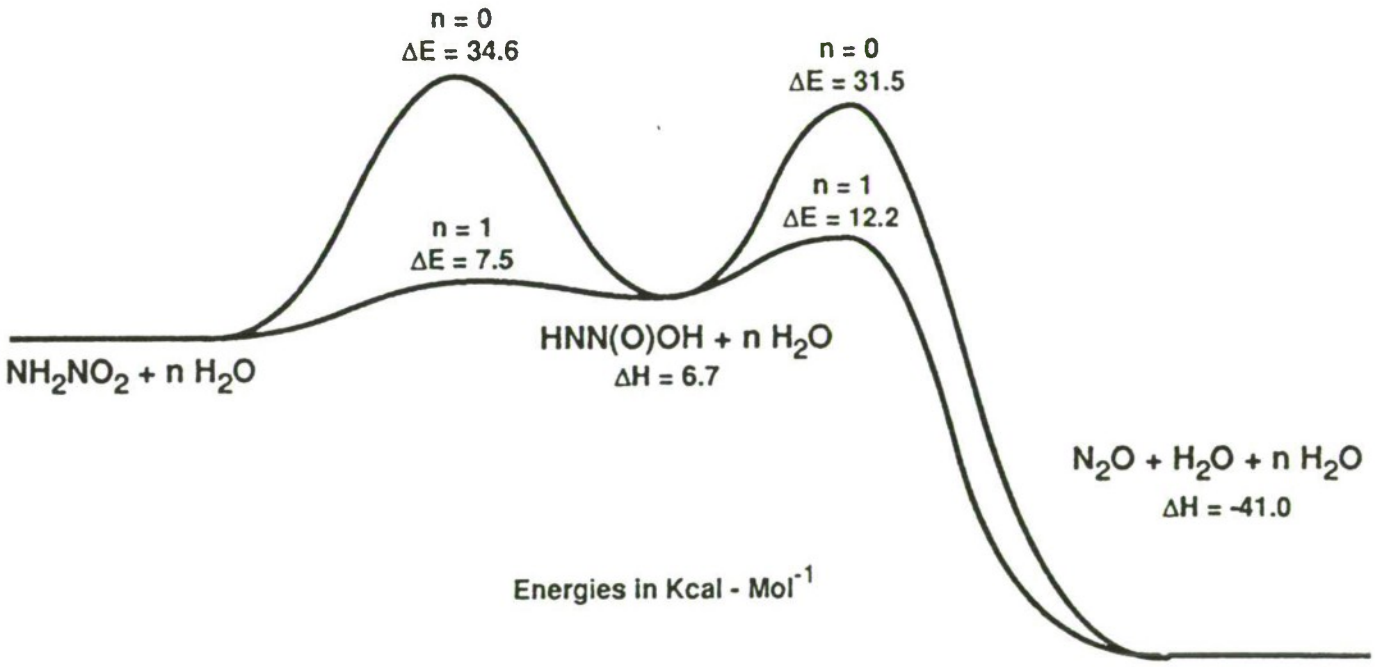

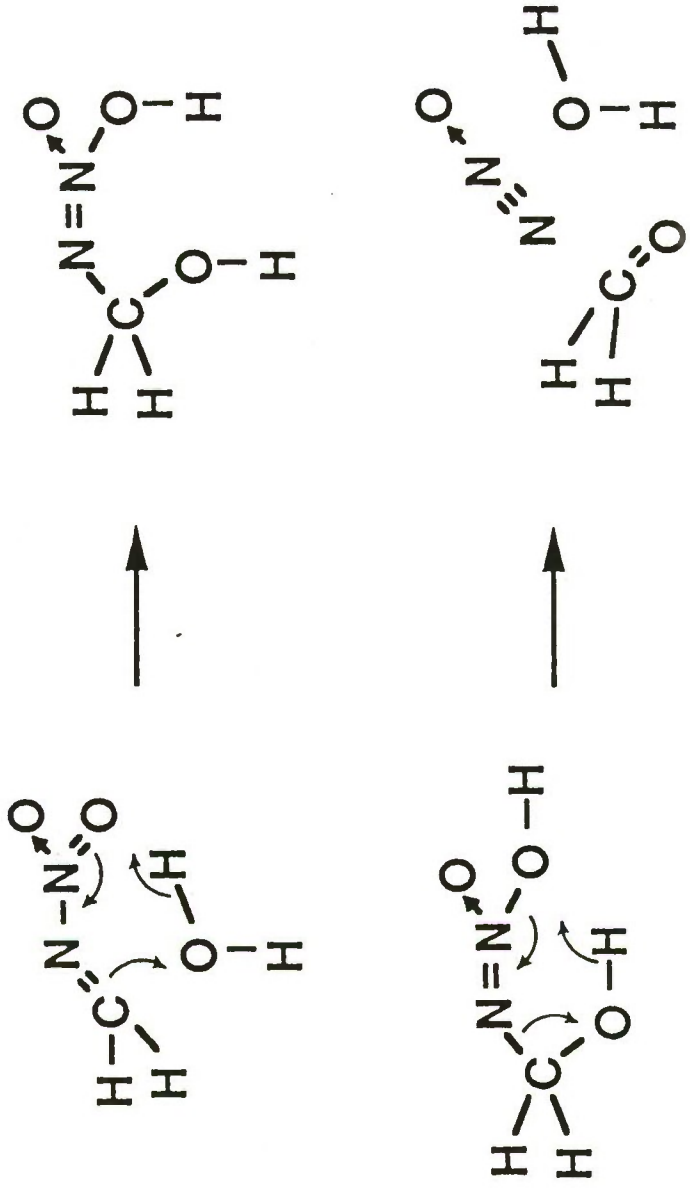

$$CH_2NNO_2\ (+H_2O) \rightarrow CH_2O + N_2O\ (+H_2O)$$

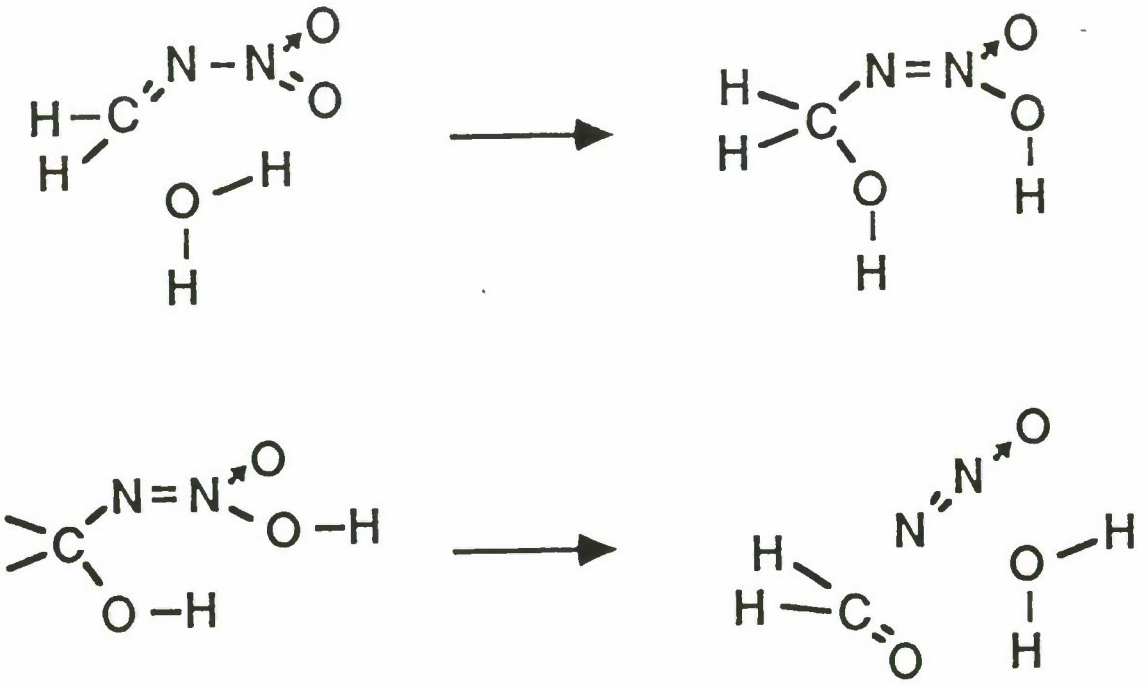

1st Step: Rate Constant = $10^{8.92}\ e^{-24.1/RT}$

Deuterium Kinetic Isotope Effect (DKIE): 1.29 @ 600K
0.97 @ 300K

Water Catalyzed Decomposition of Ringed Nitramines RDX & HMX

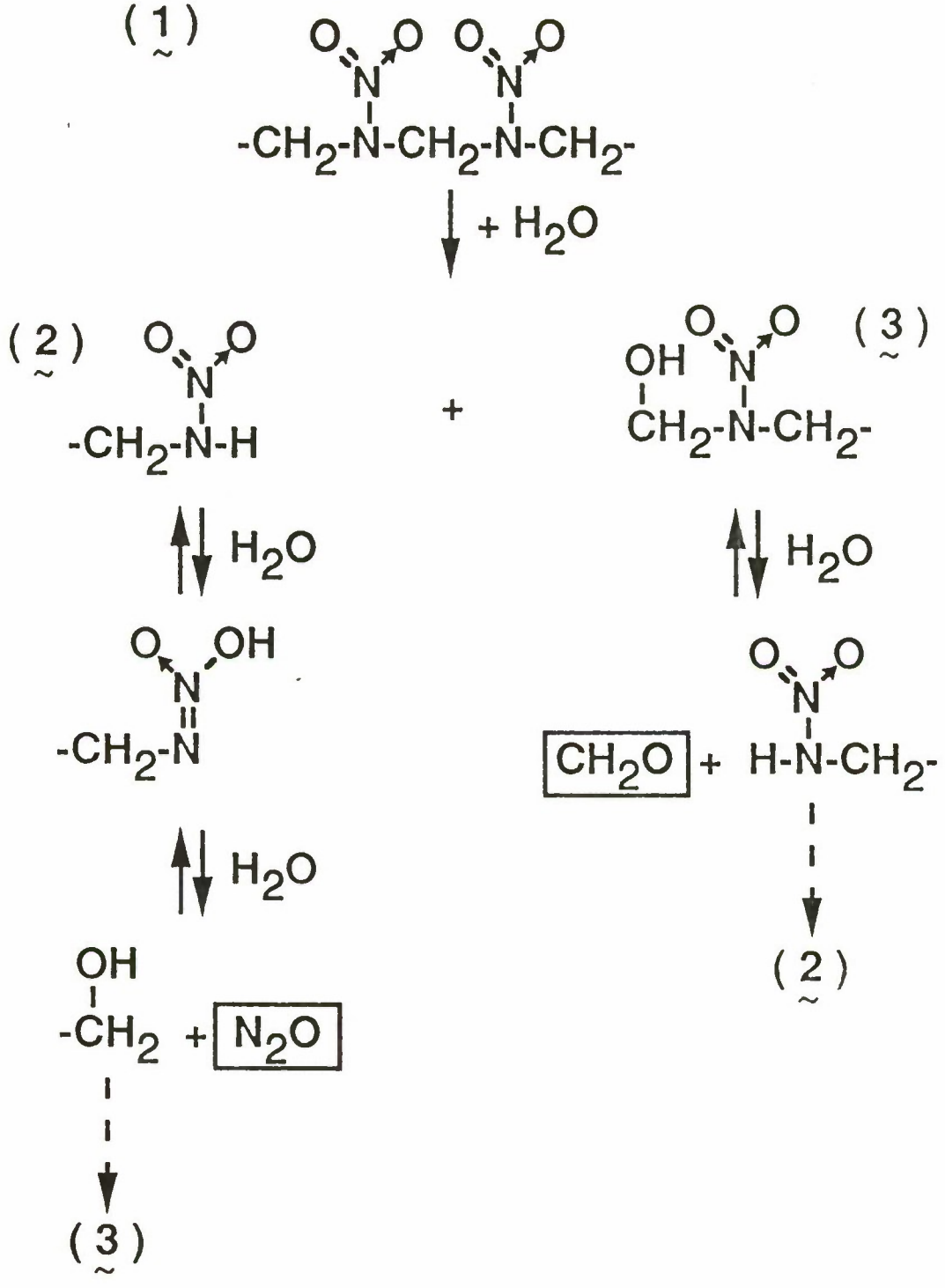

Time-Dependent Flame Code

Has been Applied to Pressure Ramping of RDX and HMX flames

Rapid Ramping (1 $\rightarrow$ 10 Atm. in 0.4 sec) Lead to Second Steady-state Solution with Higher Burn Rate

Rapid Deramping (10 $\rightarrow$ 1 Atm. in 0.4 sec) Lead to Extinguishment

Can be Used to Study Ignition, Combustion Instabilities, Etc.

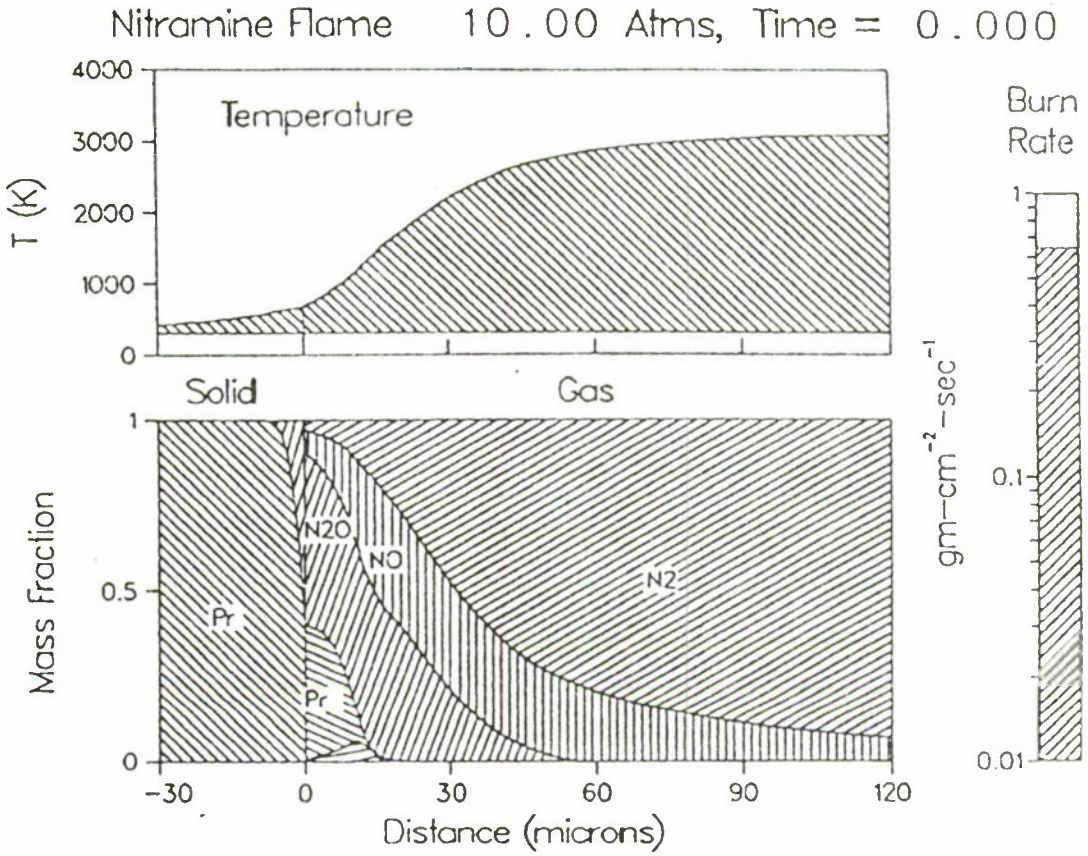
Nitramine Flame 10.00 Atms, Time = 0.000
Temperature
T (K)
4000
3000
2000
1000
0
Solid
Gas
Mass Fraction
1
0.5
0
N2O
NO
N2
Pr
Pr
−30
0
30
60
90
120
Distance (microns)
Burn Rate
gm−cm⁻²−sec⁻¹
1
0.1
0.01

R. Gilardi

Energetic Material and Related Crystal Structures

June, 1991

Structure Analyses of Energetic and Strained Organic Compounds

by Richard Gilardi,
Laboratory for the Structure of Matter [Code 6030]
Naval Research Laboratory,
Washington, D.C. 20375 U.S.A.

At the beginning of the 1980s, the U. S. Office of Naval Research [ONR] identified a strong need for the production of new 'high energy density materials' , an emerging area of research. Better materials in this area would enable improvements in performance coupled with increased safety in the next generation of naval ordnance. To meet these requirements, a number of research initiatives were spawned which focussed on the synthetic chemists who synthesize new energetic materials, but also engaged the expertise of researchers from many scientific disciplines, from rocket engineering to quantum chemistry.

The sudden production of hundreds of new energetic compounds (and precursors to energetic compounds) by this ONR program provided an opportunity for NRL's Laboratory for the Structure of Matter (LSM) to demonstrate the utility of rapid structural analysis to a synthesis program . X-ray diffraction analysis can often provide the detailed structure of a new material from a single crystal, even when the structural and empirical formula are not completely known. This technique is thus particularly valuable for primary identification when a new energetic material is very scarce. In recent years, small

quantities of many new crowded and highly strained molecules have been synthesized in academic, industrial & government labs in ONR programs. The structures of over 300 of these new molecules were identified or corroborated with X-rays at NRL.

The question of detonability of materials at the molecular level depends on many factors other than ground-state molecular structure; some of these factors are unfamiliar to me, and that is a prime reason for my attendance at this workshop. On the other hand, the molecular structure and the crystal packing of a material are essential to any specific study. One question which is often asked of me is: can you see features in the structure which indicate strain, and does this strain lead to weak bonds, which in turn might lead to increased sensitivity? The answer to this question is not at all simple. Some of the more strained compounds will be briefly discussed.

Strained Molecules

A molecule, by definition, is strained when its bond distances, angles and torsions must deviate from the "normal", or lowest-energy values to achieve the final determined connectivity and structure. Bond angles usually show the largest distortions. In some of the compounds studied at NRL, angles are distorted by up to 30° from normal tetrahedral and trigonal values. Severely twisted olefins, several cubane derivatives, and new cubyl-cubanes will be among those discussed. The cubyl-cubanes [Gilardi, Maggini & Eaton, J. Am. Chem. Soc. *110*, 7232-4 (1988)] are made up of two cubane cages linked by a C-C bond, and probably contain more overall strain energy than any other compounds yet made, yet they appear to be stable

indefinitely at room temperature. It was once thought that non-symmetrical cubanes would be unstable, but now a number of unsymmetrical derivatives have been made which appear to be as stable as cubane itself.

Nitramine Structure Analyses

Over 80 of the new materials submitted to NRL/LSM for analysis and subsequent archiving in the LSM energetic database are nitramines; when such a large number of related structures have been studied, basic structural parameters, such as preferred bond distances and angles for chemical groupings, can be derived through statistical analysis. In addition, subtler structural features may be ascertained. For example, examination of the structures of the nitramine groups in the Cambridge and NRL/LSM databases shows that the amino nitrogen atoms in nitramines are quite flexible; i. e., in some molecules, the three bonds to the amino nitrogen atom are coplanar, while in others they are decidedly nonplanar, and the N atom is best described as 'pyramidal'. The distribution of the out-of-plane bending angles for the amino group is illustrated in one of the Figures. The histogram for the amino bend ranges from 0 to 60°; though dominated by small [0-20°] angles of bending, they range up to one example observed to be 59°. The nitrogen atom in the nitro group of the nitramine is much less flexible and seldom departs from a planar conformation by more than a few degrees, as may also be seen in the same Fig. In the flexible amino portion of the nitramine, it is also of interest to note that a correlation exists between the C-N-C angle and the amino bend . This means that nitramines which are part of small rings, and thus

adopt a small CNC bond angle, will have a tendency to be pyramidal at the amino nitrogen atom. An example of such a structure is 1,3,3-trinitroazetidine (see Fig.), a dense strained nitramine wherein the N1-N5 bond makes a 39.7° angle with the C2-N1-C4 plane.

After (and partly as a result of) the NRL study of nitramine structures, an extensive quantum-mechanical analysis of a simple nitramine, dimethylnitramine, was carried out at the Univ. of Texas [F. R. Cordell; "Ab initio Study of Dimethylnitramine", 1987 Report, Univ. Texas, Austin, TX. Gov. Rep. Announce. Index (U.S.) 87, Abstr. No. 750,665. NTIS order No. AD-A183414, 112 p.]. This calculation indicated that a dimethylnitramine model containing a planar amino nitrogen has the lowest energy, but that only 400 calories/mole were needed to bend the amino-nitro bond 40° out of the plane. This is a very small amount, comparable to the thermal energy of any molecule at room temperature. Thus, the X-ray structural analyses and the quantum chemical analysis both indicate that weak forces can produce large changes in the amino bend since the energies are not much different for the in-plane and the out-of-plane configurations. This type of structural information is of great interest to the theoretical chemists studying the electronic properties of energetic groups, and is also helpful in the computer modeling of hypothetical energetic materials.

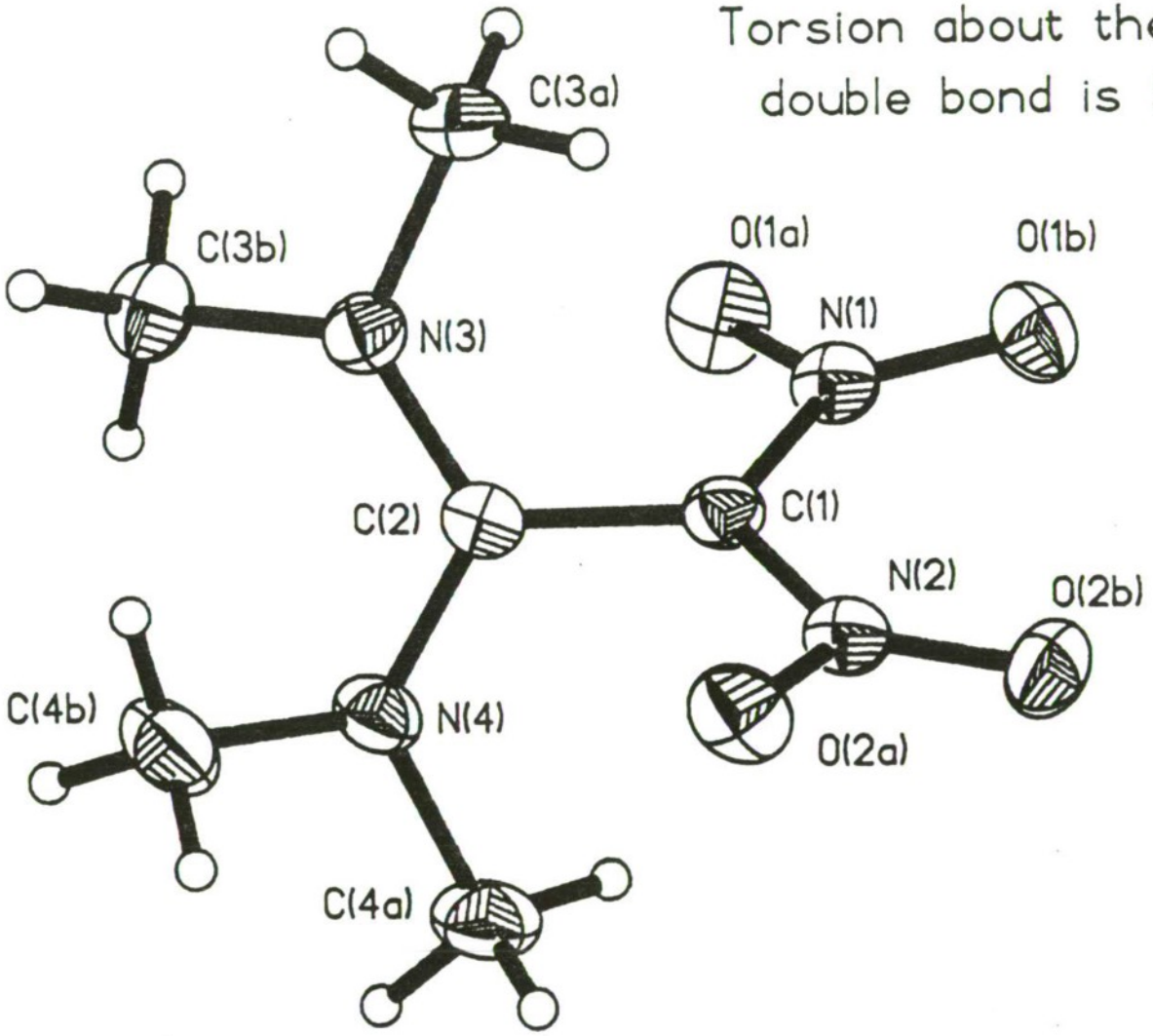

Torsion about the C1-C2 double bond is 51.4 deg.

1,1-Dinitro-2,2-di(dimethylamino) Ethylene

Twisted 1,1-Diamino-2,2-dinitro Olefins

Twisted 1,1-Diamino-2,2-dinitro Olefins

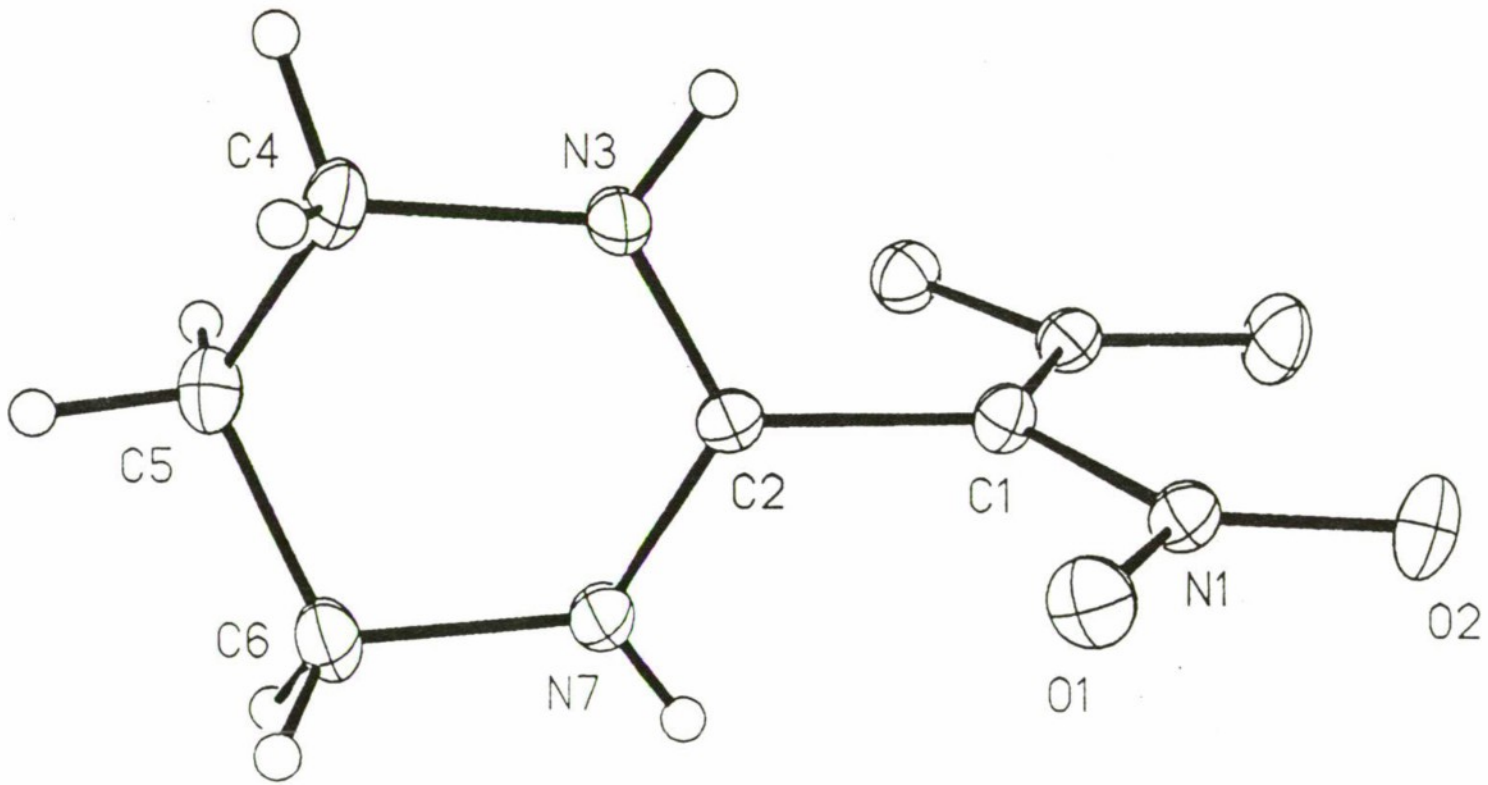

Torsion about the polarized C1-C2 double bond is 89.0°

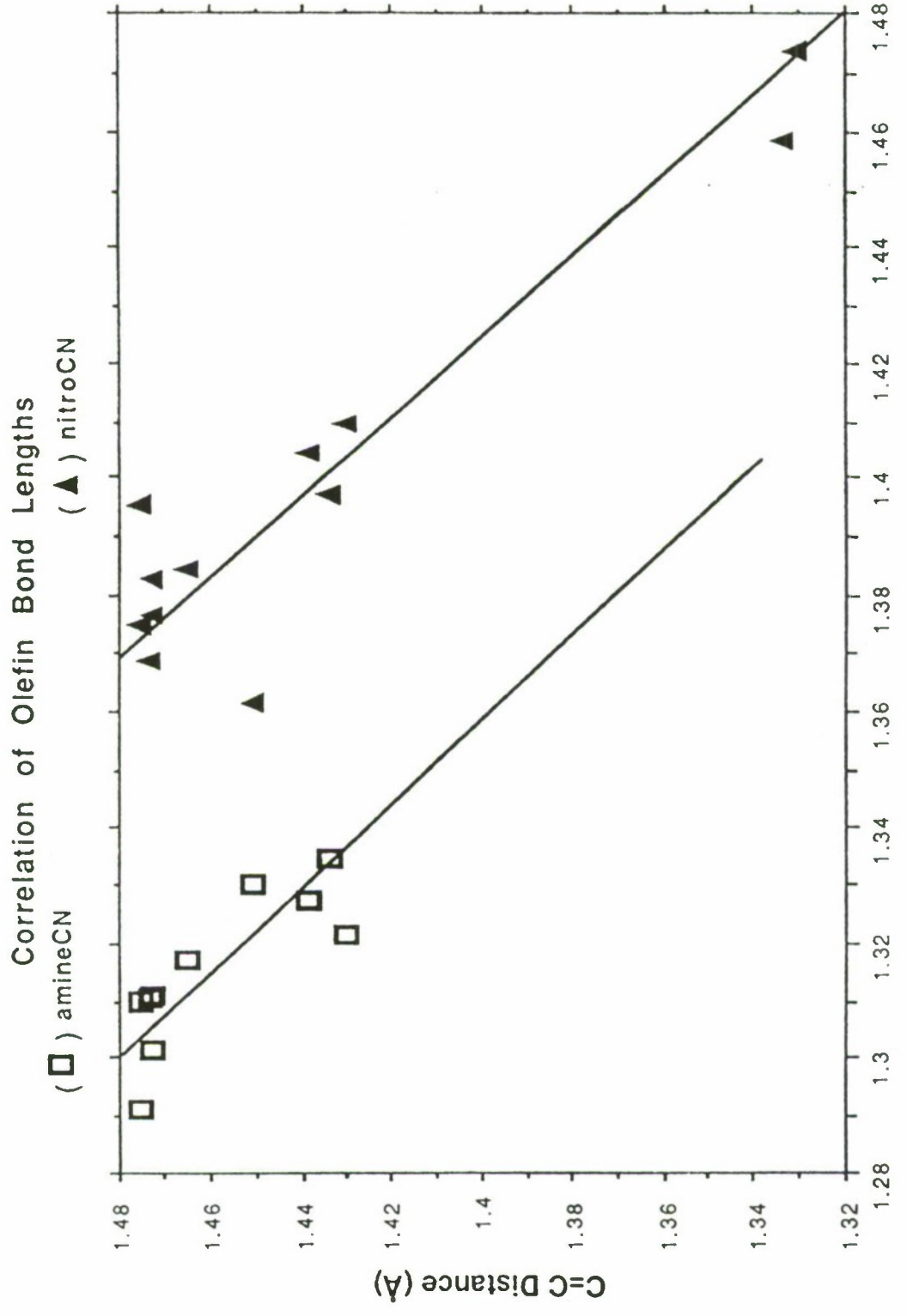

Twisted 1,1-Diamino-2,2-dinitro Olefins

CUBYL CUBANE

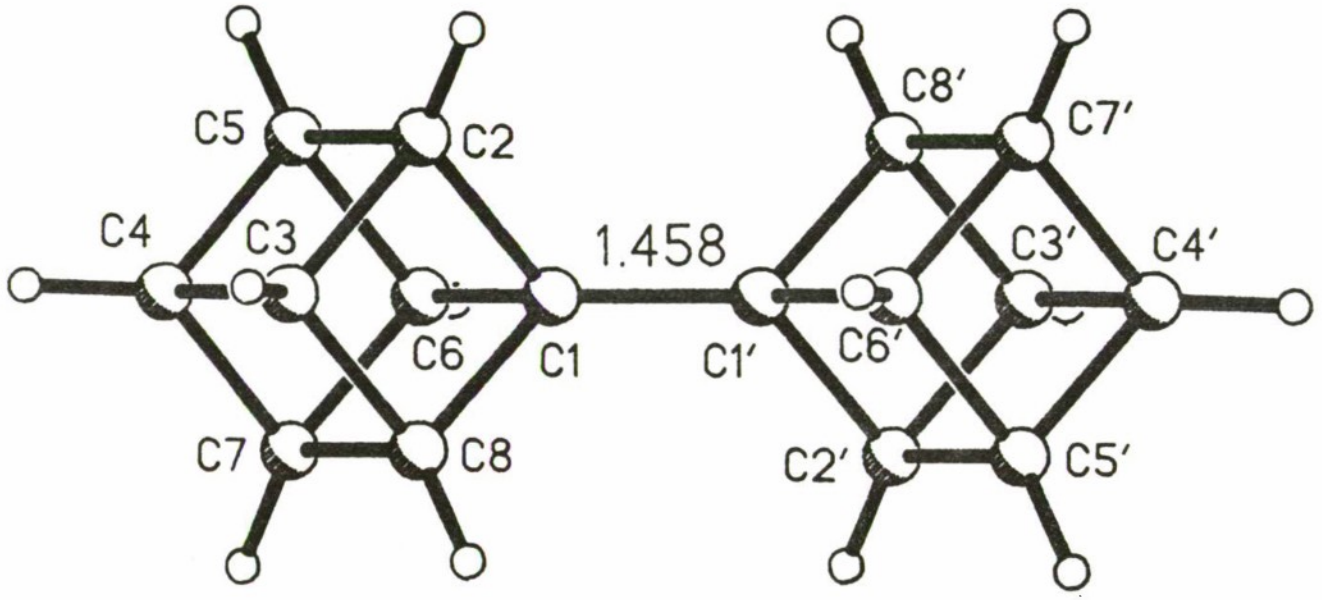

THE CUBES ARE VIRTUALLY REGULAR, AND ARE PERFECTLY STAGGERED WITH RESPECT TO EACH OTHER (D3v MOLECULAR SYMMETRY). THE AVERAGE CUBE EDGE LENGTH IS 1.568(9) FOR EDGES ADJACENT TO THE LINKAGE, 1.553(8) FOR ALL OTHERS.

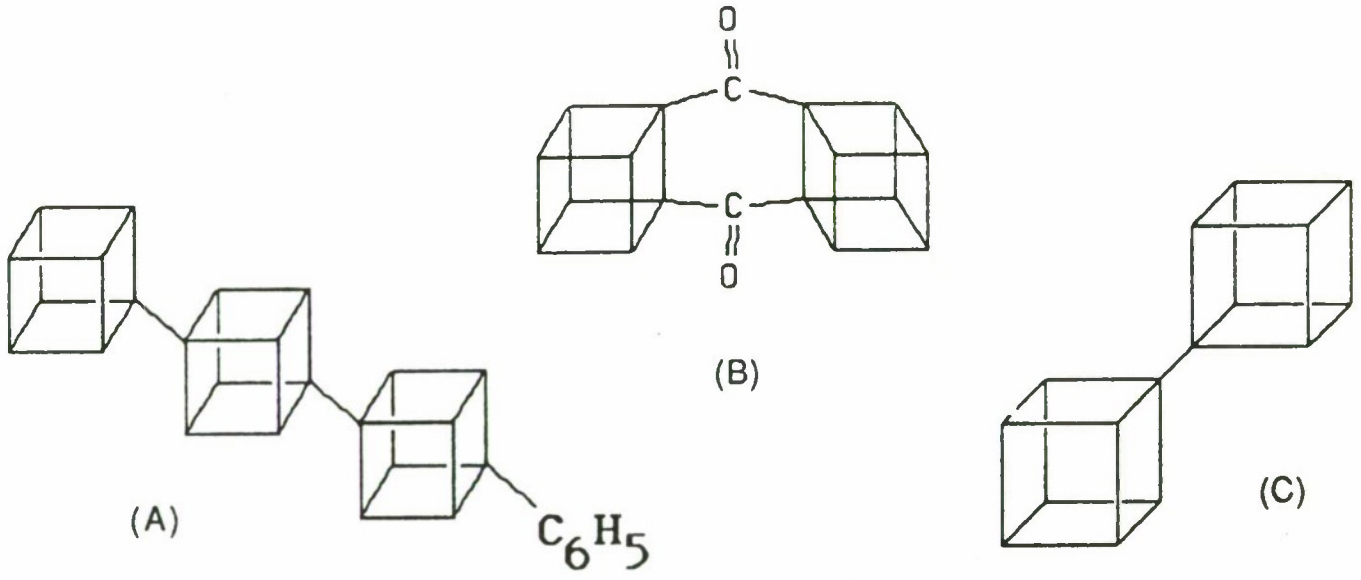

New polycubyl compounds: (A) a phenyltercubane;
(B) a cubane/cyclohexadione fusion, and (C) cubylcubane.

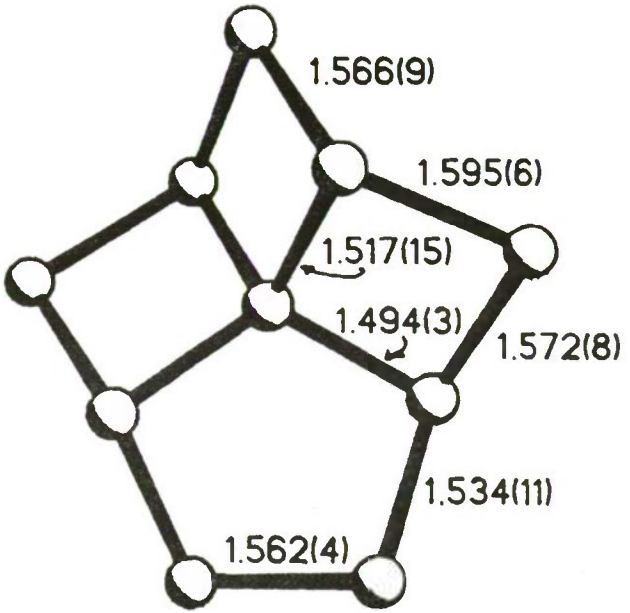

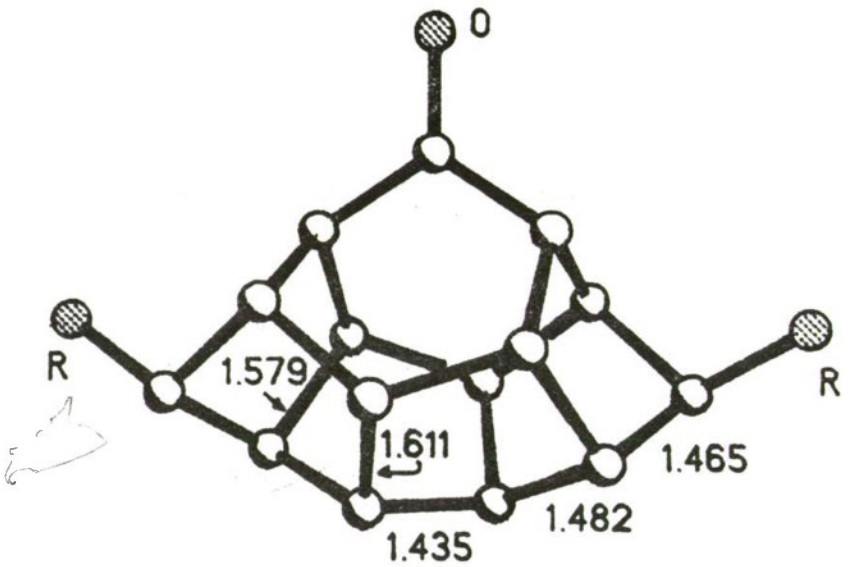

[4.4.4.5]FENESTRANES
(AVE OF 4 DETNS)

A HEPTACYCLOPENTADECANONE

RING CLOSURE COMPRESSION/TENSION

Both of these systems display angular distortions of ±20 deg. or more from tetrahedral which are virtually required in order to close all the rings. Mol. Mech.(MM2) predicts angles well, but tends to minimize distance deviations. Too much bond stiffness?

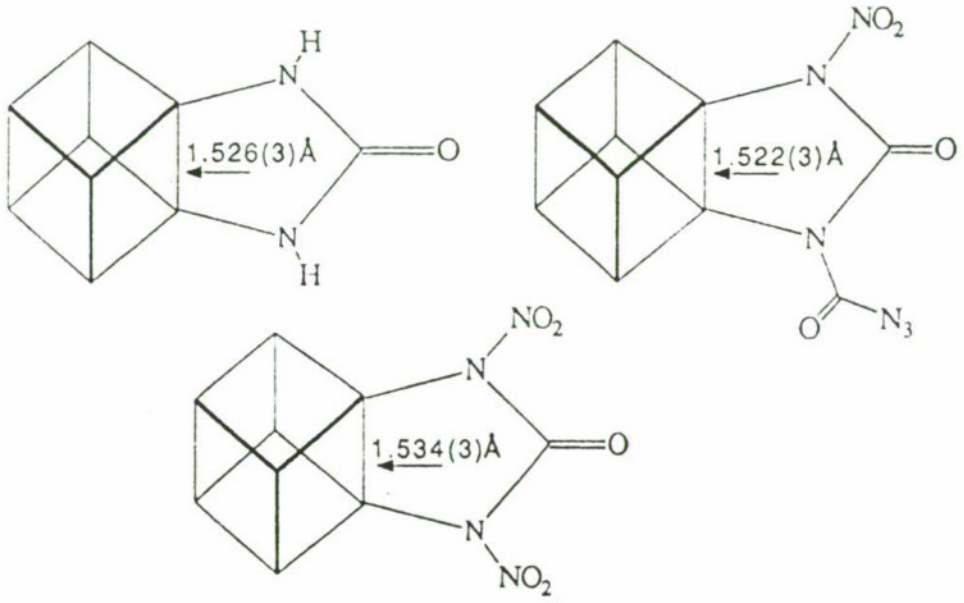

Shortened 1,2-substituted Cubane Bonds

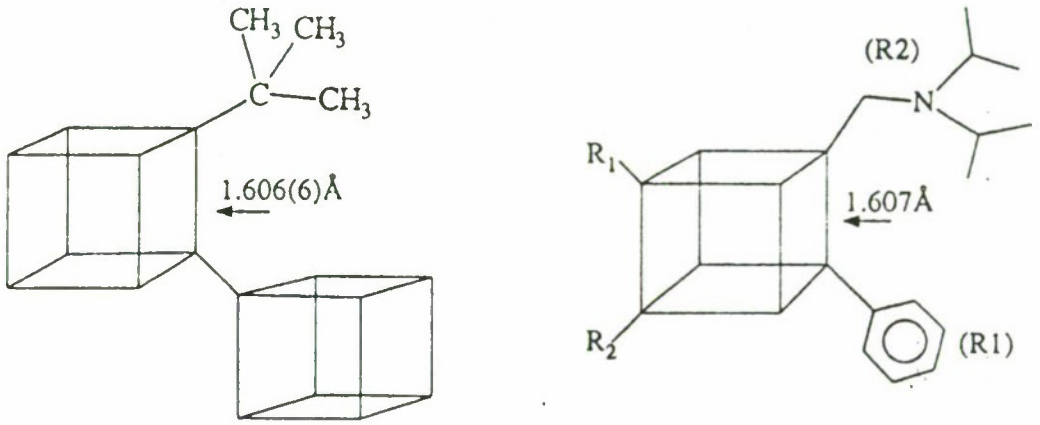

Elongated 1,2-substituted Cubane Bonds

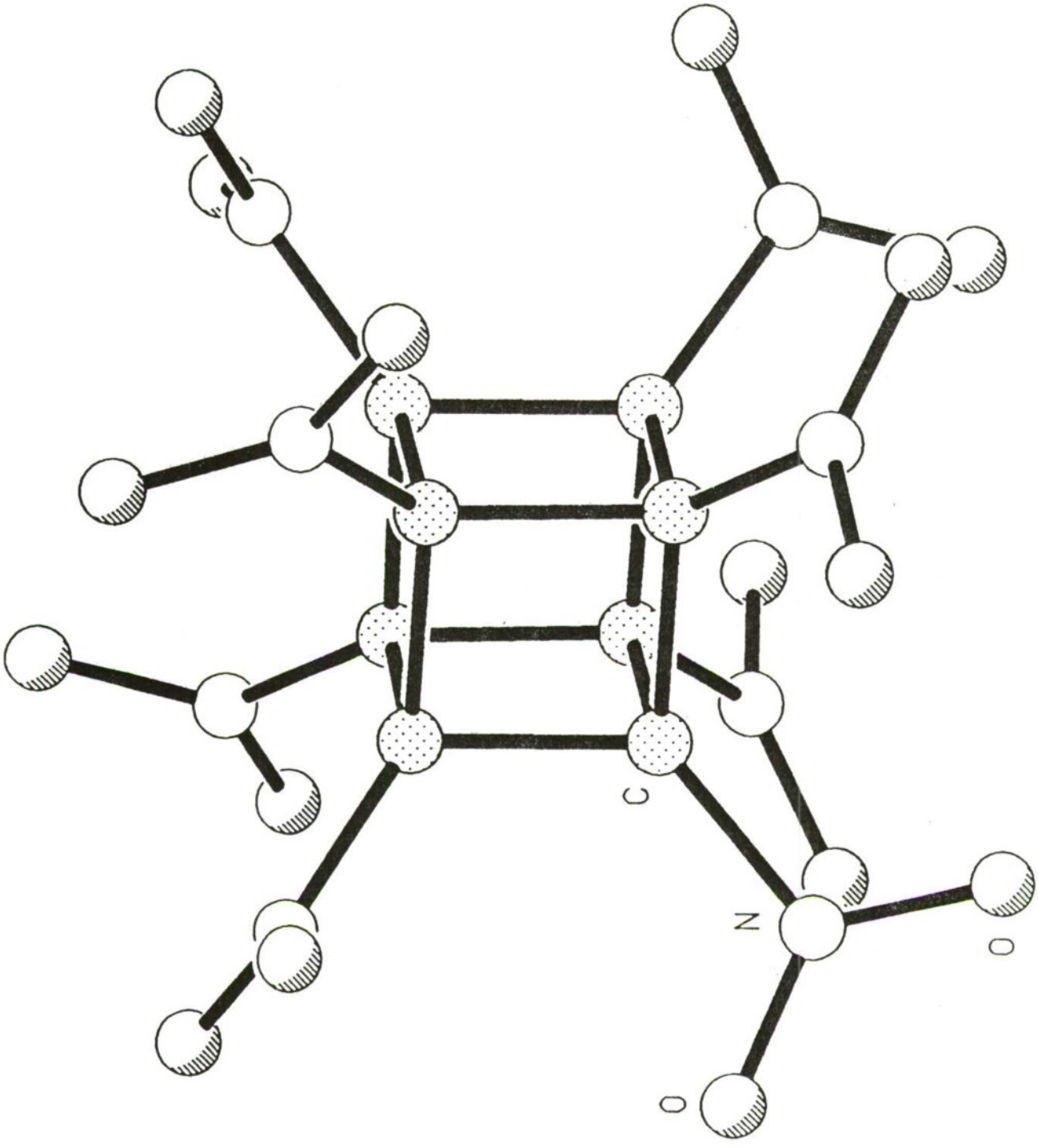

Energy-minimized model of octanitrocubane.

Table One. Shortest Nonbonded Approaches in an Energy-Minimized Octanitrocubane Model.

Type	No. of occurrences	Distance (Å)	vdW Contact(Å)
N...O	8	2.98	2.90
O...O	4	3.08	2.80
O...C	8	3.02	3.10
O...C	8	3.06	3.10

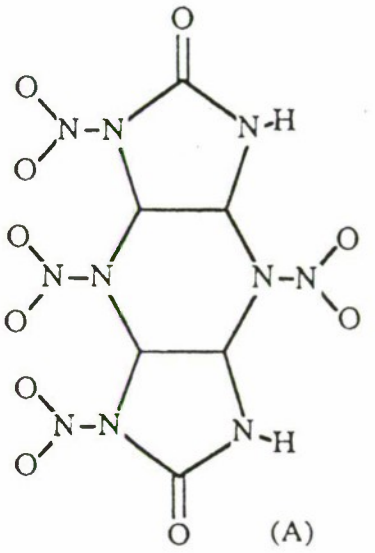

(A)

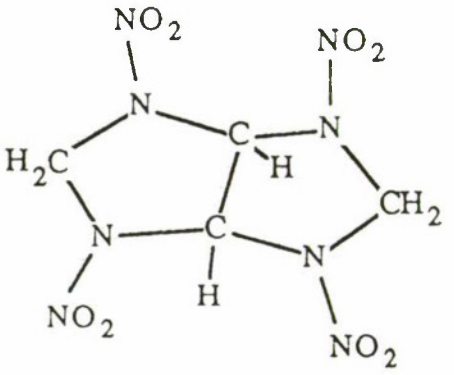

(B)

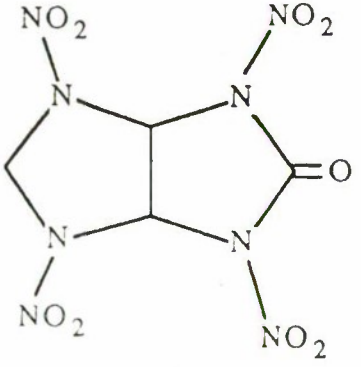

(C)

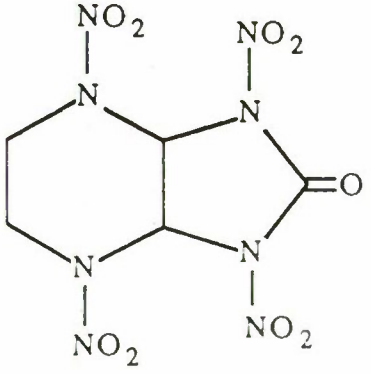

(D)

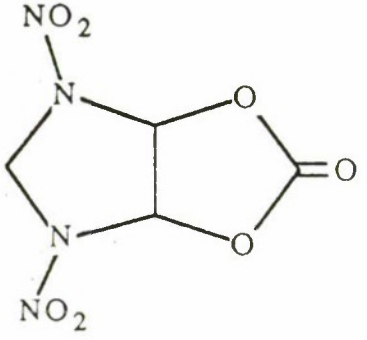

(E)

Structural formulae of several dense polycyclic nitramines made at the Naval Surface Warfare Center and at the Livermore National Laboratory. The structural subcomponents of these compounds resemble those in proven monocyclic materials such as RDX and HMX. The densities of these compounds range from 1.868 (for B) to 1.969 g/cc (for D).

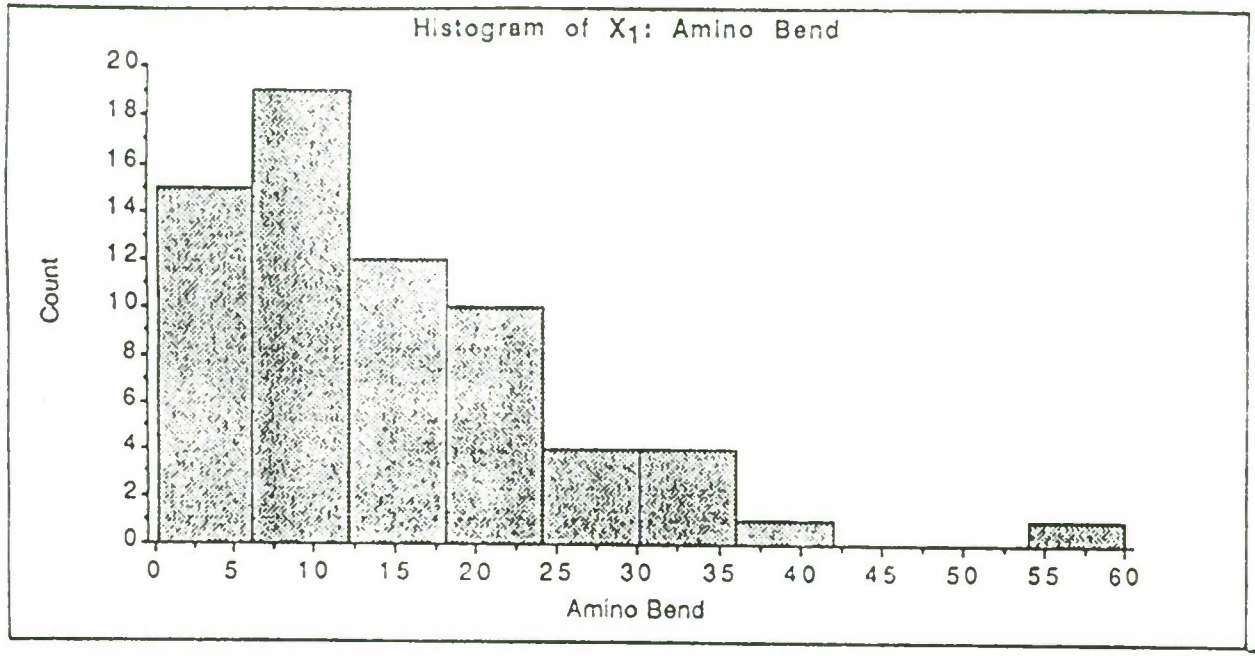

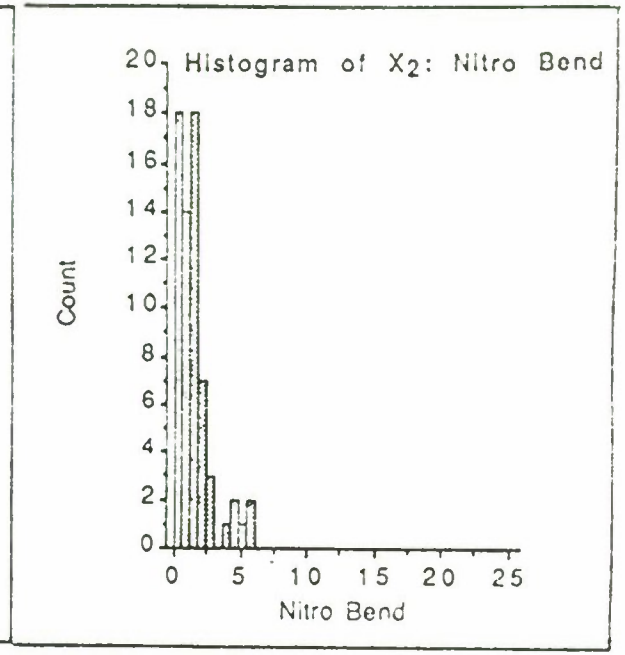

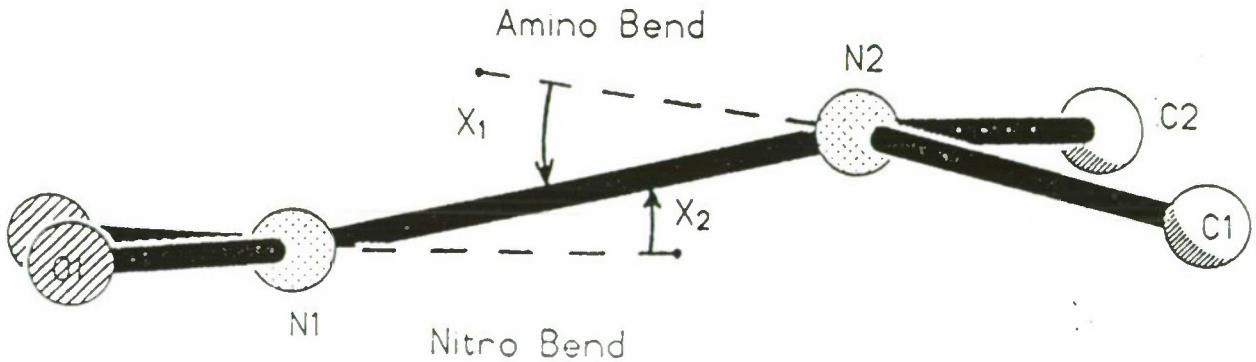

Flexible Nitramines

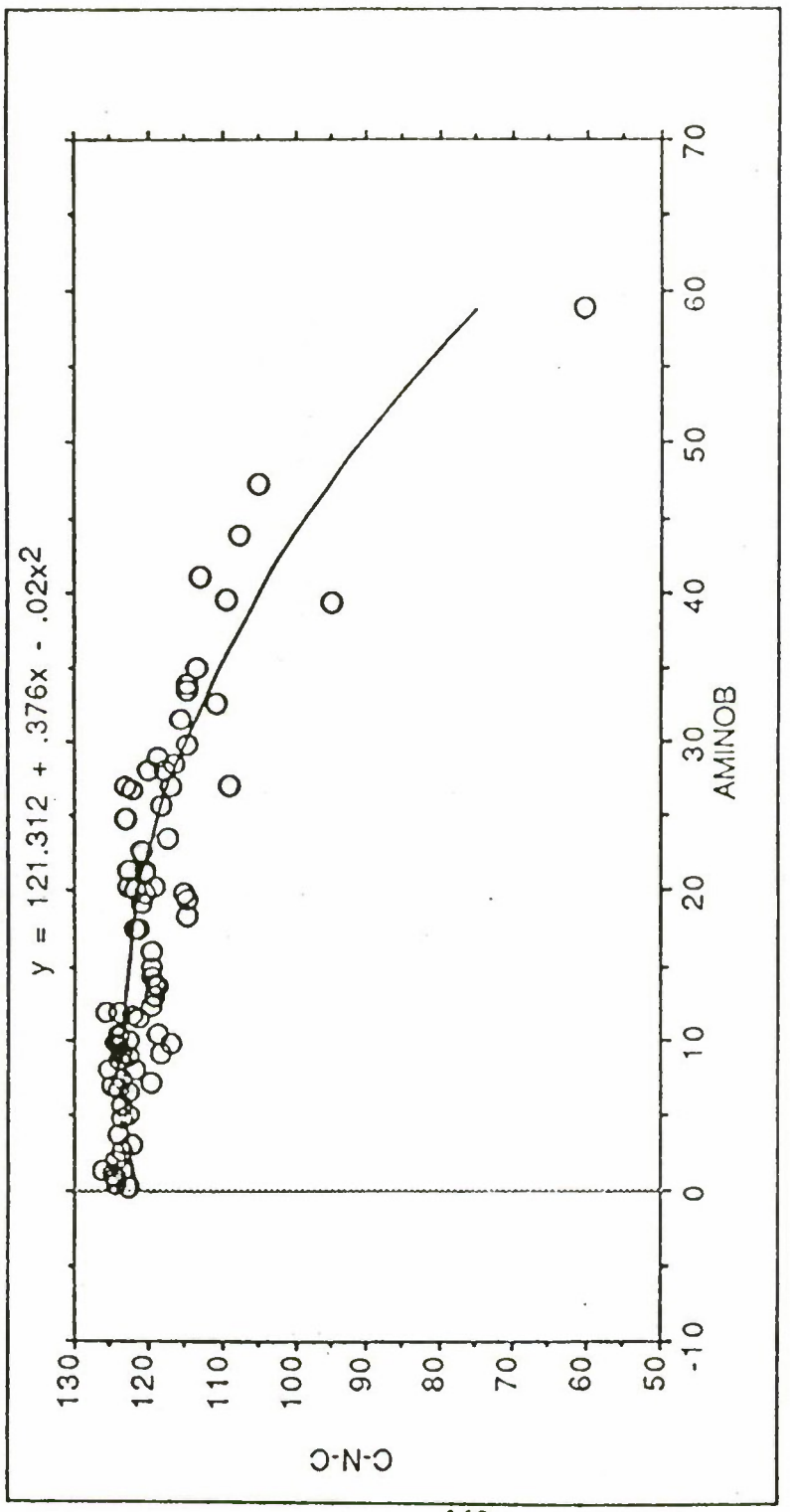

Flexible Nitramines

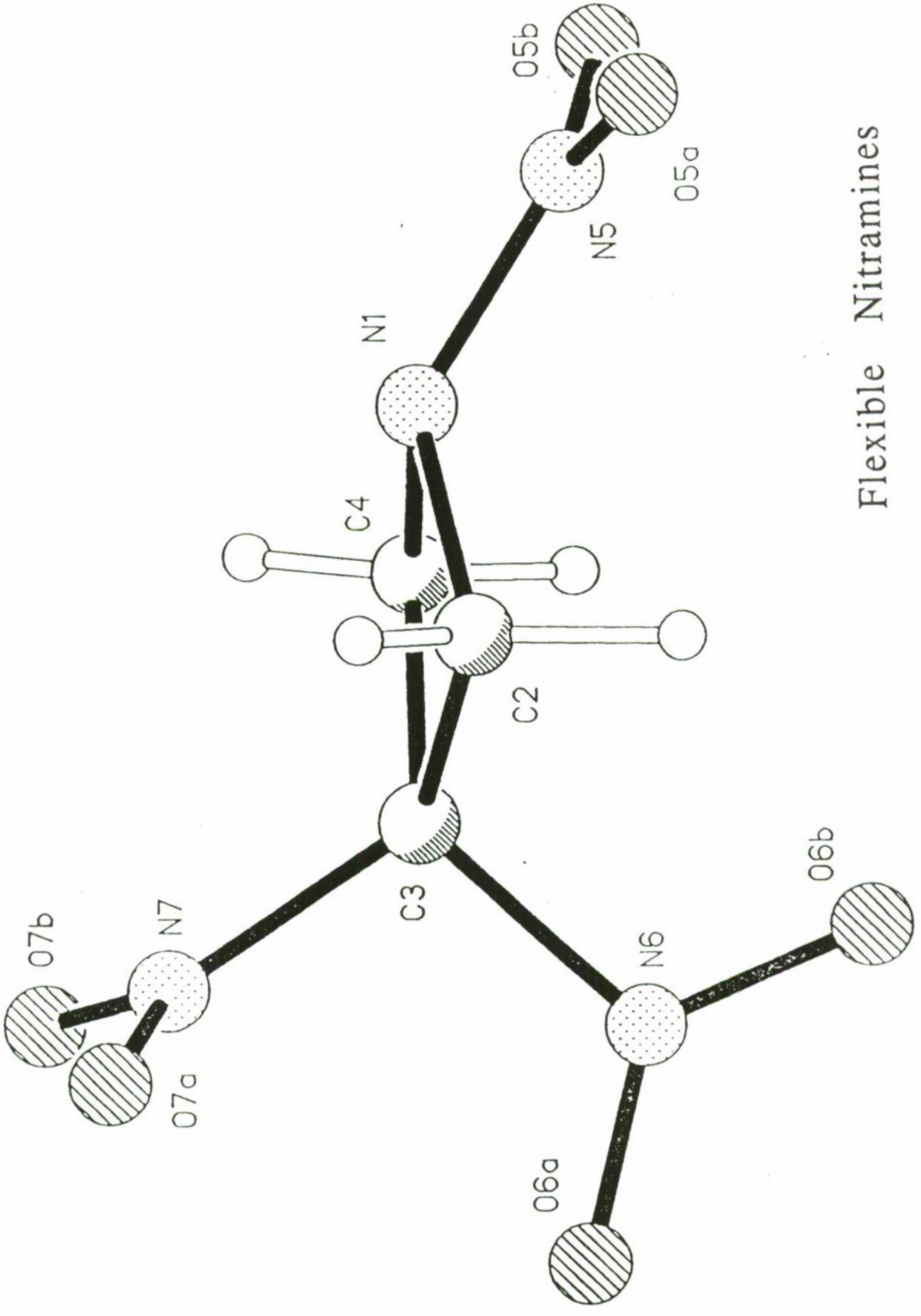

Flexible Nitramines

The 1:1 Acrylonitrile Channel Complex

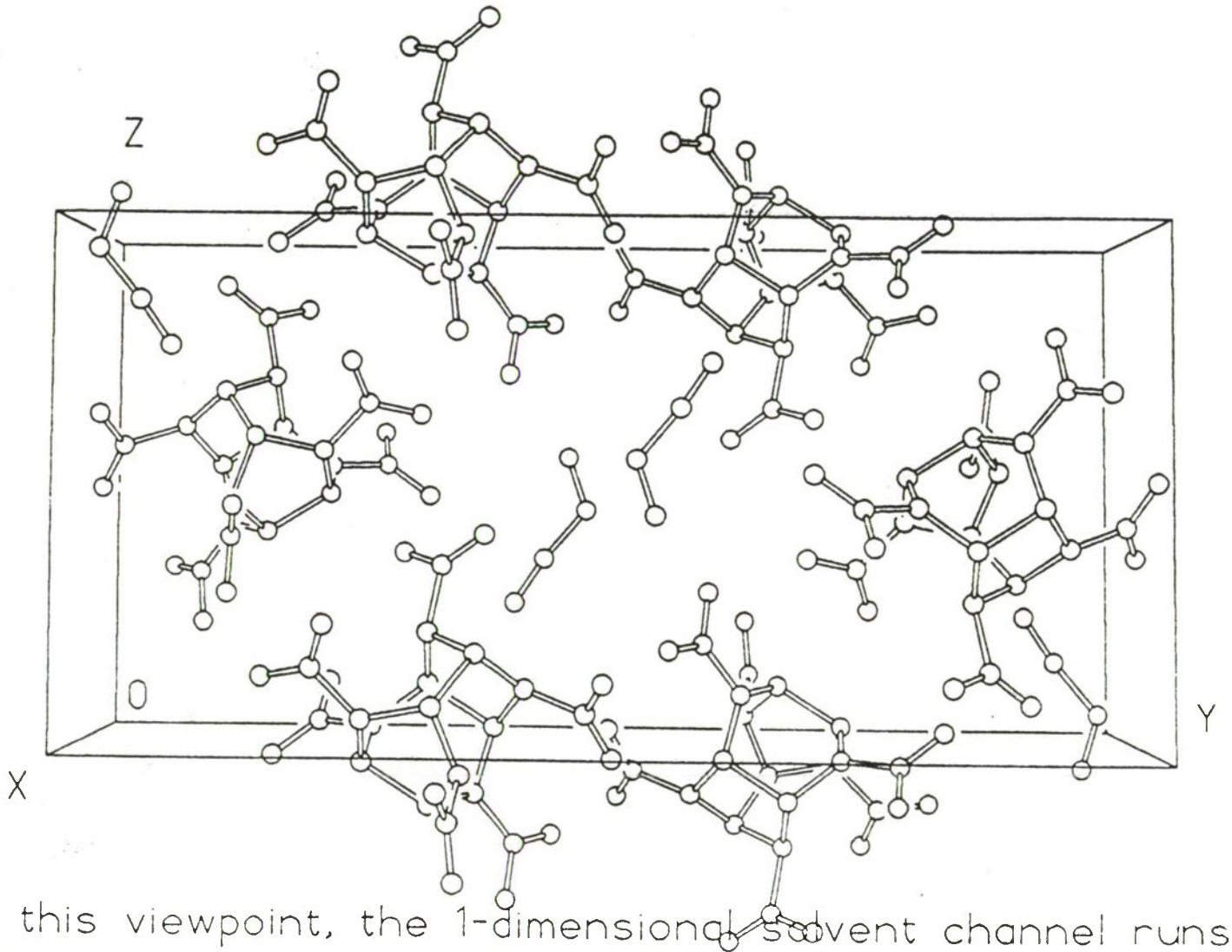

From this viewpoint, the 1-dimensional solvent channel runs towards you, through center of unit cell (2 solvents shown).

A view of the ACRYONITRILE complex with the HNIW framework omitted.

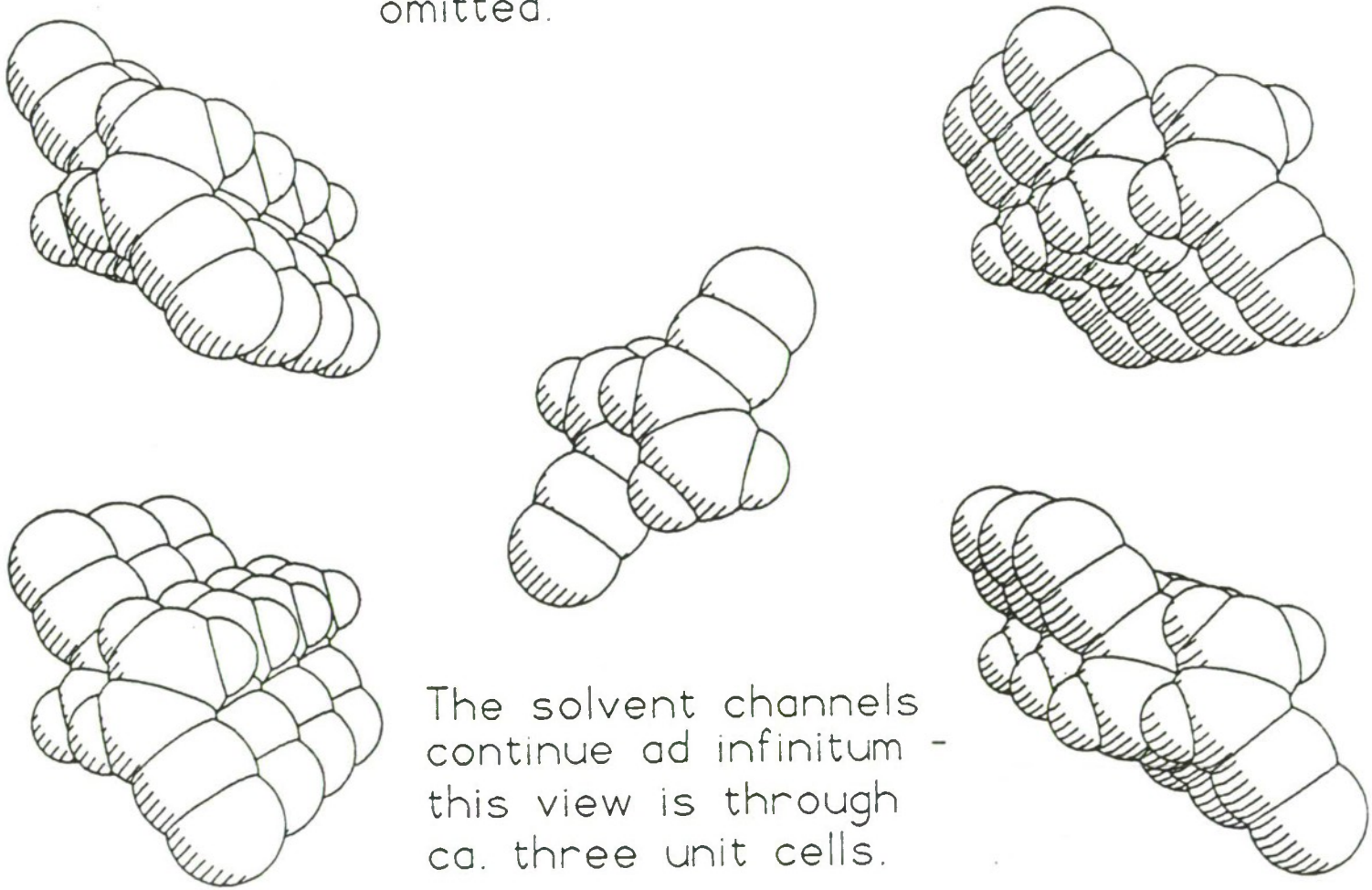

The solvent channels continue ad infinitum - this view is through ca. three unit cells.

R.Gilardi Code 6030
Naval Research Lab

07/25/91

X-ray diffraction analyses have been performed for over 300 molecules synthesized in energetic materials research programs. An up-to-date listing of the database containing structural formulae & densities is available from the authors:

Richard Gilardi 202-767-3463
Clifford George
Judith L. Flippen-Anderson

Laboratory for the Structure of Matter (Code 6030)
The Naval Research Laboratory
Washington, D.C. 20375

07/25/91

R.W. Armstrong, A.L. Ramaswamy, and J.E. Field

Thermomechanical Influences on Combustion

THERMOMECHANICAL INFLUENCES ON THE COMBUSTION OF RDX CRYSTALS

R.W. Armstrong*, A.L. Ramaswamy** and J.E. Field**

*Office of Naval Research European Office
223/231 Old Marylebone Road
London NW1 5TH, U.K.

**University of Cambridge
Cavendish Laboratory
Cambridge CB3 0HE

SUMMARY/OVERVIEW

Preliminary experiments have been performed at the Cavendish Laboratory, University of Cambridge, using a grazing laser beam to melt and ignite local surface regions of nearly perfect cyclotrimethylenetrinitramine (RDX) crystals provided by John Sherwood and David Sheen of the Department of Pure and Applied Chemistry, University of Strathclyde. The purpose is to investigate whether the type of mechanical stress influences that occur for the impact sensitivities and shock-induced detonation of energetic crystals also produce relevant influences on their combustion properties, particularly, when incorporated as ingredients in nitramine composite propellants. Properties of interest for such thermomechanical influences are, for example, burning rates and their pressure dependent exponents.

INTRODUCTION

A comprehensive review of previous combustion studies and, also, the obtainment of new results were reported by Blomshield (1) of the Naval Weapons Center, particularly involving propellants containing cyclotetramethylenetetranitramine (HMX) crystals. The total results have indicated that crystal size dependent shattering may occur in propellants under relatively high burning rate/pressure conditions. Larger crystals were indicated to shatter more easily.

Both the monoclinic beta polymorph $P2_1/n$ of HMX and the orthorhombic Pbca structure of RDX have an unusual combination of mechanical properties in that they are relatively hard, elastically-compliant, and brittle (2). Such mechanical characteristics coupled with the low thermal conductivities of these crystals provide an added incentive for investigating the nature of any cracking behavior that might be associated with their combustion properties. A further interesting feature is that combustion of HMX and RDX occurs after a melt layer forms on the crystal surfaces. This should facilitate the occurrence of cracking below the liquid because a lower liquid/solid interfacial energy is then required for the formation of crack surfaces rather than the larger surface energy of solid/vapor interfaces.

Experimental results reported here were obtained on RDX crystals that were made available from the University of Strathclyde. Considerable information on the dislocation properties of such crystals has been obtained at Strathclyde (3). Related results have been reported for similar crystals that were produced at the Los Alamos Laboratory and tested at the Naval Surface Warfare Center, White Oak Laboratory (4). For example, the easy occurrence of cleavage cracking across (001) surfaces has been confirmed for the orthorhombic crystal structure of RDX (2,4).

PRELIMINARY RESULTS

The light from a neodymium glass laser capable of delivering 10 J in a 300 ns pulse was put through a 50 micrometer diameter fiber optic guide inclined at a glancing angle of approximately 10 degrees onto local regions of essentially specular growth faces of individual RDX crystals of approximately 5 mm size. Energies in the range of 0.1 to 1.0 J are estimated to have been delivered to the crystals. Only post-irradiation observations have been made thus far of obvious melt (and combustion) zones that have occurred at generally smaller regions in the irradiated crystal surface areas. The cause for localized melting is attributable, presumably, to the nonuniform distribution of energy in the incident laser beam and to the possibility of certain defect-containing regions being more prone to melting.

Figure 1 is a transmission optical micrograph of an irradiated region centered on a ($\bar{2}10$) RDX crystal growth surface. The Figure shows several lateral (001) cleavage cracks within an elliptical melt zone also containing a central lens-shaped burn spot of semi-transparent brownish residue. Behrens has given a physical description of a brownish residue in his studies of the controlled combustion of RDX and identification of gaseous products (5). The smallest (001) crack spacing in Figure 1 is approximately 3 micrometers.

Figure 2 shows another example of fine scale lateral (001) cracking in a melt zone formed adjacent to a larger prominent (001) crack emanating from the long axis of a Knoop microhardness indentation put into the ($\bar{2}10$) crystal surface prior to irradiation with the laser beam. The fine scale (001) cracks are approximately 1 micrometer deep. The two relatively large vertical cracks, inclined to varying degrees to the ($\bar{2}10$) surface, are indicated to have segments of ($\bar{1}00$) and (010) crack lengths as well as other crystallographic segments.

DISCUSSION

A main point of interest --- whether the cracking at melted and burned spots has occurred during heating or while at the combustion temperature as compared with occurring on cooling after the laser irradiation --- is not yet known and further experiments are in progress to resolve the issue. If the cracks are formed on heating or at the burn temperature, then they

provide a ready explanation for the observation of crystal shattering at high burn rates, also leading to an increase in the burn rate/pressure exponent. Sufficient pressure build-up over the microcracks would drive them through the crystal. Crack formation caused by thermal stresses on cooling, though a normal expectation, would have to relate in a more complicated thermal cycling mechanism to crystal shattering occurring at increasing burn rates. For this reason, various thermomechanical models are being investigated for the possibility of explaining the occurrence of cracking at constrained zones on a crystal surface subjected to localized heating, especially, for a hard, elastically-compliant, and yet brittle crystal with a low thermal conductivity.

A first consideration is that circumferential tensile stresses are produced in the constraining matrix when resisting the expansion of a heated zone. Hahn and Armstrong have described the inverted situation for a low thermal expansivity inclusion resisting the contraction of a matrix material that has plastically yielded (6). Atkinson has obtained this result for the elastic expansion from a point heat source (7). Cracking has been observed in unmelted zones around inclusions in RDX.

A second interesting consideration involves the outward bulge-type expansion of a free surface region when locally heated. If a sufficient "bend strain" is introduced into the surface layer, then wedge-type cracks will penetrate to a certain small depth. The cracks will be stable in the sense of being prevented from propagating into the compressive stress state of the deeper surface layer. Such cracking would be promoted underneath a liquid layer and, also (8), would be promoted by the dislocation flow needed to satisfy this strain condition. Such cracking might be expected for a material with the kind of properties exhibited by RDX or HMX.

REFERENCES

1. F.S. Blomshield, "Nitramine Composite Solid Propellant Modelling", Naval Weapons Center Report NWC TP 6992, (1989).
2. R.W. Armstrong and W.L. Elban, Materials Science and Engineering, A111, 35, (1989); Ibid., A122, L1, (1989).
3. P.J. Halfpenny, K.J. Roberts, and J.N. Sherwood, Philosophical Magazine, A53, 531, (1986).
4. W.L. Elban, R.W. Armstrong, K.C. Yoo, R.G. Rosemeier, and R.Y. Yee, Journal of Materials Science, 24, 1273 (1989).
5. R.G. Behrens, Sandia National Laboratories, Livermore, CA, private communication.
6. T.A. Hahn and R.W. Armstrong, in "Thermal Expansion 7", Ed. D.C. Larson, (Plenum Press, NY, 1982), p. 195.
7. C.A. Atkinson, Department of Mathematics, Imperial College, London, U.K., private communicaton.
8. R.W. Armstrong and W.H. Robinson, Journal of the Physical Society of Japan, 38, 1221, (1975).

Figure 1. Combustion residue and microcracking at an RDX ($\bar{2}10$) crystal surface burn spot after laser irradiation.

Figure 2. Extensive cracking within a melt zone occurring in the strain field of a Knoop microhardness indentation.

Nitramine Composite Solid Propellant Modelling

by
F. S. Blomshield
Research Department

NAVAL WEAPONS CENTER
CHINA LAKE, CA 93555-6001

89. Cole, J. E. and Fifer, R. A., "Burn Rate Behavior of High Density Binderless HMX," 16th JANNAF Combustion Meeting, CPIA Pub. 308, Vol. II, pp. 1-15, December 1979.

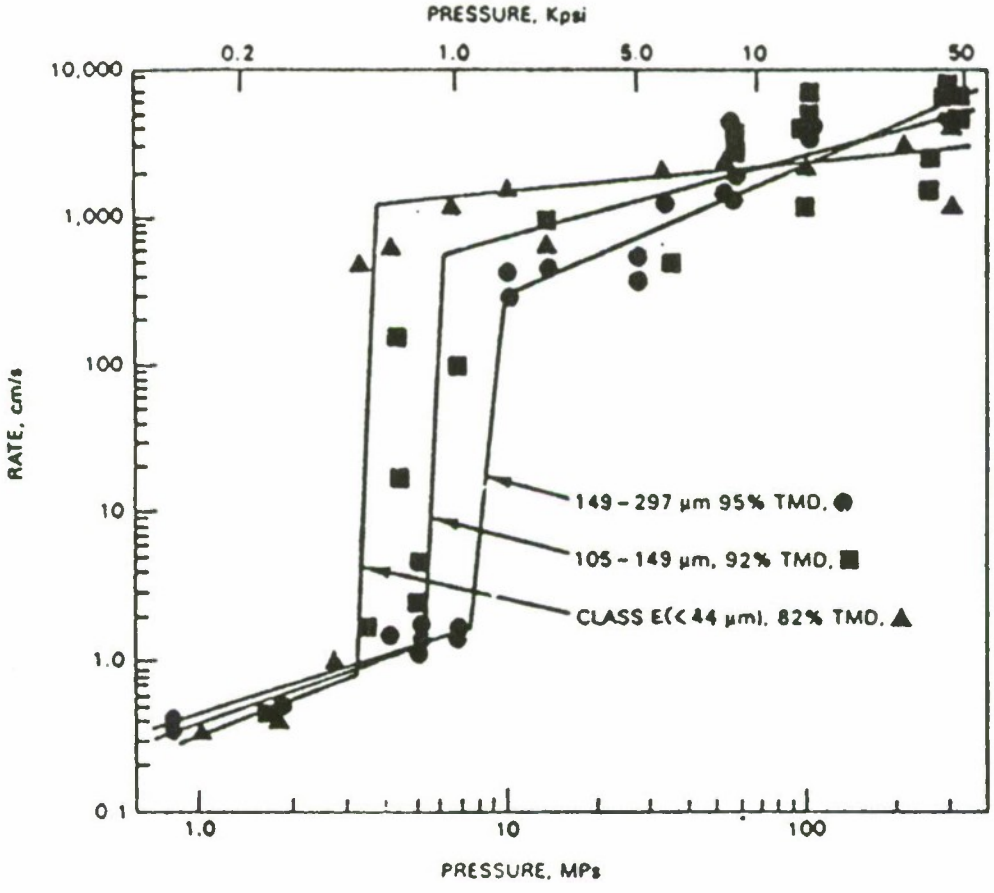

Figure 12
Apparent Burning Rates of HMX

Dislocation micromechanics approach to investigating nitramine-filled propellant combustion

07/25/91

I. Slip- or twinning-induced cleavage cracking

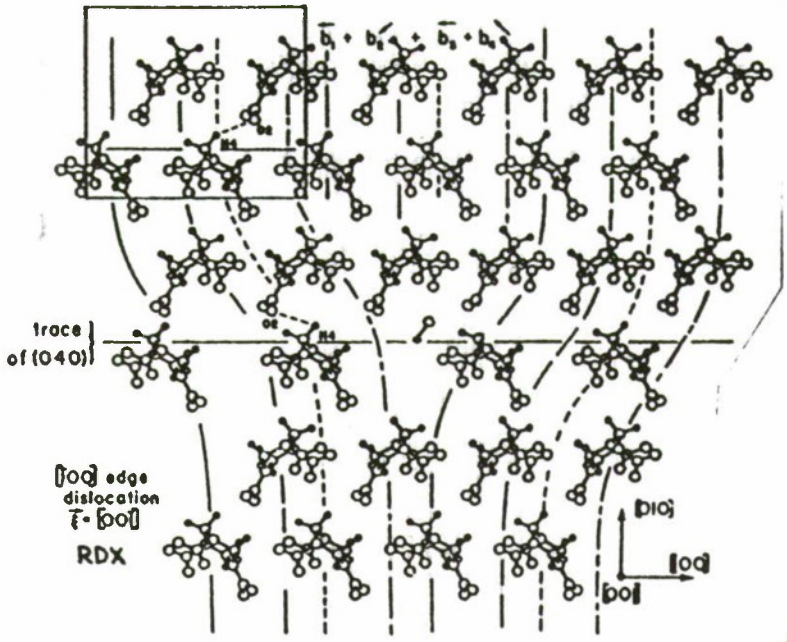

Predicted deformation and cracking systems in other compounds?

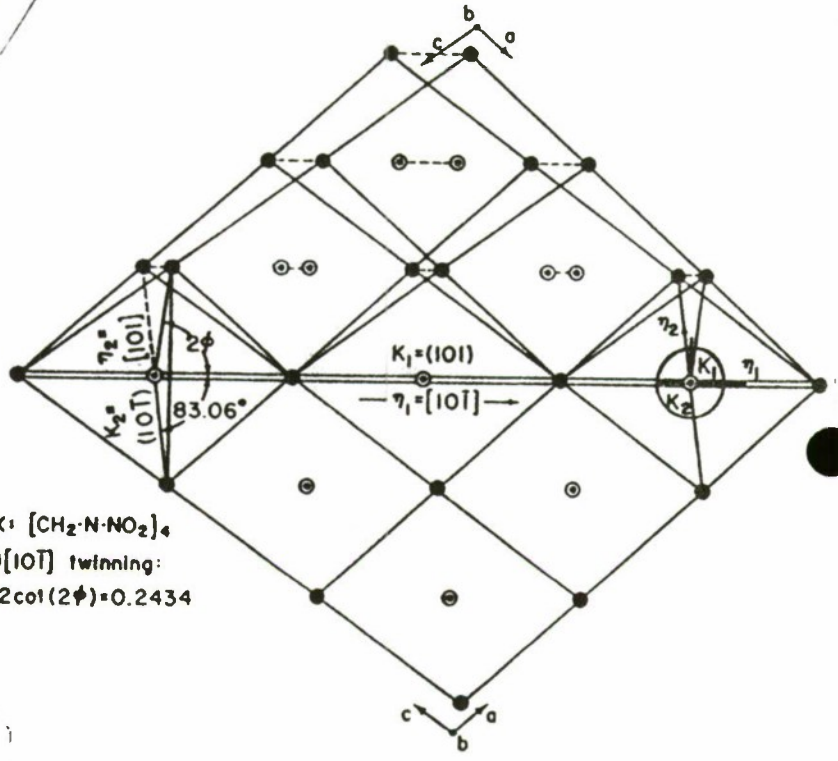

HMX: $[CH_2{\cdot}N{\cdot}NO_2]_4$
(101)[10ī] twinning:
$\gamma_{12} = 2\cot(2\phi) = 0.2434$

II. Pile-up avalanche model for shear banding and hot spots

(a) isothermal stress build-up: n_1 dislocations

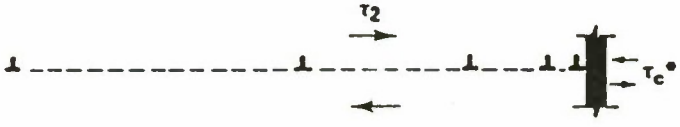

(b) critical stress concentration: $n_2 \tau_2 = \tau_c^*$

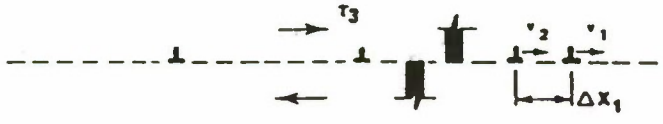

(c) adiabatic collapse-discontinuous load drop

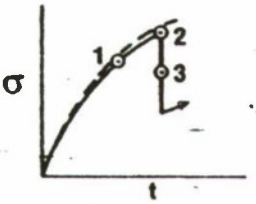

(d) pressure-time curve for τ_1, τ_2, and τ_3

$$\Delta T \leq (k_s/16\pi)[2\ell v/c^* K b]^{1/2}$$

k_s = pile-up stress intensity
ℓ = pile-up length
v = dislocation velocity
c^* = specific heat/volume
K = thermal conductivity
b = dislocation Burgers vector

Hot spot size, lifetime, and extent of reaction?

Dislocation micromechanics approach to investigating nitramine-filled propellant combustion

07/25/91

III. Drop height sensitivity (H_{50}) dependence on crystal size (ℓ) — through the stress-driven dislocation velocity, v:

$$v = v_0 e^{-\frac{G_0}{RT} + \frac{1}{RT}\int_{\tau_{Th^\circ}}^{\tau_{Th}} (Ab)\, d\tau'_{Th}}$$

$$Ab = w_0 / \tau'_{Th}$$

$$v = v_0 e^{-\frac{G_0}{RT}} \left(\frac{\tau_{Th}}{\tau_{Th}^\circ}\right)^{\frac{w_0}{RT}}$$

$$\tau_{Th} \propto H_{50}^{1/n}$$

$$v = v_0 e^{-\frac{G_0}{RT}} \left(\frac{H_{50}}{H_{50}^\circ}\right)^{\frac{w_0}{nRT}} .$$

Substituting for v in the ΔT expression:

$$\ln H_{50} = \ln H_{50}^* + \frac{2nRT}{w_0} \ln \ell^{-1/2}$$

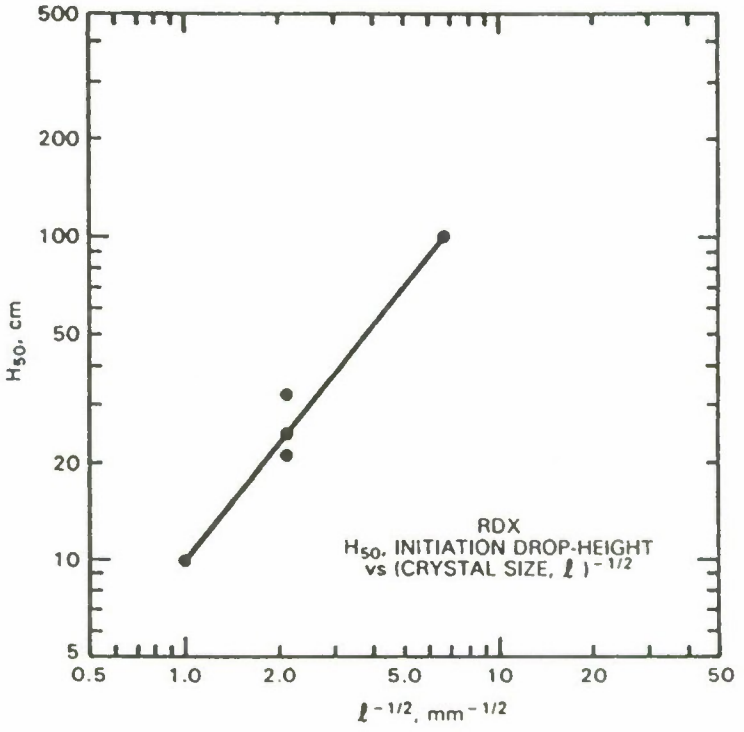

Size effect in propellant composites?

IV. Comparison with thermal decomposition properties:

Boddington result for thermal decomposition of liquid

Hot spot model leading to melting and superheating:

$$T \leq T_0 + \frac{Gb^2}{64\alpha\, \Delta x_1^2} \left[\frac{\ell \nu}{c^2 K}\right]^{1/2}$$

At $\ell = 1.0$ mm, $T \approx 900°K$

hot spot radius ≈ 400 Å

hot spot lifetime ≈ 40 ns

rel. amt. reacted ≈ 0.3

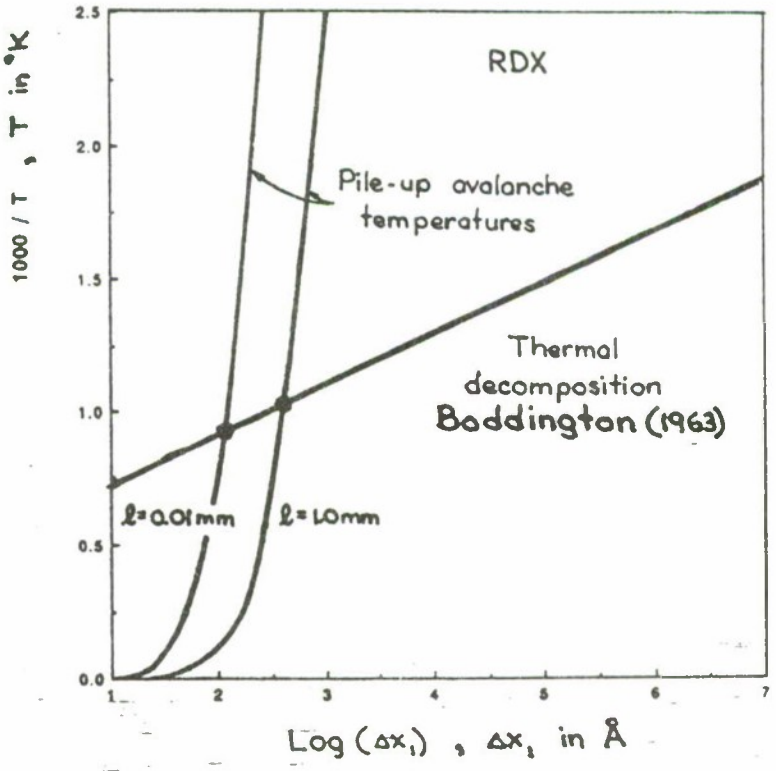

Application to propellant composites?

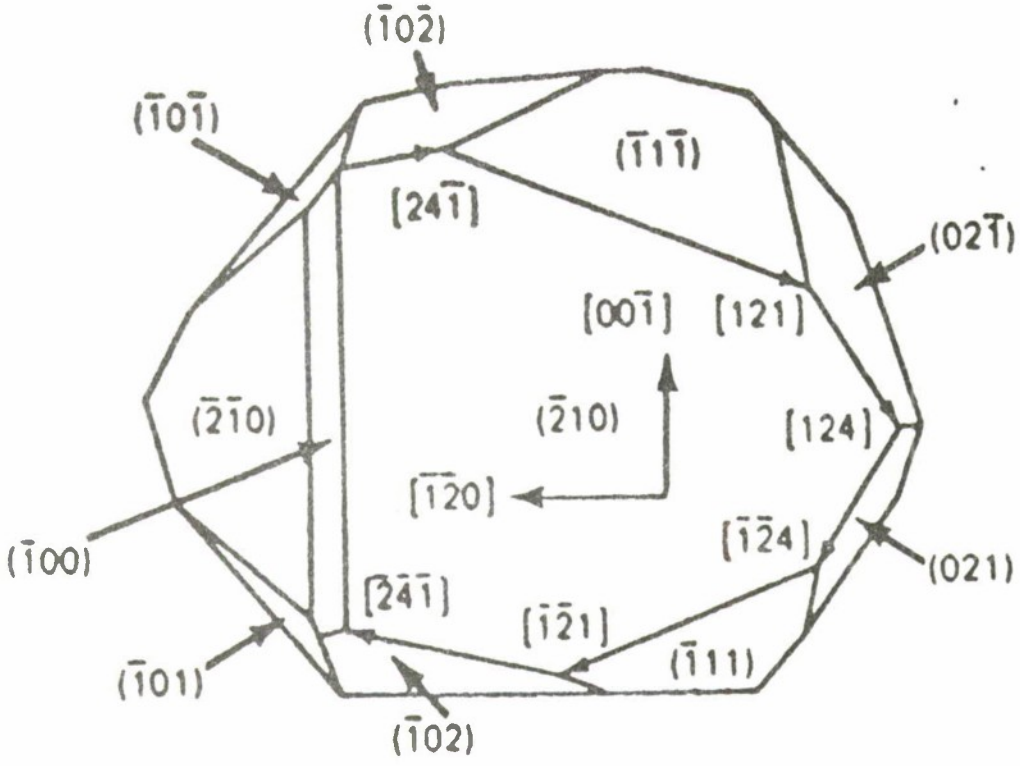

175

Combustion residue and microcracking at an RDX ($\bar{2}10$) crystal surface burn spot after laser irradiation.

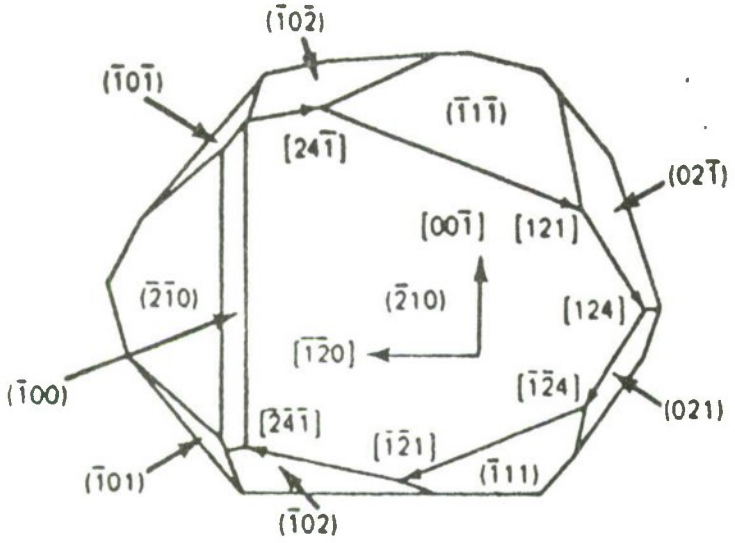

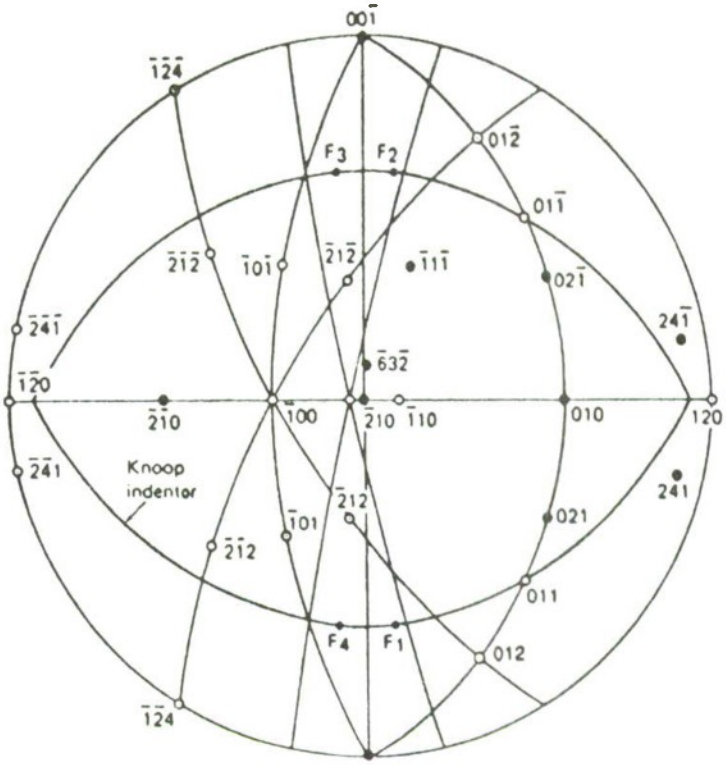

Extensive cracking within a melt zone occurring in the strain field of a Knoop microhardness indentation.